NASA Contractor Report 179549
DOT/FAA/CT-TN87/1
M/NAFA/TR-1

Jet Engine Simulation With Water Ingestion Through Compressor

T. Haykin and S.N.B. Murthy
Purdue University
West Lafayette, Indiana

January 1987

Prepared for
Lewis Research Center
Under Grant NAG3-481

National Aeronautics and
Space Administration

U.S. Department of Transportation
Federal Aviation Administration

PREFACE

The investigation was conducted under a grant from the Lewis Research Center of the National Aeronautics and Space Administration, grant No. NAG 3-481, related to NASA-FAA Agreement No. DTFA03-83-A00328. Mr. R. Steinke was the grant technical monitor at NASA and Mr. T. Rust at FAA.

Dr. S.N.B. Murthy was principal investigator of the project, and was assisted in the current effort by Mr. T. Haykin, Research Assistant in Mechanical Engineering. The report is based on a thesis, entitled, "Jet Engine Simulation with Water Ingestion in Compressor," dated May 1986, submitted by T. Haykin in partial fulfillment of the requirements for the award of the M.S.M.E. degree in the School of Mechanical Engineering, Purdue University.

EXECUTIVE SUMMARY

The transient performance of jet engine during power setting operations is affected in several ways when water is ingested at the front end of the engine. The nature and magnitude of effects depend primarily upon (1) the initial design of the engine and the control system, including limit switches incorporated in them, (2) the mass fraction and volumentric droplet size of water, (3) the ambient conditions including pressure, temperature and degree of saturation with water vapor, (4) the rate at which power resetting is carried out and (5) any errors in data acquisition with sensors that are providing input to the engine control.

An attempt has been made to establish the effects of water ingestion through simulation of a generic high bypass ratio engine with a generic control. In view of the large effects arising in the air compression system during water ingestion, attention has been focussed on those effects and the resulting changes in engine performance. In order to confine the effects of water ingestion to the air compression system, it is assumed that water is either drained out completely at the end of compression processes in the bypass and the core streams or is removed in part by draining and the rest by flash evaporation at either entry or the exit of the burner. Such treatment of water, while leaving the turbines and the nozzles with single phase, gaseous flow, will cause changes in turbine entry mass flow and temperature.

Engine simulation has been carried out in the afore-mentioned cases utilizing the PURDU-WINCOF code, that is suitable for obtaining the performance of a fan-compressor unit with water ingestion, and an engine simulation code that is flexible enough for handling a generic high bypass ratio engine and its control.

Engine performance with ingestion of 1, 2, 4, and 8 per cent mass fraction of water, mean volumetric diameter of water droplets being 600 microns, during power setting in accel and decel modes between idling and maximum power at sea level standard, static conditions, shows highly nonlinear variation with the magnitude of water mass fraction. Most of the change in performance occurs with one per cent water ingestion. No simulations have been possible with 8 per cent water ingestion.

The performance of the generic engine deteriorates under hot day operating conditions even with dry air operation. No appreciable further deterioration occurs during water ingestion, although the air compression system shows some improvement due to increased heat and mass transfer at the higher temperatures.

Evaporation of water in the burner to any extent larger than 0.5 per cent, especially at the exit section of the burner, causes appreciable changes in the performance of the low pressure spool. It appears significant to test engines with small amount of water ingestion during power setting operations.

While small changes in temperature sensor (submerged in centrifuged water) reading, that is utilized as an input to the control, does not affect the performance of the generic engine, an error of about 10F does not permit engine simulation between the desired initial and final conditions. The compressor seems to surge.

It is often of interest to establish if, during water ingestion, the time-rate of change of power setting should be reduced to obtain a smooth, surge-free operation. In the case of the generic engine with an automatic provision for operating with a pre-set acceleration fuel schedule, appreciable slowing down of power lever angle changes seems to be necessary to ensure that there is an adequate margin between acceleration schedule operation and compressor surging condition.

TABLE OF CONTENTS

LIST OF SYMBOLS

AK1	Adjustable parameter in deviation rule, non-dimensional.
AK2	Adjustable parameter in nondimensional wake momentum thickness rule, non-dimensional.
AK3	Adjustable parameter in equivalent diffusion ratio rule, non-dimensional
D_{30}	Volume-mean drop diameter, microns.
D_{eq}	Equivalent diffusion ratio, non-dimensional.
i	Incidence angle, degrees of angles.
$\dot{M}$	Mass flow rate, 16m./sec.
M	Mach number, non-dimensional
N	Rotor rotational speed, revolutions/sec.
r_1	Radial location of streamline at entry to blade row, feet.
r	Ratio of specific heats, non-dimensional.
V_{z1}	Axial velocity at rotor inlet, ft./sec.
V_{z2}	Axial velocity at rotor outlet, ft./sec.
X_w	Mass fraction of droplets, non-dimensional.
X_{ww}	Mass fraction of large droplets, non-dimensional.

Greek Letters

β_1	Relative flow angle at rotor inlet, degrees of angle.
β_2	Relative flow angle at rotor outlet, degrees of angle.
detal	Deviation, degrees of angle.

Θ/C	Non-dimensional wake momentum thickness.
σ	Solidity, non-dimensional.
ϕ	Flow coefficient, non-dimensional.
ψ	Work coefficient, non-dimensional.
ψ_1	Pressure coefficient, non-dimensional.
ω	Rotor angular velocity, degres of angle/sec.
$\bar{\omega}$	Pressure loss coefficient, non-dimensional.

Subscript

corr	Pertaining to values corrected or ambient conditions
max	Pertaining to maximum values
F	Pertaining to fuel
ML	Pertaining to minimum loss point
R	Pertaining to values corrected for ambient conditions
1	Pertaining to rotor inlet
2	Pertaining to rotor outlet
*	Pertaining to design point

Engine Simulation Output Symbols

PCN25R	Corrected to core rotor speed
PCN12R	Corrected booster rotor speed
P13Q12	Fan pressure ratio
P23Q2	Booster pressure ratio
P3Q25	High pressure compressor pressure ratio

W2R	Corrected mass flow rate of mixture at booster inlet
W25R	Corrected mass flow rate of mixture at high pressure inlet
WFE	Engine fuel mass flow rate, lbm.
SFC	Engine specific fuel consumption, lbm/lb of the rust.
FG	Engine gross thrust, lbs.

CHAPTER I

INTRODUCTION

An aircraft gas turbine engine and its control system are normally designed for operation with air as the working fluid. All of the components of an engine except the burner are then expected to operate with a single phase, gaseous fluid. The burner in an aircraft gas turbine is commonly supplied with a liquid fuel and occasionally also with water. The design objective in those cases then is to obtain an adequate amount of atomization and vaporization in the shortest time and space within the burner to complete the desired heat and mass transfer and combustion processes. Thus under all of the flight conditions, defined by altitude, Mach number and power setting, the engine is designed to perform with a gaseous fluid except for local processes in the burner.

There are, however, a number of environmental conditions under which the air utilized by an engine may contain a second phase in the form of dust, sand, or volcanic ash (References 1 to 3) and also water (References 4 and 5). The effects of the presence of a liquid in the ingested air are in several respects similar to those obtained with solid particles, but there are certain specialized effects in the case of water ingestion. It is considered of interest to establish the effects of the presence of water on individual engine components and the overall engine system with a given control. Based on such studies, one may proceed to obtain some guidelines for engine operation with current designs and also, possibly, for modifying engine and control design.

Ingestion of water may arise in various ways. Water vapor is often present in ambient air giving rise to changes in density, molecular weight, and ratio of specific heats of the working fluid. Modern engines and their control systems are designed to accommodate appreciable humidity in the ambient air. When the humidity is high, however, engine inlet condensation may be severe enough under certain operating conditions to cause noticeable amounts of liquid water to be ingested into the engine (References 6 and 7). An air-liquid water mixture may also enter an engine directly during take-off from rough runways on which there are puddles of water and during flight through a rainstorm (References 4 and 8). Water may then be present along the gas path of an engine, starting from the inlet face all the way up to the thrustor nozzle exit, in droplet, film, or vapor form in different proportions at different locations.

The problem of water ingestion is of interest in the case of all aircraft gas turbines, although in the case of turboprops there may be some shielding provided by the propeller installation. The effects of water ingestion can be particuraly severe in the case of a two-spool engine with a fan and a bypass flow, since the design, matching and control fo the engine involve a core engine and asupercharger. Although the basic effects of water ingestion appear even in a single shaft engine, a high bypass ratio engine such as used in many civil aircraft applications, provides a special opportunity for examining the effects of water ingestion on "matching" and control of a system with two shafts and thrustor nozzles but with a part of the working fluid passing through the entire engine and with a single control. It is such an engine that is chosen

for the current investigation. Figure 1 provides a schematic of a typical high bypass ratio engine and control.

In practice, the effects of water ingestion on an aircraft gas turbine need to be determined taking into account the installation of the engine in the aircraft. Several considerations resulting from installation are (i) changes introduced by the installation on water ingestion into the engine, (ii) thrust requirement of the integrated aircraft-engine system and (iii) the role of aircraft or flight control on engine operation and control. It is clear that those considerations make the problem aircraft-specific in addition to being engine installation-specific. Therefore, in the current investigation the engine is examined as though it is on a test bed with standard inlet and nozzle and with provision for obtaining any desired air-water mixture in front of the engine.

The nature and magnitude of the effects of water ingestion depend upon some or all of the following: (i) characteristics of air-water mixture ingested, (ii) design of each of the components of the engine and its control system and the nature of the component performance matching scheme utilized for obtaining equilibrium running of the engine, (iii) operational changes introduced following water ingestion and (iv) design and performance of sensors feeding the control system.

1.1. Air-Water Mixture

An air-water mixture ingested into an engine is characterized by pressure and temperature of air, temperature, mass fraction and mechanical state of liquid water and water vapor content. In general, the mixture may be fully saturated with respect to water vapor during flight operations in rain storm conditions. The temperature of air and liquid water may also be unequal under such conditions. The pressure and temperature of the gas phase (air-water vapor mixture) depend upon the altitude of engine operation and flight speed, when applicable. There may be deviations in temperature and pressure from "standard" data at some altitudes due to meteorological phenomena. In this investigation the pressure, is assumed to correspond to the standard value (14.7 P.S.I.A.) and the temperature to either the standard (518.7R) or selected hot day (for example, 589.7R) conditions. During hot day conditions, the initial water vapor content under saturation conditions and any phase change process within the compression subsystem are also affected.

The liquid in the air-water mixture is assumed in the current investigation to enter the engine entirely in droplet form, although in practice the liquid may flow into the engine in film form from a wing, fuselage, or inlet surface. Within the engine, the liquid may flow over material surfaces in film form or in the free stream in droplet form. At the trailing edge of a blade surface, a water film may be entrained in the form of droplets. In the free stream droplets may coalesce into large droplets or break up into smaller droplets (References 9 and 10). There is considerable uncertainty about the mechanical state of water in curved ducting (such as the one utilized for interconnecting the low pressure compressor and the high pressure compressor in the engine shown in Figure 1), diffuser (such as that following the high pressure compressor), burner (with primary and coolant streams), and nozzles. In the current investigation no account is taken of the existence of a film of water in any of these components.

The water droplets in the air-water mixture may be characterized by values of size distribution and mass fraction. One method of characterization consists in using a reference local volume-mean diameter, D_{30}, as defined by A.S.T.M. Standards (Reference 11) and number density per unit volume of the mixture. The droplets found in rainfall are of the order of hundreds of microns and in some cases, larger than 1000 microns (References 12 and 13). Within the engine, especially following droplet breakup and vaporization, a portion of the droplets may be small enough to follow the gas phase motion. No data seem to be available for droplet size in aircraft wheel-generated sprays. The mass fraction of water may vary over an appreciable range in practice, for example 0.5 to 15 per cent (Reference 8). It may be useful to note that 1.0 per cent by weight of water in droplet form of size $D_{30} = 1000$ microns is equal to a number density of 54,200 per cubic foot of air-water mixture under standard conditions, with a total surface area of 264 square inches and a volume of 1.73 cubic inches.

1.2. Engine Components and System

The generic engine shown in Figure 1 may be divided broadly into the engine and the control system. The engine consists of a large number of components. They may be grouped for convenience under (i) stationary, cold flow components, namely inlet, ducting, diffuser, and bypass stream thrustor nozzle, (ii) air compression subsystem consisting of fan (bypass stream), booster (fan core stream, and low pressure compressor) and core or high pressure compressor, (iii) burner, (iv) turbines and (v) stationary hot flow components, namely core stream thrustor nozzle. During water ingestion, the working fluid may contain the liquid phase in any or all of the groups of components. All of the groups of components are, in general, affected by the presence of water in any of the groups since the engine has to function as a single integrated system whether or not the performance of various components is exactly matched for equilibrium running under a given set of conditions.

The engine also incorporates, in general, a number of bleeds through valves located between various stages and also sections of the compression subsystem. The performance of such bleeds is affected by the presence of water in the working fluid.

The control system consists of sensors, signal processors, and actuators. Typically it is designed to control engine speed in response to power setting and values of temperature and pressure at various locations. During equilibrium running under given ambient conditions and at a given power setting, the high pressure turbine work output matches the work input required by the high pressure compressor operating at a speed corresponding to the power setting, and the work input required by the fan and low pressure compressor by the output of the low pressure turbine. When the ambient conditions and/or the power setting are changed, the latter causing a different fuel flow-rate, the control is actuated by the sensor, that is providing data for it, and functions such that the engine attains the equilibrium running point corresponding to the new operating conditions. The core engine speed is often controlled directly while the low pressure system speed is not. However, the low and high pressure system are coupled through the enthalpy and the mass flow rate of the core stream working fluid so that the low pressure system attains an equilibrium speed

corresponding to the controlled speed of the core or the engine. Now, during water ingestion, under similar conditions of changes in operation (for example, power setting) the component performance matching will become affected. This may be due to changes in working fluid characteristics along the gas path as well as changes in the output of sensors which feed the control system. For example, a temperature sensor that provides an input to engine control may become immersed in liquid water and transmit the water temperature rather than the gas phase temperature (Reference 14) and cause a malfunction of engine.

1.3. Operational Changes During Water Ingestion

During normal gas phase operation there are various modes or states in which it is required to run an engine. These modes include (a) steady state operation at various power settings, (b) changes in flight conditions such as altitude and Mach number, (c) changes in ambient conditions such as temperature, pressure and composition of the working fluid, and (d) transient operation during and following power setting changes. In the design of an aircraft power plant there are ranges of flight conditions, ambient conditions and power settings over which the engine may be operated. The limits of these ranges define the operating envelope of the engine. During water ingestion the available operating envelope may be altered. Also inherent in an engine design are limits on rates of change for various operational parameters, that will result in stable engine operation at the end point of a transient. The presence of water in the working fluid may also alter these allowable rates of change.

Each of the components and the engine system as a whole can be expected to be affected by the presence of liquid water in the working fluid entering the engine. The effects of water ingestion are both aerothermodynamic and mechanical. The affects can arise "immediately" or in a short time scale during water ingestion as well as in a cumulative fashion over a long period of time due to sustained or repeated ingestion and consequent deterioration of engine components and system (Reference 15). Although aerothermodynamic and mechanical effects are in general coupled attention is focused in the current investigation on aerothermodynamic changes. For example, the loading of a turbomachine blade can be expected to change when the working fluid contains liquid water. The aerothermodynamic effects may also lead to aero-elastic phenomena due to altered bending and torsional loading on blades and other structural elements. However, in view of the central nature of aerothermodynamic effects, attention is focused here on those effects.

In general, it is of interest to establish the effects of water ingestion on a time-dependent basis. Every engine and control, including sensors, have inherent dynamic characteristics due to inertia and time delays in the system. A change in the working fluid therefore cannot be accommodated instantaneously. Furthermore, the engine operating condition may be altered, for example, by pilot action, through a resetting of the power demand over a short but finite interval of time. It may also be possible that the characteristics of air-water mixture entering the engine may themselves not be steady with respect to time. In all cases, the principal interest is in the time dependent changes between one condition of operation and another. It may be observed that there is no certainty that at any finite length of time following ingestion

of water, the engine in fact attains an equilibrium running point. In general the following are of interest in a two-spool engine at every instant of time in any chosen interval of time of operation with water ingestion: (i) speeds of the two spools, (ii) surge margin of compressors, (iii) fuel cut-off, (iv) flame-out in the burner, and (v) thrust output.

A detailed time-dependent analysis requires a knowledge of the dynamical characteristics of each component of the engine and its control as a system. Such characteristics are required during engine operation both with air and with various air-water mixtures. Moreover, a given air-water mixture at entry to the engine can be expected to undergo substantial changes along the gas path, from component to component. There may also be resulting changes in the dynamical characteristics of components. Accounting for all of those is unmanageable at this time since only a hybrid analytical-experimental study can provide the required data. No such study is available to date.

The current investigation is therefore limited to determining time-dependent changes for an engine under quasi-steady approximations wherein it is assumed that (a) the performance of each component is that obtained under steady state conditions and (b) inertias and delays remain unchanged from reference values obtained under a set of specified design operating conditions. In conducting a quasi-steady calculation of performance, the time steps chosen should of necessity be larger in duration than any of the delay times associated with the engine. At the same time, the time steps should be small enough to recover any time-dependent, oscillatory behavior of the engine during a transient.

In general, an investigation of the effects of water ingestion on an engine requires consideration of effects on all of the components and also the matching and control of the engine as a system. This is a formidable task in view of various uncertainties associated with modeling of air-water mixture flow through various engine components. It has therefore been felt that the effects of water ingestion on the engine may be determined with respect to effects on one component at a time. Among the engine components mentioned earlier, the compression subsystem is most directly exposed to water ingestion. There are reasons to believe that the effects of water ingestion can be severe in the compression system directly and through induced effects on the engine (Reference 15). In the current investigation, therefore, attention is focussed on the air compression subsystem and the performance of the engine is then established with respect to the changes in the performance of that subsystem.

All of the current investigations are conducted on a generic engine with a control system, such as that shown in Figure 1, and described briefly in the Appendix. The performance of the engine is examined in three categories of problem areas, namely: (i) various types of air-water mixtures entering the engine and chosen power setting changes; (ii) operational conditions related to different types of power setting changes; and (iii) behavior of major sensors feeding the control system.

The principal tools utilized in the investigation are a computer code for obtaining the performance of an axial flow compressor with water ingestion and a computer code capable of predicting the dynamic performance of a typical high bypass ratio turbofan

engine. There are various compressor modeling codes available such as those presented in References (16) and (17). Similarly, there are a number of engine simulation programs with the required capabilities such as those discussed in References (18) and (19). The programs chosen for this investigation are (i) the so-called PURDU-WINCOF code, a computer program capable of obtaining the performance of multi-spool, axial flow compressor operating with an air-water mixture working fluid (References 20), and (ii) an engine simulation code (Reference 21).

1.4. Organization of Report

The objectives of the investigation, along with details of the approach utilized, are given in Chapter II. A computer program has been modified and utilized to generate the compressor performance maps under various operating conditions. A description of the code and details concerning its modification for use in generating performance maps are provided in Chapter III. In Chapter IV, the generic high bypass ratio turbofan engine and its standard control system are described. A description of the engine simulation program is also included. Finally, the specific test cases used in the investigation are discussed. Chapter V presents results of both the compression subsystem performance analysis and the engine performance simulation. In Chapter VI, the results are discussed with some conclusions.

Some aspects of the investigation and initial results are discussed in References 34 and 35.

CHAPTER II

OBJECTIVES AND APPROACH

The objectives of the investigation are as follows:

(i) To establish a procedure for determining time-dependent changes in the performance of a high bypass ratio turbofan engine with water ingestion effects confined to the compression subsystem; and

(ii) To determine operability or controllability characteristics of a selected high bypass ratio turbo fan engine with a given control under various conditions of water ingestion and operation.

For the purposes of current analysis, controllability of the engine may be defined as the ability of the engine and the control system to respond effectively as a combined system to operator-initiated power setting changes.

The PURDU-WINCOF code has been modified to generate performance maps for the fan (with respect to the bypass stream), the booster (fan with respect to the core stream, and low pressure compressor) and the core or high presure compressor under various ambient conditions Such conditions include ambient temperature and inlet mass fraction of water. For each set of ambient or water ingestion conditions, specific compressor performance maps must be generated.

The effects of water ingestion on the engine are to be established in the current investigation with respect to changes in performance of the air compression subsystem. In order to isolate the effects of water ingestion to the air compression subsystem, a number of assumptions are introduced as follows: (a) the performance of inlet, ducting, and diffuser is not significantly affected; (c) the performance of bleed valves is not affected, and (c) water can be removed or converted into vapor form before the working fluid in the core stream leaves the burner and before that in the bypass stream enters the cold flow thrustor nozzle. The assumptions remove the need for examining any two phase effects in any of the components except the air compression subsystem and the burner. Insofar as the burner is concerned, some of the water entering it can be expected to undergo evaporation. It is clearly difficult to establish where evaporation may begin or become completed along the burner. Accordingly, two limiting cases have been postulated regarding such evaporation: (i) at entry and (ii) at exit of the burner.

The engine simulation program uses a gas path analysis along with stored component performance data, limits and schedules imposed by the control system, and information on mechanical characteristics and limits of the engine (such as inertias and speed limits) to obtain a series of equilibrium operating points in response to an input representing a set of operational conditions. In other words, the time dependent response of the engine to operator-initiated (input) changes in power setting and operational altitude and flight Mach number is obtained in the form of a series of local equilibrium operating points corresponding to discrete time steps between the initial and the desired final, steady state operating points. In order to accomplish this, an

engine simulation code requires, typically, data that completely define the performance of each engine component over as large a part of the range of operational parameters (such as mass flow rate, rotational speed, temperature, pressure, composition of the working fluid, etc., whichever is applicable) as possible for which the component and the engine system have been designed. This information is stored in tabular form and is referred to collectively as the component performance maps. Both the WINCOF code and the generic engine simulation code have been modified as required for application to the given air compression subsystem and engine under conditions of water ingestion.

In order to examine operability and controllability a series of simulation test cases have been chosen. The test cases may be grouped under the following types of studies for the effects of: (i) amount of water ingested, (ii) location and extent of water vaporization, (iii) elevated ambient temperature, (iv) errors in input to control system and (v) operational changes with respect to power-setting operations.

CHAPTER III

PERFORMANCE OF COMPRESSION SUBSYSTEM WITH WATER INGESTION

In this section a general description of the WINCOF code is given along with a discussion of the assumptions and modifications introduced for obtaining the performance of the compression subsystem in the form of "maps" that are suitable for use in the engine simulation program.

3.1. Description of the WINCOF Code

The WINCOF code provides a scheme for a one-dimensional, or designated-streamtube, performance calculation for a fan or a compressor stage, and through a stage-stacking procedure, a multi-stage compressor. Considering axisymmetric coordinates (r, radial, Θ, circumferential, and Z, axial directions) a one-dimensional analysis, by definition, does not account for the radial velocity component. The streamtube is always assumed to be parallel to the Z-direction over its entire length. However, the streamtube can be located arbitrarily, as desired, in the spanwise direction from blade row to blade row within a compressor.

The WINCOF code can be used for obtaining the performance of a fan or a compressor while operating with air or air-water droplet mixture. The performance calculations are done with consideration of the following processes that are of interest during water ingestion.

(i) Ingestion of the working fluid at the turbomachine face;

(ii) Impact and rebound at material surfaces;

(iii) Film formation and film flow on material surfaces;

(iv) Modification of boundary layer thickness, deviation, and aerodynamic losses;

(v) Centrifugal action on droplets causing their radial displacement;

(vi) Interphase heat and mass transfer;

(vii) Reingestion of water into wakes of blades from film flow over blades;

(viii) Droplet size adjustment based on Weber number considerations (Reference 22); and

(ix) Division of work input between the two phases.

Some of those processes occur at specific locations with respect to a given blade row, while others are distributed over a blade surface and a blade wake. The WINCOF code is based on lumping the processes at specific locations. Thus, considering the aforementioned list of processes, it is assumed that (a) (i) occurs at a specific location upstream of the blade row under consideration; (b) (ii), (iii), and (ix) can be combined suitably to obtain work output and losses; and (c) (v) to (viii) can be

considered at the exit plane of the blade row under consideration.

Regarding centrifugal action and heat and mas transfer processes, characteristic length and velocity scales are assumed for each blade row to yield a characteristic length of time over which such processes occur for that blade row.

Centrifugal action on water droplets is assumed to occur both over blade surfaces and in the free stream. Centrifugal action displaces water radially from the hub towards the tip of a blade. It is assumed that water removed from any spanwise location accumulates only at the tip of blades, in the vicinity of the outer casing wall.

The various processes are a function of the local state of air-water mixture, defined by the mass fraction of water and the mean volumetric droplet size. They have a combined effect on the balance of forces as well as on heat and mass transfer processes. Thus, although gravitational force has not been included for consideration, it may become significant in relation to momentum and drag forces under certain conditions of number density and size distribution of droplets. The heat and mass transfer from a conglomeration of droplets of different sizes is also significantly different from that for a single droplet or droplets of homogeneous size and small concentration.

In the current investigation droplets are generally visualized as falling into two categories, namely, small and large. Small droplets are assumed to follow the gas phase motion and to absorb work input. Large droplets are assumed to move independently of the gas phase and to absorb no work input. Both types of droplets are expected to undergo change of size based on mechanical equilibrium consideration, and are subjected to heat and mass transfer processes.

The WINCOF code is set up to perform the following three types of calculations.

(i) Design point calculation: Given the design rotational speed, mass flow rate, axial flow velocities (at inlet and exit planes of each blade row) or, equivalently, streamtube area (at inlet and exit planes of each blade row), pressure ratio across each blade row, stage efficiency, and blade metal angles for each blade row, the code determines the relative and the absolute flow angles, the incidence and the deviation angles and the design point equivalent diffusion ratio. For a multistage machine, overall performance parameters are established by extending a blade row-by-blade row single stage calculation utilizing a "stage stacking" procedure.

(ii) Off-design point calculation for operation with air-flow: Given values of operating speed and flow coefficient, the code calculates all of the flow velocities and angles, pressure ratio, and efficiency for each blade row based on (a) design point data and (b) certain rules regarding deviation, diffusion factor and momentum thickness of boundary layer over the blade (Reference 23). Again, "stage stacking" is used for a multistage machine.

(iii) Off design point calculation for operation with air-water droplet mixture: Given values of operating speed, flow coefficient, mass fraction of water, and volumetric mean droplet size in the mixture, the code establishes flow velocities and angles, pressure ratio, efficiency, water mass fraction redistribution, and water droplet size reorganization based on (a) design point data, (b) certain rules regarding deviation, diffusion factor, and momentum thickness of boundary layer over the blade, and (c) various assumptions related to the presence of water in film and droplet form (Reference 20).

In applying the WINCOF code to a fan or a compressor, it is necessary as stated earlier to choose a streamtube along which calculations are to be performed. A streamtube is defined by its location and cross-sectional area. The location may be the hub, the tip or another spanwise section. The cross-sectional area may be chosen based on design point data pertaining to mass flow and axial flow velocity. However, a blade is designed to yield specific aerodynamic performance at each spanwise section through a choice of blade metal angles, incidence and deviation. Furthermore a compressor stage consists usually of at least two blade rows. Some trial and error may become necessary in choosing location and cross-sectional area along the stage in a piecewise continuous fashion such that they are compatible with, for example, the design point performance for given design point air flow angles and rotational speed.

In general, it can be expected that one blade row differs from another and thus one stage from another. The two major parameters of interest in the application of the WINCOF code for determining the performance under a given set of operational conditions are (i) aerodynamic design of blading and (ii) operating rotational and axial flow velocities. The latter also determine the duration of time available for centrifugal action and heat and mass transfer processes.

Regarding the aerodynamic performance of blading, the WINCOF code incorporates a simple procedure for choosing rules for deviation and losses that are appropriate for a given compressor. A brief description follows.

The model used to estimate the blade outlet flow angle and the loss due to turbulent flow of gaseous phase over the rigid blade surface incorporates the concept of equivalent diffusion ration (Reference 24). The equivalent diffusion ratio is dependent upon the ratio of the maximum suction surface velocity and the trailing edge velocity. This parameter is defined as follows (15):

$$D_{eq} = \frac{\cos\beta_2 V_{Z1}}{\cos\beta_1 V_{Z2}} \left\{ 1.12 + 0.0117(i - i^*)^{1.43} + 0.61 \frac{\cos^2\beta_1}{\sigma} \cdot K \right\} \cdot AK3 \qquad (1)$$

where

$$k = \tan\beta_1 - \frac{r_2}{r_1} \frac{V_{Z2}}{V_{Z1}} \cdot \tan\beta_2 - \frac{\omega r_1}{V_{Z1}} \left(1 - \frac{r_2^2}{r_1^2} \right),$$

β = flow angle, V_Z = axial velocity, i = incidence angle, σ = solidity, r = streamline

radius, and ω = rotor rotational speed. The subscripts 1 and 2 refer to the blade row inlet and outlet, respectively. The asterisk superscript refers to the design point case. The design point equivalent diffusion ratio, D^*_{eq}, is found using this expression with the incidence angle term set equal to zero. In order to obtain the blade row outlet axial velocity and flow angle, an iteration scheme is employed to arrive at the correct value of axial velocity, but the flow angle, β_2, is assumed to be the outlet angle of the blade. A value for the equivalent diffusion ratio is then calculated using Equation 1. The deviation angle, δ, may be calculated using the following empirical expression:

$$\delta = \delta^* + 6.40 - 9.45(M_1 - 0.60)(D_{eq} - D^*_{eq}) \text{ x AK1} \quad , \qquad (2)$$

where M_1 = inlet Mach number. A value for the outlet flow angle is then calculated by adding the deviation angle to the blade outlet angle and a final value for the outlet flow angle obtained by iteration. The iteration procedure involves the determination of density at blade outlet. In order to determine density, the pressure rise across the blade row, if any, and the pressure loss must both be established. The total pressure rise is a function of axial and rotational velocities and the inlet and outlet flow angles.

The total pressure loss coefficient is dependent upon the non-dimensional wake momentum thickness, which is calculated using the following empirical expressions:

$$(\Theta/c) = (\Theta/c)^* + (0.827M_1 - 2.692M_{12} - 2.675M_{13})(D_{eq} - D^*_{eq})^2 \text{ x AK2}$$

for $D_{eq} > D^*_{eq}$; and

$$(\Theta/c) = (\Theta/c)^* + (2.89M_1 - 8.71M_{12} + 9.36M_{13})(Deq - D^*_{eq})^2 \text{ x AK2}$$

for $D_{eq} < D^*_{eq}$. (3)

The total pressure loss coefficient may then be calculated using the following expression:

$$\bar{\omega} = (\Theta/c) \cdot \frac{2\sigma}{\cos\beta_2} \left[\frac{\cos\beta_1}{\cos\beta_2}\right]^2 \qquad (4)$$

This procedure is employed in each cycle of the iteration scheme for the blade outlet axial velocity.

Now, the empirical expressions presented above apply to the class of blades for which the correlations were originally performed (Reference 24). They may not apply to other blades. Even in the general class of blades for which the correlations may apply, there may be need for modifying the rules for various types of blades. It is for permitting such modifications that in equations (1), (2), and (3), three parameters, AK1, AK2, and AK3, have been introduced. These may be adjusted for a given blade to alter deviation angle, pressure less coefficient, and equivalent diffusion ratio, respectively, both individually and relative to one another. Changes in the values of

the constants modify the predicted performance for a compressor blade row or stage substantially. Accordingly, given, for example, details of velocities and flow angles and of work done and efficiency at design for a specific compressor stage, the values of constants can be determined through trial and error such that the predictions of the WINCOF code match the given performance. It may be pointed out that (a) the overall performance of a compressor is extremely sensitive to the choice of the values for the constants and (b) the trial and error procedure is not computationally simple. Furthermore, it is possible that in certain cases, there may be more than one set of constants that can yield the same overall performance. However, it is assumed that the values of the constants once determined for a compressor provide the deviation and the equivalent diffusion rules that are specific to the compressor under consideration and may be so utilized in all of the predictions, including those under off-design conditions.

3.2. Modifications to the WINCOF Code to Obtain Compressor Performance Maps Suitable for Use in an Engine Simulation

In order to simulate the operation of the high bypass ratio turbofan engine, data which define many operating points must be known for each component under various ambient conditions. Typically, for a computer-based engine simulation, these data are stored in tabular form. Engine performance is established for given operating conditions by reference to tabulated data of performance of each engine component or subsystem. The simulation program continues to search component tables until a "performance-match" point for all components is found. If the operation of a component or subsystem in the engine is changed such that performance data stored for the component no are no longer valid, then the stored data table must be replaced by an approximately corrected data table. In the problem under investigation, the performance of the compression subsystem is altered by the effects of water ingestion. The WINCOF code was utilized to generate the corrected performance data.

Traditionally, the performance of a compressor has been represented by plots of overall pressure ratio and adiabatic efficiency as functions of inlet mass flow rate for a range of rotor rotational speeds. These performance data plots are called compressor maps. Typically, a limited number of curves of constant corrected rotational speed are plotted for corrected mass flow rate ranging from a high flow condition to the surging condition flow or a slightly lower value of flow for each speed.

It is well known that relations among the quantities on a compressor map are highly nonlinear and that no useful similarity relations can be found with respect to operating speed or mass flow-rate, regardless of the nature of the working fluid. Thus, compressor maps may have to be stored as discrete data points in an engine simulation program. In general, the operating point required by the simulation program many not be one of the stored data points so that interpolation between stored data points becomes required. Because of the highly nonlinear nature of the compressor performance curves, a large number of data points must be stored in such a procedure to achieve sufficient accuracy when interpolation is employed. Unfortunately, storing large amounts of data for the compression subsystem as well as for other components in an engine simulation results in a large, inefficient program. It

is for this reason that new types of compressor map representation have been developed.

One approach to compressor map representations is to base the maps on the use of similarity parameters derived from further consideration of the basic physics of the component performance (Reference 25). This approach has been used for this investigation. In order to define performance, (i) flow coefficient, (ii) work coefficient, and (iii) loss along the minimum-loss curve, known as the "backbone" of the map, must be specified; as well as variations of (iv) loss and (v) flow rate along the speed lines. These five curves together contain the same information as traditional maps. At the same time, they are approximately piecewise linear so that fewer data point are required to achieve the same accuracy when interpolation is necessary.

The five curves can be broken into two groups: (i) efficiency representation and (ii) flow representation. Rather than using efficiency directly, loss and work coefficient and their variation with respect to the minimum loss point values are used for efficiency representation. The definitions of work coefficient, pressure coefficient, flow coefficient, and loss are illustrated in Figure 2. The characteristics of loss versus flow or work coefficient curves that make loss a good basis for a map fitting procedure are that the loss is always positive and finite and it exhibits a definite minimum value. The WINCOF code has been modified to calculate the loss and the work coefficient. In order to determine the minimum-loss values at each speed the compressor performance is calculated at each speed over a range of mass flow rates (specified by inputting a set of compressor inlet flow coefficients). Although performance calculations are performed for each stage, it is sufficient in calculations of overall engine performance through simulation to obtain the loss as an overall loss for an entire machine or any section of it such as fan, LPC, or HPC. Corresponding to each loss value, there is a work coefficient, which may also be obtained as an overall value for a machine or section thereof. After the calculations have been performed for the desired range of flow coefficient at a given speed, the minimum-loss value and, hence, the corresponding minimum-loss work coefficient and minimum-loss flow coefficient for the given speed are found.

After the minimum-loss point (minimum loss, minimum-loss work coefficient, and minimum-loss flow coefficient) has been found at each speed in a desired range, the minimum-loss and minimum-loss work coefficient are plotted as a function of rotational speed. These two curves are called "backbone" curves. The "off-backbone" loss is then represented by a plot of the difference between loss at a value of speed and flow coefficient and the minimum loss value at that speed versus the square of the difference between the work coefficient and the minimum loss work coefficient. The sign of the work coefficient difference is retained and is used in plotting the two branches of the bi-variate loss representation. Plots of this loss correlation are fairly linear over a wide range of work coefficient. Breaks often occur near points of positive stall and choking. These three curves, shown schematically in Figure 3, complete the efficiency representation. Because the curves are fairly linear, fewer points are needed for accurate tabular representation in an engine simulation than for traditional maps.

The flow representation consists of two curves. The first curve defines the mass flow for operation on the "backbone" of the map and is a plot of minimum-loss flow

coefficient versus rotational speed. The second is the "off-backbone" flow representation which is obtained based on the following consideration. If it is assumed that the Mach number is unity at some point in the gas path of the machine when it is operating at the choking or the maximum mass flow rate condition, then a critical flow area can be calculated. Furthermore, if this flow area is assumed to be constant over the entire range of operation at a given rotational speed, then all mass flow rates at that speed can be expressed relative to the choking mass flow rate using a pseudo-Mach number defined as follows:

$$\frac{\dot{m}_{corr}}{\dot{m}_{corr,max}} = \frac{M}{\left(1 + \left(\frac{\gamma - 1}{2}\right) M^2\right)^{\frac{\gamma+1}{2(\gamma-1)}}} \left(\frac{\gamma + 1}{2}\right)^{\frac{\gamma+1}{2(\gamma-1)}} \qquad (5)$$

This pseudo-Mach number is plotted as a function of the difference between the work coefficient and the minimum-loss work coefficient for each speed and the set of these curves is referred to as the off-backbone flow representation These curves along with the "flow-backbone" curve define the mass flow. Again, the curves are fairly linear or piecewise linear so that a "table look-up" can be set up in an engine simulation code that will yield good accuracy with a relatively small number of entries. It is often found that the solution becomes unstable at Mach numbers close to unity. Thus, the calculations for choking mass flow rate could not be carried out in the case of the selected generic engine. However, since the mass flow rate which results in a choking condition serves merely as the reference value for all other mass flow rates, the maximum mass flow rate for which WINCOF calculations may be carried out in practice in any given case can be used as an appropriate reference flow. It is also noted that the ratio of corrected mass flow rate to maximum corrected mass flow rate in Equation 5 is equivalent to the ratio of flow coefficient to maximum flow coefficient. The locus of values of pseudo-Mach number as a function of the difference between work coefficient and minimum-loss work coefficient for each speed is determined by solving Equation 5 for M for the range of values of flow coefficient desired.

3.3. Generating the Performance Maps for the Compression Subsystem with Water Ingestion

In conducting engine simulation with the compressor performance modified for effects of water ingestion, several other considerations become necessary. Figure 4 shows the streamtubes of interest in a typical high bypass ratio compressor. In general, the performance of a compressor is different for different radial positions across the gas path. That is, the work coefficient and loss and the mass flow rate per unit area vary in the radial direction at the exit of the compressor or section of the compressor. With water ingestion, these radial differences in compressor performance can become even more pronounced. During operation with air, acceptable representation of the overall performance values can probably be made by performing calculations along streamline 2 for the bypass stream and streamline 5 for the core stream (Figure 4).

During water ingestion, two processes which must be taken into account in turbomachinery are (i) centrifugal action on droplets and (ii) interphase heat and mass transfer. These processes cause continuous and substantial changes in the air-liquid water mixture ratio along a streamtube, which in turn causes changes in the local aerodynamic performance along a streamtube. Water will tend to become depleted along streamtubes 1 and 4. These changes in the state of the working fluid when combined with the changes caused by aerodynamic effects and heat and mass transfer can in most cases be expected to give rise to nonlinear changes in performance between the hub and the tip sections The result is that streamtubes such as 2 and 5 may no longer be adequately representative, mean streamtubes for the bypass and the core flows.

Considering the core and the bypass streams, there is no simple way of assigning a mean performance for either. Carrying out performance calculations for an infinitely large number of streamtubes and averaging the resulting values is unacceptable. However, simple averaging of performance obtained for a limited number of streamtubes will in general not yield a meaningful mean performance. A fully three-dimensional analysis of the compressor performance may provide a basis for establishing the overall performance. Such an analysis is beyond the scope of this investigation. It appears that in the current state of knowledge, it is only possible to consider certain streamlines as being representative of certain flows. On that basis it is assumed that streamtubes 2 and 5 are representative of the bypass stream and the core stream, respectively. It is clear that the performance of the fan, the LPC and the HPC are different and may be critical along streamtubes 1 and 4 during operation with water ingestion. However, for this investigation it is assumed that the fan and the compressor tip effects may be considered separately from the determination of engine system performance changes.

The streamtubes 2 and 5 were established by connecting the locus of points which divide the flow in the bypass and the core streams, respectively, in half during operation at the design point. The location of each of these streamtubes has been assumed to remain unchanged for all other operating conditions also. In general, the radial position of the streamline that divides the bypass or the core stream into two equal parts will change with speed and mass flow rate, but the change is assumed to be small enough so that the streamtubes chosen remain equally representative of the mean compressor performance for all operating conditions Furthermore, the bypass ratio also changes with operating conditions. Again, for this investigation the bypass ratio has been assumed to remain constant under various operating conditions.

In this investigation the steady state performance of each section of the compressor subsystem (fan bypass, booster, and core compressor) has been obtained separately over appropriate ranges of mass flow rate and rotational speed. The results of these calculations are three sets of steady state compressor performance maps.

In the generic high bypass ratio turbofan engine (Figure 1) the compression subsystem has provision for bleeds (both between stages and between sections, (LPC and HPC), and also for variable stator blade stagger angle settings. The engine control system meters the bleed flow and changes the stator vane stagger setting.

The compression subsystem performance has been calculated by making certain assumptions about the changes that are expected to be made by the control system. Firstly, in regard to variable stator blade stagger angles, it has been assumed that the setting schedule is "fixed". That is, the stagger setting is related to a single engine operating parameter namely the rotational speed. The performance maps for the compression subsystem at various rotational speeds have been established using the "fixed" schedule. Secondly, in regard to bleed flows, they fall into two categories. The first category includes interstage bleeds the discharge from which does not reenter the engine flow. For this investigation since the engine has been considered as operating on a test stand, it is assumed that all interstage bleed valves remain closed. The second type of bleed flow is that which passes through a variable area door from the core stream just aft of the supercharger to the bypass stream just forward of the bypass nozzle. It has been assumed that the performance of that bleed valve remains the same in the case of two-phase flow as in the case of air flow. However, the operation of the bleed valve during air-water mixture flow may become altered by the input of modified values of temperature, pressure, and speed to the controller. Thirdly, regarding the nature of the air-water mixture entering the bleed valve, it may be observed that in the fan core stream and the low pressure compressor some of the liquid water is centrifuged. Thus, at the exit of the supercharger, there is a higher mass fraction of water in the tip region or at the core engine casing. Since the variable bleed valve door is located at the core compressor outer casing there is some ambiguity about the state and composition of the air-water mixture that can be expected to pass through the bleed valve door. In that connection, it is assumed that the mass fraction of water in the bleed flow mixture is the same as the local mass fraction of water in streamtube 5. Fourthly and finally, it is assumed that in the swan neck-shaped duct between the supercharger discharge and the core compressor inlet, liquid water which accumulates in the blade tip region and vapor which accumulates in the hub region in the supercharger is redistributed across the entire cross section; in other words, that a homogeneous air-water vapor-liquid water mixture enters the core compressor.

3.4. Procedure for the Use of the WINCOF Code

It may be pointed out that in the case of the generic engine, it is assumed a priori that only design point data are made available. It is necessary therefore to obtain details of (a) location and flow area of streamtubes 5 and 2 and (b) deviation, momentum thickness, and equivalent diffusion ratio corresponding to the design point and then utilize such data for undertaking off-design calculations with air-water droplet mixture flow. In other words the location and the flow area of streamtubes are treated as fixed in all of the subsequent calculations performed with air-water mixture. It may be recalled that the WINCOF code incorporates a stage-stacking procedure in obtaining the performance of a multistage machine.

The procedure for performance prediction consists of four major parts: (i) applying two-phase flow related assumptions to the WINCOF code and creating necessary input data set for the code; (ii) exercising the WINCOF code to obtain design point/reference values of data needed for subsequent design point calculations including streamtube area, equivalent diffusion ratio, incidence angle, deviation angle,

and momentum thickness for each blade row; (iii) adjusting coefficients AK1, AK2, and AK3 in the aerodynamic rules to obtain an accurate prediction of the design point performance of the compression subsystem, and (iv) exercising the WINCOF code for obtaining off-design performance over appropriate ranges of mass flow rate, speed, and water mass fraction. The procedure is repeated for each section of the compression subsystem.

The first part of the procedure requires that physical data describing the mechanical elements of the compression subsystem and performance data specifying the design operating point of the subsystem be available. The blade metal angles, stagger settings, stator outlet flow angles, blade chords, blade hub and tip radii, design point rotational speed, design point stage pressure ratios and efficiencies, and ambient conditions at design are needed for each section of the subsystem. Details regarding these data for the compression subsystem of the chosen generic engine are included in the Appendix.

In part two of the procedure, the WINCOF code was run with the design point operating parameters and physical dimensions of each compressor section as input. In order to duplicate the exact design point performance for each section some additional information was needed, namely: (i) the axial velocity at rotor inlet, rotor outlet, and stator outlet of each stage and (ii) absolute flow angle at rotor inlet and rotor outlet of each stage. With this information, the absolute velocity was calculated at each station, namely rotor inlet, rotor outlet, and stator outlet. Stagnation temperature and pressure were calculated at the rotor inlet, rotor outlet, and stator outlet of each stage using the design point rotor and stage pressure ratios and stage efficiency. Using those values and the absolute velocity, the static temperature and pressure, and hence density were calculated at each station. Finally, using Equations (1) and (4) from Section 3.1, the design point/reference values of the non-dimensional wake momentum thickness and the equivalent diffusion ratio were calculated for each blade row.

Part three of the procedure consists in carrying out a performance calculation utilizing Equations (1), (2), and (3) at the design point operating conditions and flow coefficient as input and comparing the resulting predicted performance with the given design point performance. In general, and as was observed in the case of the given compression subsystem, such a comparison may reveal a need to adjust the parameters AK1, AK2, and AK3 in Equations (2), (3), and (1), respectively, to obtain performance predictions that match given design point data for each section of the compression subsystem. In the WINCOF calculation scheme, the stator outlet deviation determines the net stage rotor inlet incidence. Thus by lowering coefficient AK1 in Equation (2), the incidence and deviation angles for each blade row can be lowered, thereby reducing the work input and the resulting pressure ratio for each stage. The efficiency can be raised by reducing parameter AK2 in the non-dimensional wake momentum thickness rule (Equation 2). Using a trial and error procedure with the above trends taken into consideration, a set of values for the three parameters which resulted in an accurate prediction of the design point performance was found for each section of the compression subsystem. It may be noted that the values of the three parameters were held constant for all subsequent (off-design) calculations.

The final step was then to exercise the WINCOF code over a range of speeds. The range of mass flow rates utilized at each speed was chosen so that a sufficient number of calculation points were obtained on either side of the minimum-loss point. Carrying out the calculations for the above range of speeds and mass flow rates for one section of the compression subsystem yields a performance map for that section which is specific to the working fluid properties existing at the section inlet. These properties include composition, temperature, and pressure. The final mapping step was repeated for each compressor section for (i) standard temperature and pressure and discrete values of inlet liquid mass fractions of zero, one, two, four, and eight per cent and (ii) a so-called "hot day" temperature and standard pressure and water mass fractions of zero and four per cent.

CHAPTER IV

ENGINE SIMULATION WITH WATER INGESTION

The generic engine for which the investigation of time-dependent changes in performance with water ingestion has been conducted can be described as a two spool, high bypass ratio turbofan with a bypass ratio of about 1.5. The core stream and the bypass stream exhaust through separate thrustor nozzles. The engine is typical of those used in large commercial and military aircraft.

The control is assumed to be designed to control fuel flow and variable stator vane position. It is basically a speed governor which senses engine rotational speed and adjusts the fuel flow as necessary to maintain the desired speed as set by the power lever. The control system for both engine speed and variable stator vane setting is an analog, electro-mechanical system.

The control system incorporates a fuel flow schedule as a function of engine speed, which is then corrected with respect to various other performance parameters under existing operating conditions. In order for the control to follow the resulting schedules, the required parameters, namely, compressor discharge pressure, compressor inlet temperature and engine speed, must be accurately sensed. The controller acquires the parameters through various sensors and then amplifies the signal, computes the fuel flow acceleration and deceleration limits, and imposes the limits. The fuel flow is regulated by regulating fuel pressure. Part of the actuation mechanism may consist of a three dimensional cam. Moving the power lever then rotates the cam to set the basic fuel flow schedule required for the chosen power setting. The cam moves laterally according to the operating conditions and thus imposes appropriate limits on the base schedule.

The variable stator vanes are controlled separately from the engine speed. The actuation may be hydraulic with engine fuel as the medium. The hydraulic signal is determined utilizing two of the sensed parameters, namely compressor inlet temperature and engine speed.

4.1. Description of Engine Simulation Code

The engine simulation program (Reference 21) used in this investigation is designed to operate as a free standing program or as a subroutine in an aircraft simulation program. The program contains performance maps for each of the components in the engine system, logic which models the control system including prescribed control schedules, and logic which makes certain that the components are matched at the operating point calculated. For each component in the engine there is a subroutine. The subroutines are arranged in the order in which the components appear along the gas path. They contain the logic required to extract data from the performance maps based on the initial and operating conditions chosen for each component at the design point. However, the initial and operating conditions for any component can be expected to vary depending upon the operating conditions of the engine. Corrections are applied to the base values of performance data stored in the component maps. These corrections, which are in the form of scalars and adders, can be considered

analogous to control system functions in an actual engine.

The program contains provisions for specifying the following: (i) control system logic options, (ii) fixed flight/ambient conditions and (iii) time dependent quantities which prescribe the simulation case to be run. The control system logic options include some that are of importance to the investigation. In the compressor analysis since no interstage customer bleed flows are considered, options for turning off such bleeds in the engine simulation are used. Another option used is the idle selection switch. This sets a minimum limit on the desired core engine speed regardless of how low the power lever angle is set. The fixed flight/ambient conditions include temperature, pressure, geopotential pressure altitude, and absolute humidity. The temperature and pressure are input as increments added to the U.S. Standard Atmosphere, 1962 (Reference 26). The temperature and pressure increments may also be given as a function of time. The inputs which specify a simulation case are functions of time. Piecewise linear functions are established by giving the value of a variable at the beginning and end of any specified time period. The value of the variable at times which fall between the end points of the specified time period are found by linear interpolation. The time dependent parameters available for specifying a case are flight Mach number, geopotential pressure altitude, and power lever angle.

The outputs available in the engine simulation program include overall engine performance parameters such as thrust, engine pressure ratio, specific fuel consumption, total fuel flow rate, total inlet air mass flow rate, core speed, supercharger speed, etc. Also, fluid properties are available at various stations in the core and the bypass streams.

The engine simulation program also provides diagnostic output of two types in the form of numerical status indicators (N.S.I.'s) pertaining to: (i) engine performance and (ii) computer system or program status. The engine performance N.S.I.'s are printed when a specified engine performance limit is reached. The engine performance N.S.I.'s correspond to various physical limits on operating parameters of each component. During simulation program execution, if the value of an operating parameter exceeds a preset physical limit, an engine performance N.S.I. is printed and the calculations continue with the value of the operating parameter set equal to its physical limit. The engine performance N.S.I.'s are useful in analyzing results of simulation cases. Some examples of these are "fuel flow exceeds pump limit," "low pressure turbine inlet temperature exceeds maximum allowable," "physical or corrected core speed exceeds maximum allowable," etc.

System N.S.I.'s indicate fatal errors, that is, those which cause program execution to stop. Typical system N.S.I.'s give the name of a component subroutine in which the calculation pro- fails to converge to a stable value, or they may tell the user that the maximum number of interactions selected originally is exceeded before convergence. System N.S.I.'s also indicate when part of the input data is out of the allowable range or is incorrectly given.

4.2. Incorporating Water Ingestion into an Engine Simulation Code

As stated earlier, in the component subroutines the base values of performance parameters are retrieved from the stored component maps and the base values are modified according to control system specifications and specific operating conditions. The effects of water ingestion on the compression subsystem performance and subsequent overall engine performance are incorporated into the simulation code in a manner which follows logically from the original program structure.

The WINCOF code was used to obtain the performance maps (in the form of the five linearized curves giving flow and efficiency representation) for the fan bypass stream, the supercharger section stream, and the core compressor stream individually for a series of values of inlet liquid water mass fraction with other operating conditions held constant. For each point stored in the base maps a corresponding correction value was stored in another table, the correction representing the deviation in the value of the performance parameter during water ingestion from the base value for dry air operation. The correction values actually vary for different sets of inlet conditions including temperature, pressure, humidity, and mass fraction of water in the mixture entering the engine. The basic engine simulation program can provide engine performance for any given set of the ambient conditions. However, the interphase heat and mass transfer processes, that occur in the compression subsystem, are greatly affected by the ambient temperature. These processes in turn have a significant effect on the overall compression subsystem performance and hence on the engine. An unreasonable approach to the problem would be to store correction maps for an infinite set combinations of inlet conditions. Furthermore, there is no simple method for modifying the values obtained for a few sets of inlet conditions such that they are valid for all cases. Accordingly, performance calculations have been carried out at two selected values of temperature, namely (i) standard day, 518.7R, and (ii) hot day, 589.7R. The inlet air is assumed to be saturated with water vapor when either temperature is used. In this investigation the ambient pressure has been held constant at standard value of pressure. Four inlet mass fractions of water, X_w, equal to one, two, four, and eight per cent, were considered. The performance map correction tables were established for each of the inlet water mass fractions for the standard day temperature and, as a representative case, for a water mass fraction of four per cent for the hot day temperature. In view of changes in water concentration along the gas path that occur under any engine operating condition, necessary logic has been added to the engine simulation program for utilizing at any desired location the correction tables corresponding to one of the integral values of water mass fraction nearest to the actual value of water concentration.

In the current investigation, the emphasis is, as stated in Chapter II, on the determination of engine performance changes due, solely, to modification in the performance of the air compressor subsystem with air-water mixture flow. The effects of air-water mixture flow on the performance of the other engine components are not considered. In that context, two limiting cases have been selected in order to isolate and to explain the effects of compression subsystem changes on engine overall performance. The cases are as follows: (i) all liquid water is removed before the

mixture enters the burner and (ii) all or some of the water entering the burner undergoes flash-evaporation at some location in the burner. In both cases all of the water is assumed to be removed from the bypass stream before the mixture enters the bypass stream nozzle. Thus, in both cases all of the "hot" components and the two thrustor nozzles are expected to operate with gaseous working fluid except for the fuel and water entering the burner. The second case has been further specialized to examine two possibilities of burner location where flash-evaporation may occur. The evaporation is assumed to occur at either the burner entry or the burner exit. The enthalpy, temperature, and composition of the gaseous phase are adjusted at the station at which the evaporation is assumed to take place. The mass fraction of liquid assumed to evaporate is added to the local water vapor mass fraction. The enthalpy of the gaseous phase is reduced by an amount equal to the product of the mass rate of vaporization and the latent heat of vaporization at the local pressure.

4.3. Procedure for the Use of the Engine Simulation Code

The procedure for using the engine simulation code is given for two cases of simulation of engine operation during water ingestion with standard control: (i) operation with standard and high ambient temperature values and (ii) operation with an error in the high pressure compressor inlet temperature value which is an input to the control system.

4.3.1. Simulation Procedure for Water Ingestion During Standard and Hot Day Conditions

Subroutines were added to correct the three compression subsystem section performance maps in order to take into account water ingestion effects. These subroutines are organized such that there is a complete set of water ingestion performance data, corresponding to the original performance map data, for each temperature and mass fraction of water considered. These water ingestion data are in the form of additive corrections to be applied to the compressor performance map data that are retrieved by the engine simulation subroutines. The water ingestion performance data are specific for each ambient temperature considered (standard day, 518.7R, and hot day, 589.7R) and water mass fraction (zero, one, two, four, and eight per cent).

Modifications to the subroutines were necessary to account for the draining and evaporating of the water as specified in the input data. In the bypass stream, the subroutine which models the fan discharge was modified to account for the reduction in mixture mass flow rate when liquid is drained off. The subroutine modeling the high pressure compressor discharge was modified in a similar fashion. The burner subroutine was modified to calculate the enthalpy change of the gaseous mixture working fluid due to evaporation of water at the entry or the outlet sections of the burner.

The modified engine simulation code is exercised exactly as the original code is, except for the requirement that additional input must be supplied to specify initial conditions of the water ingestion case.

4.3.2. Simulation of an Engine with Control Input Error

It has been stated in Reference (14) that the observed anomalous performance during water ingestion tests could be traced to the error in the output of a thermocouple located on the casing wall at the entry to the high pressure compressor and providing an input to the engine control. The thermocouple which may have become immersed in the water centrifuged to the casing wall could have sensed and transmitted the water temperature rather than the local gas temperature. When fairings were placed around the thermocouple, the engine performance became closer to that expected under the given operating conditions. It was concluded that the fairing employed helped to prevent the thermocouple from becoming submerged in water, and therefore, the thermocouple could transmit the local gas phase temperature to the control system.

Considering those observations, a test case was chosen for simulation in which it was postulated that there occurred an error in the output of the thermocouple that sensed the temperature, T_{25}, at entry to the core compressor. In the generic engine that temperature is an input to the control system. The control system regulates the position of the variable bleed valve and also the stator stagger angles. Those features have been included in the engine simulation code wherein the base values of the variable bleed valve area schedules and the stator stagger angles are stored in the form of maps. In order to analyze the test case with an error in the thermocouple sensing the temperature. T_{25}, it is therefore necessary to set up procedures for varying the schedules for the variable bleed valve and the stator stagger angles.

For the variable bleed valve area the change corresponding to the temperature error is applied quite simply. The corrected speed and the compressor inlet temperature itself are parameters in the variable bleed valve map. The corrected speed is recalculated using the sensed temperature. Necessary additions were made to the simulation code for utilizing this value along with the sensed temperature itself in order to obtain the variable bleed valve area from the stored maps.

The method of accounting for the relationship between temperature, T_{25}, and stagger setting of the stators in the engine simulation code is more complicated. The performance of the core compressor depends on (a) the conditions at entry to it, (b) the true corrected speed, and (c) the corrected speed corresponding to the incorrectly sensed temperature. The latter determines the stator stagger angle setting and hence the aerodynamic performance. The compressor is operating at the true corrected speed but with stagger setting corresponding in the erroneous temperature-based corrected speed. The procedure for calculating the performance, utilizing the compressor performance maps, for any given value of temperature error is then as follows.

Now, in the actual engine, adjustments are made to the stator setting as a function of the sensed value of T_{25} through the action of the control.

In the engine simulation code, there is a fixed (meaning, function of speed only) stator setting schedule. The stator schedule is stored as a function of corrected speed corresponding to a reference T_{25}. The effect of stator setting adjustments on

compressor performance maps is provided in the form of corrections represented by functional relationships.

In a given case of error in T_{25}, then, the stator setting value is obtained corresponding to the true corrected speed as well as the corrected speed with respect to the sensed (erroneous) temperature. The difference between the two stator setting values is utilized in the functional relationships to obtain the adjustment to the compressor performance. The adjustment is in the form of scalars to be applied to the performance maps corresponding to the true corrected speed.

The procedure thus involves applying a correction for the error in T_{25} with reference to the compressor performance that should have been obtained at the true value of T_{25} and the rotational speed of the compressor.

The procedure described in the preceding discussion applies both to the case of operation with air flow and to that with air-water mixture flow.

CHAPTER V

RESULTS

The results of the performance prediction calculations are divided into two groups: (i) those pertaining to the air compression subsystem and (ii) those pertaining to the engine system. Both sets of results apply to the generic engine with its standard control system. The cases for which the compression subsystem performance has been obtained and the test cases carried out utilizing the engine simulation code are outlined in the first section. The results of the compression subsystem performance calculations are presented next. Finally the engine simulation results are discussed.

5.1. Test Cases

Complete performance maps for each of the three sections of the compression subsystem are necessary corresponding to operation during water ingestion with each inlet mass fraction of water and each ambient temperature selected. The performance maps have been obtained for the following cases: (i) compressor operation at standard ambient temperature with water ingestion inlet mass fractions of one, two, four, and eight per cent and (ii) compressor operation at hot day ambient temperature with a water ingestion inlet mass fraction of four per cent.

With the compression subsystem performance data, corresponding to operation with various water ingestion cases stored in the engine simulation code, the code can be exercised for a variety of cases. The results of each test case are plots of various quantities describing engine performance as a function of time. These data are divided into three groups and plotted on three separate sets of axes. The three groups are as follows:

(i) Core rotor corrected speed as a percentage of design point core rotor corrected speed, PCN25R; or $\%N_{2c}$; booster rotor corrected speed as a percentage of design point booster rotor corrected speed, PCN12R; or $\%N_{1c}$; fan pressure ratio, P13Q12; or FAN P.R; and booster pressure ratio, P23Q2 or BOOSTER P.R.

(ii) High pressure compressor pressure ratio P3Q25; or HPC P.R; booster inlet corrected working fluid mass flow rate in pounds per second, W2R; or $\dot{m}_{2c}$ and high pressure compressor inlet corrected working fluid mass flow rate in pounds per second, W25R or $\dot{m}_{25c}$.

(iii) Flow rate of fuel in pounds per hour, WFE; or $\dot{m}_f$; specific fuel consumption in pounds per hour of fuel per pound of thrust, SFC; and gross thrust in pounds, FG or THRUST.

The test cases run include the following types:

(i) Acceleration from ground idle power setting to maximum power setting with the power lever change occurring over a

one-second period, ACCEL.

(ii) Deceleration from maximum power setting to ground idle setting with the power lever change occurring over a one-second period, DECEL.

The cases are further distinguished by the mass fraction of water ingested, the ambient temperature and the method of handling the water after compression. When the case is based on assuming an ambient temperature of 130 F, the case is designated HOT DAY. When all of the liquid is assumed to be drained from the core stream and the bypass stream after compression the case is designated DRAINED. When all of the water in the core stream is assumed to be evaporated at the burner entry the case is designated EVAPORATED. Other cases not involving complete evaporation are described according to the location and mass fraction of evaporation, for example, "two per cent ingested; one per cent evaporated at burner entry." Finally, there are cases in which a temperature sensing error of either 10 F or 40 F is simulated; these are designated by either 10 F TEMPERATURE ERROR or 40 F TEMPERATURE ERROR.

The following is a list of engine simulation cases presented in this Report. All of the cases pertain to static operation on ground.

1) DRY, ACCEL;
2) 1% INGESTED, DRAINED, ACCEL;
3) 2% INGESTED, DRAINED, ACCEL;
4) 4% INGESTED, DRAINED, ACCEL;
5) 1% INGESTED, EVAPORATED, ACCEL;
6) 2% INGESTED, EVAPORATED, ACCEL;
7) 4% INGESTED, EVAPORATED, ACCEL;
8) DRY DECEL;
9) 1% INGESTED, DRAINED, DECEL;
10) 2% INGESTED, DRAINED, DECEL;
11) 4% INGESTED, DRAINED, DECEL;
12) 2% INGESTED, 1% EVAPORATED AT BURNER ENTRY, ACCEL;
13) 2% INGESTED, 1/2% EVAPORATED AT BURNER ENTRY, ACCEL;
14) 2% INGESTED, 1% EVAPORATED AT BURNER EXIT, ACCEL;
15) 2% INGESTED, 1/2% EVAPORATED AT BURNER EXIT, ACCEL;

16) HOT DAY, DRY, ACCEL;

17) HOT DAY, 4% INGESTED, DRAINED, ACCEL;

18) HOT DAY, 4% INGESTED, 1% EVAPORATED AT BURNER ENTRY, ACCEL;

19) HOT DAY, 4% INGESTED, 1/2% EVAPORATED AT BURNER ENTRY, ACCEL;

20) HOT DAY, 4% INGESTED, 1% EVAPORATED AT BURNER EXIT, ACCEL;

21) HOT DAY, 4% INGESTED, 1/2% EVAPORATED AT BURNER EXIT, ACCEL;

22) 10 F TEMPERATURE ERROR, DRY, MAX POWER;

23) 40 F TEMPERATURE ERROR, DRY, MAX POWER;

24) 10 F TEMPERATURE ERROR, 2% INGESTED, DRAINED, MAX POWER;

25) 40 F TEMPERATURE ERROR, 2% INGESTED, DRAINED, MAX POWER;

26) 20 F TEMPERATURE ERROR, DRY ACCEL;

27) 10 F TEMPERATURE ERROR, 2% INGESTED, DRAINED, ACCEL;

28) 40 F TEMPERATURE ERROR, DRY ACCEL; AND

29) 40 F TEMPERATURE ERROR, 2% INGESTED, DRAINED, ACCEL.

It will be observed in the foregoing list of test cases that no mention has been made of the predictions carried out for the case of eight per cent water ingestion. It was found that, with eight per cent water ingestion, even in the most favorable case of all of the water being drained at the end of compression (both in the bypass and in the core stream, it was not possible with the engine simulation code to obtain acceleration or deceleration of the engine with power lever angle changes carried out over one second. Accordingly, it has been considered not useful to provide details of performance for those cases.

5.2. Performance of the Compression Subsystem Operating at Standard Temperature with Water Ingestion

The WINCOF code has been used to generate performance maps for each of the three compressor sections (fan bypass, booster, and H.P.C.) for operation with water vapor-air-liquid water mixtures. The resulting maps are shown in Figures 5.1 to 7.3.

The high pressure compressor backbone curves (which have been defined in Section 3.2) for three air-water mixture compositions and dry air are given in Figure 5.1. At

low rotational speeds, the difference between operation with dry air and air water mixture in work coefficient and flow coefficient at minimum loss is small. It may be interesting to note that experiments have shown (Reference 27) that water ingestion degrades the performance of an axial flow compressor much more at high flow coefficients and/or speeds than at low flow coefficients and/or speeds. At high rotational speeds, the difference in the same quantities between operation with dry air and air-water mixture becomes noticeable. Both at low and high speeds, there is a significant difference in minimum loss between the same two cases of operation. These observations may be related to the influence of the following: (a) centrifugal action that causes most of streamtube 5 to be depleted of water; (b) blockage due to presence of water and (c) increased aerodynamic losses due to presence of water film on blade surfaces.

Next, considering Figure 5.2 wherein the "off-backbone" performance is shown, it can be seen that the "off-backbone" performance does not vary in a consistent manner for various mass fractions of water in relation to performance with dry air. Similar trends may be observed in some experimental results (Reference 27). These results may be related to the nature and magnitude of various losses assumed to be occurring during water ingestion.

In general, for the high pressure compressor, the effects of water ingestion occur in a nonlinear fashion with respect to mass fraction of water in the inlet flow. That is, the difference between performance parameters predicted for the compressor operating with one per cent mass fraction of water and those for dry air operation is much greater than the difference in performance parameters predicted for the compressor operating with two, four, and also eight per cent mass fraction of water and those for operation with one per cent mass fraction of water. This may be due to the fact that many of the later stages of the compressor are operating with all of the liquid water centrifuged from the stream tube for which calculations are being done. Thus, any differences in calculated overall performance for various mass fractions of water may be due to differences which occur in the first four to six stages in which liquid water is present at the mean streamline.

The predicted booster performance (streamtube 5) is presented in Figures 6.1 to 6.3 and the predicted fan performance (streamtube 2) is presented in Figures 7.1 to 7.3. It can be observed, consistent with the arguments presented in the case of the core compressor, that the effects of mass fraction of liquid in the inlet flow are increasingly greater for the booster and the fan which have fewer stages than the high pressure compressor. In the booster, some of the water is centrifuged but most stages operate with liquid water along streamtube 5. In the fan even less of the water is centrifuged out of streamtube 2.

The "backbone" curves for both the fan and the booster have some characteristics which differ from those of the high pressure compressor "backbone" curves. Comparing the predicted performance given in Figure 5.1 for the core compressor with that given in Figure 6.1 and 7.1 for the booster and the fan, respectively, the following can be observed. For inlet mass fractions of liquid water greater than one per cent, the minimum loss work coefficient is greater than that for dry air at all speeds. Similarly, for water mass fractions greater than one per cent, the minimum loss flow coefficient is

less than that for dry air at all speeds. These are the same as the trends in the high pressure compressor performance. However, for an inlet mass fraction of liquid water of one per cent, at low speeds the minimum-loss work coefficient and minimum-loss flow coefficient are less and greater, respectively, than those for dry air operation.

It is next considered of interest to examine the individual influence of various processes considered with respect to flow of air-water mixture in the compression subsystem. The booster has been chosen for this study. Figure 8 contains the "backbone" curves for the booster operating with dry air and with a water mass fraction of one per cent. For the water ingestion condition, three cases are shown: 1) both heat and mass transfer and centrifugal effects included, 2) centrifugal effects included but heat and mass transfer not included and 3) only heat and mass transfer included. The "backbone" curves for both cases 2 and 3 are closer to curves for dry air operation than the curves for case 1; case 1 includes all of two-phase flow effects treated in the analysis used in the WINCOF code. The removal of centrifugal effects causes the minimum-loss flow coefficient for one per cent water ingestion to be less than that for dry air operation at all speeds. On the other hand, in the absence of centrifugal effects, the minimum-loss coefficient for one per cent ingestion is greater than that for dry air at all speeds. The centrifugal action has a greater effect on compressor performance than do transport processes. Furthermore, the centrifugal effects are independent of water mass fraction since gravitational and droplet-droplet interaction effects are small for the range of mass fractions considered (References 28 and 29).

The foregoing considerations may also explain the fact that the behavior of the fan and booster are similar at low speeds. At higher rotational speeds, more liquid is centrifuged but the booster performance deteriorates with water ingestion in a manner similar to that of the high pressure compressor.

The "off-backbone" performance of both the fan and booster with water ingestion is similar to that for the high pressure compressor in that relative to the "backbone" performance no consistent trends appear with respect to water mass fraction. The "off-backbone" performance of the fan with water ingestion, both the efficiency representation and the flow representation (Figures 7.2 and 7.3), is very close to dry air performance for high and low speeds. The "off-backbone" performance of the booster with water ingestion (Figures 6.2 and 6.3), however, does not resemble the dry air performance.

5.3. Hot Day Compression Subsystem Performance

Figures 9.1 to 11.3 are the so-called "hot day" performance maps for the high pressure compressor, the booster and the fan, calculated for an ambient temperature of 130 F and a water mass fraction of four per cent. The air is assumed to be fully saturated at 130 F. An inlet water mass fraction of water of four per cent has been chosen as an example, also because the military specifications for water ingestion engine tests specify four per cent (Reference 30). In each figure, the performance parameters for dry air at standard temperature, dry air at 130 F, saturated air-liquid water mixture ($X_w = 0.04$) at 130 F are plotted for comparison. The effect of elevated temperature is, in general, a deterioration in performance relative to that obtained

under standard temperature conditions. However, the "off-backbone" performance, both flow and efficiency representations, are similar for standard and hot day temperatures as seen in Figures 9.2 and 9.3, 10.3, and 11.2 and 11.3. This result may be explained in relation to experimental observations (Reference 27) noting that the performance of compressors operating under conditions far from minimum loss or high efficiency points is most strongly influenced by the aerodynamic and mechanical design of the machine rather than by the ambient conditions or water mass fraction.

Some trends in the "backbone" curves for the high pressure compressor (Figure 9.1) may be of interest. First, the minimum-loss flow coefficients of the dry, hot day conditions are higher than those for the dry, standard temperature conditions at all speeds. The minimum-loss flow coefficients for four per cent water ingestion and hot day conditions, however, are significantly lower than those for the same mass fraction of water ingestion under standard temperature conditions. It may be recalled that the predictions have been based on the assumption that the location in a compressor where the flow becomes choked when the machine is operating with the maximum mass flow rate is the same for all inlet conditions and that the effective flow area at that location remains constant. Within the compressor the difference in working fluid temperature for standard and hot day conditions decreases after a few stages of compression, absolutely and as a percentage of the local working fluid temperature. Thus the performance difference between hot day and standard day operation in the later stages of the compressor is small. However since the density of ingested fluid is a function of inlet temperature, the flow coefficient becomes higher for the hot day to obtain the same mass flow rate as for the standard day. On the other hand, when water is ingested during hot day conditions, the mass transfer rate from liquid to vapor state is significantly higher than for standard temperature operation, causing the gas phase mass flow rate to increase along the flow path.

The minimum-loss and minimum-loss work coefficient curves as a function of speed (Figure 9.1) are affected significantly by high ambient temperature. The minimum-loss work coefficient "backbone" curve for hot day conditions differs form that for standard temperature conditions in a complex way. At some speeds the hot day work coefficient curve falls above the standard day condition work coefficient curve and at others it falls below. The minimum-loss is higher for hot day, dry conditions than for standard day conditions. Since the minimum loss curve is smooth and the difference between hot day and standard day minimum loss is approximately constant, the wide variation of minimum-loss work coefficient then indicates that the pressure coefficient at the minimum-loss point is also varying widely.

It is interesting also that while the minimum-loss values for hot day, dry conditions are higher than those for dry standard day conditions, the minimum-loss values for operation with four per cent water ingestion and hot day conditions are lower than those for standard day temperature and four per cent water ingestion. The energy absorbed by liquid water during phase changes lowers the gas phase temperature yielding a higher adiabatic efficiency or lower loss.

5.4. Engine Simulation Results

The engine simulation test cases investigated can be divided into four groups in which engine performance is examined with respect to (i) various water ingestion mass fractions, (ii) various assumptions about the two-phase flow in the engine, (iii) high ambient temperature, and (iv) errors in control system input. The performance parameters obtained in each case as well as the list of cases studied are given in Section 5.1.

5.4.1. Effects of Mass Fraction of Water Ingestion

As a basic study on engine performance with water ingestion, the engine simulation code has been exercised for acceleration tests from idle to maximum power setting, and for deceleration tests from maximum power setting to idle setting. The ambient conditions are standard temperature and pressure with either dry air or saturated (with respect to water vapor) air-water droplet mixture flow. The operating condition is static and the power lever angle changes are made in all cases in one second. The water ingestion mass fractions used are one, two, four, and eight per cent. Two cases of engine operation are considered as follows: (i) cases in which all of the liquid water is drained form the core stream and the bypass stream after compression and (ii) cases in which all of the liquid water is drained from the bypass stream after the fan and all of the liquid in the core stream is flash-evaporated at the burner entry. In each of the test cases, a program execution period, called hereafter the simulation period, is chosen as the period at the end of which the desired terminal equilibrium state is expected to be obtained.

The results of engine simulation cases with zero, one two, and four per cent water ingestion are shown in Figures 12.1 to 22.3. In general the nonlinearity in compressor performance deterioration with respect to the magnitude of water ingestion mass fraction is evident in the overall engine performance. The difference between dry air performance and performance with one per cent water ingestion is much greater than the difference in performance between cases of one per cent and two per cent water ingestion, and so on. However, the performance changes do increase with water mass fraction, such that for high values of water mass fraction the program terminates execution (as indicated by a system N.S.I. or a fatal numerical status indicator) before the end of the stipulated simulation period.

For the acceleration tests performed while assuming that water is drained from both the core stream and bypass stream after compression, the controllability of the engine is not affected significantly. This can be seen by comparing the transient performance of the engine during an acceleration test for the case of dry air operation as shown in Figures 12.1 to 12.3 with that for the case of operation with air-water mixture, with mass fractions of water of one, two, and four per cent, as shown in Figures 13.1 to 13.3, 14.1 to 14.3, and 15.1 to 15.3, respectively. During water ingestion, the engine reaches a steady state condition in a period one-half to one second longer than it does when operating with dry air. The steady state point, however, varies for different cases of water ingestion and all of them differ form the dry air case. The rotational speeds of both the core engine and the booster decrease with increasing inlet mass fraction of water. The work input to the air-water droplet

mixture is then decreased resulting in reduced thrust. The specific fuel consumption increases with increasing inlet water mass fraction.

The controllability of the engine during the deceleration tests is not significantly affected when all of the liquid is drained from both streams after compression. This can be seen by comparing Figures 16.1 to 16.3, which represent dry air operation, with Figures 17.1 to 17.3, 18.1, and 19.1 to 19.3, which represent operation with water ingestion mass fractions of one, two, and four per cent, respectively. The rotor speed, mass flow rate of mixture into the engine, engine pressure ratio, etc. and consequently the thrust and specific fuel consumption show degradation similar to that for the acceleration tests. However, when the inlet mass fraction is four per cent (Figures 19.1 to 19.3), program indicates that the low pressure turbine inlet temperature exceeds the maximum allowable value. This condition is not fatal and the program continues to run.

The next test cases to be examined are those in which liquid in the core stream is flash evaporated at the burner entry and liquid in the bypass stream is drained aft of the fan. Flash evaporation of water at burner entry causes significant performance changes compared to draining the liquid from the two flow streams, as seen in Figures 20.1 to 22.3. For all four water mass fractions used, the engine simulation code encounters difficulties in completing the calculations between the chosen power settings. Only when the inlet mass fraction of water is one per cent or less can the engine simulation code complete a test run.

For one per cent mass fraction of water (Figures 20.1 to 20.3), the calculated match points at nearly every time step fall out of the range of the stored burner performance maps. This suggests that during a similar test on an actual engine the control system may cause the burner to operate outside its specified range, perhaps with respect to air and/or fuel mass flow rates or temperature. For a mass fraction of water of two per cent, the same type of burner performance is obtained as for the one per cent case. However, the calculation fails to converge for this value of water ingestion and after approximately eight tenths of a second of simulation time the program aborts, before the instant of time when the power lever change is completed. This can be seen in Figures 21.1 to 21.3. At that condition, the N.S.I. displayed shows that the core stream thrustor nozzle inlet pressure becomes less than ambient pressure.

When the inlet mass fraction of water is four per cent additional problems are encountered as evident in Figures 22.1 to 22.3. The calculated operating point is off the fan map, and also, the fuel flow required to reach the desired operating point exceeds the pump limit. After three tenths of a second of simulation time an error condition, namely, nozzle inlet pressure becoming less than the ambient pressure is indicated.

In summary, the deterioration in performance due to water ingestion seems to be nonlinear with respect to inlet mass fraction of water both individually in the compression subsystem and in the engine and also interactively. The effects on the engine system appear as reductions in thrust and increases in specific fuel consumption and reduced engine controllability. In the limiting case wherein water is flash evaporated at burner entry there appear considerable difficulties in operation. For

example, only acceleration type operations, and then none with more than one per cent water ingestion run to completion, and no deceleration type operations from maximum power setting to ground idle setting are possible since even the first calculation point produces a fatal error.

As the foregoing observations pertain to evaporation of water at one location of the burner, namely the inlet, it is next of interest to examine the influence of choosing other locations for evaporation of water, for example the burner exit as noted earlier in the section.

5.4.2. Effects of Location and Magnitude of Flash Evaporation of Water

In order to study the effects of location and magnitude of flash evaporation of water, the engine simulation program has been run with the inlet mass fraction of water held constant at two per cent while specifying that one and one-half per cent or one per cent of water is drained from the core stream and correspondingly, the balance of either one-half or one per cent mass fraction of liquid is evaporated at either the burner entry or burner exit. It may be pointed out that each of these cases involves partial drainage of water and evaporation of the balance of water entering the burner. The results from these simulation runs are given in Figures 23.1 to 26.3. In each case the power lever change that is introduced is from ground idle setting to maximum power setting in a period of one second.

In the previous section the results of simulating an acceleration-type power lever change with all of the water in the core stream undergoing flash vaporization were presented. In those cases, the program was unable to complete the simulation for inlet mass fractions of water greater than one per cent. On the other hand it is observed that the current four cases, each with two per cent water ingestion, run to a steady state, though not necessarily the specified state, thereby indicating some improvement in operation. However, the engine performance deviates greatly from the dry air cases for all four cases of water vaporization examined here. In particular, it may be observed that in the current case of a low value of water ingestion, namely, two per cent, it is possible to accomplish an acceleration only with one per cent water (that is, half of the ingested liquid) undergoing flash evaporation at burner entry, as seen in Figures 23.1 to 23.3. In this case the core speed falls from an initial value of 65 per cent of design speed, which is nearly the same as ground idle speed with dry air, to about 60 per cent of design speed at the end of one second of simulation time. Then the core engine accelerates to about 83 per cent design speed as opposed to 92 per cent for dry air operation. The booster follows a similar deceleration-acceleration pattern finally reaching a steady state value of 54 per cent of design speed as compared to 111 per cent obtained during an acceleration simulation with dry air as the working fluid. In all cases it appears that the change in low pressure spool speed is what limits the engine performance. Since part of the energy made available by combustion of fuel is utilized for evaporation of water, the energy available at entry to the high pressure as well as, later, the low pressure turbine is reduced. The reduced output of the low pressure turbine lowers the booster pressure ratio and, thus, the high pressure compressor inlet temperature. Meanwhile, the controller does tend to increase the fuel mass flow-rate to compensate for the energy absorbed by the phase change. However,

it is observed that the core engine speed is in fact low. Since the fuel flow schedule depends on core rotor speed, the reduction in temperature due to the phase change cannot be completely compensated for by the small increase in fuel.

In the other three cases, namely one per cent water evaporating at burner exit and one and one-half per cent water evaporating at burner entry or exit, the specified final state could never be reached. The amount of energy absorbed by water undergoing vaporization is in all cases, large enough to reduce the output of the high pressure turbine as well as that of the low pressure turbine. The core rotor speed then falls and the fuel flow, which is independent upon the core speed, is reduced. This in turn reduces the energy content of the gas at the high pressure turbine entry, causing further reduction in core and booster speeds. Along the path to the steady state operating condition of the engine and at the final, possible operating point itself, the simulation program indicates that the calculated operating point is off the fan map, the low pressure turbine map, and the burner map.

5.4.3. Effects of High Ambient Temperature of Engine Performance

The effects of high ambient temperature (130 F) on compressor performance were presented in an earlier section (Section 5.3). The results of various "hot day" engine simulation cases are given in Figures 27.1 to 32.3.

The mass fraction of water ingested in the hot day simulation cases is assumed to be four per cent. In each case the power lever is changed from ground idle setting to maximum power setting in a period of one second. The simulation has been carried out for operation with dry air at an ambient temperature of 130 F also, and the results are shown in Figures 27.1 to 27.3. Comparing the engine performance under dry, high ambient temperature conditions with that under dry, standard temperature conditions, it is found that there is a significant deterioration in engine performance even without water ingestion. The pressure ratios in each compressor section, the core and bypass stream air mass flow rates, and the core and booster rotor speeds are all lower than the values obtained under corresponding conditions at standard temperature. These reductions result in lowered thrust and increased specific fuel consumption. It is interesting to note that as in the case of water ingestion with flash evaporation in the burner, either at entry or exit, the low pressure system performance deteriorates to a greater extent than does the core engine.

The trends in engine performance during operation with water ingestion with a high ambient temperature are generally the same as those for standard temperature operation. When all the liquid is drained from the core and bypass streams aft of the compression subsystem, the controllability of the engine is not greatly affected, as shown in Figures 28.1 to 28.3. The thrust and specific fuel consumption during the engine transient and at the final steady state operating condition are adversely affected compared to those values obtained during operation under dry, standard temperature conditions as well as to those values obtained during operation with four per cent water ingestion and standard temperature. Recalling that the performance of each section of the compression subsystem operating with four per cent mass fraction of water ingestion is better during hot day operation than during standard temperature operation, as seen in Figures 9.1, 10.1 and 11.1 in Section 5.3, it is

interesting that the engine performance does not follow the same trend. The hot day performance deterioration of the other components perhaps counteracts any small improvement in compression subsystem performance.

When portions of the liquid are assumed to flash-evaporate in the combustor during hot day water ingestion simulations, again the trends in engine performance are similar to those observed in the standard temperature engine performance. The increase in power lever angle fails to accomplish an acceleration of the engine when one-half per cent of mass fraction of liquid flash evaporates at the burner entry or when one per cent mass fraction of liquid flash evaporates at the burner exit, as seen in Figures 30.1 to 30.3 and 31.1 to 31.3. When one-half per cent mass fraction of liquid flash-evaporates at the burner exit, the case presented in Figures 32.1 to 32.3, the power lever angle is an observed engine acceleration. However, the actual core and booster rotor speed increases are about one-half and one per cent of design speed, respectively. The steady-state operating condition reached during the simulation is different from that for dry air with equal ambient temperature and operational inputs; therefore, the end condition should still be considered a failed condition. When the mass fraction of water which evaporates at the burner entry is reduced to one per cent, the engine does respond to the power lever change. The core engine accelerates from about 63 per cent design speed to about 86 per cent speed as compared to an acceleration from about 65 per cent speed to 91 per cent speed for standard air. Nevertheless, the thrust and specific fuel consumption are considerably deteriorated in comparison with dry, standard temperature values.

The results of the investigation of engine operation under high ambient temperature conditions lead to some general observations. The effects of high ambient temperature on engine performance as predicted by the simulation program depend on the assumption made concerning the evaporation of water after the compression subsystem. If all liquid is drained from both the core stream and the bypass stream, the engine operates with normal controllability but with deteriorated performance parameters, such as thrust and specific fuel consumption. The difference between engine performance with water ingestion when the ambient temperature is high and that when the ambient temperature is standard is very close in magnitude to the difference in engine performance for dry, hot day operation, and standard day performance. In other words, high ambient temperature has an equally adverse effect on engine performance for either dry air or saturated air-water-droplet mixture flow operation. This may be understood by noting the performance changes introduced by phase change processes associated with the presence of water.

If it is assumed that some portion of the liquid water evaporate somewhere other than the inlet in the combustor, the engine performance as predicted by the simulation is severely and adversely affected for both hot day and standard day operation. In the case of partial evaporation of liquid, the high ambient temperature causes slight improvement over the standard temperature conditions indicated by the observed acceleration during idle-to-maximum power-setting operations. Still, the overall performance and the controllability are so far deteriorated compared to those for dry air operation that the slight improvement has little effect on the general

conclusions. That is, when there is evaporation of the water in the burner, the engine performance is unacceptable regardless of ambient temperature.

5.4.4. The Effects of an Error in the Temperature Sensed for the Control System

During water ingestion tests on actual turbofan engines it has been observed that the thermocouples used to measure temperatures for use as control system inputs give erroneous readings. The thermocouple junctions become immersed in the liquid water film flowing along the engine cases (Reference 14). For investigating the effects caused by such a sensor error, interest in the generic engine is in the high pressure compressor inlet temperature, as stated earlier in Section 4.3.2. It may be recalled that variable bleed valve area, variable stator vane setting and fuel flow rate depend on the core compressor inlet temperature. Simulations have been carried out for two values of temperature sensing error, namely 10 F and 40 F. The predicted results are presented in Figures 33.1 to 40.3. For comparison, simulation cases have been performed for dry air operation with the same values of temperature error as though there was a malfunction in the signal processor or a defect in the thermocouple.

Four simulation cases were tried initially that involve no change in power level angle. The four cases include the following conditions: (i) operation with dry air and a temperature error of 10 F, (ii) operation with dry air and a temperature error of 40 F, (iii) operation with an inlet mass fraction of water of two per cent under the assumption that the water is drained completely after compression and with a temperature error of 10 F, and (iv) operation with an inlet mass fraction of water of two per cent under the assumption that the water is drained completely after compression, and with a temperature error of 40 F. In all four cases the power lever is set and held at maximum power-setting. These engine simulation cases were started under the condition that the temperature sensor was functioning properly. In the case of operation with dry air the temperature sensor was assumed to begin providing the control system with an erroneous input at the end of one second from the initiation of simulation. In the case of water ingestion, the sensor was assumed to be erroneous at the same instant as the beginning of water ingestion, which was, however, assumed to begin after one second of simulation time. The temperature error and water ingestion are continued throughout the simulation period. When there is water ingestion it is assumed that all liquid is drained from the core and the bypass streams aft of the compression subsystem. The results for these cases are given in Figures 33.1 to 35.3.

During operation with dry air in the case of a temperature error of 10 F, the performance of the engine is affected significantly, as seen in Figures 33.1 to 33.3, and various control or engine operation limits are reached or exceeded. The temperatures at the high pressure turbine inlet and low pressure turbine inlet exceed the maximum allowable values. The fan speed exceeds the design operating limit and the high pressure compressor discharge pressure is greater than its maximum allowable value. In comparison with the maximum power operating condition without a temperature error, the error in temperature causes rotor speeds to increase, total mass flow rate of air into the engine to increase and fuel flow rate to increase, resulting in increased engine pressure ratio and increased thrust. Thus the output of the engine increases when a temperature error occurs. Unfortunately, the new operating point is not as

efficient as the maximum power operating point that the engine attains when there is not a temperature error and, moreover, the specific fuel consumption is also increased.

Figures 34.1 to 34.3 are the results for case (ii), in which there is a temperature error of 40 F all other conditions remaining the same as in case (i). As seen in the figures a fatal error causes execution to cease after eight seconds of simulation time. Initially, the trends which occurred during engine operation with a 10 F temperature error are followed. The rotor speeds, pressure ratios, mass flow rates, etc., increase. High inlet temperatures for the high pressure and low pressure turbines are indicated. Then the trends are reversed as the high pressure compressor appears to begin to surge, a condition reported by a numerical status indicator. The surge condition leads to the fatal error.

The water ingestion cases are identical to the dry air temperature error cases in ambient conditions and power-setting except for a two per cent mass fraction of liquid water in the flow. The results for the water ingestion cases, shown in Figures 35.1 to 36.3, are very similar to those for the corresponding dry air cases. The increases in speeds and mass flow rates over the cases of engine operation with no temperature error are less during water ingestion than during dry air operation. The steady state thrust and specific fuel consumption are lower and higher, respectively, than those for dry air operation with a temperature error. The same control limits and error conditions are indicated. The fan speed and turbine inlet temperatures are too high as is the high pressure compressor pressure ratio. For the 40.0 F temperature error, the simulation ends with a fatal error after only five seconds of simulation time. Also, the condition leading to the fatal error is high pressure compressor urge. In general, the presence of liquid water changes the steady state operating point of the engine as compared to that during engine operation with dry air with the same operational input. However, the error in the temperature sensed by the control system has a greater effect on steady state running than does the presence of two-phase flow.

Next, four simulations involving a power lever angle change from ground-idle-setting to maximum power-setting were carried out for dry air and water ingestion conditions for both the 10.0 F and 40.0 F temperature errors. These results are presented in Figures 37.1 to 40.3. During dry air and air-water droplet mixture operation, these simulations end in fatal errors. The duration of pressure simulation depends upon the temperature error and not the nature of the working fluid entering the engine.

When the temperature error is 10.0 F (Figures 37.1 to 37.3 and 38.1 to 38.3), the simulation runs for just under three seconds. The engine begins to accelerate as the power lever is advanced; however, the temperature error effects observed in the steady state simulation have an effect on engine controllability. The speeds, pressure ratio, and air (or air-water droplet) mixture mass flow rates for both the high and low pressure systems decrease while the fuel flow rate increases. The calculated points go out of range of the combustor, the low pressure turbine, and the booster maps and the high pressure turbine inlet temperature exceeds its maximum allowable value. The simulation ends when no stable operating point can be calculated.

When the temperature error is 40.0 F, no acceleration is observed during the power lever angle change and the simulation aborts during the change, as can be seen in Figures 39.1 to 40.3. As soon as the temperature error is encountered the pressure ratios for the fan and booster increase sharply while the working fluid mass flow rate decreases; these changes indicate the possibility of surging in the fan and booster. The high pressure compressor pressure ratio and core speed fall while the fuel flow rate and turbine inlet temperature rise. The final error scenario is the same as that for the 10.0 F temperature error, namely no stable operating point is found.

CHAPTER VI

DISCUSSION

The discussion is divided into three parts as follows: (i) Methodology; (ii) General conclusions from predictions of compression subsystem performance; and (iii) Conclusions on transient performance of engines with water ingestion.

6.1. Methodology

In this section some features of the methodology used in this investigation are discussed with respect to the strengths and limitations inherent in them. The features discussed are as follows: (i) approach to engine simulation with isolation of effects of water ingestion in the compression subsystem, (ii) compression subsystem model, and (iii) engine simulation code.

6.1.1. Simulation of Engine Operation with Water Ingestion Isolated in Compression Subsystem

(i) The method of simulating engine performance when water ingestion effects are taken into account only in the compression subsystem has been found successful for simulating cases in which (a) there are power-setting operations and (b) there is an incorrect input to control system from a sensor that can be expected to be affected by the presence of water in the working fluid.

(ii) The performance data obtained for the compression subsystem operating with water ingestion and the data stored in the engine simulation code which represents the performance of each of the components in the engine correspond to steady state equilibrium operating points. The transient engine performance calculated using these data in the engine simulation code is thus quasi-steady performance.

(iii) The choice of limiting conditions pertaining to disposal of water following compression of air-water mixture has permitted an examination of the effects of other variables such as change in mass flow in the hot section and thrustor nozzles, change of fuel flow rate and change of combustor exit temperature.

6.1.2. Compression Subsystem Model

(i) The WINCOF code, because of the nature of the calculation scheme employed, specifies an equivalent machine to any given compressor in the following manner: (a) a chosen streamtube is assumed to represent the given compressor; (b) a high, reference Mach number which sets a limit to mass flow in a blade passage and on which the compressor flow representation is based is assumed to exist at each speed of operation; and (c) deviation, non-dimensional wake momentum thickness, and equivalent diffusion ratio rules obtained corresponding to design point performance are expected to apply throughout the range of operation.

(ii) The WINCOF code has been found generally useful for obtaining performance of fan, booster, and high pressure compressor with respect to the bypass and the core streams.

(iii) The validity of the choice of representative streamtube location depends upon several parameters, which include ambient conditions, inlet mass fraction of water, mass flow rate of compressor working fluid, and rotational speed of the compressor.

6.1.3. Engine Simulation Code

The modular architecture/organization of the engine simulation code employed is such that any desired model or modification to performance maps can be introduced for any component in the generic engine. In addition, control system parameters and limits can be altered.

6.2. Predictions of Compressor Performance

In this section, some general observations are made about the performance of a compression subsystem and how the performance is affected by various mechanical characteristic, operational conditions, and ambient conditions.

6.2.1. Performance Parameters Selected

(i) Because the "off-backbone" performance of a compressor is nearly identical for a variety of ambient conditions and mass fractions of water ingested, useful comparisons of performance under various conditions can only be made with respect to such parameters as work coefficient, flow coefficient and loss, and the associated "backbone" or minimum loss values.

(ii) However, in compressor maps utilizing those performance parameters, the stall and surging conditions are not readily apparent.

6.2.2. Effects of Speed of Rotation and Flow Coefficients on Water Ingestion

A relationship between the rotational speed and the flow coefficient and the two phase flow phenomena can be based on the residence time of a fluid particle in a compressor. An overall characteristic time representing the residence time of a fluid particle, has been defined as follows (Reference 31)

$$t_o = \frac{1}{\phi_o} \cdot \frac{L}{D} \cdot \frac{1}{N} \cdot \frac{1}{\pi}$$

where ϕ_o is the flow coefficient at the compressor inlet, and is arbitrarily chosen as the reference flow coefficient, L is the compressor length, D is the compressor outer casing diameter, and N is the rotational speed. The characteristic time decreases with increasing flow coefficient and rotational speed. With a reduction in characteristic time, the effect of centrifugal action on mixture ratio decreases, as well as the effects of heat and mass transfer processes. In other words, in such cases, the compressor operates with two-phase fluid flow.

In this investigation, performance calculations have been carried out along streamtubes which divide the flow into two equal parts both in the bypass stream and the core stream. Along these streamtubes, centrifugal action and transport processes tend to deplete the liquid. As the water content is depleted the compressor performance becomes more like that which occurs during single phase flow operation.

It can be concluded, then, that as the overall characteristic time increases, the performance of a compressor operating with water ingestion will approach that of the compressor operating with dry air.

(i) The performance predicted for the compression subsystem of the generic engine reflects the foregoing arguments to a certain extent. The overall characteristic times for the fan and the booster are similar while the overall characteristic time for the high pressure compressor is higher. For example, the overall characteristic times at design point for fan, booster and high pressure compressor are 0.22 msec, 0.36 msec, and 1.03 msec, respectively. The changes in the performance of the fan and the booster due to water ingestion are similar.

(ii) The dependence of the performance changes on characteristic time during water ingestion can be seen in the "backbone" performance of the high pressure compressor, for example, where at low-speeds, corresponding to higher characteristic time, the water ingestion effects are small compared to those at high rotational speeds.

6.2.3. Effects of Operating Conditions

The conditions for which compression subsystem performance calculations have been carried out include various inlet mass fractions of water droplets and two ambient temperatures. The effects of these conditions on the compression subsystem performance can be summarized as follows:

(i) The performance of the compression subsystem deteriorates when water is ingested and the magnitude of the deterioration increases with increasing mass fraction of water ingestion.

(ii) The magnitude of the compressor performance deterioration is a non-linear function of inlet mass fraction of water; that is, the magnitude of the difference between the performance of the compressor operating with an inlet mass fraction of water of one per cent and that of the compressor operating with dry air is higher than the difference between the performance of the compressor operating with an inlet mass fraction of water of two per cent and that of the compressor operating with an inlet mass fraction of one per unit.

(iii) The performance of a compression subsystem deteriorates at a high ambient temperature.

(iv) The difference between the performance of the compressor operating with water ingestion and that of the compressor operating with dry air is smaller when the compressor is operating at high ambient temperature.

In all cases, deteriorated performance refers to decreased pressure coefficient and flow coefficient and increased work coefficient and loss at the minimum-loss point for a given speed.

6.3. Transient Performance of Engine with Water Ingestion

In this section the engine simulation test cases studied are reviewed with reference to their applicability in practical cases. Some general conclusions about the results of the test cases are made.

6.3.1. Applicability of Test Cases

The test cases involve changes in (a) quality of air-water mixture ingested, (b) power-setting under sea level static conditions, and (c) output of a sensor that provides information to the control system. The test cases are based on limiting assumptions concerning the handling of water in the gas path such as drainage and evaporation.

(i) The amounts of water drained at the end of the compression subsystem and evaporation in the burner have been selected purely on a parametric basis.

(ii) The identification of the location of flash-evaporation in the burner and its magnitude permit examination of changes in engine performance with low and high power settings and small and large amounts of water ingestion.

(iii) The limiting cases studied provide a means of establishing the validity of standard testing procedures (Reference 30) for determining the behavior of engines with water ingestion and also a means of determining what type of test may prove to be the most crucial. For example, testing at idling and full power conditions with small amounts of water, in the range of 0.5 per cent, may prove significant in revealing several aspects of engine operation during certain aircraft flight operation.

6.3.2. Effects of Water Mass Fraction and the Limiting Assumptions

The mass fraction of water ingested into an engine affects the engine performance in the present study through (a) effects on the compressor subsystem and (b) effects of drainage or evaporation of water following compression. The effects of water ingestion into an engine are described here in terms of performance degradation, that is, reduced thrust and increased specific fuel consumption, and includes slow response to, or even inability to respond to, operational changes such as power-setting operations.

(i) The effects of water ingestion on the performance of the generic engine are similar to those on the compression subsystem in that there is a nonlinear relationship between the magnitude of performance degradation and the mass fraction of liquid in the working fluid.

(ii) For engine simulation cases run under the assumption that all of the liquid is drained from both the core stream and the bypass stream after compression, the predicted performance is characterized by (very slightly) slower response to power-setting operations and degraded steady state performance.

(iii) For the cases in which a portion of liquid evaporates at burner entry or exit, that portion being a mass fraction of at least one-half per cent, both the controllability and the steady state performance are significantly degraded.

(iv) When all of the liquid is assumed to evaporate at the burner entry, increasing the power lever angle results only in an unsuccessful simulation which stops with indication of a fatal error in calculation.

6.3.3. Effects of Increased Ambient Temperature

Test cases, including dry air operation and water ingestion operation under the limiting assumptions, were carried out with an ambient temperature of 130°F. There are two general observations about the results.

(i) The effect of high ambient temperature is, in general, degraded final steady state performance. While the compression subsystem performance at high ambient temperature is slightly improved with the presence of water, the engine performance is not affected significantly in that manner.

(ii) The controllability of the engine is not affected by the high ambient temperature. That is, the characteristics of the transient engine performance predicted for a given test case carried out under high ambient temperature conditions are the same as those for a corresponding test case carried out under standard temperature conditions.

6.3.4. Influence of Rate of Change of Power Lever on Transient Performance of Engine

In all the test cases studied in this investigation, the period of time specified for carrying out the desired power setting change has been one second. In practice problems with engine operability or controllability can be overcome, it is recommended, by changing, in general reducing, the rate of power setting operations. Some investigation into this aspect of the subject has been performed.

For a case in which the engine operates with dry air as working fluid under standard conditions, the period over which the power-setting change takes place was increased from one second to five seconds in one case and then to ten seconds in another case. When the power setting change occurs in one second, the engine attains a steady state condition in just over five seconds, as may be observed, for example in Figures 12.1 to 12.3. When the power lever is moved in five seconds over the same range of angle the engine responds more smoothly but there is little change in the total time required for the engine to reach steady state condition. When the power setting operation is performed next over a ten second period, the engine responds even more smoothly and, as expected, reaches a steady state condition in just over ten seconds. It may be pointed out that the control system for the generic engine incorporates an acceleration schedule for fuel flow as a function of core rotor speed. The schedule limits the rate of fuel delivered in response to power setting changes in order to maintain a safe surge margin. The schedule becomes operative whenever the rate of change of core rotor speed is greater than a preset value. Thus, when the power lever is moved in engine simulation from ground idle setting to maximum power setting in less than about five seconds, the engine seems to be forced to follow a preset acceleration schedule.

During all of the test cases examined in the current investigation with water ingestion, the control system is found to force the engine to operate according to such a preset acceleration schedule, regardless of the rate at which the power setting operation is performed. This can be explained as follows. The ingestion of water causes the performance of the compression subsystem to deteriorate and the core compressor inlet temperature and core compressor discharge pressure become reduced. The control system responds by increasing the flow rate of fuel. Then, in the event of a power lever change corresponding to an acceleration from ground idle to maximum power, the control system further increases the flow rate of fuel, as is to be expected. However, the desired fuel flow rate exceeds the maximum pre-set rate for maintaining a safe surge margin; and therefore, the control system seems to impose a limit on the fuel flow rate as specified by the acceleration schedule.

This investigation into the influence of rate of change of power-setting and a given acceleration schedule leads to an observation about engine operation in practice. If the engine is already accelerating according to the built-in acceleration schedule for any reason, water ingestion, under those circumstances, could cause the engine to stall, especially when the margin remaining between the prescribed acceleration schedule and the surging condition is small.

6.4. Effects of Control System Input Errors

The results of engine simulation cases involving temperature sensing errors show several features observed in certain reported water ingestion engine tests (Reference 14). The mechanical effects noticed in the experiments are an excessively high booster speed, suggesting incorrect booster-core performance matching, and an opening of stator vanes, which increases the choking mass flow rate. The resulting performance change due to the observed mechanical effects is compressor stall. This type of stall occurs in the last stages of a compressor when operating with high mass flow rates. As the mass flow rate increases the pressure ratio decreases in each stage. Thus, at any point in the compressor flow path the working fluid density becomes lower than that at design conditions. This causes increased flow velocity through the blade passages. In the later stages there is then a possibility of a rotor blade becoming stalled, which is thought to cause surge at high speeds (References 32 and 33).

The effects of an error in temperature signal transmitted to the controls system are apparent in the resulting action of the controller. As a result of such action, the component performance matching process is disrupted, that is, the performance of various components at the resulting operating points during transient engine operation may not be properly matched.

(i) When the temperature error is small, in this investigation 10 F, the effects of incorrect component performance matching are as follows: (a) the time required for the engine to reach steady state operation after an operational change is increased and (b) the overall engine performance is characterized by increased thrust and specific fuel consumption compared to normal operation.

(ii) When the temperature error is large, in this investigation 40 F, the engine simulation program is unable to carry the performance calculations through until a

steady state operating point is reached. A fatal error condition, namely surging of the high pressure compressor, is indicated.

LIST OF REFERENCES

1. Tabakoff, W. and Hamed, A., "Installed Engine Performance in Dust-Laden Atmosphere," AIAA Paper No. AIAA-84-2488, October, 1984.

2. Butler, D. and Bridges, J., "Sand Environmental Test Facility," AIAA Paper No. AIAA-84-0411, January 1984.

3. Balan, C. and Tabakoff, W., "A Method of Predicting the Performance Deterioration of a Compressor Cascade Due to Sand Erosion," AIAA Paper No. AIAA-83-0178, January 1984.

4. (a) "Concorde Completes Flooded Runway Tests," *Aviation Week and Space Technology*, p. 22, October 4. (b) "Board Assays Crash of DC-9 in Storm," Ibid, pp. 63-67, July 24, 1978. (c) "Storm Traced in Southern DC-9 Crash," Ibid, pp. 59-61, July 31, 1978. (d) "Damage Assessed in Southern Crash," Ibid, pp. 59-63, August 7, 1978. (e) "Thrust Loss Cited in Southern Accident," Ibid, pp. 55-58, August 221, 1978. (f) "Board Urges Improved Thunderstorm Reporting," Ibid, pp. 63-64, August 28, 1978.

5. Parikh, P., Hernan, M., and Sarohia, V., "Quantitative Determination of Engine Water Ingestion," AIAA Paper No. AIAA-86-0307, January 1986.

6. Zerkie, R.D., Colley, W.C., and Doel, D.S., "Analysis of Moisture Condensation in Engine Inlets," *Proceedings of the Symposium on Particulate Laden Flows in Turbomachinery*, edited by M. Tabakoff, C.J., Crowe, and D.V. Cale, American Society of Mechanical Engineers, New York 1982.

7. MacGregor, C.A. and Bremer, R.J., "An Analytical Investigation of Water Ingestion in the B-1 Inlet," Rockwell International NA-73-181, June 1981.

8. Murthy, S.N.B., *et al*, "Water Ingestion into Axial Flow Compressors," Report No. AFAPL-TR-76-77, Air Force Systems Command, Wright-Patterson Air Force Base, August 1976.

9. Wallis, G.B., *One-Dimensional Two-Phase Flow*, McGraw- Hill, Inc., New York, 1969.

10. Moore, M.J. and Sieverding, C.H., *Two Phase Steam Flow in Turbines and Separators*, p. 49, McGraw-Hill, New York, 1976.

11. Annual Book of ASTM Standards, General Methods and Instrumentation, Vol. 14.02, No. E694, 1985. American Society of Materials Testing, Philadelphia, PA.

12. Danielson, K. and Higgins, A.W., "Raindrop Size Distribution Measurement of High Elevation Continental Cumuli," *Conference on Cloud Physics*, pp. 305-310, October 1974.

13. Killel, G.J., "Rain and Hail Extremes at Altitude," AIAA Paper No. 79-0539, February 1979.

14. Russell, R.E. and Victor, I.W., "Evaluation and Correction of the Adverse Effects of (i) Inlet Turbulence and (ii) Rain Ingestion on High Bypass Engines,"AIAA Paper No. 84-2486.

15. Tsuchiya, T. and Murthy, S.N.B., "Analysis of Water Ingestion Effects in Axial Flow Compressors," Technical Report AFAPL-TR-78-35, Air Force Systems Command, Wright-Patterson Air Force Base.

16. Chambler, C.E., Davis, M.W., and Himyey, W.F., "A Multistage Axial Flow Compressor Mathematical Modeling Technique with Application to Two Current Turbofan Compression Subsystems," AIAA Paper No. 80-0051, January 1980.

17. Davis, Jr., M.W., "A Stage-by-Stage Dual Sppol Compression System Modelling Technique," AIAA Paper No. AIAA-85-1354, 1985.

18. Sadler, G.G. and Melcher, K.J., "DEAN: A Simulation Program for Turbofan Engines," AIAA Paper No. AIAA-85-1354, 1985.

19. Sellers, J.F. and Daniele, C.J., "Dyngen-A Program for Calculating Steady-State and Transient Performance of Turbojet and Turbofan Engines," NASA TN D-7901, National Aeronautics and Space Administration, April 1975.

20. Leonardo, M., Tsuchiya, T., and Murthy, S.N.B., PURDU-WINCOF - A Computer Code for Establishing the Performance of a Fan-Compressor Unit with Water Ingestion, Report No. NASA CR-168005, National Aeronautics and Space Administration, 1982.

21. Murthy, S.N.B., Private Communication.

22. Tsuchiya, T. and Murthy, S.N.B., "Effect of Water Ingestion into Axial Flow Compressors," Technical Report AFWAL-TR-80-2090, Air Force Systems Command, Wright-Patterson Air Force Base, Part I: Analysis and Predictions, October 1980.

23. Swan, W.C., "A Practical Method of Predicting Transonic-Compressor Performance," *Jr. of Engineering*; Transaction of the ASME, July, 1961.

24. Lieblein, S., Schwenk, F.C., and Broderick, R.L., "Diffusion Factor for Estimating Losses and Limiting Blade Loadings in Axial-Flow Compessor Blade Elements," NACA RM E53D01, 1953.

25. Converse, G.L. and Giffin, R.G., Extended Parametric Representation of Copessor Fans and Turbines, Report No. NASA CR 174645, 1984.

26. *U.S. Standard Atmosphere*, United States Committee on Extension to the Standard Atmosphere, 1962.

27. Murthy, S.N.B., Tsuchiya, T., Ehresman, C.M., and Richards, D., "Water Ingestion into Axial Flow Compressors: Part III, Experimental Results and Discussion," Technical Report AFWAL-TR-80-2090, Air Force Systems Command, Wright-Patterson Air Force Base, June 1981.

28. Marble, F.E., "Mechanism of Particle Collision in the One-Dimensional Dynamics of Gas-Particle Mixtures," *The Physics of Fluids*, Vol. 7, No. 8, pp. 1270-1282, August 1964.

29. Pinkus, O., "Liquid Particle Dynamics and Rate of Evaporation in the Rotating Field of Centrifugal Compressors," ASME Paper No. 82-GT-86, December 1981.

30. Code of Federal Regulations, Title 14-Aeronautics and Space, Chapter I - Federal Aviation Administration Article 33.77, paragraphs (c) and (f), January 1980.

31. Tsuchiya, T., Aerothermodynamics of Axial-Flow Compressor with Water Ingestion, Ph.D. Dissertation, Purdue University, May 1982.

32. Cohen, H., Rogers, G.F.C., and Saravanamutto, H.I.H., *Gas Turbine Theory*, Longman Group Limited, Burnt Mill, U.K., 1972.

33. Stone, A., "Effects of Stage Characteristics and Matching on Axial-Flow-Compressor Performance," Trans. ASME, 80, 1958, pp. 1273-93.

34. Haykin, T., "Jet Engine Simulation with Water Ingestion in Compressors," M.S.M.E. Thesis, Purdue University, May, 1986.

35. Haykin, T. and Murthy, S.N.B., "Dynamic Performance of a High Bypass Ratio Engine with Water Ingestion," Interim Report No. DOT/FAA/CT-TN86/14, October, 1986.

APPENDIX

I. Generic Engine and Control

The generic engine studied in this investigation has been chosen because it contains many features that are interesting for study and it is typical of those used in large military and civilian transport aircraft. The engine can be described as a two-spool high bypass ratio turbofan with a bypass ratio of about 4.5. The core stream and the bypass stream exhaust through separate thrustor nozzles. There are various features in the compression subsystem of the generic engine which are of particular interest. Some of the stators in the high pressure compressor can be adjusted through a range of stagger settings. There is a variable area bleed valve door located in the outer casing of the core stream aft of the booster.

The engine control system for the generic engine is assumed to control fuel flow and variable stator vane position. The system is considered as an electro-mechanical analog speed governor which senses the core rotational speed, the core compressor inlet temperature and the core compressor discharge pressure and adjusts the fuel flow to attain or maintain a desired speed, as set by a chosen value of power lever angle. Under design ambient and operating conditions there is a fixed flow rate of fuel corresponding to any given power lever angle. Furthermore, there is a core speed value corresponding to any given power lever angle. However, in the event of a change in power lever angle, a step change in fuel flow rate from that corresponding to the initial power lever angle to that corresponding to the final power lever angle is not the desired action. Such setup change could cause unstable combustion or more generally, unstable engine operation. Thus in the event of a power-setting change the fuel flow rate changes gradually as opposed to a step change. The gradual fuel flow rate changes are made according to a schedule which is a function of core compressor speed only.

As stated in the foregoing, the control system operates with signals related to compressor discharge pressure and compressor inlet temperature in addition to core speed. The control system uses these signals to correct the fuel flow rate schedule for deviations from design ambient and operating conditions. The signals are compared with their respective values under design conditions and a correction that is a function of the difference between the compressor inlet temperature and the compressor discharge pressure under design conditions and those under a specific set of operating conditions is applied to the base fuel flow schedule. Typical control systems regulate fuel flow by regulating the injection nozzle delivery pressure. The pressure regulation can be accomplished using a bypass loop in the fuel line delivering fuel from the pump to the injectors. The fuel pressure at the injectors is inversely proportional to the flow rate of fuel in the bypass loop; this flow rate is regulated with valves under the action of the control.

The variable stator vanes have a schedule of stagger settings which is a function of compressor speed. The schedule is corrected for specific operating conditions as a function of compressor inlet temperature. A hydraulic actuator is typically used for making the stator stagger setting adjustments and the medium in many cases is engine fuel.

II. Data Utilized for Calculation of Compression Subsystem Performance

In order to specify the compression subsystem of the generic engine used in the investigation, specific data pertaining to the compressor subsystem must be provided as input to the WINCOF code. The data include information common to an engine compressor section (fan, booster, and high pressure compressor) as well as radii, streamtube areas, blade metal angles, design point stage performance, etc., which is specific to the actual streamline used in the investigation. A list of required input data and descriptions of each follows:

NS	number of stages
NSF	number of fan stages
NSLPC	number of low pressure compressor stages
NSHPC	number of high pressure compressor stages
RRHUB(i)	hub radius at ith stage rotor inlet
RC(i)	chord length of ith stage rotor
RBLADE(i)	number of blades for ith stage rotor
STAGER(i)	stagger angle for ith stage rotor
SRHUB(i)	hub radius at ith stage stator inlet
SC(i)	chord length of ith stage stator
SBLADE(i)	number of blades for ith stage stator
STAGES(i)	stagger angle for ith stage stator
SIGUMR(i)	solidity of ith stage rotor
SIGUMS(i)	solidity of ith stage stator
BET2SS(i)	stator outlet absolute flow angle
FND	core rotor corrected speed at design point
TOID	compressor inlet temperature at design point
POID	compressor inlet pressure at design point
FNDLPC	LPC rotor corrected speed at design oint
GAPR(i)	gap between ith stage rotor and (i - 1)th stage stator
GAPS(i)	gap between rotor blade and stator blade for ith stage
RRTIP(i)	blade tip radius at ith stage rotor inlet
STRIP(i)	blade tip radius at ith stage stator inlet
RM(i)	rotor inlet radius at which mean line performance calculation is carried out
SM(i)	stator inlet radius at which mean line performance calculation is carried out
BLOCK(i)	blockage factor for ith stage rotor
BLOCKS(i)	blockage factor for ith stage stator
BET1MR(i)	blade metal angle at ith stage rotor inlet
BET2MR(i)	blade metal angle at ith stage rotor outlet
BET1MS(i)	blade metal angle at ith stage stator inlet
BET2MS(i)	blade metal angle at ith stage stator outlet

DSMASS	streamtube design mass flow rate
BYPASS	bypass ratio at design point
PR12D(i)	total pressure ratio for ith stage rotor at design speed
PR13D(i)	total pressure ratio for ith stage at design point
ETARD(i)	adiabatic efficiency for ith stage rotor
DVZ1(i)	ith stage rotor outlet axial velocity at design point
DVZ3(i)	ith stage stator outlet axial velocity at design point
BET2SR(i)	ith stage rotor outlet relative flow angle at design point

III. Data Utilized for Engine Simulation

The compression subsystem performance calculations are performed for each inlet mass fraction of water and ambient temperature. The results of the calculations are performance maps in the form suitable for use in an engine simulation code for each inlet mass fraction of water and each ambient temperature. Each map contains the following data:

(i) Minimum loss as a function of compressor speed, MIN LOSS vs. N.

(ii) Work coefficient at the minimum loss points as a function of speed, ψ'_{ML} vs. N.

(iii) Flow coefficient at the minimum loss points as a function of speed, (ϕ_{ML} vs. N).

(iv) Pseudo-Mach number as a function of the difference between the work coefficient at the given operating point and the minimum loss work coefficient for the given operating speed. These data are needed over the range of operating speeds for which the minimum loss points were found, M vs. $\psi - \psi'_{ML}$ for each N.

(v) Loss at the given operating point minus minimum loss at the given operating speed as a function of the square of the difference between the work coefficient at the given operating point and the minimum loss work coefficient at the given operating speed. These data are needed over the range of operating speeds for which the minimum loss points were found. The sign of the difference between the work coefficient at the given operating point and the minimum loss work coefficient at the given operating speed is preserved

$$(\text{LOSS} - \text{MINLOSS}) \text{ vs. } \left\{ (\psi' - \psi'_{ML})\big|_1 \times (\psi' - \psi'_{ML}\big|_1 \right\} \text{ for each N.}$$

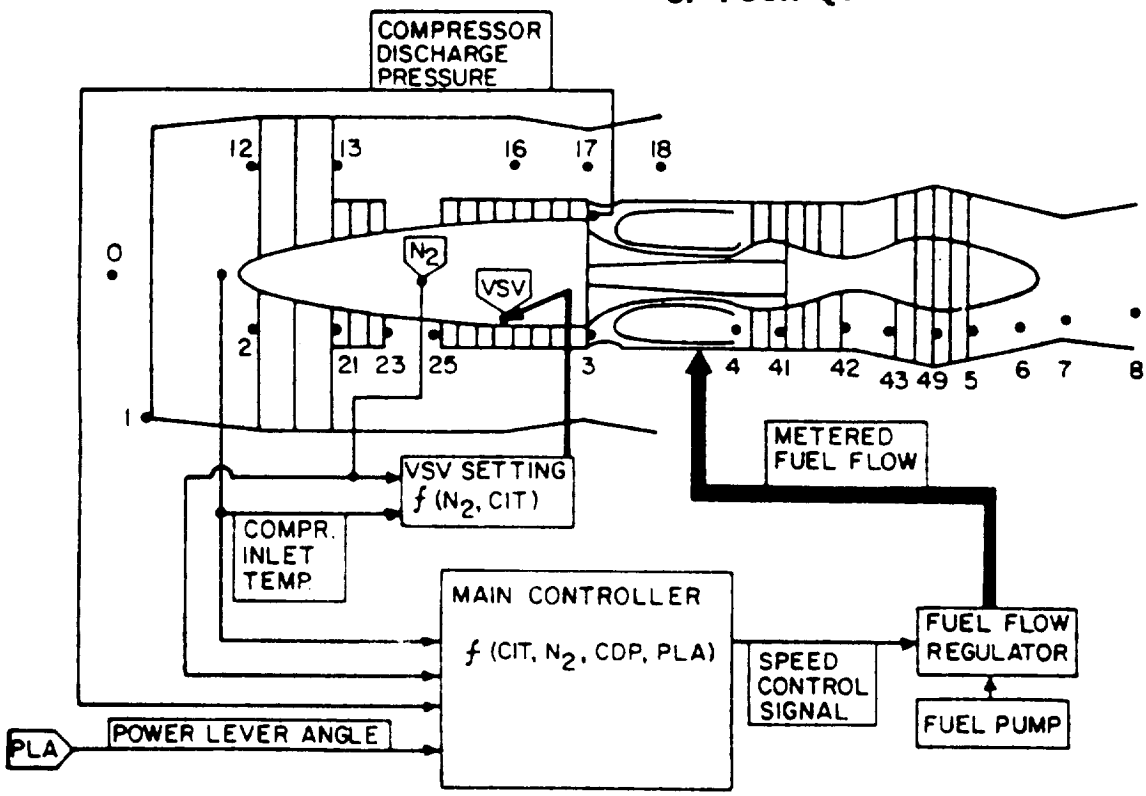

PRIMARY GAS STREAM

STATION	DESCRIPTION
0	AMBIENT
1	INLET/ENGINE INTERFACE
2	FAN FRONT FACE
21	FAN DISCHARGE AT HUB
23	BOOSTER DISCHARGE (STATOR EXIT)
25	HIGH PRESSURE COMPRESSOR INLET
3	HIGH PRESSURE COMPRESSOR DISCHARGE
4	BURNER DISCHARGE
41	HIGH PRESSURE TURBINE ROTOR INLET
42	HIGH PRESSURE TURBINE EXIT
48	LOW PRESSURE TURBINE ROTOR INLET
5	TURBINE DISCHARGE
6	EXHAUST NOZZLE/ENGINE INTERFACE
7	EXHAUST NOZZLE THROAT
8	EXHAUST NOZZLE DISCHARGE

SECONDARY GAS STREAM

STATION	DESCRIPTION
12	FAN INLET AT TIP
13	FAN DISCHARGE
16	DUCT EXHAUST NOZZLE/ ENGINE INTERFACE
17	DUCT EXHAUST NOZZLE THROAT
18	DUCT EXHAUST NOZZLE EXIT

Figure 1. Schematic of the Generic High Bypass Ratio Engine with the Generic Control. Stations identified in the drawing are described beneath the drawing.

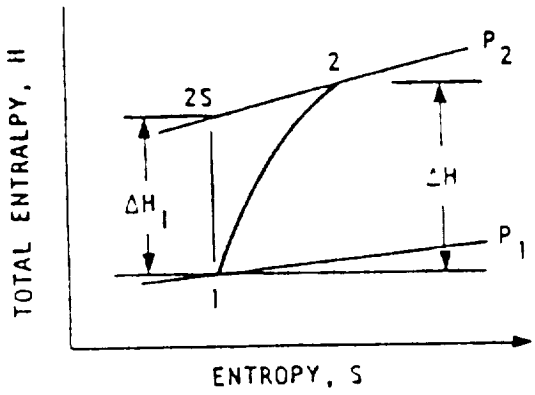

LET: C_{z_1} = AXIAL VELOCITY COMPONENT AT ROTOR INLET

v = WHEEL SPEED

DEFINE:

1. WORK COEFFICIENT, $\psi = \Delta H/(v^2/2g_oJ)$
2. PRESSURE COEFFICIENT, $\psi_1 = \Delta H_1/(v^2/2g_oJ)$
3. FLOW COEFFICIENT, $\phi = C_{z_1}/v$
4. EFFICIENCY, EFF = ψ_1/ψ
5. LOSS, XLS = $(\Delta H - \Delta H_1)/(v^2/2g_oJ) = \psi - \psi_1$

Figure 2 Definitions of Work Coefficient, Pressure Coefficient, Flow Coefficient, and Loss

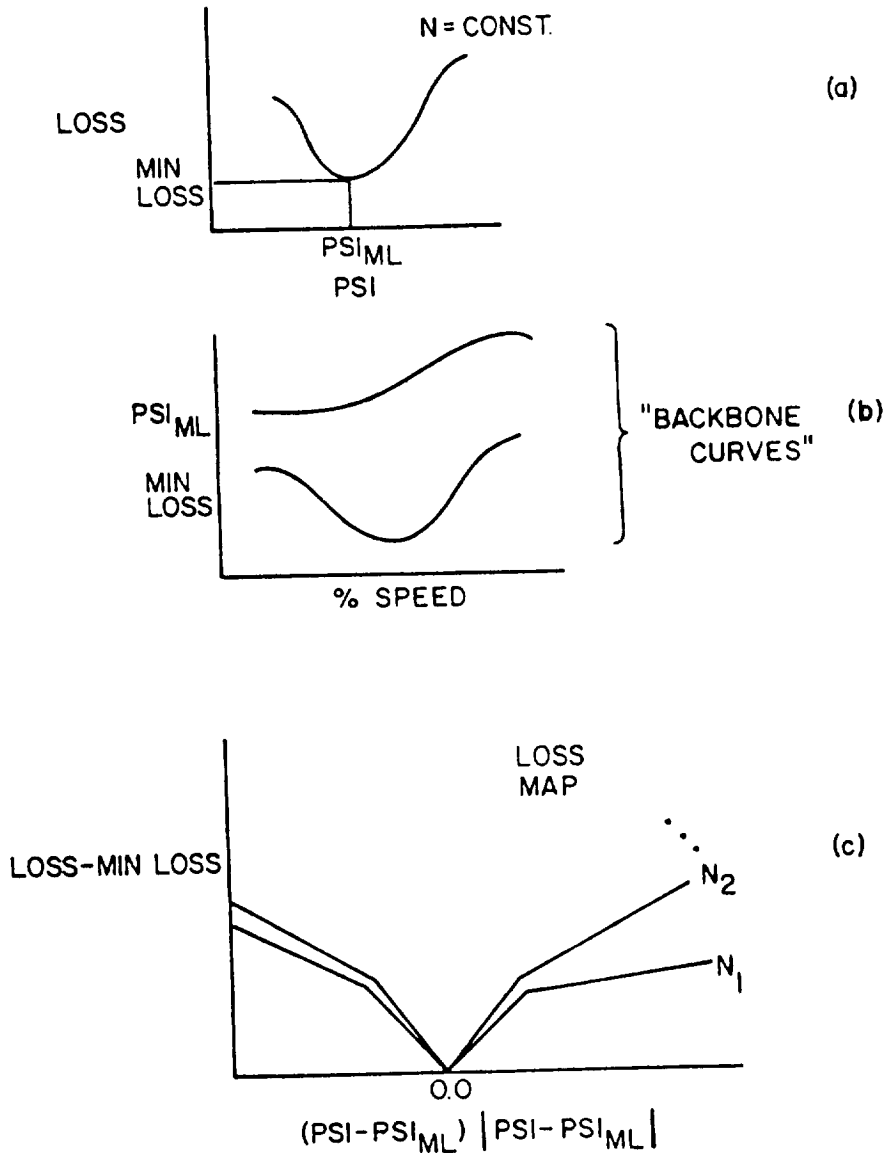

Figure 3 Schematic of Compressor Performance Maps.
(a) Loss vs. Work Coefficient
(b) Minimum Loss vs. Speed and
Minimum Loss Work Coefficient vs. Speed
(c) Loss-Minimum Loss vs. (Work Coefficient-
Minimum Loss Work Coefficient) Squared
(d) Minimum Loss Flow Coefficient vs. Speed
(e) Pseudo-Mach Number vs. (Work Coefficient-
Minimum Loss Work Coefficient)

... Continued on page 60 ...

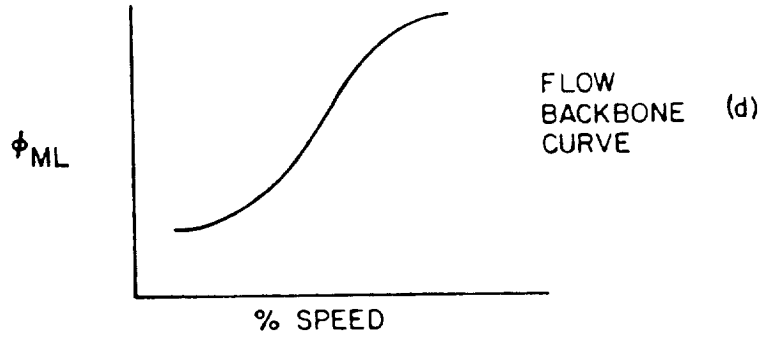

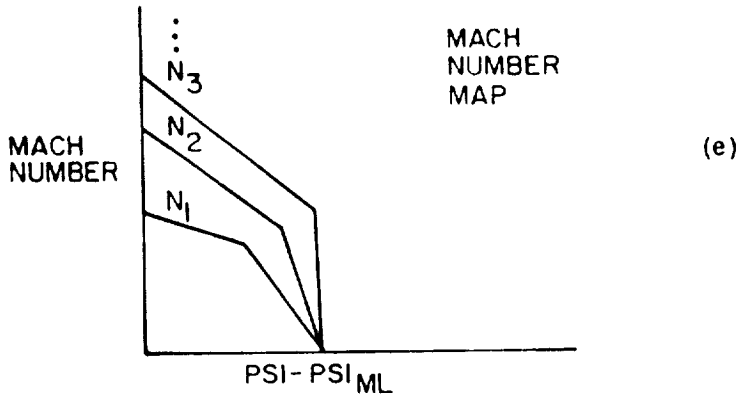

Figure 3, continued

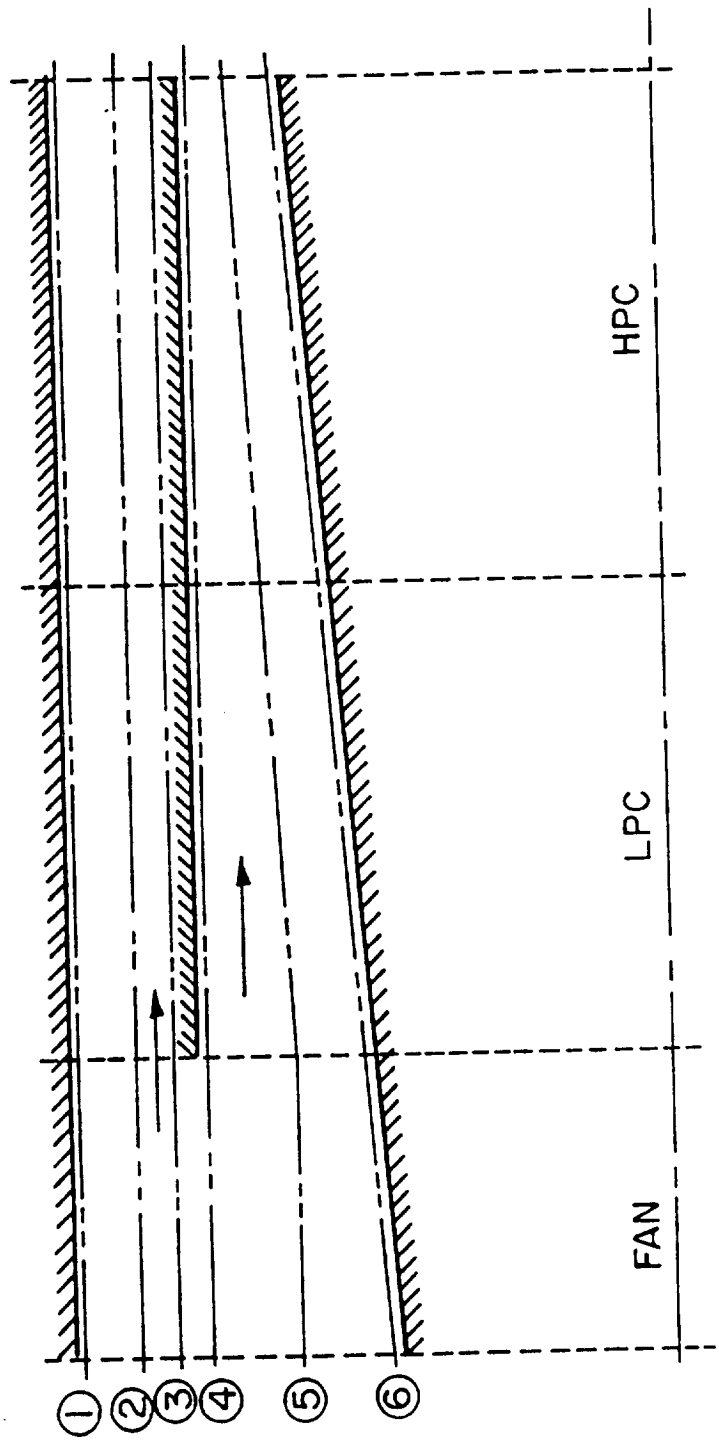

Figure 4 Streamtube Designation in Compressor

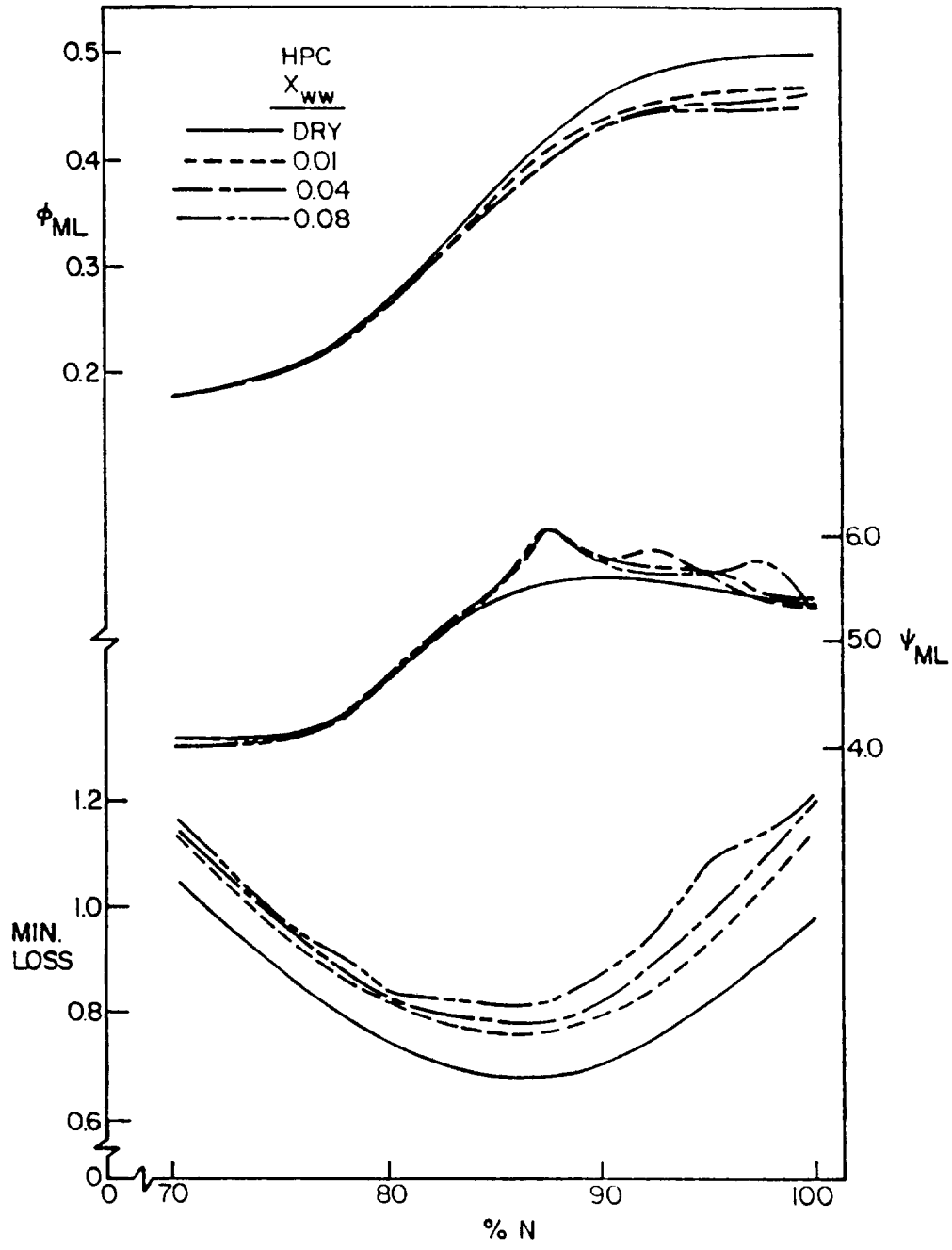

Figure 5.1 High Pressure Compressor Performance Representation: "Backbone" Curves (MIN LOSS, ψ_{ml}, and ϕ_{ml} vs. speed)

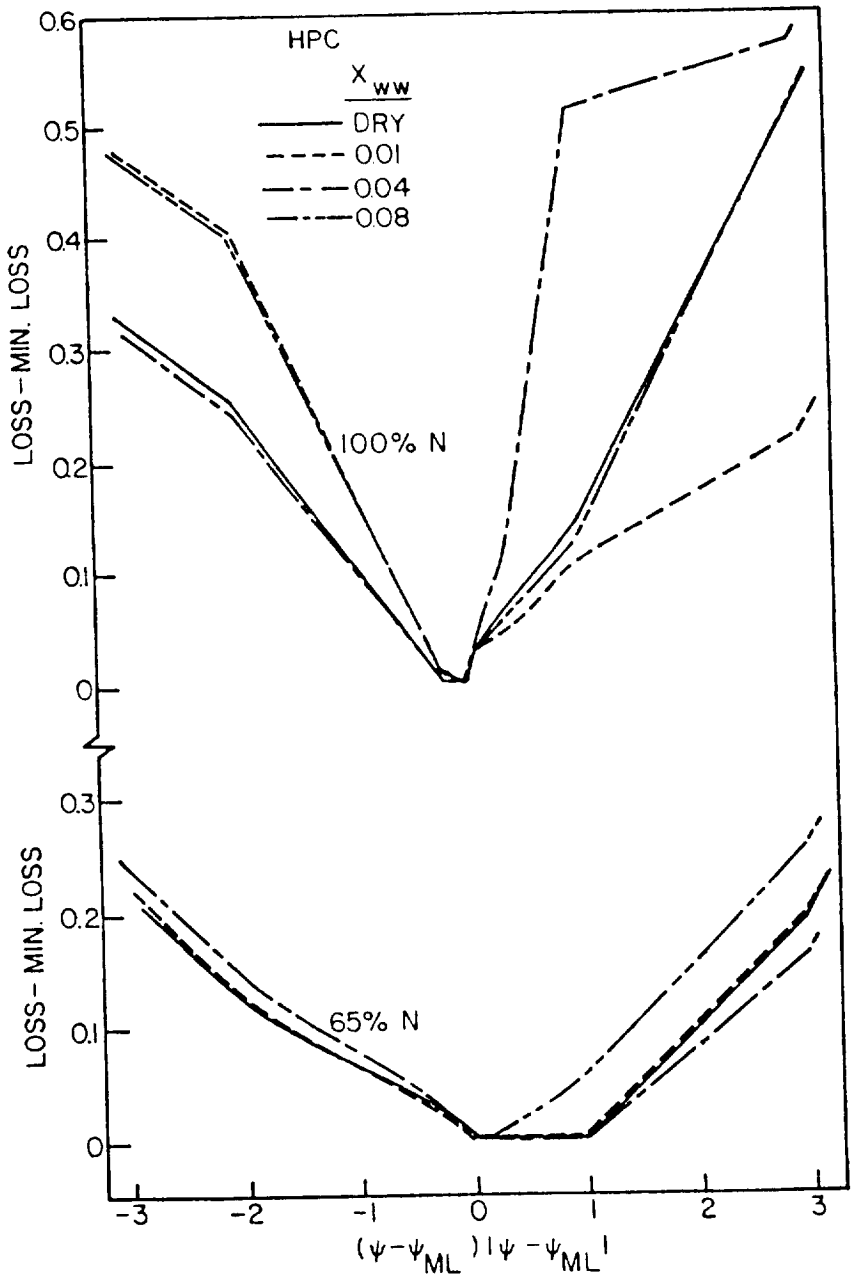

Figure 5.2 High Pressure Compressor Performance Representation: "Off-Backbone" Curves (LOSS-MIN LOSS vs. $(\psi-\psi_{ml})/|\psi-\psi_{ml}|$ for 65 per cent and 100 per cent Design Speed)

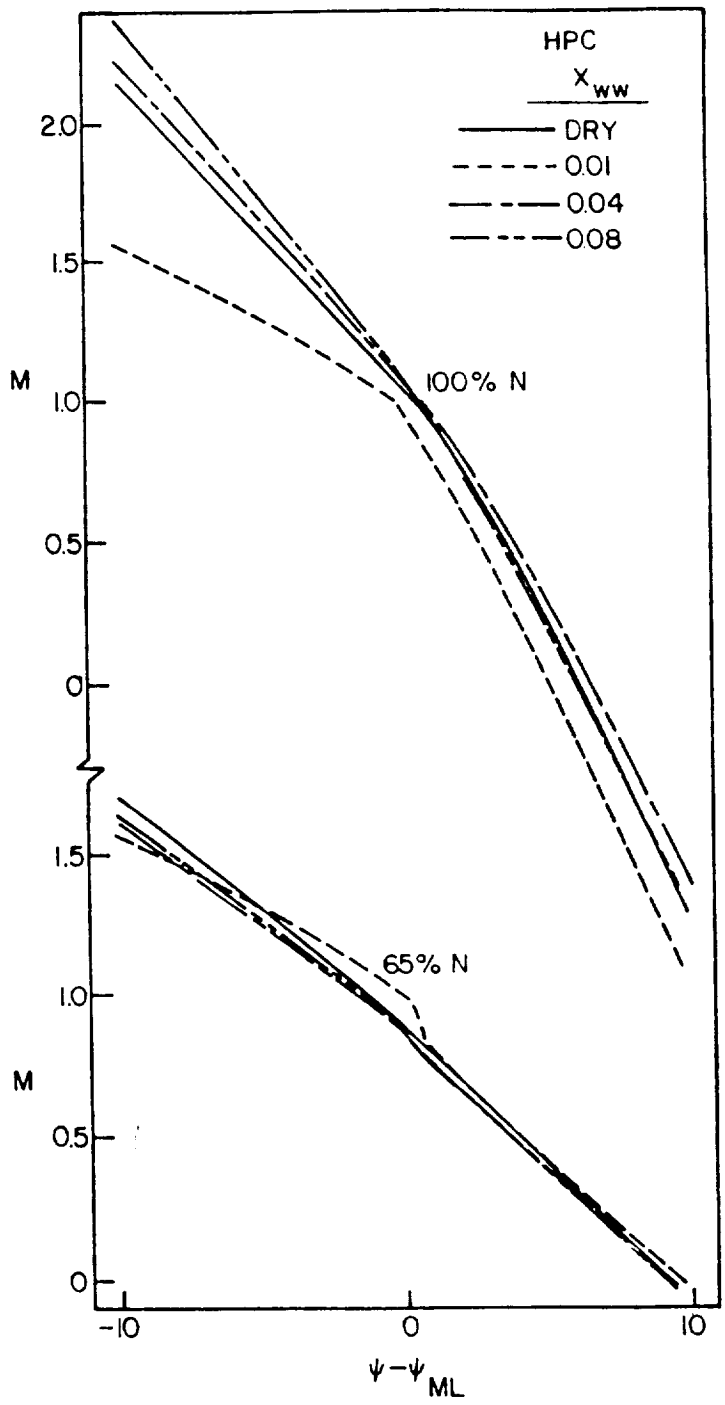

Figure 5.3 High Pressure Compressor Performance Representation: Mach Number Map (M vs. $(\psi-\psi_{ml})$ for 65 per cent and 100 per cent Design Speed)

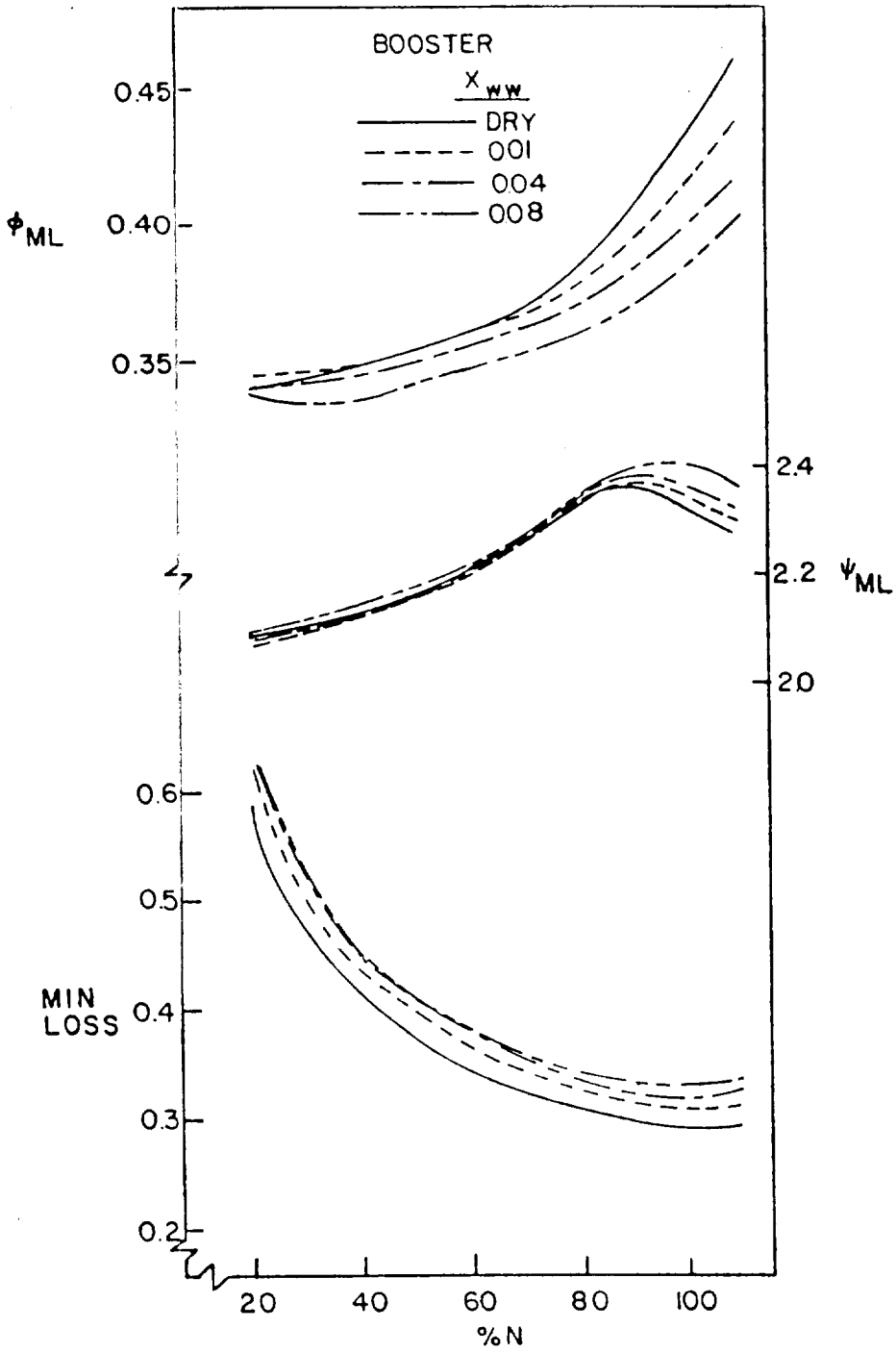

Figure 6.1 Booster Performance Representation: "Backbone" Curves (MIN LOSS, ψ_{ml}, and ϕ_{ml} vs. Speed)

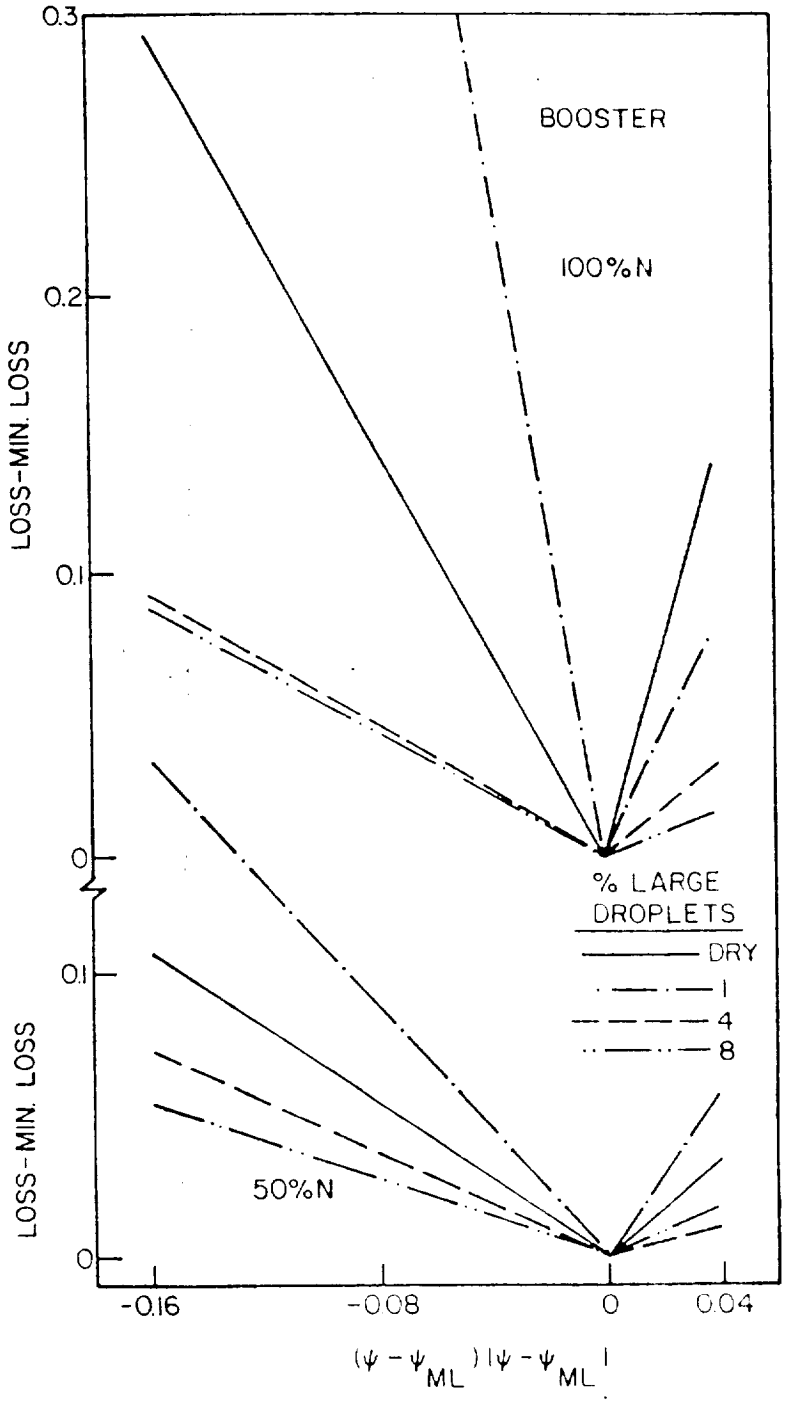

Figure 6.2 Booster Performance Representation: "Off-Backbone" Curves (LOSS-MIN LOSS vs. $(\psi-\psi_{ml})|\psi-\psi_{ml}|$ for 50 per cent and 100 per cent Design Speed)

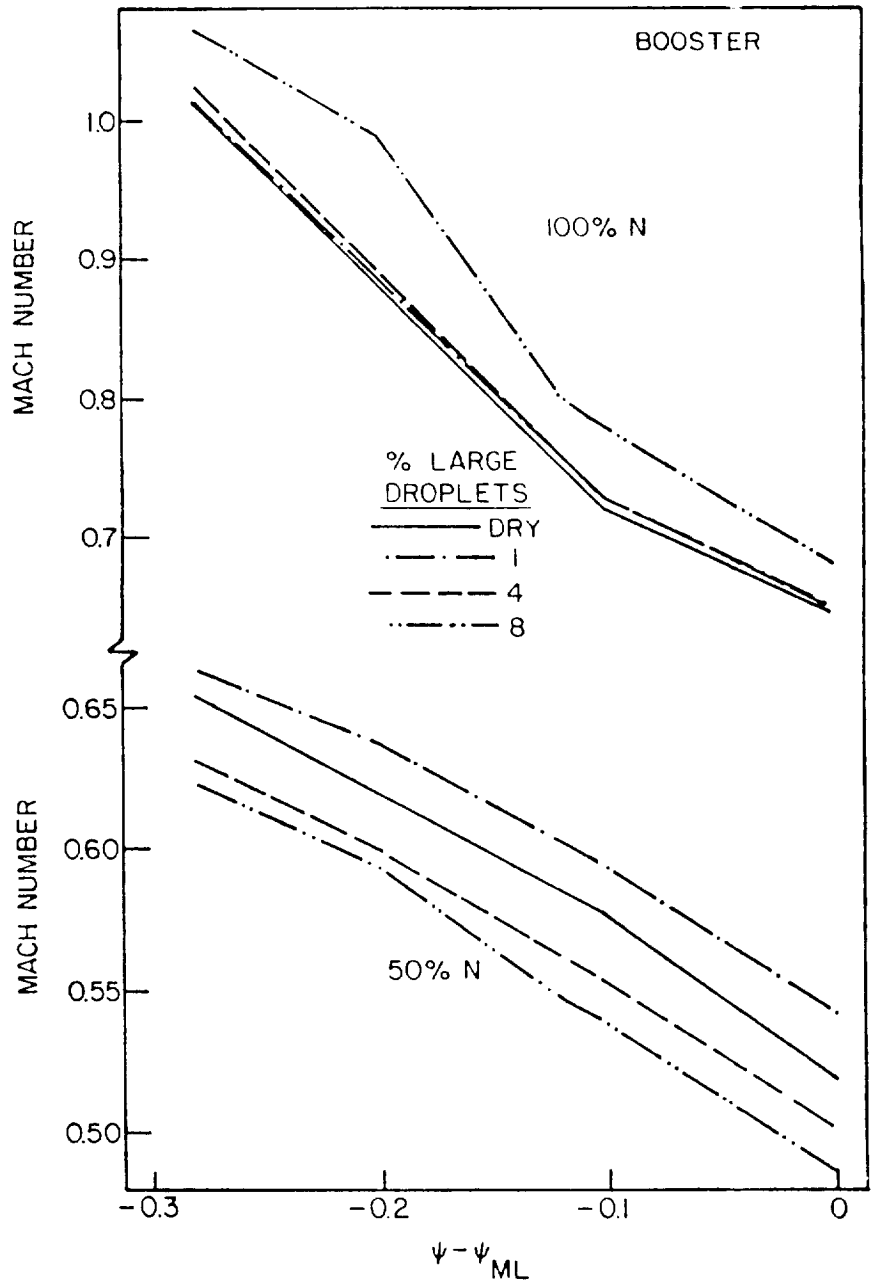

Figure 6.3 Booster Performance Representation: Mach Number Maps (M vs. $(\psi-\psi_{m_1})$ for 50 per cent and 100 per cent Design Speed)

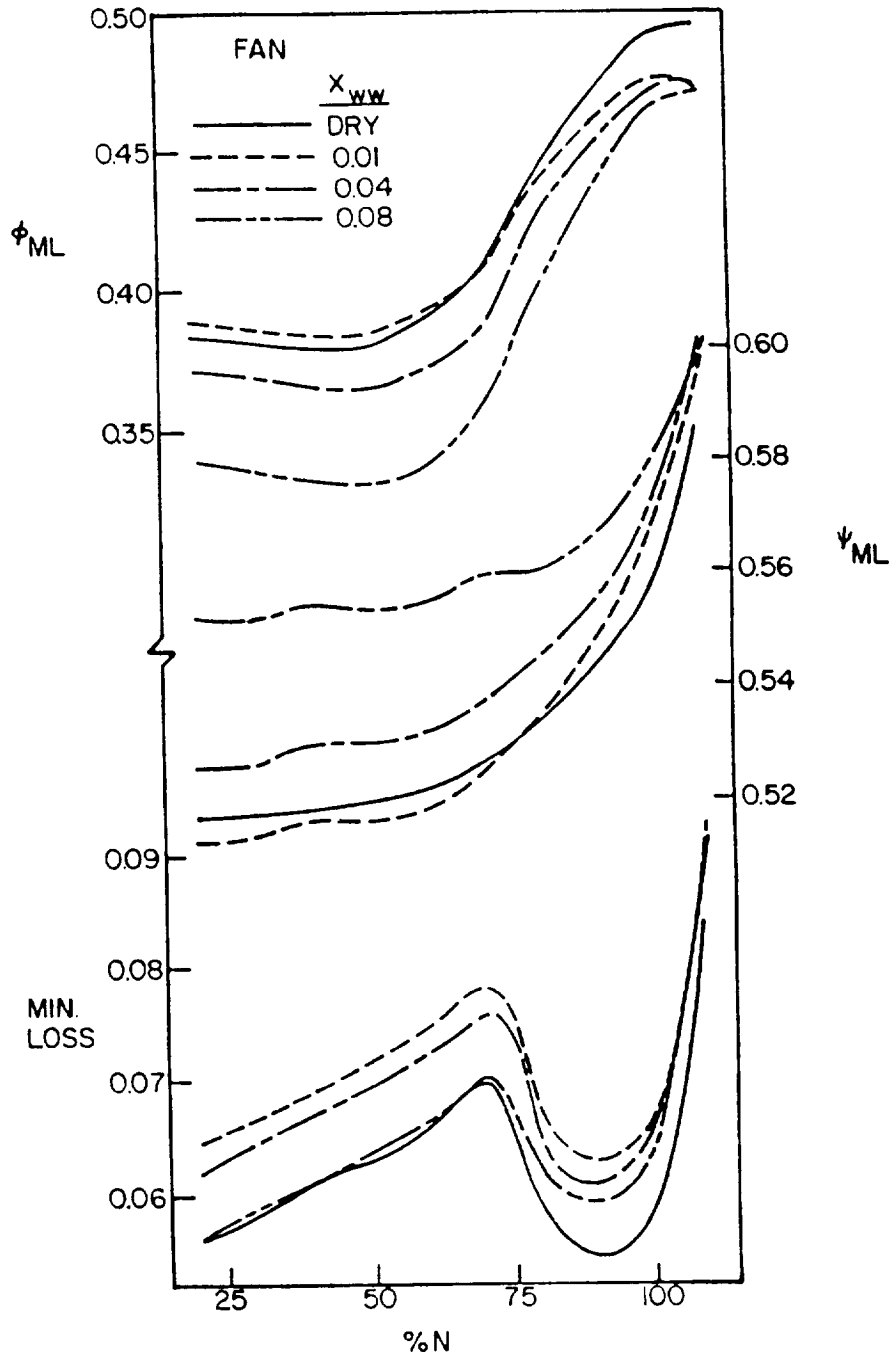

Figure 7.1 Fan Bypass Performance Representation: "Backbone" Curves (MIN LOSS, ψ_{ml}, and ϕ_{ml} vs. Speed)

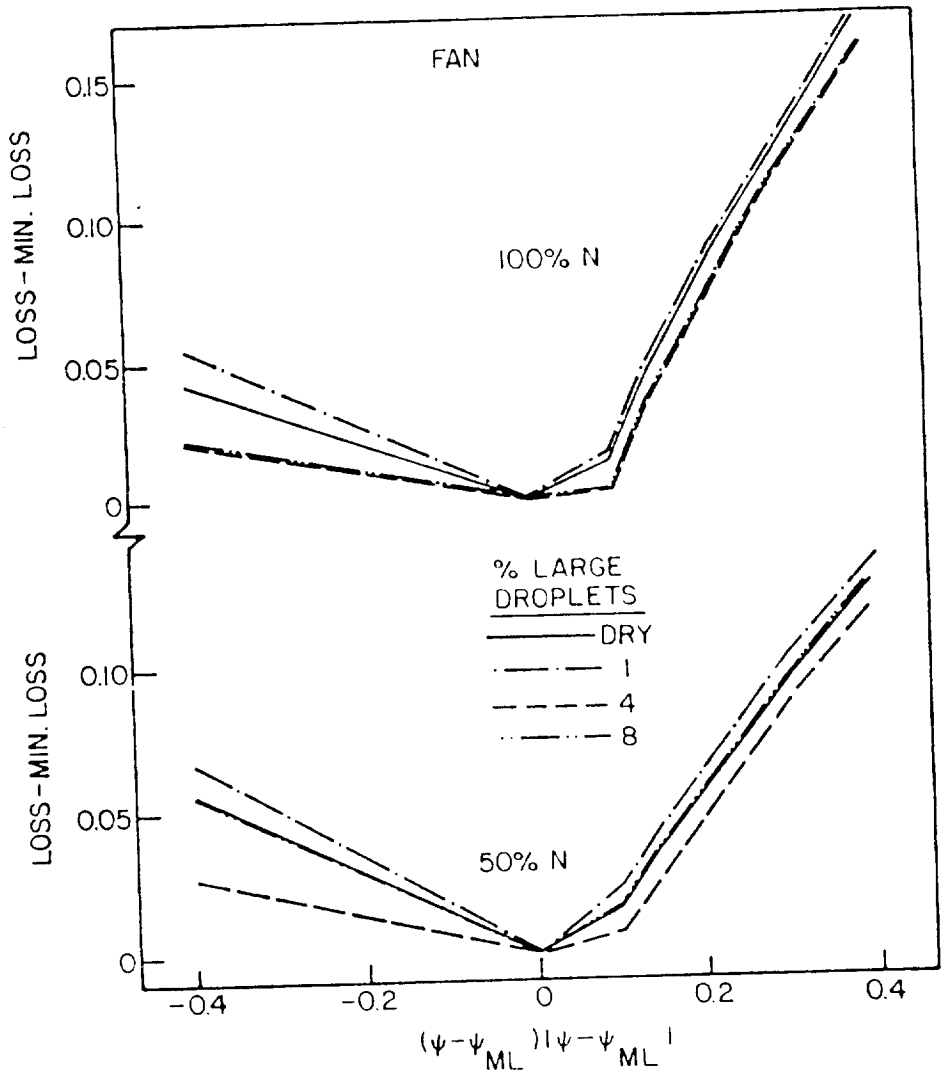

Figure 7.2 Fan Bypass Performance Representation: "Off-Backbone" Curves (LOSS-MIN LOSS vs. $(\psi-\psi_m)/|\psi-\psi_m|$ for 50 per cent and 100 per Design Speed)

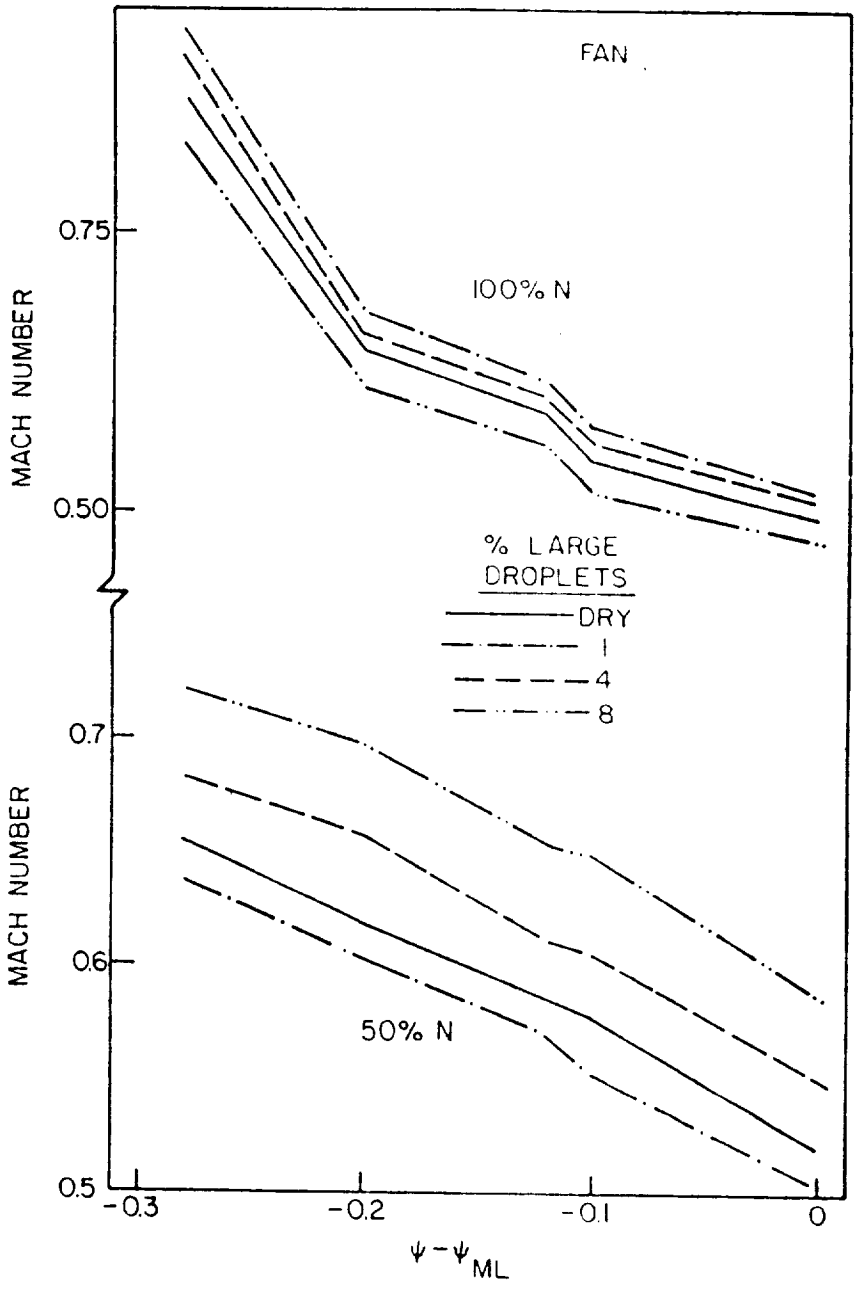

Figure 7.3 Fan Bypass Performance Representation: Mach Number Maps (M vs. (ψ-ψ_{ml}) for 50 per cent and 100 per cent Design Speed)

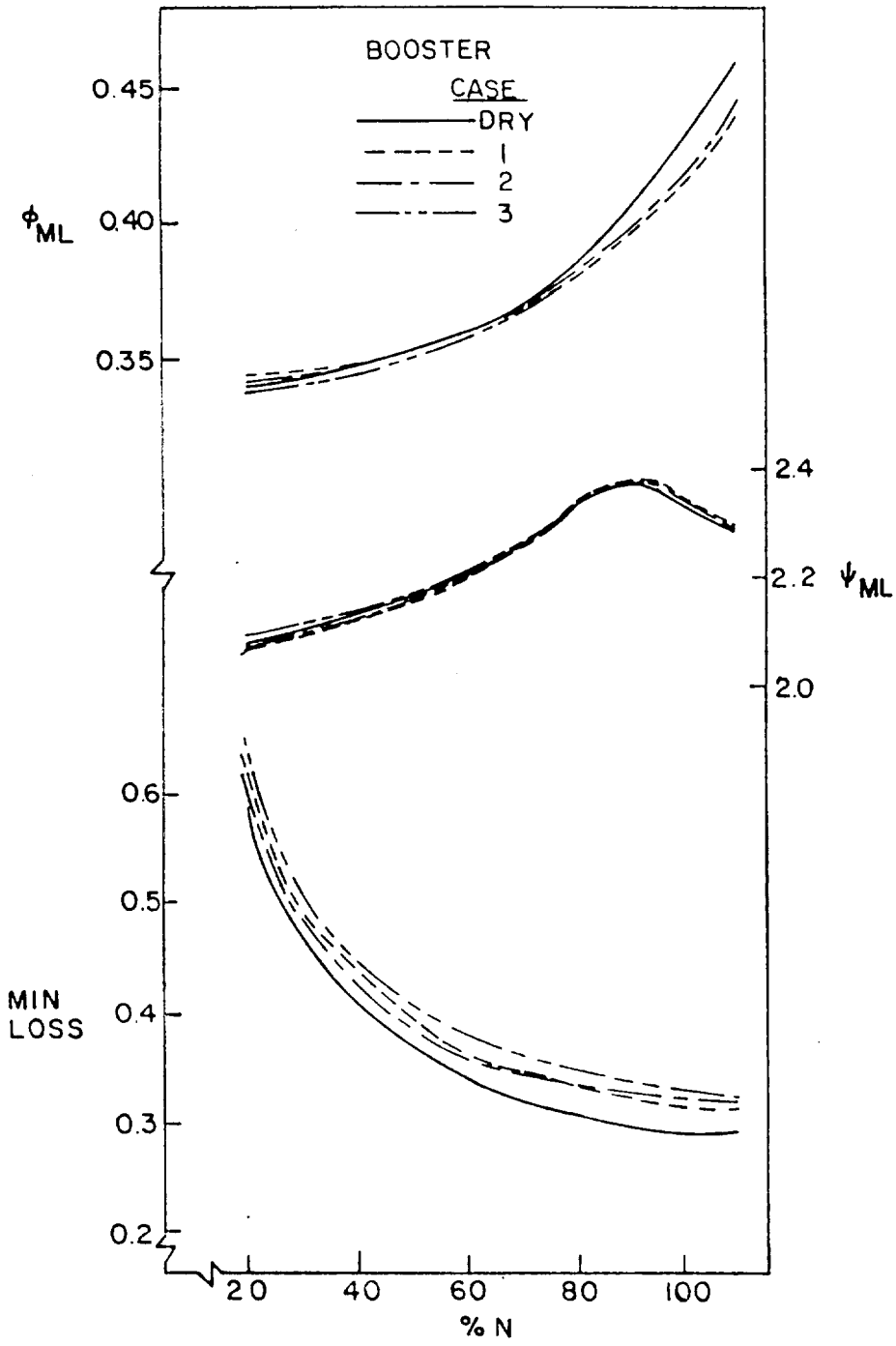

Figure 8 Booster "Backbone" Curves with Isolated Centrifugal Action and Transport Processes

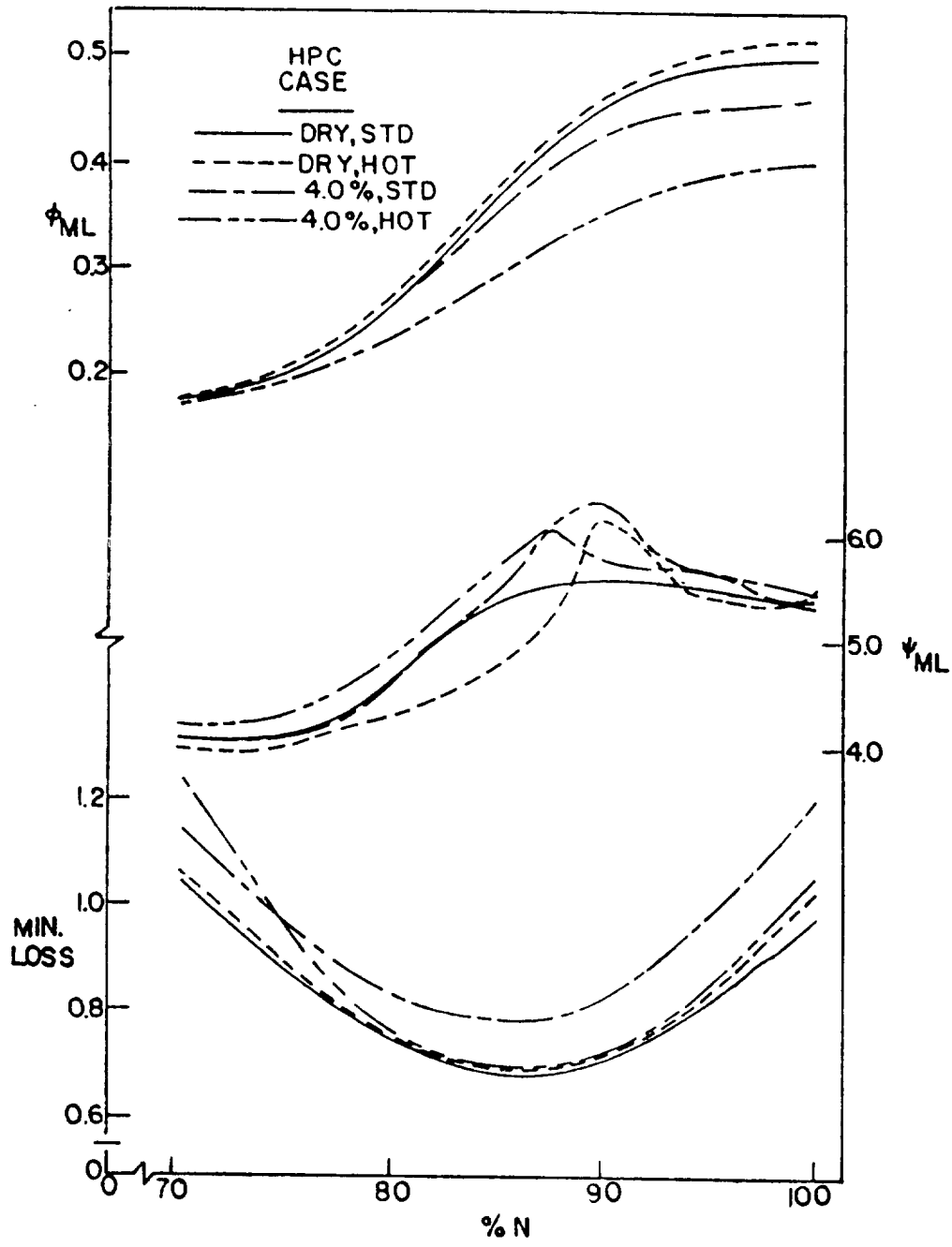

Figure 9.1 High Pressure Compressor Performance Representation: "Backbone" Curves (MIN LOSS, ψ_{ml}, and ϕ_{ml} vs. Speed) for Hot Day Conditions

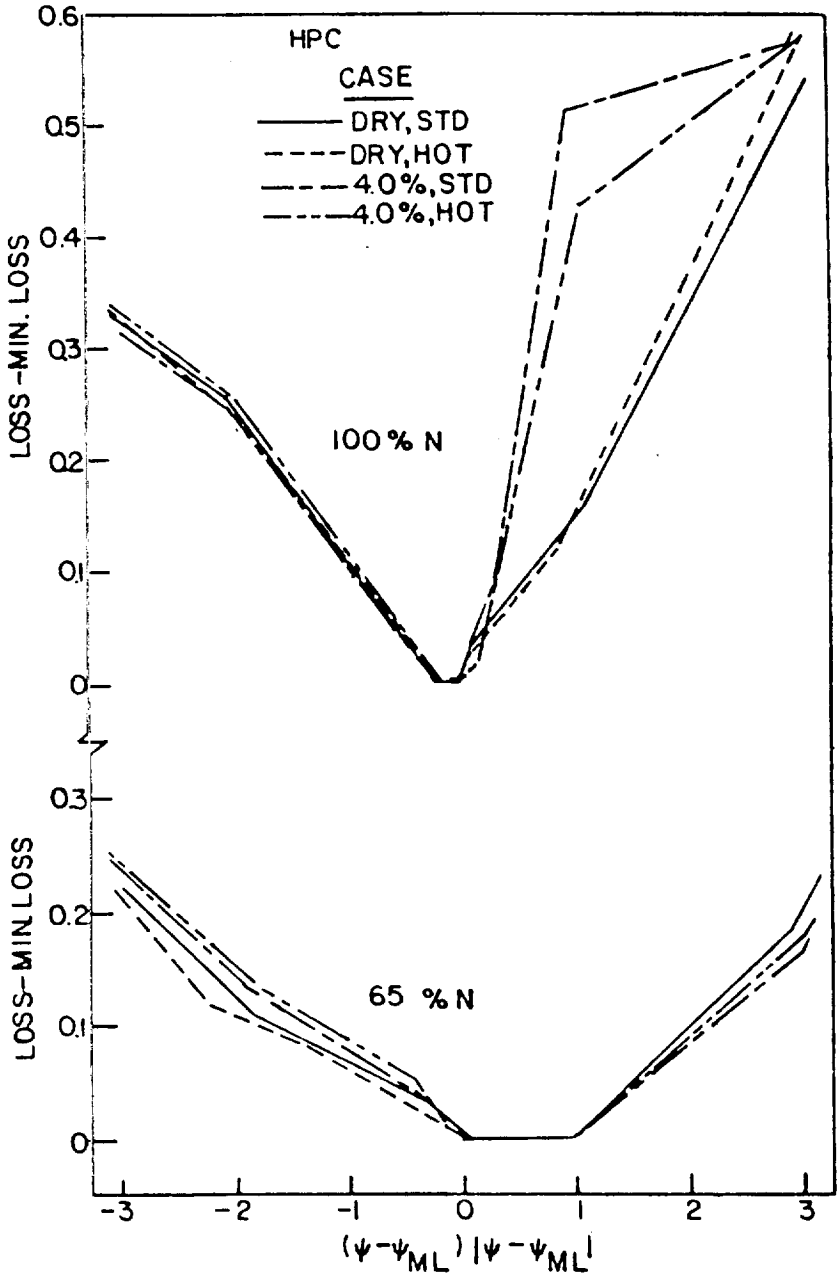

Figure 9.2 High Pressure Compressor Performance Representation: "Off-Backbone" Curves (LOSS-MIN LOSS vs. $(\psi-\psi_{ml})|\psi-\psi_{ml}|$ for 65 per cent and 100 per cent Design Speed) for Hot Day Conditions

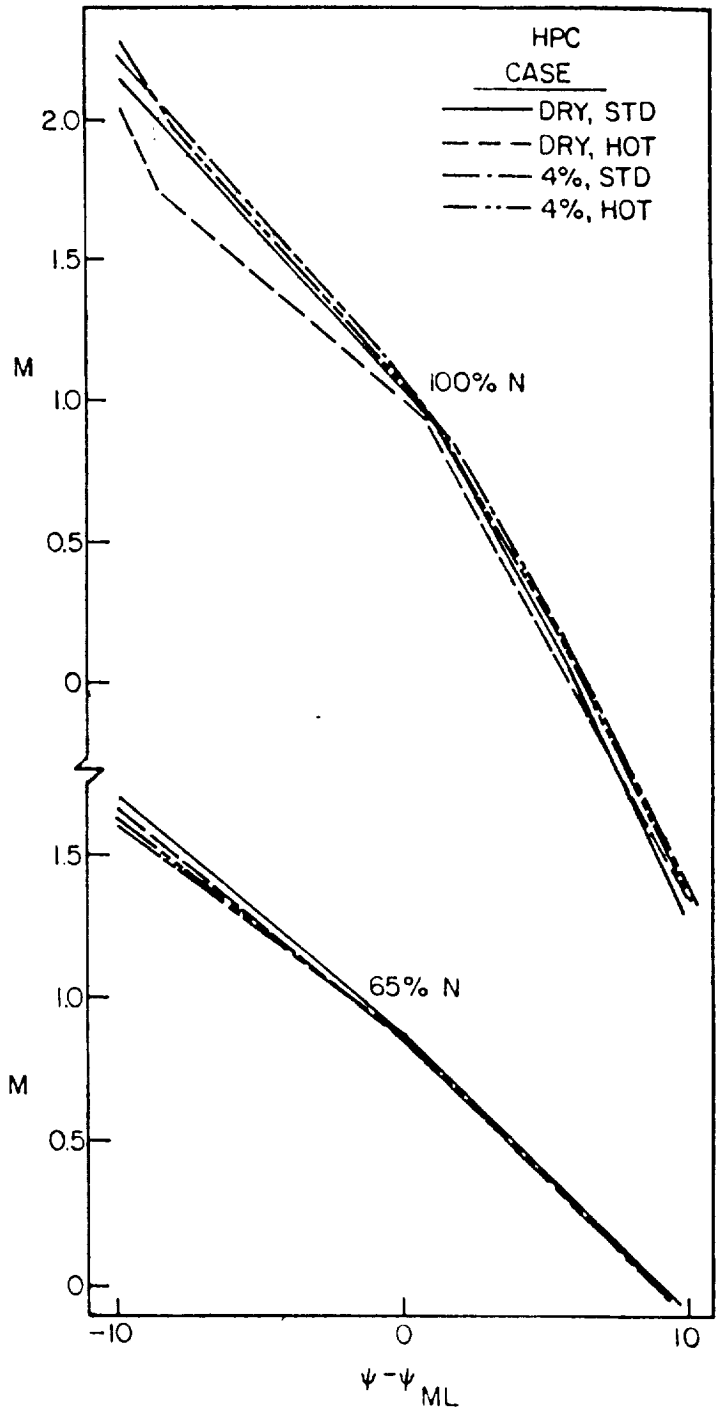

Figure 9.3 High Pressure Compressor Performance Representation: Mach Number Maps (M vs. $(\psi - \psi_{m_1})$ for 65 per cent and 100 per cent Design Speed) for Hot Day Conditions

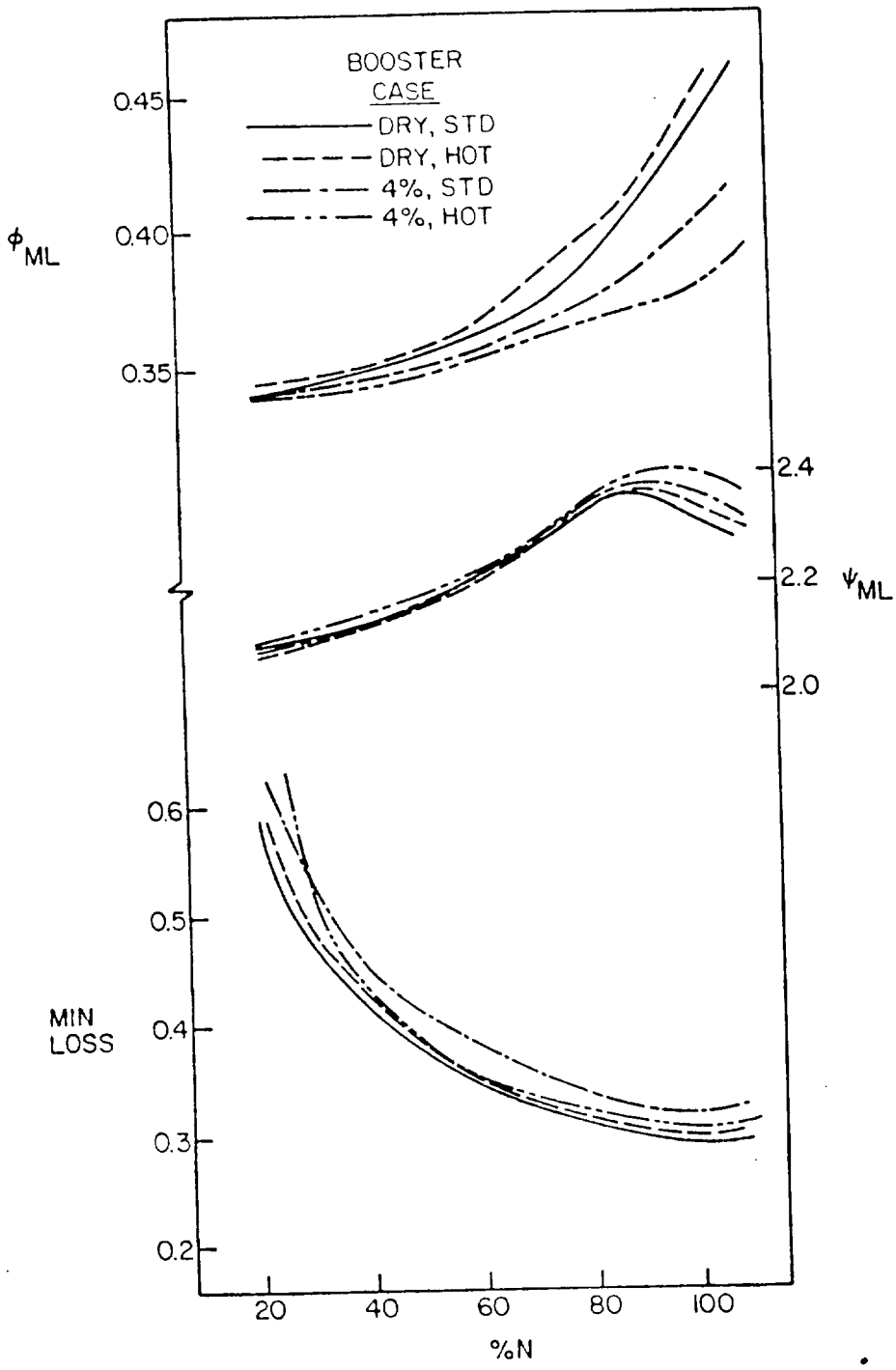

Figure 10.1 Booster Performance Representation: "Backbone" Curves (MIN LOSS, ψ_{ml}, and ϕ_{ml} vs. Speed) for Hot Day Conditions

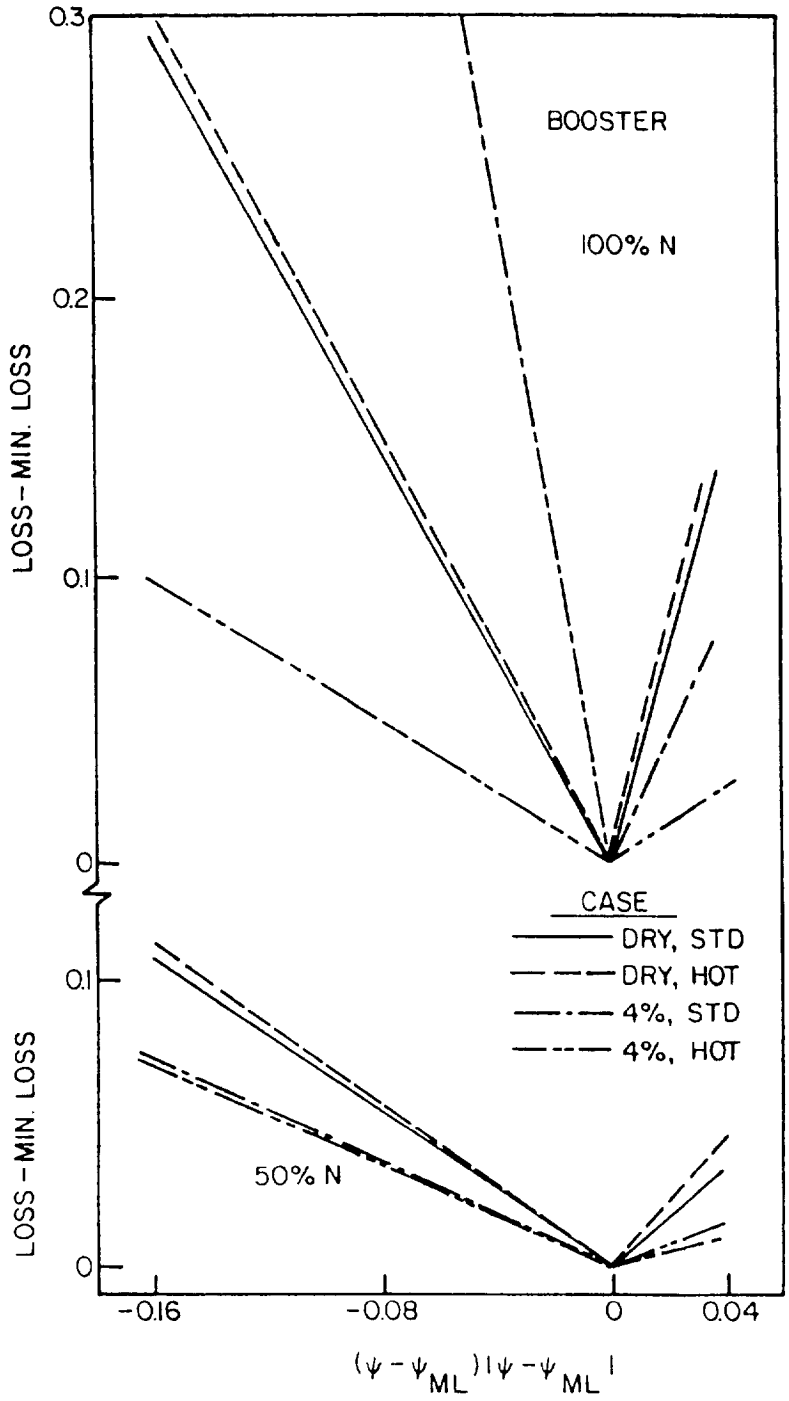

Figure 10.2 Booster Performance Representation: "Off-Backbone" Curves (LOSS-MIN LOSS vs. $(\psi-\psi_{mi})/|\psi-\psi_{mi}|$ for 50 per cent and 100 per cent Design Speed) for Hot Day Conditions

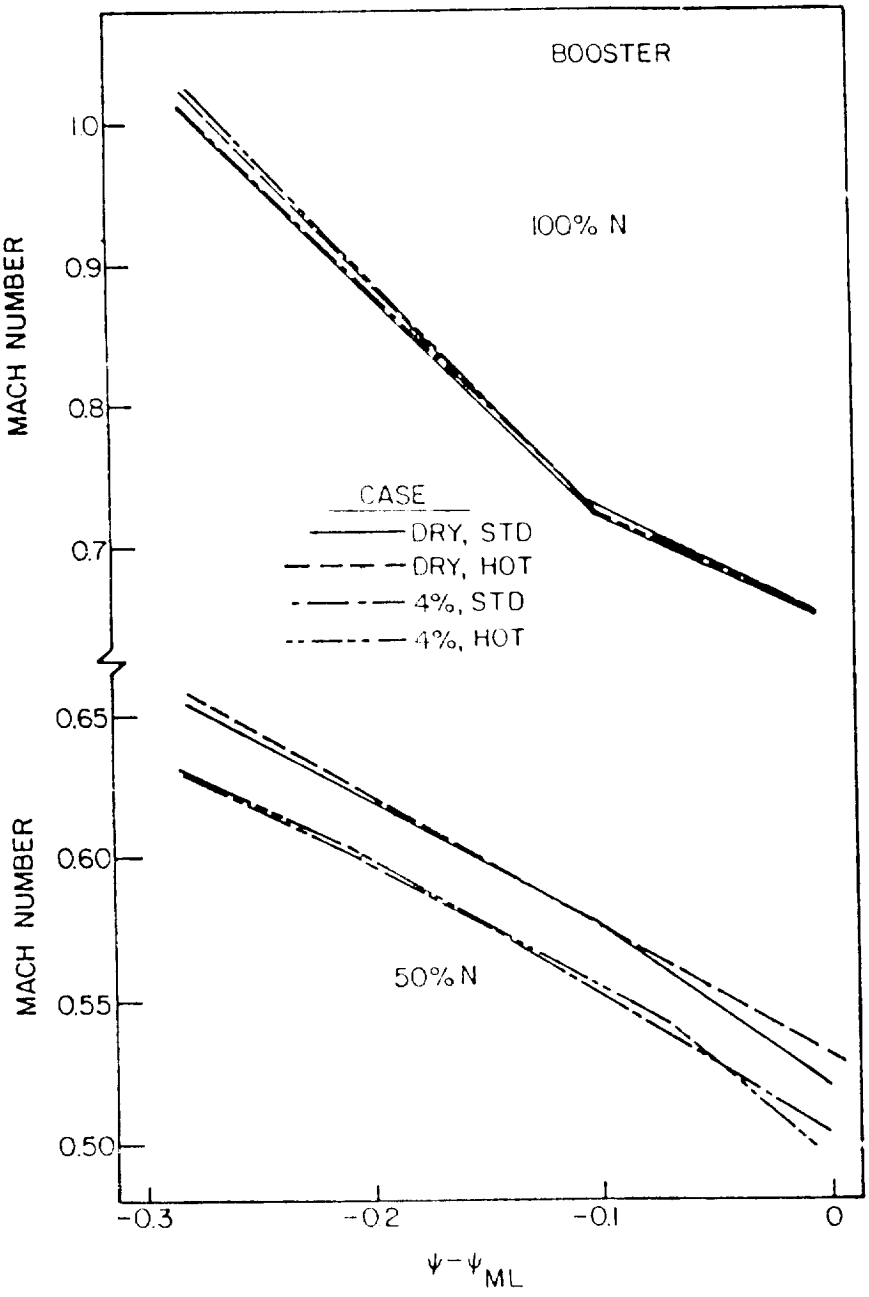

Figure 10.3 Booster Performance Representation: Mach Number Maps (M vs. $(\psi-\psi_m)$) for 50 per cent and 100 per cent Design Speed) for Hot Day Conditions

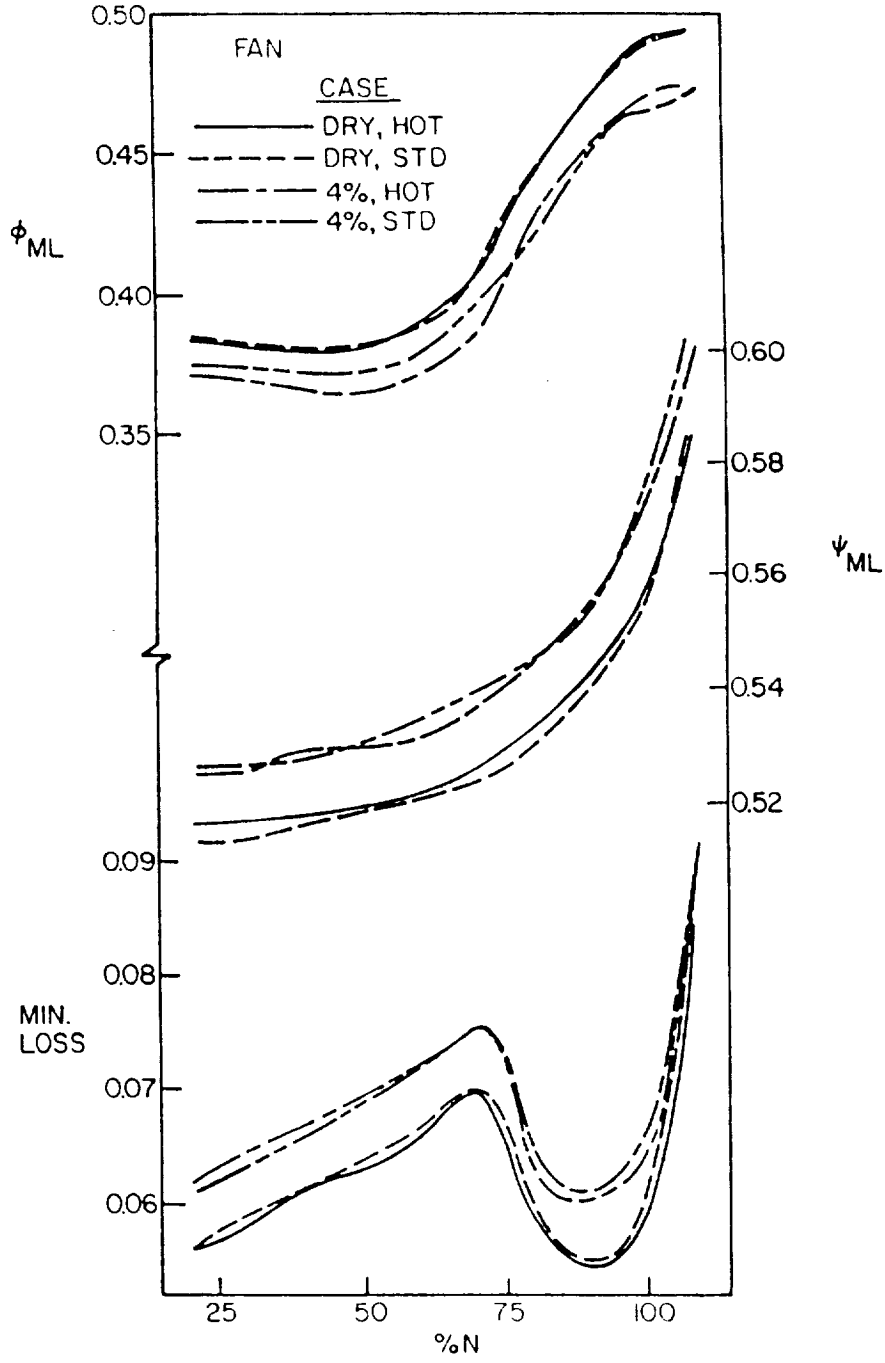

Figure 11.1 Fan Bypass Performance Representation: "Backbone" Curves (MIN LOSS, ψ_{ml}, and ϕ_{ml} vs. Speed) for Hot Day Conditions

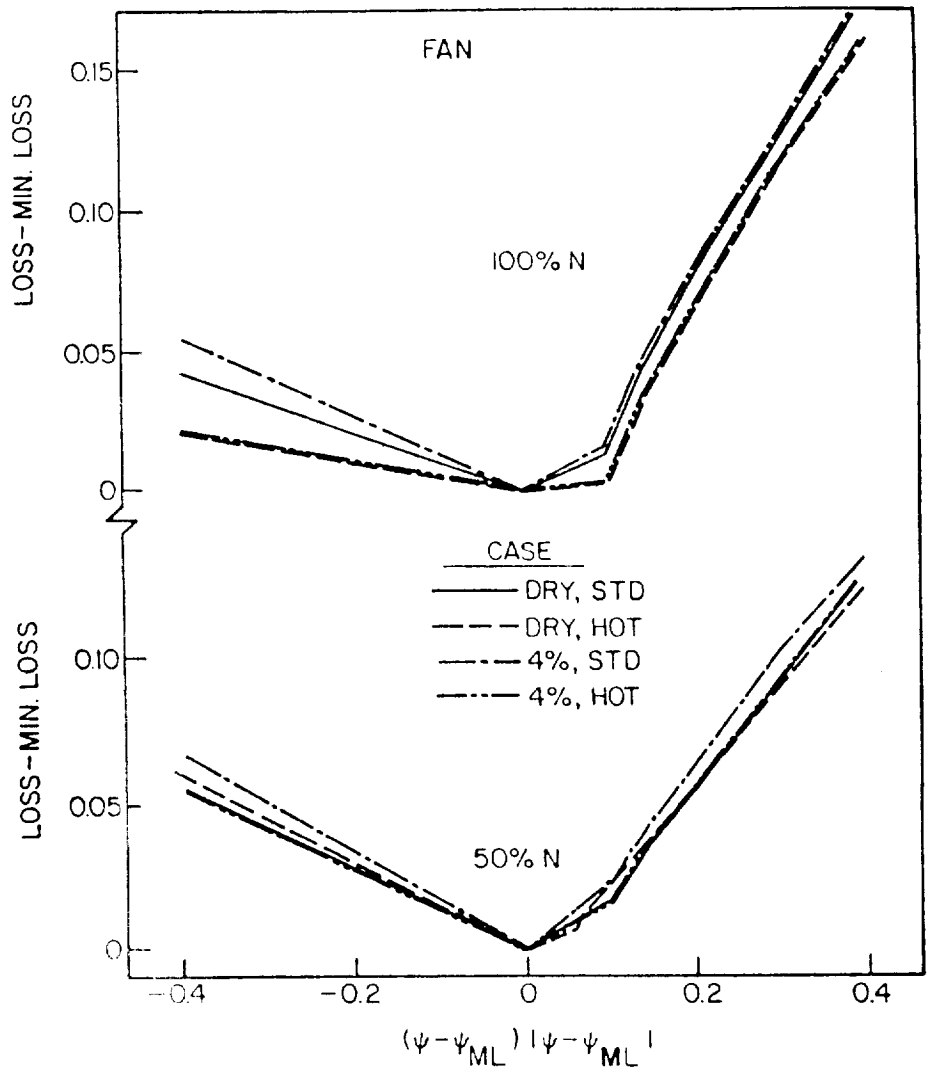

Figure 11.2 Fan Bypass Performance Representation: "Off-Backbone" Curves (LOSS-MIN LOSS vs. $(\psi-\psi_{ml})|\psi-\psi_{ml}|$ for 50 per cent and 100 per cent Design Speed) for Hot Day Conditions

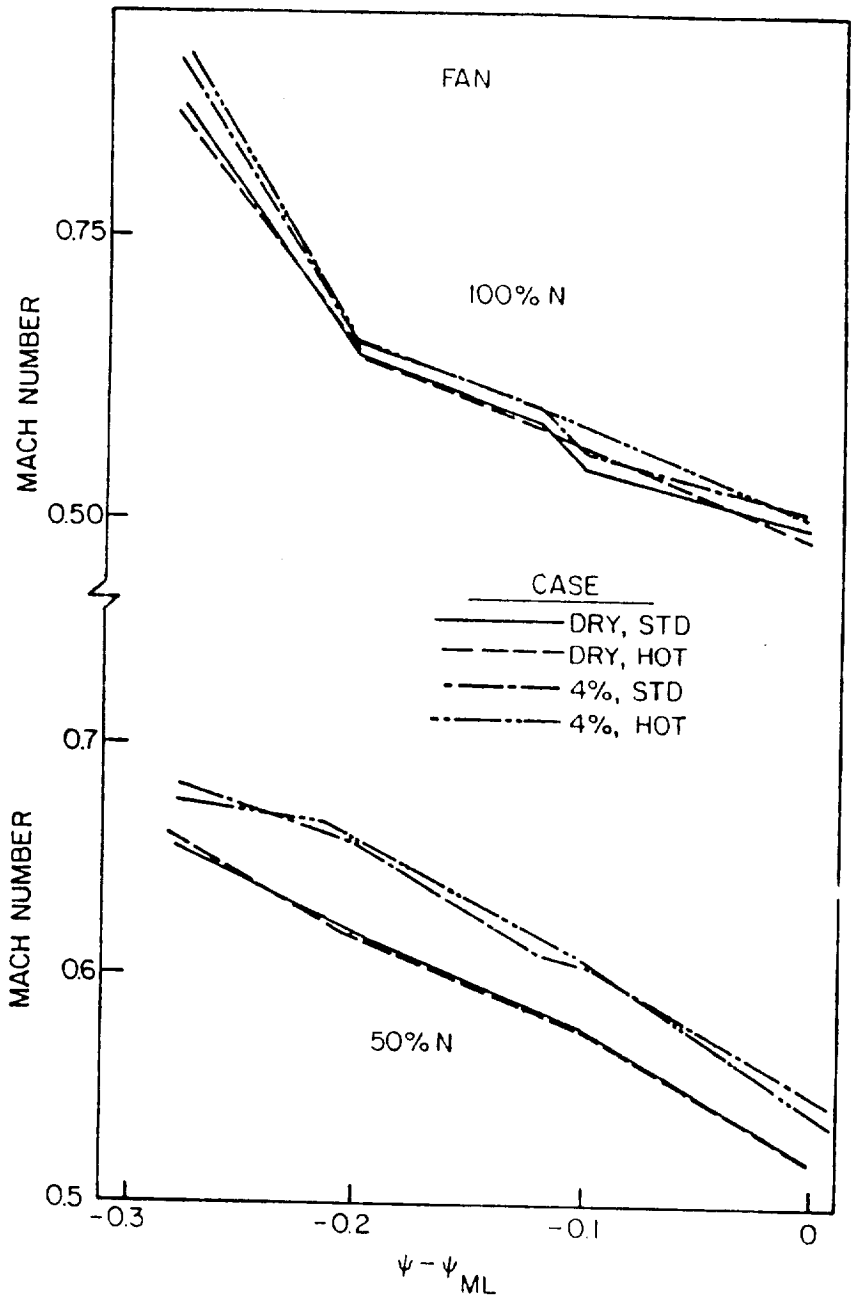

Figure 11.3 Fan Bypass Performance Representation: Mach Number Maps (M vs. (ψ-ψ_{ml}) for 50 per cent and 100 per cent Design Speed) for Hot Day Conditions

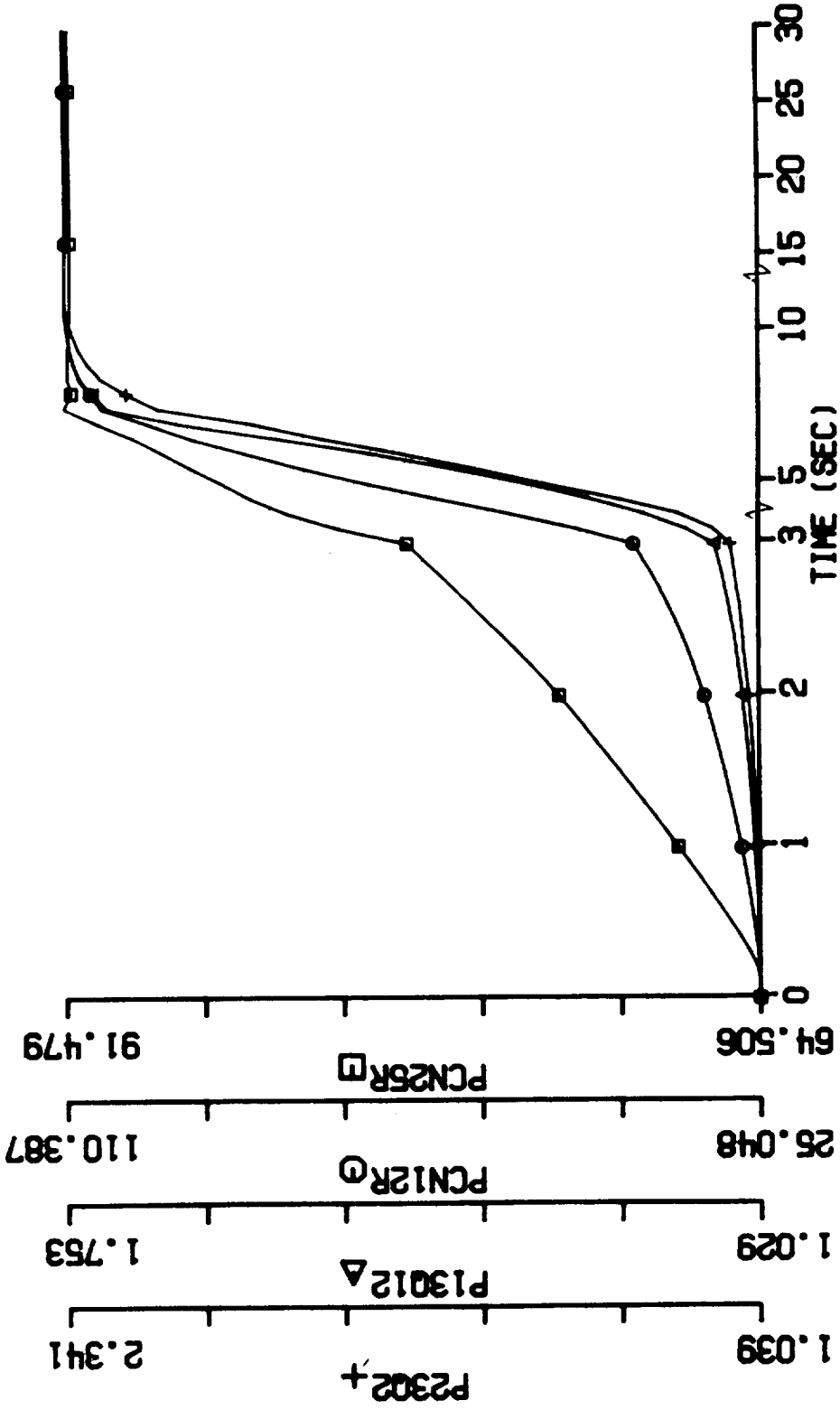

Figure 12.1 Transient Engine Performance: PLA changes from Ground Idle Setting to Max Power Setting, Dry Air Operation, Standard Temperature
(PCN25R, PCN12R, P13Q12, vs. Time)

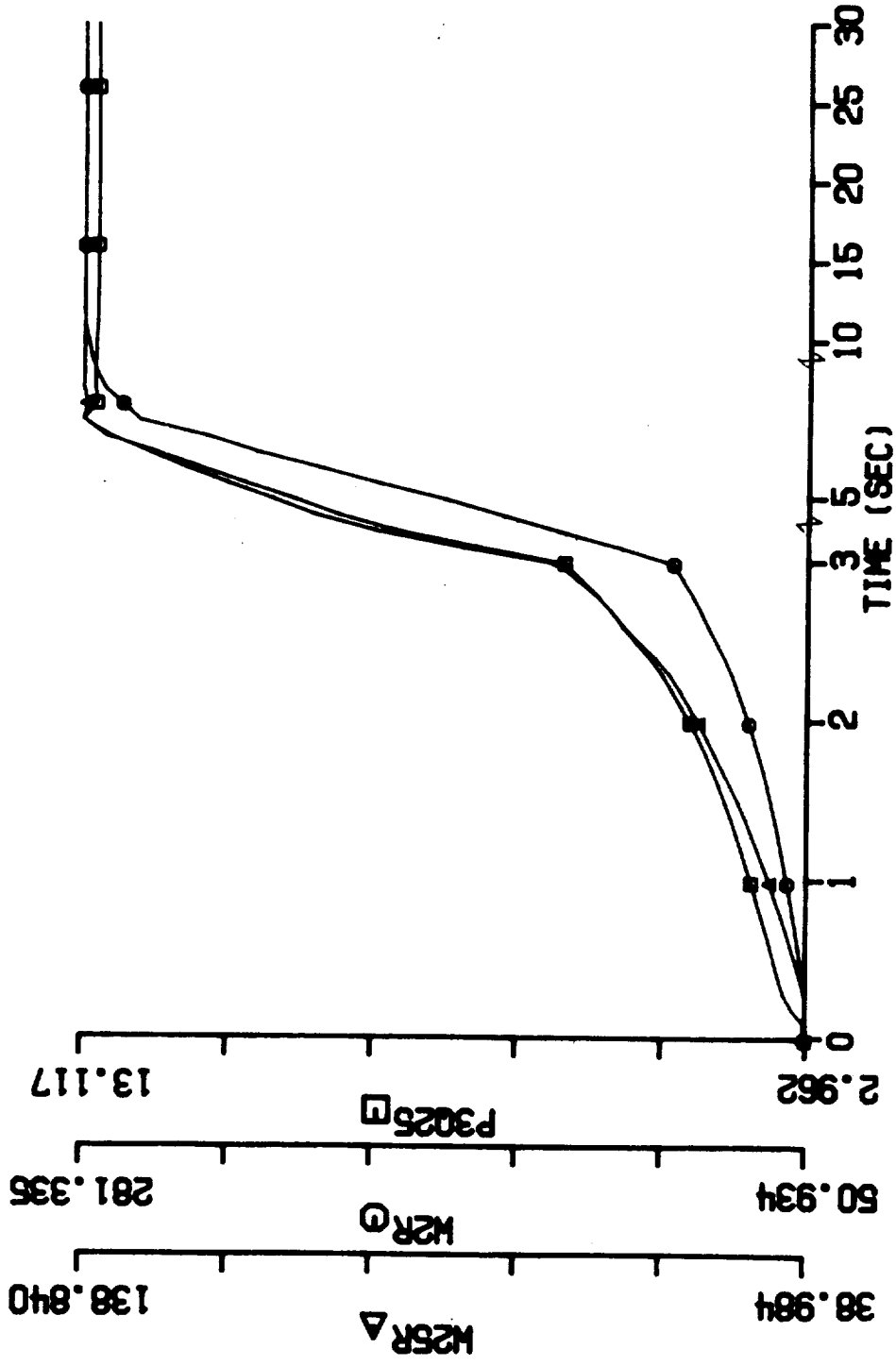

Figure 12.2 Transient Engine Performance: PLA changes from Ground Idle Setting to Max Power Setting, Dry Air Operation, Standard Temperature
(P3Q25, W2R, W25R vs. time)

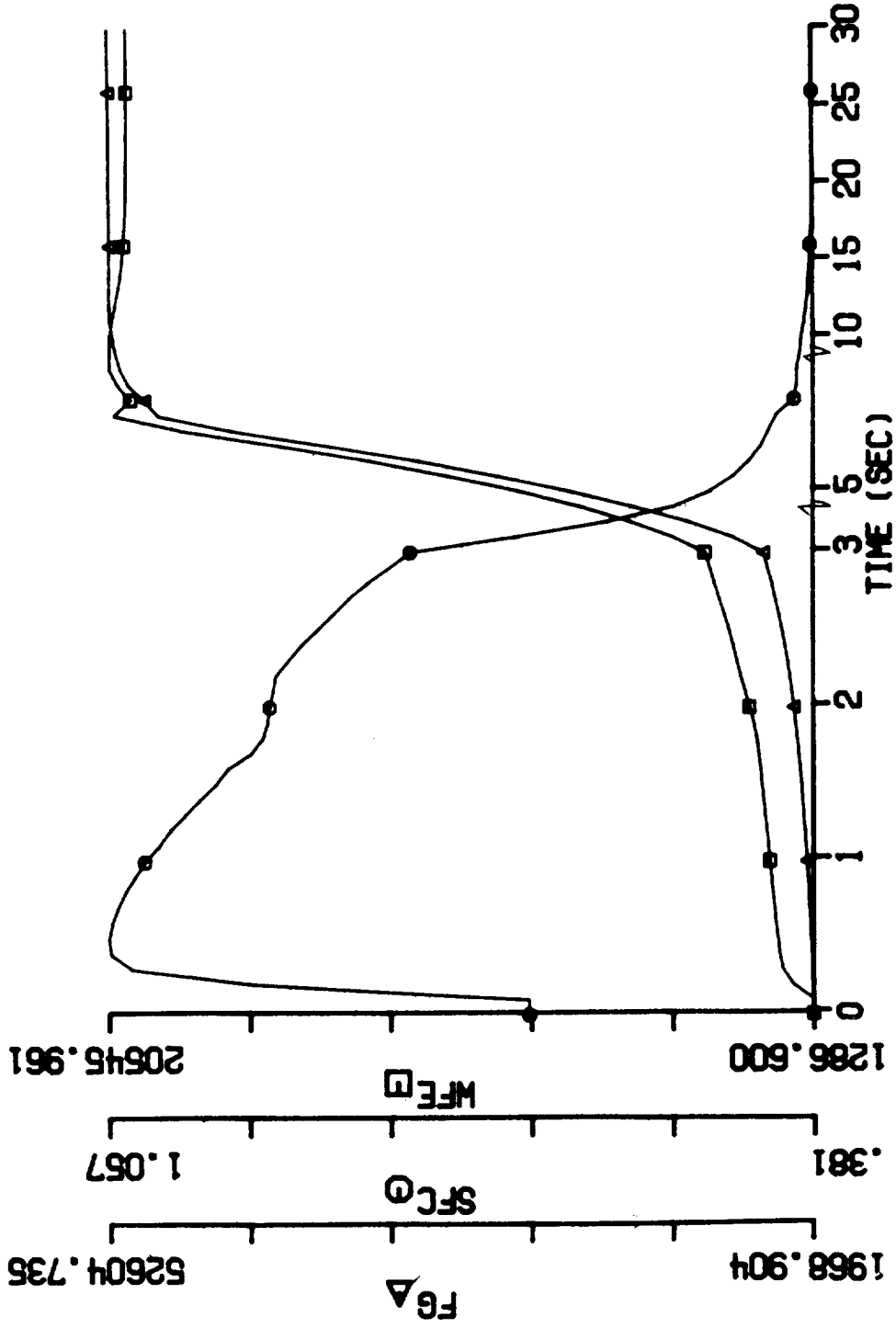

Figure 12.3 Transient Engine Performance: PLA changes from Ground Idle Setting to Max Power Setting, Dry Air Operation, Standard Temperature
(WFE, SFC, FG vs. time)

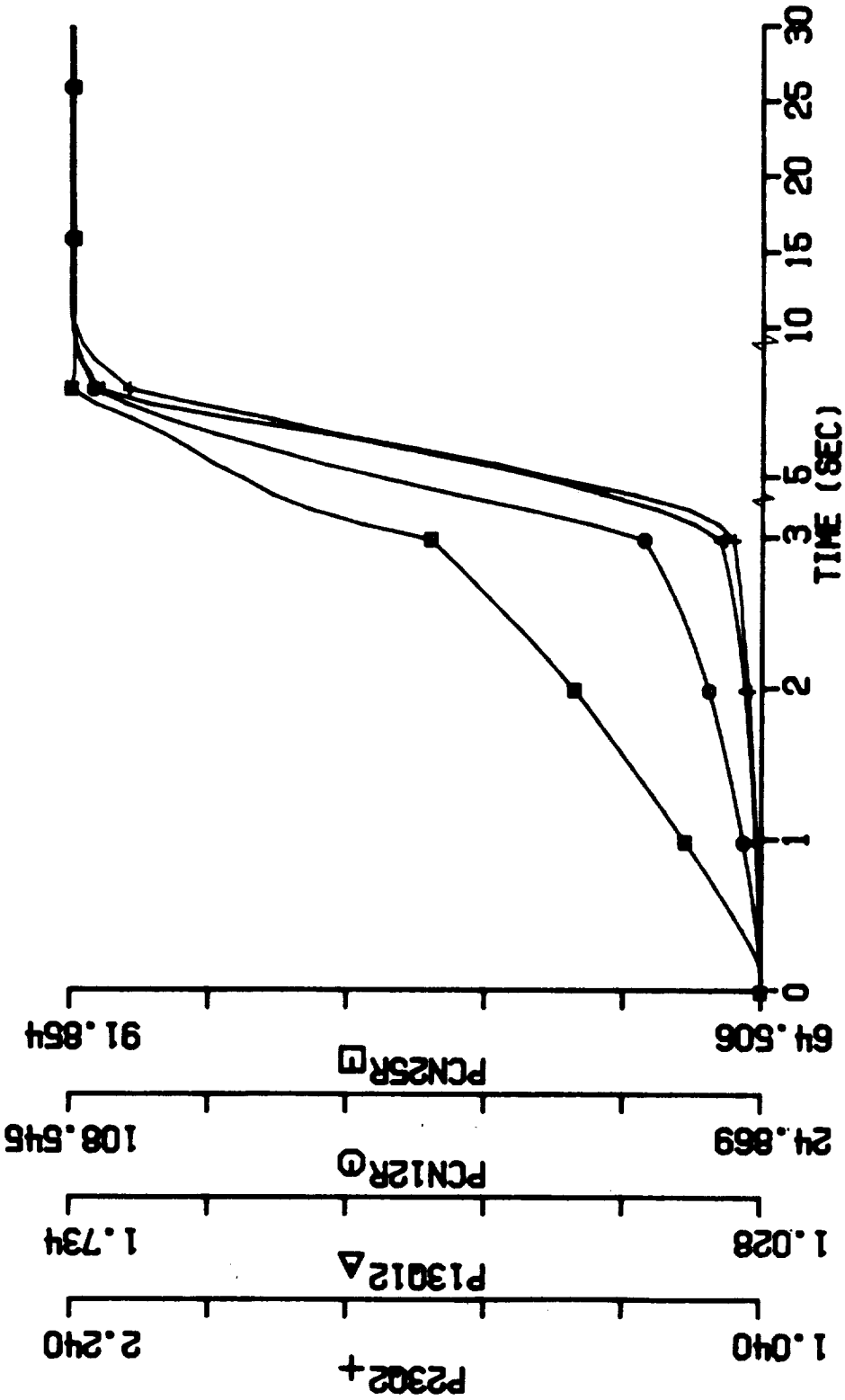

Figure 13.1 Transient Engine Performance: PLA changes from Ground Idle Setting to Max Power Setting, 1% water ingestion with all liquid drained, standard temperature (PCN25R, PCN12, P13Q12R, P23Q2, vs. time)

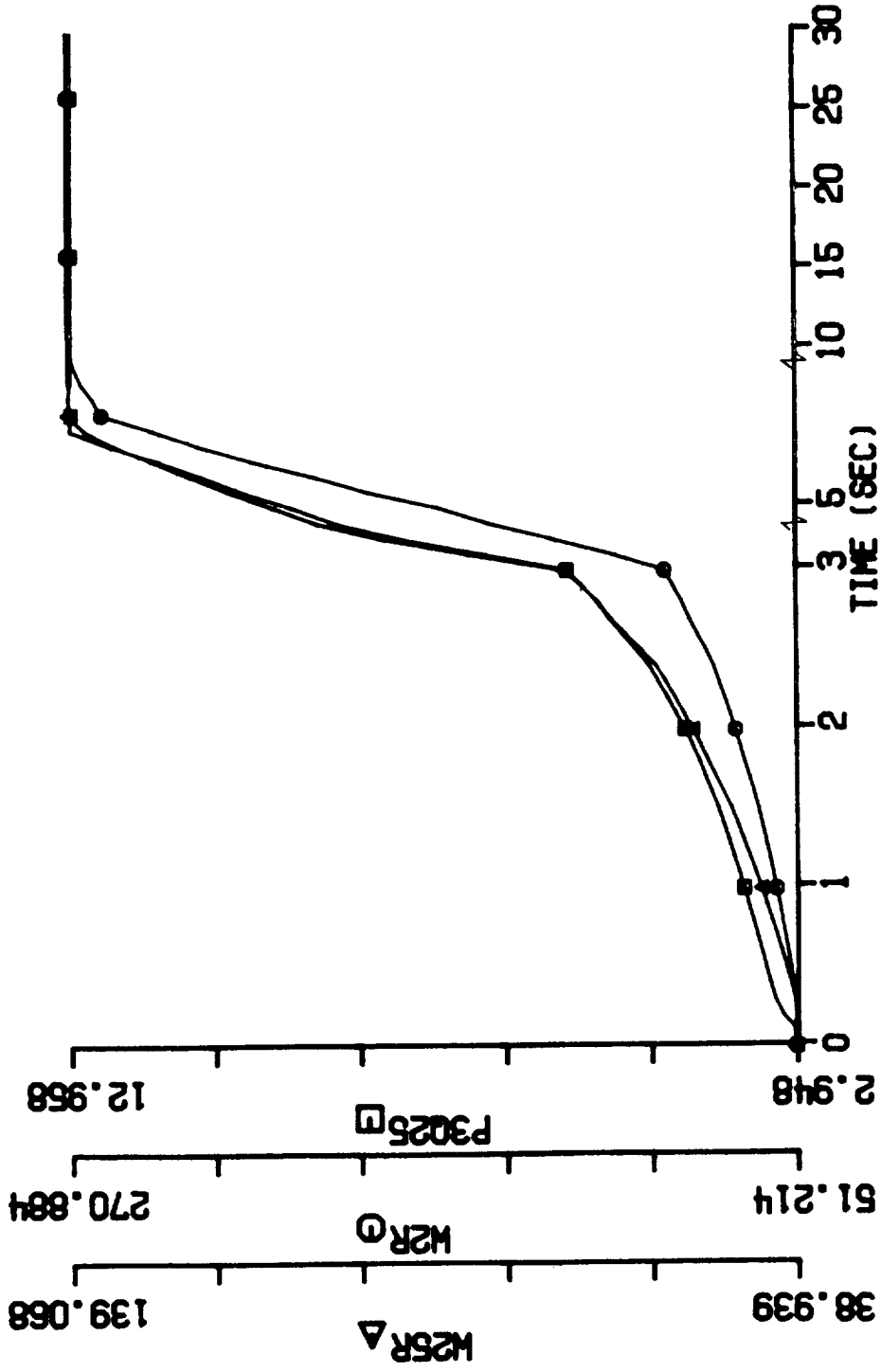

Figure 13.2 Transient Engine Performance: PLA changes from Ground Idle Setting to Max Power Setting, 1% water ingestion with all liquid drained, standard temperature (P35Q25, W2R, W25R vs. time)

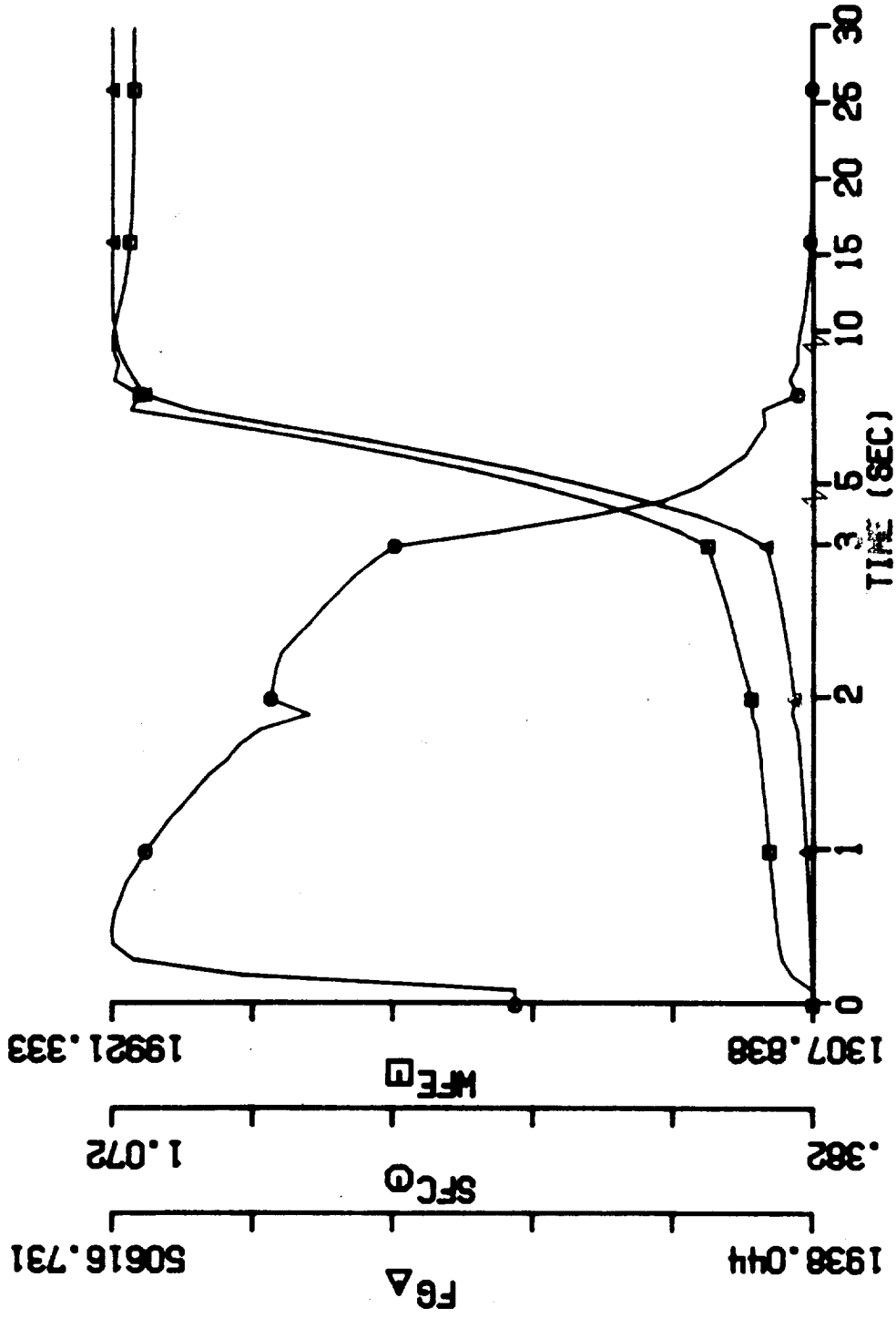

Figure 13.3 Transient Engine Performance: PLA changes from Ground Idle Setting to Max Power Setting, 1% water ingestion with all liquid drained, standard temperature (WFE, SFC, FG vs. time)

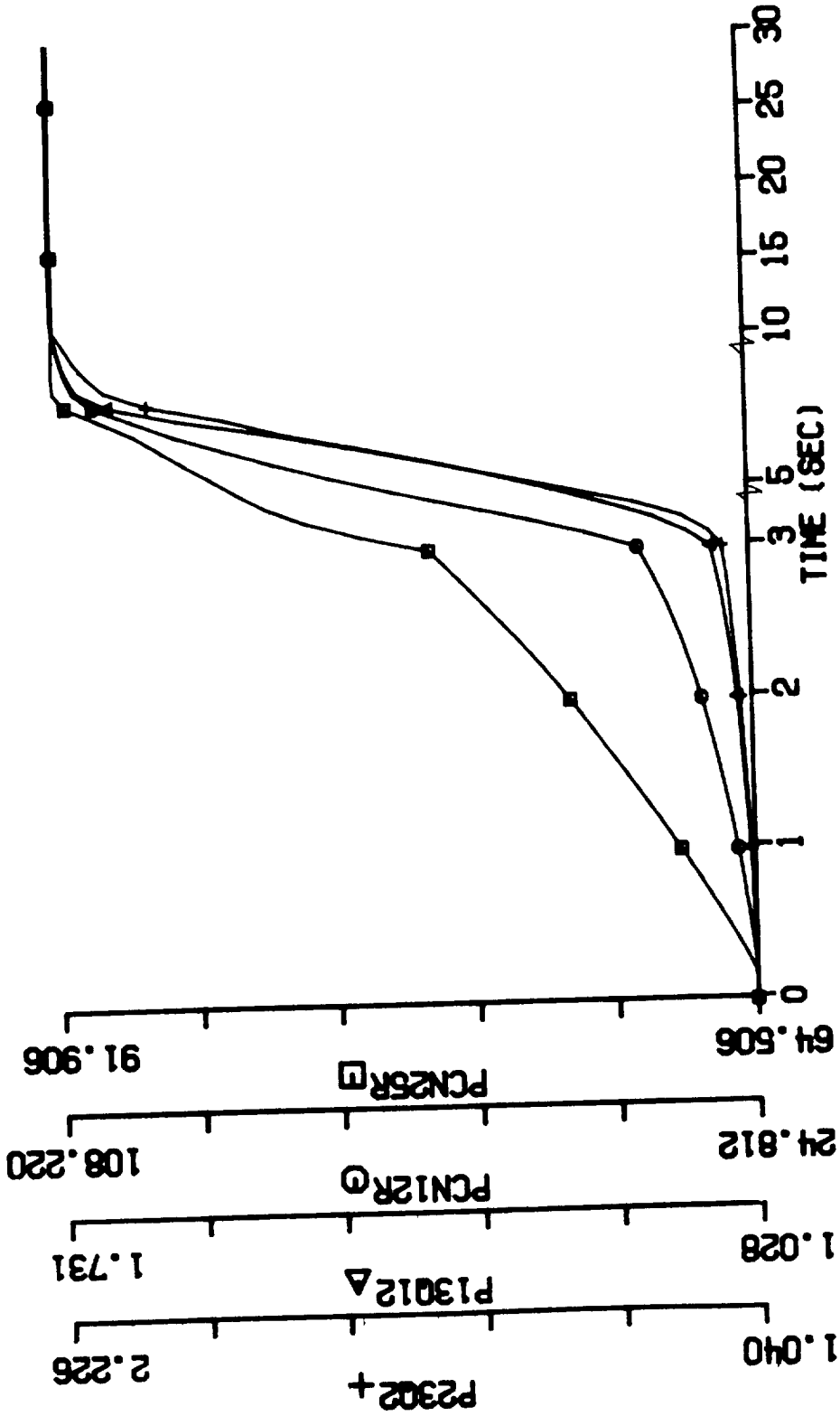

Figure 14.1 Transient Engine Performance: PLA changes from Ground Idle Setting to Max Power Setting, 2% water ingestion with all liquid drained, standard temperature (PCN25R, PCN12R, P13Q12, P23Q2, vs. time)

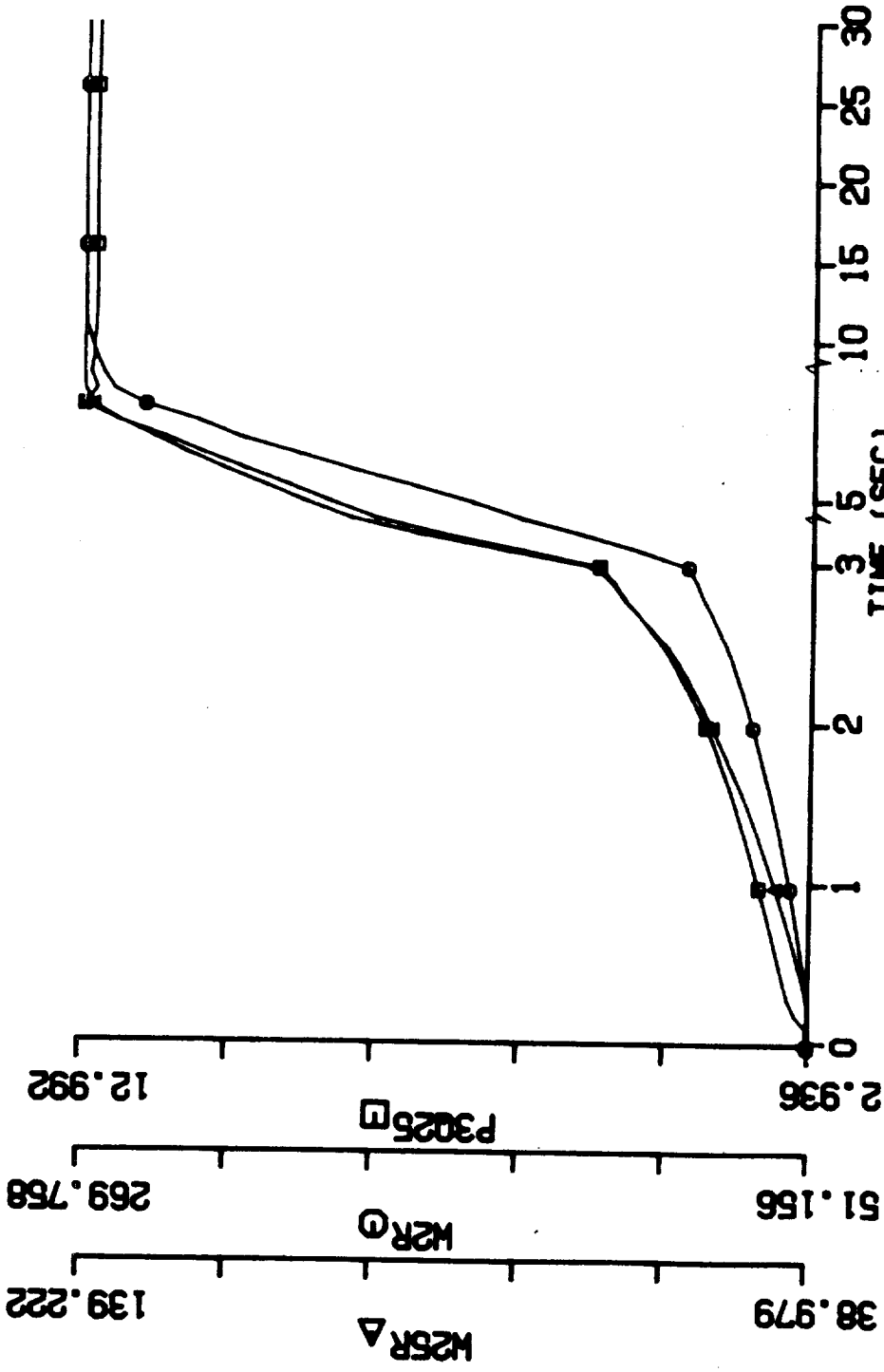

Figure 14.2 Transient Engine Performance: PLA changes from Ground Idle Setting to Max Power Setting, 2% water ingestion with all liquid drained, standard temperature (P3Q25, W2R, W25R vs. time)

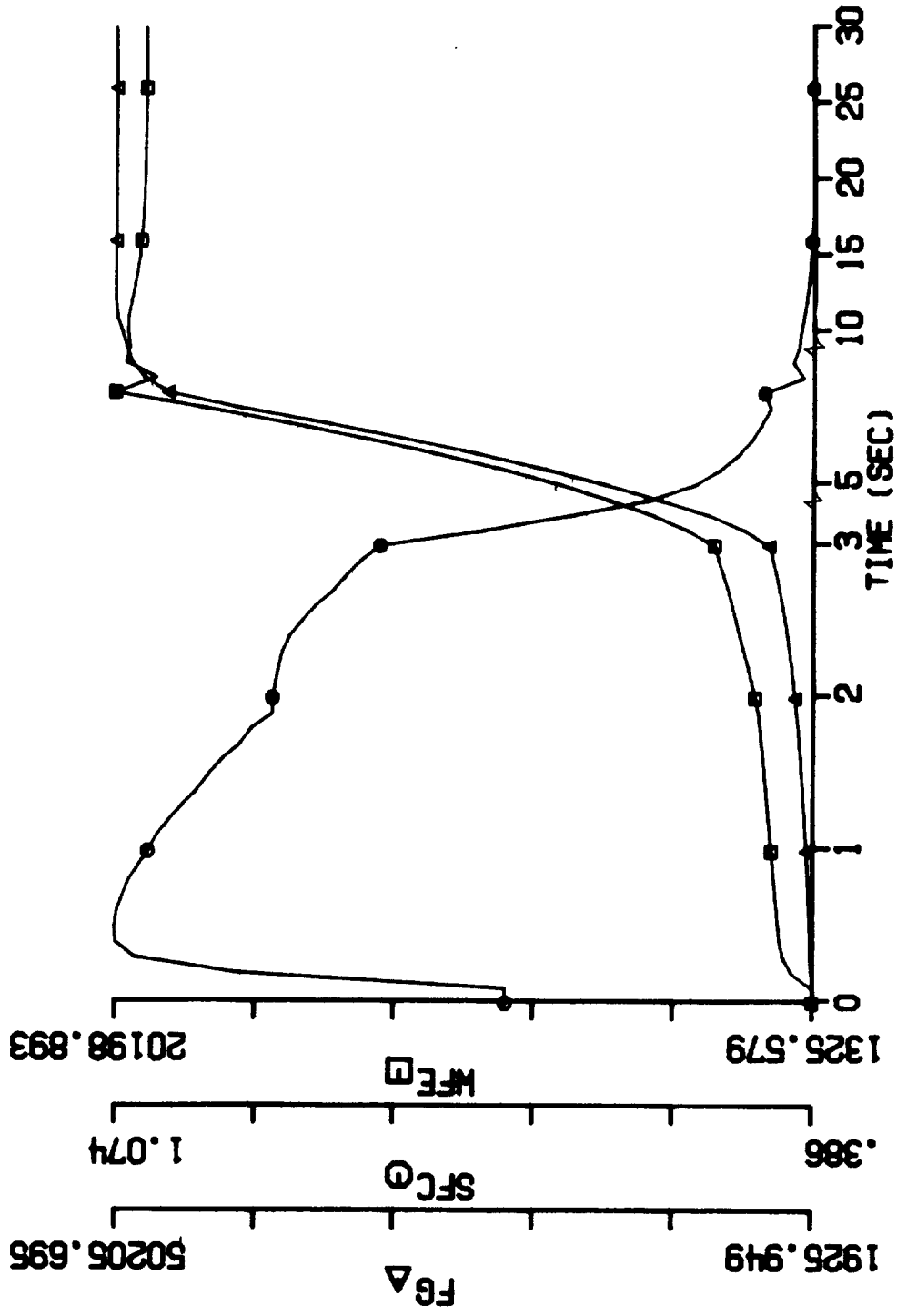

Figure 14.3 Transient Engine Performance: PLA changes from Ground Idle Setting to Max Power Setting, 2% water ingestion with all liquid drained, standard temperature (WFE, SFC, FG vs. time)

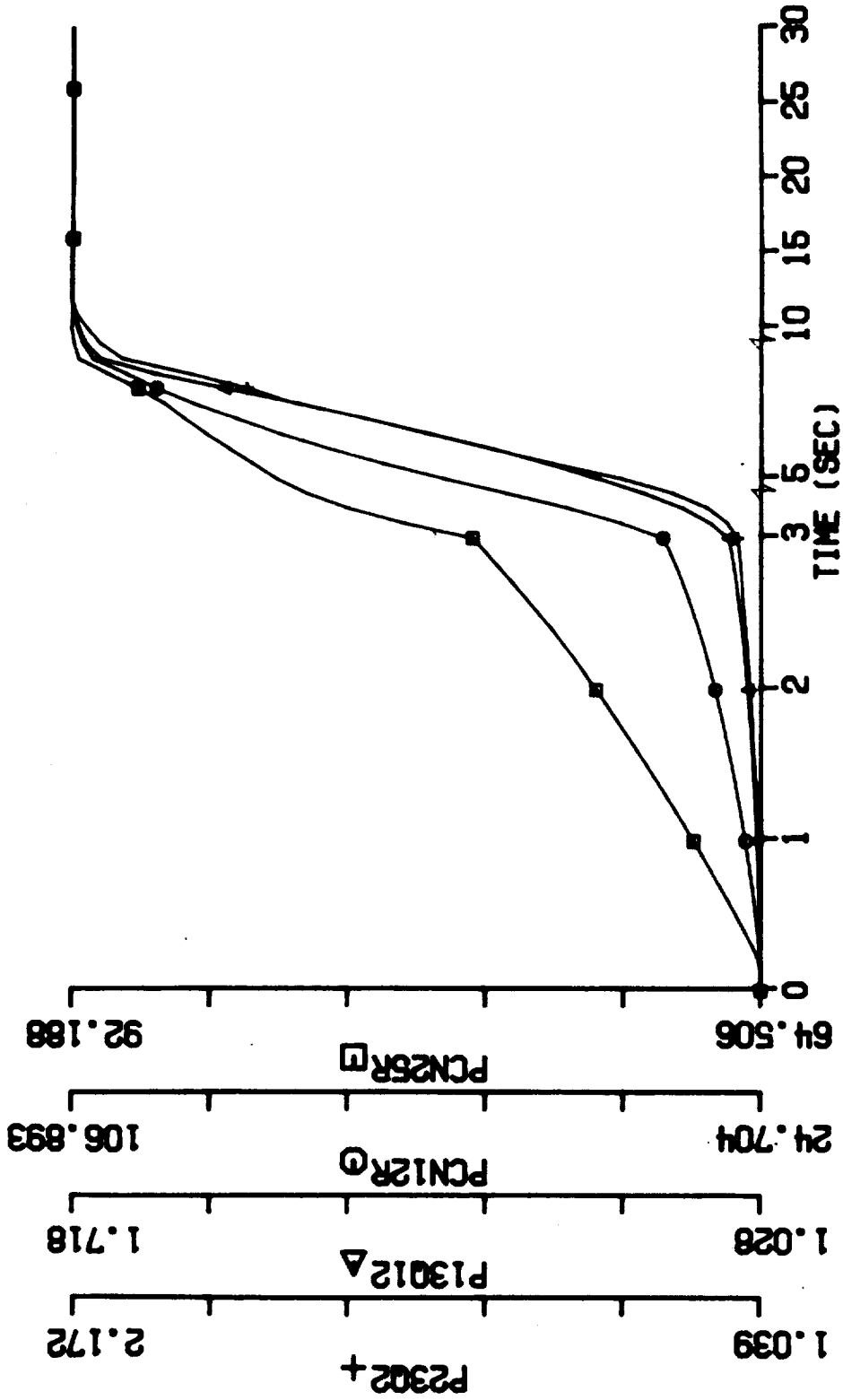

Figure 15.1 Transient Engine Performance: PLA changes from Ground Idle Setting to Max Power Setting, 4% water ingestion with all liquid drained, standard temperature (PCN25R, PCN12R, P13Q12, P23Q2 vs. time)

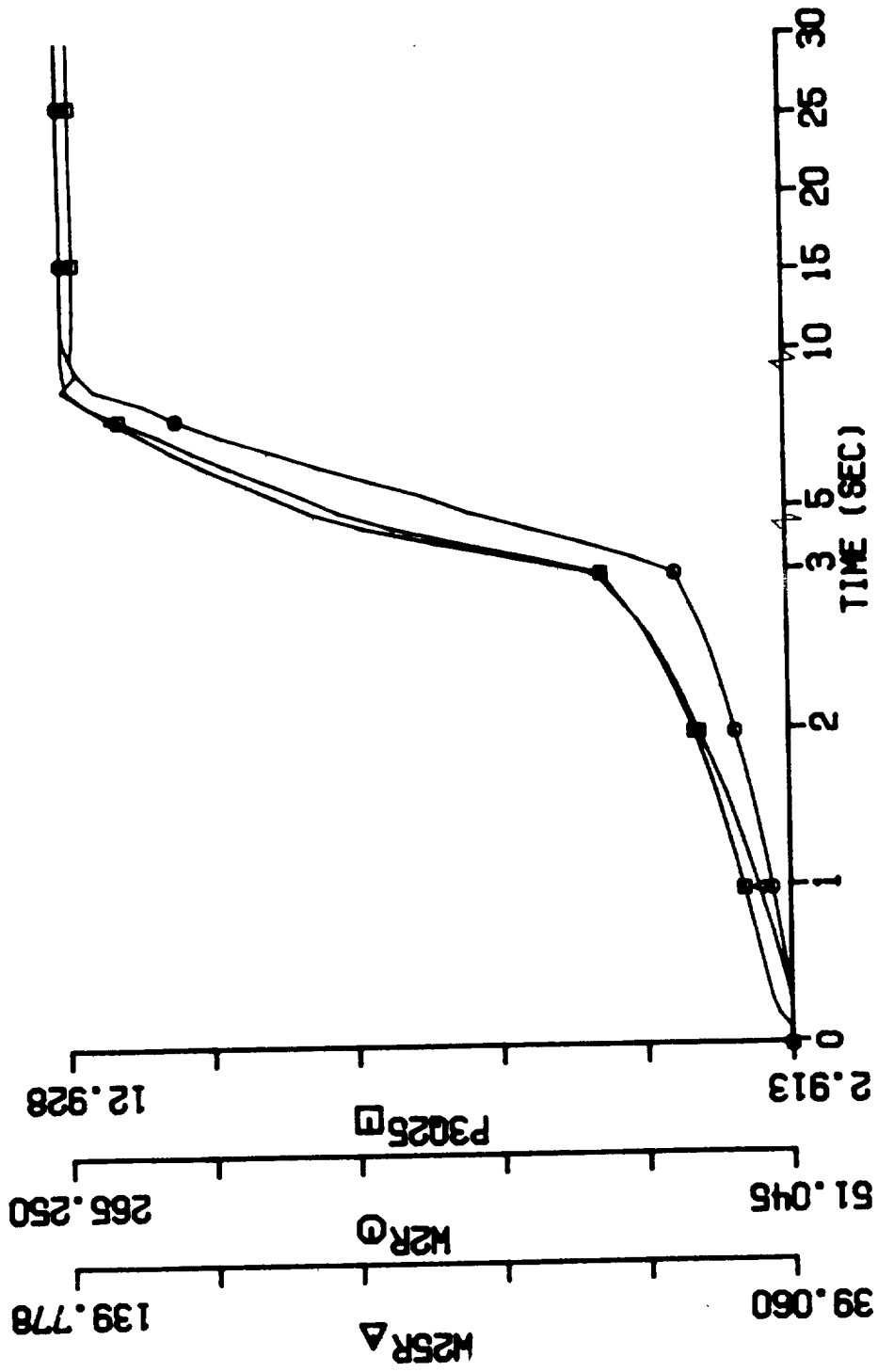

Figure 15.2 Transient Engine Performance: PLA changes from Ground Idle Setting to Max Power Setting, 4% water ingestion with all liquid drained, standard temperature (P3Q25, W2R, W25R, vs. time)

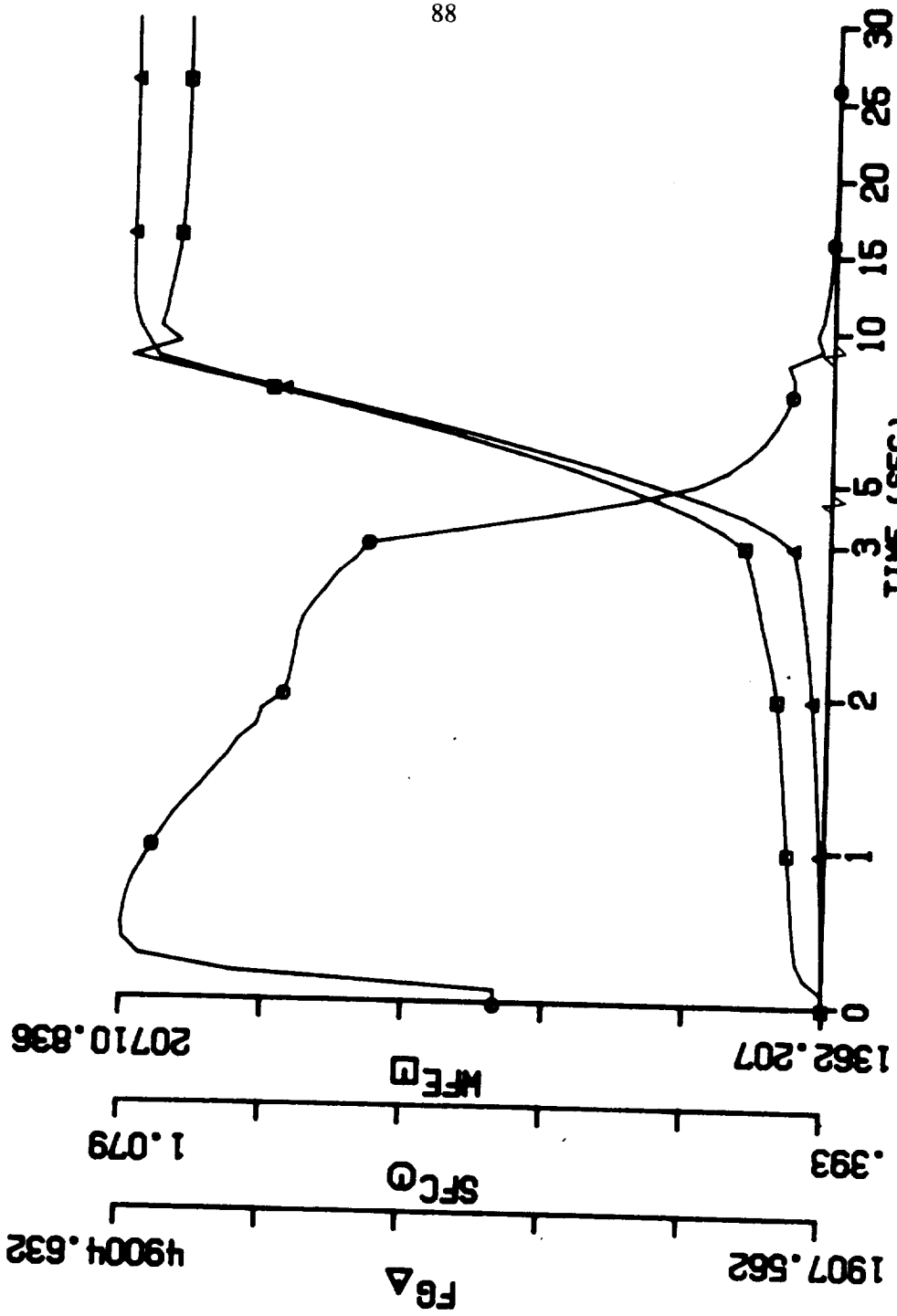

Figure 15.3 Transient Engine Performance: PLA changes from Ground Idle Setting to Max Power Setting, 4% water ingestion with all liquid drained, standard temperature (WFE, SFC, FG, vs. time)

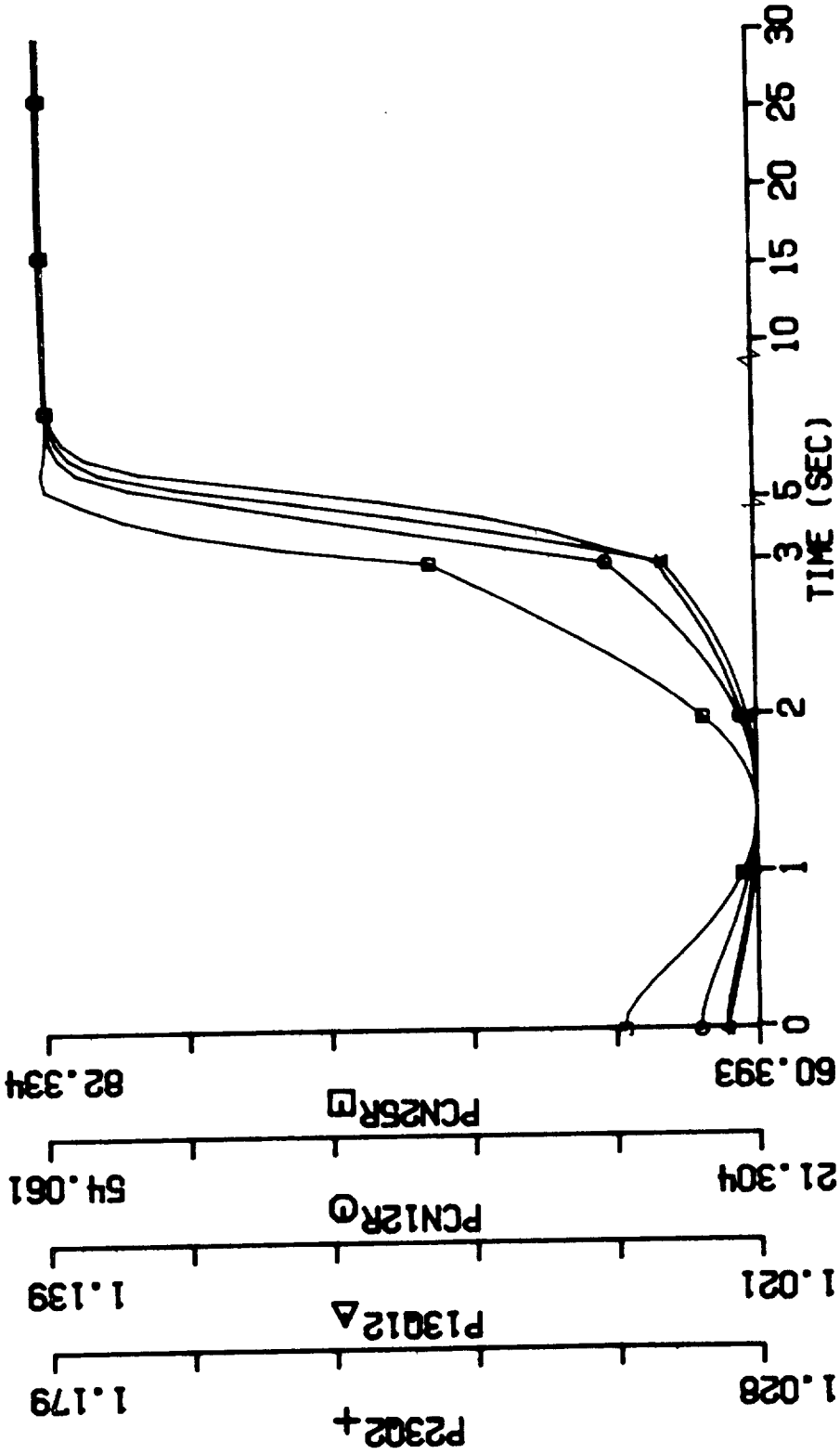

Figure 16.1 Transient Engine Performance: PLA changes from Ground Idle Setting to Max Power Setting, 1% water ingestion with all liquid evaporated at burner entry, standard temperature (PCN25R, PCN12R, P13Q12, P23Q2 vs. time)

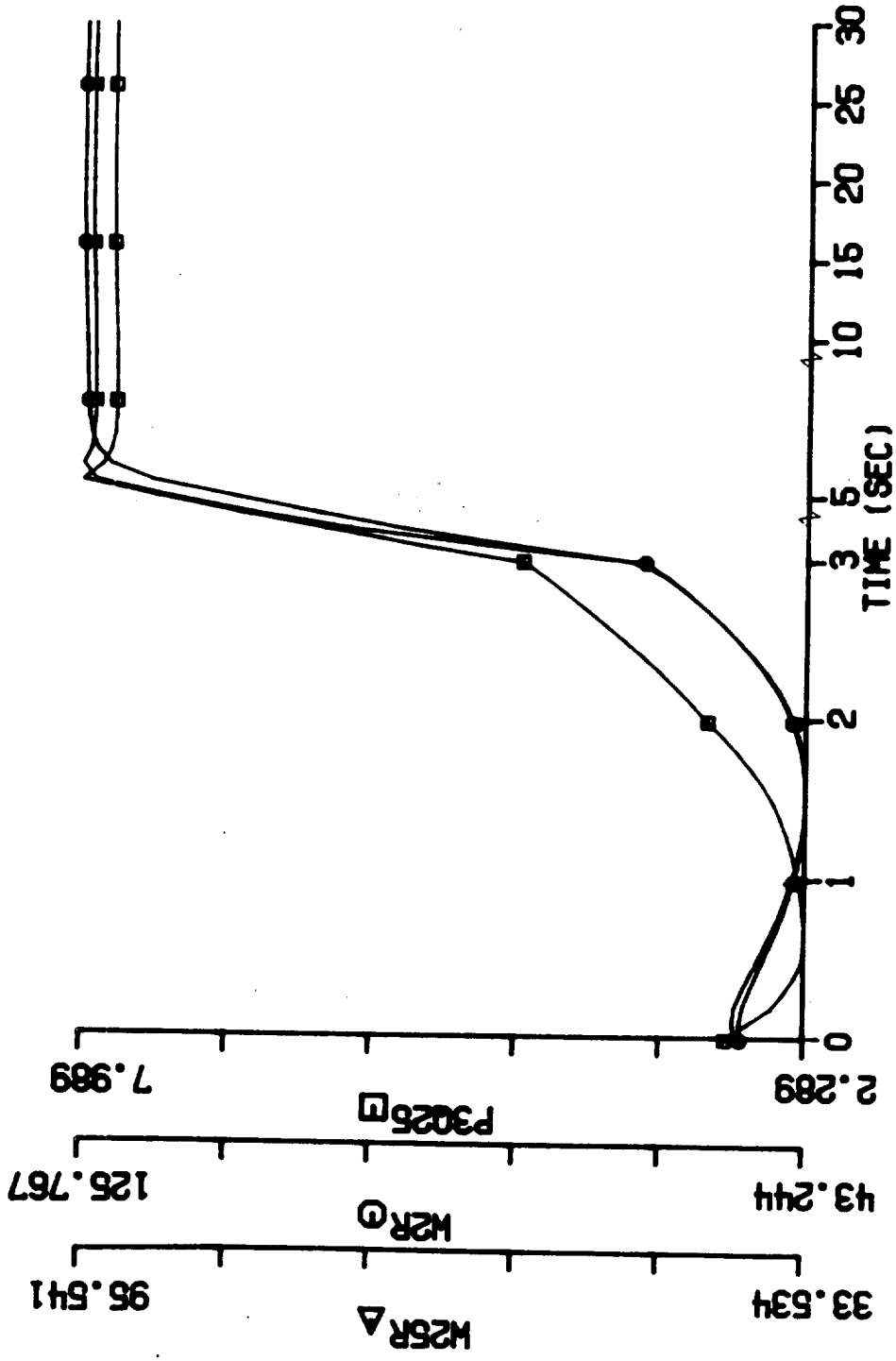

Figure 16.2 Transient Engine Performance: PLA changes from Ground Idle Setting to Max Power Setting, 1% water ingestion with all liquid evaporated at burner entry, standard temperature (P3Q25, W2R, W25R vs. time)

C-2

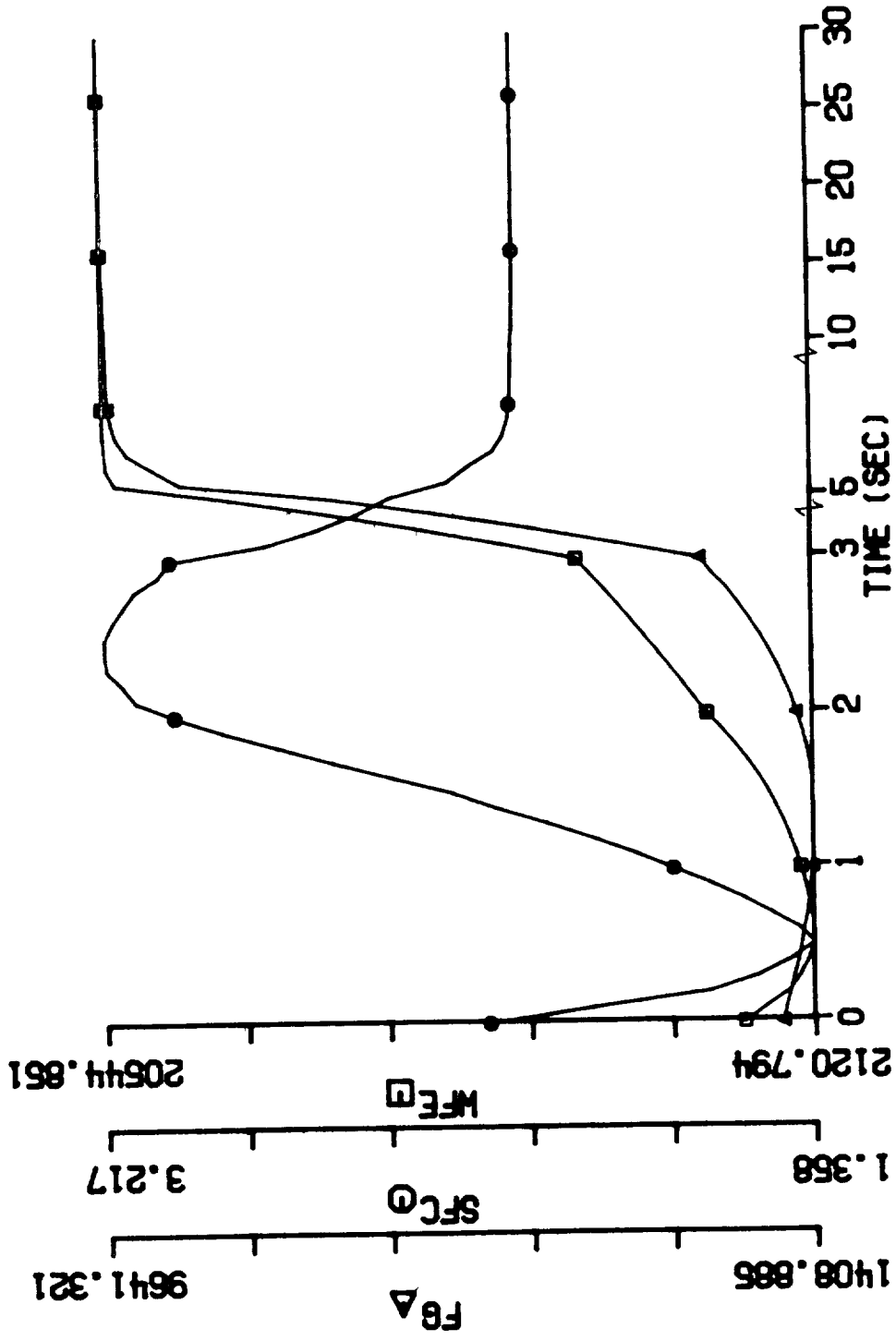

Figure 16.3 Transient Engine Performance: PLA changes from Ground Idle Setting to Max Power Setting, 1% water ingestion with all liquid evaporated at burner entry, standard temperature (WFE, SFC, FG vs. time)

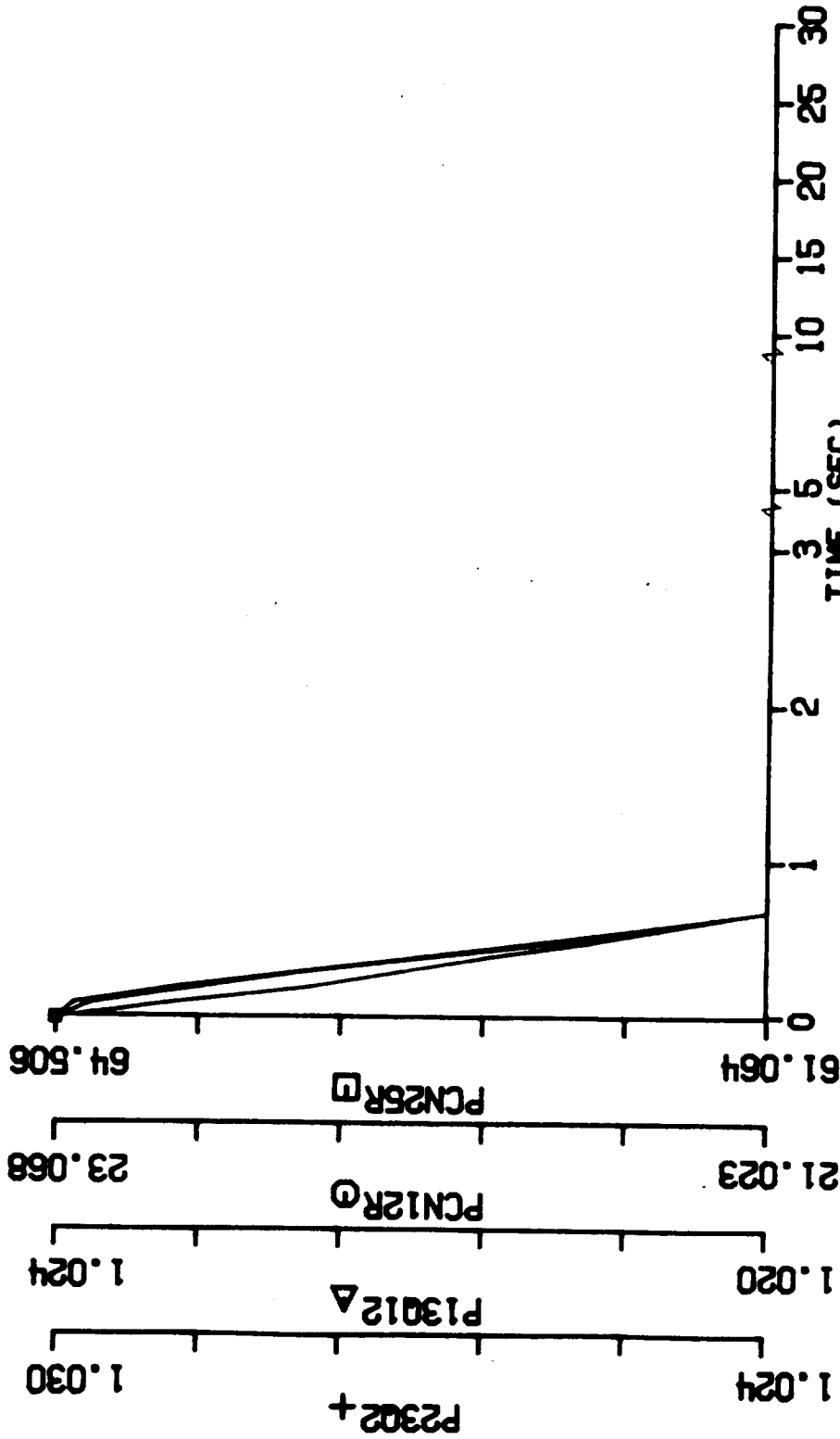

Figure 17.1 Transient Engine Performance: PLA changes from Ground Idle Setting to Max Power Setting, 2% water ingestion with all liquid evaporated at burner entry, standard temperature (PCN25R, PCN12R, P13Q12, P23Q2 vs. time)

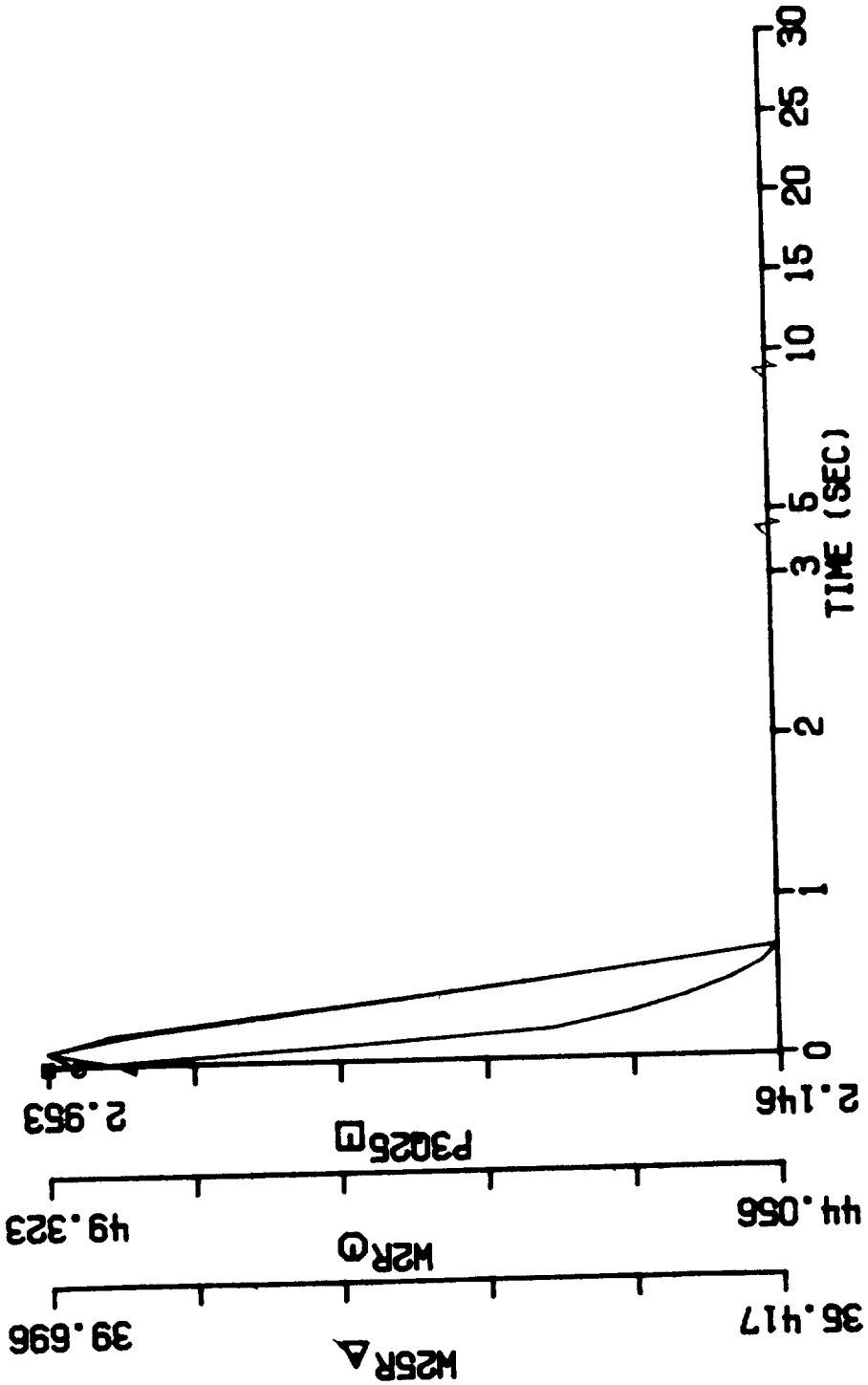

Figure 17.2 Transient Engine Performance: PLA changes from Ground Idle Setting to Max Power Setting, 2% water ingestion with all liquid evaporated at burner entry, standard temperature (P3Q25, W2R, W25R vs. time)

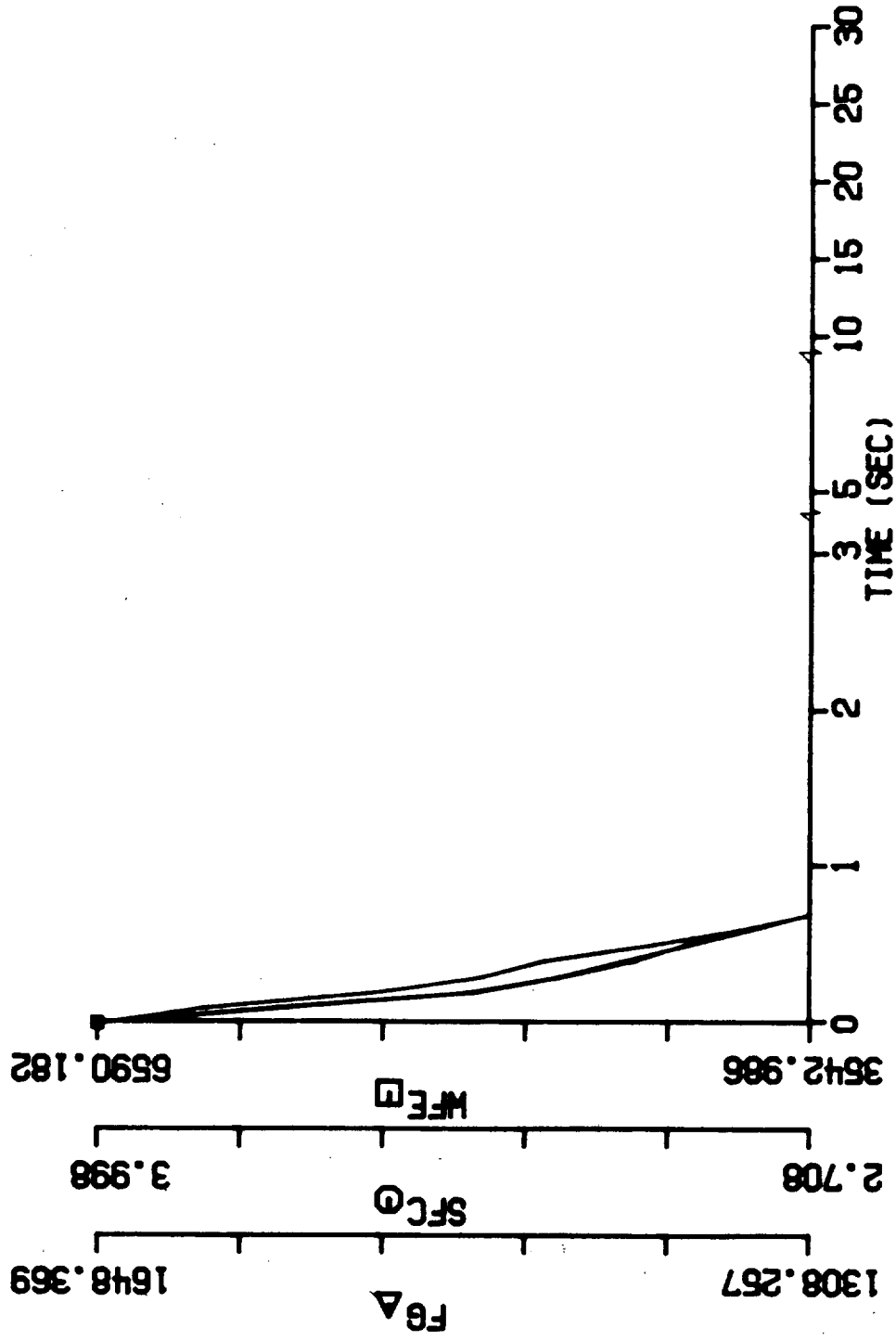

Figure 17.3 Transient Engine Performance: PLA changes from Ground Idle Setting to Max Power Setting, 2% water ingestion with all evaporated at burner entry, standard temperature (WFE, SFC, FG vs. time)

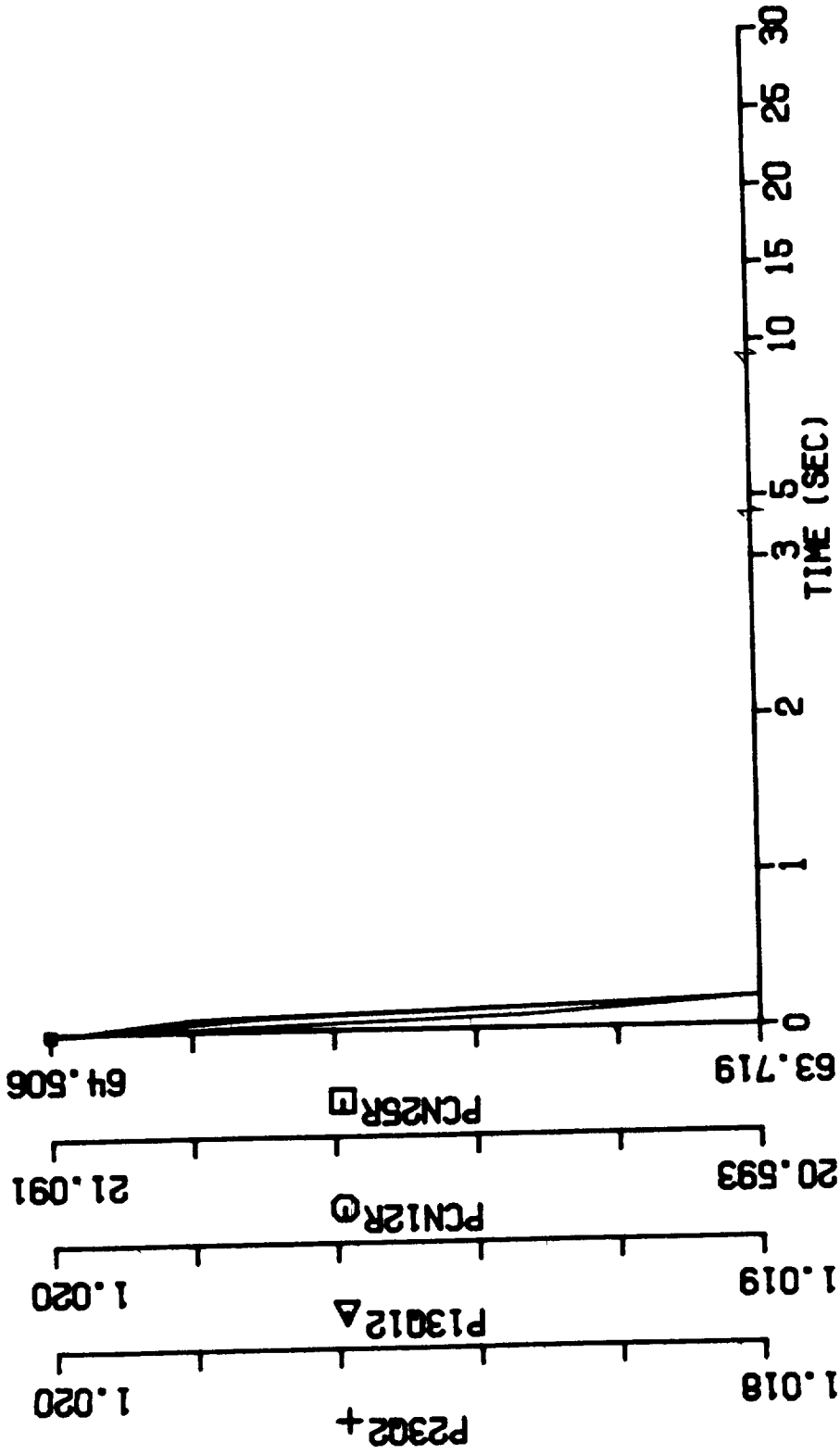

Figure 18.1 Transient Engine Performance: PLA changes from Ground Idle Setting to Max Power Setting, 4% water ingestion with all liquid evaporated at burner entry, standard temperature (PCN25R, PCN12R, P13Q12, P23Q2 vs. time)

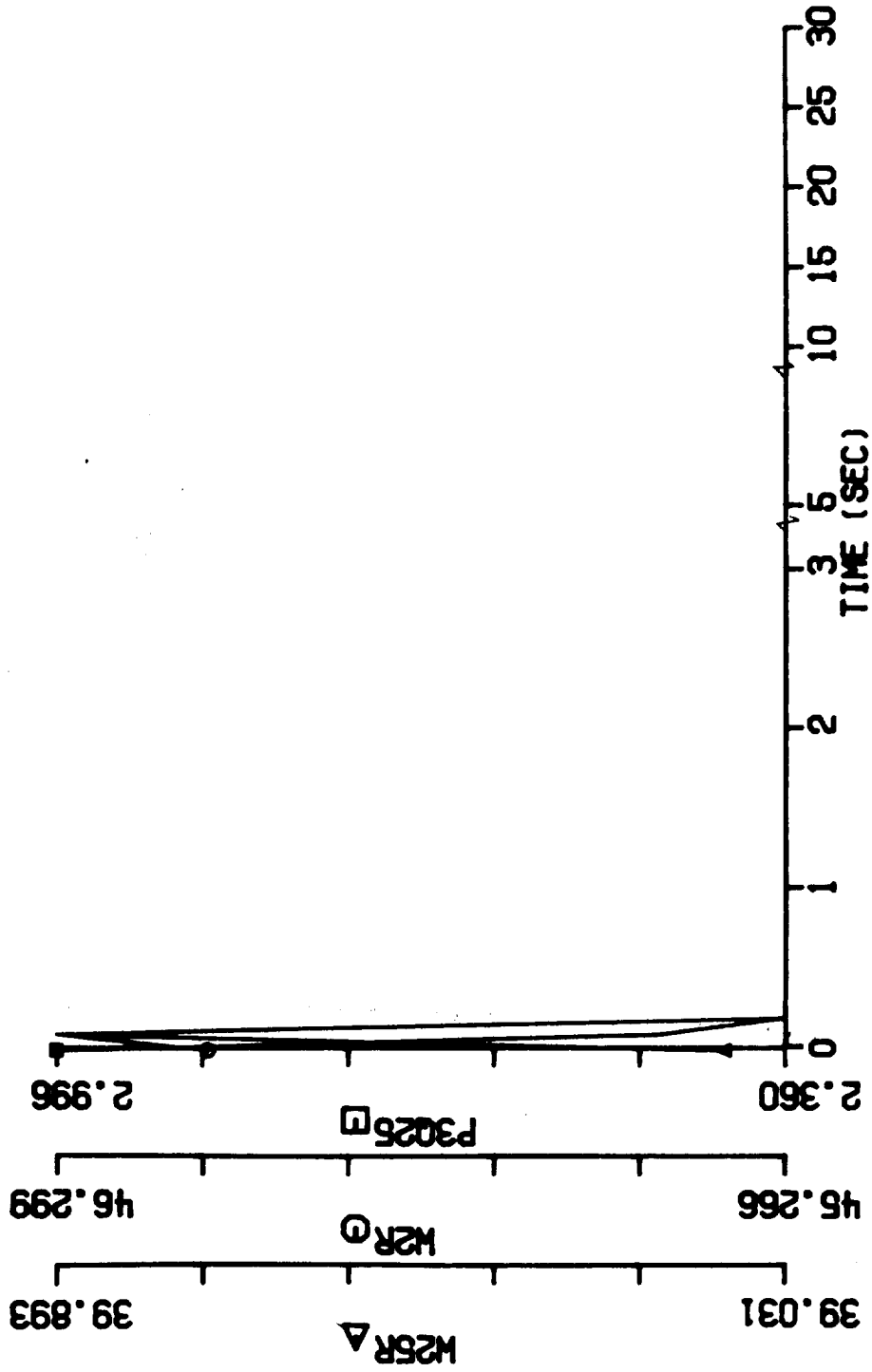

Figure 18.2 Transient Engine Performance: PLA changes from Ground Idle Setting to Max Power Setting, 4% water ingestion with all liquid evaporated at burner entry, standard temperature (P3Q25, W2R, W25R vs. time)

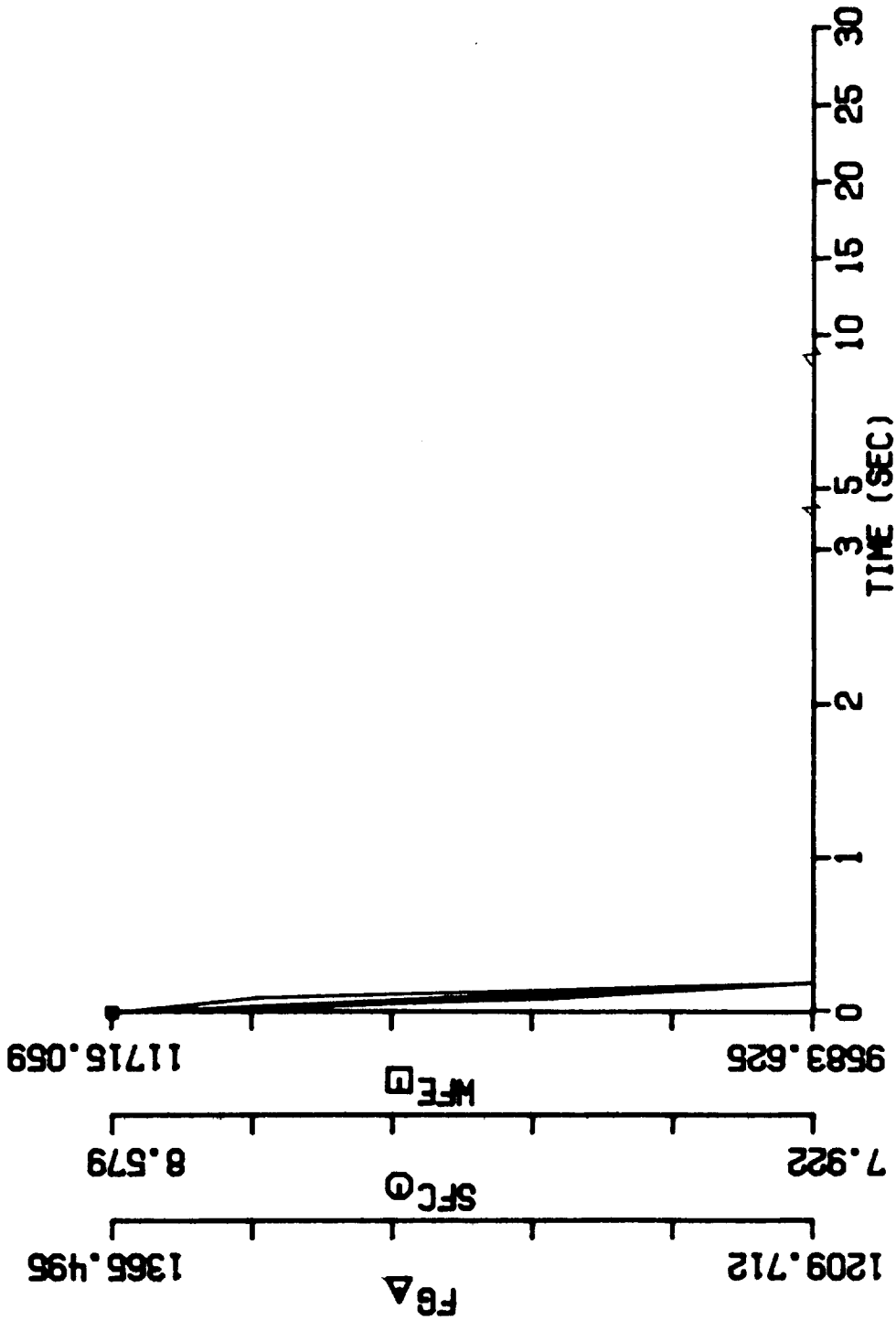

Figure 18.3 Transient Engine Performance: PLA changes from Ground Idle Setting to Max Power Setting, 4% water ingestion with all liquid evaporated at burner entry, standard temperature (WFE, SFC. FG vs. time)

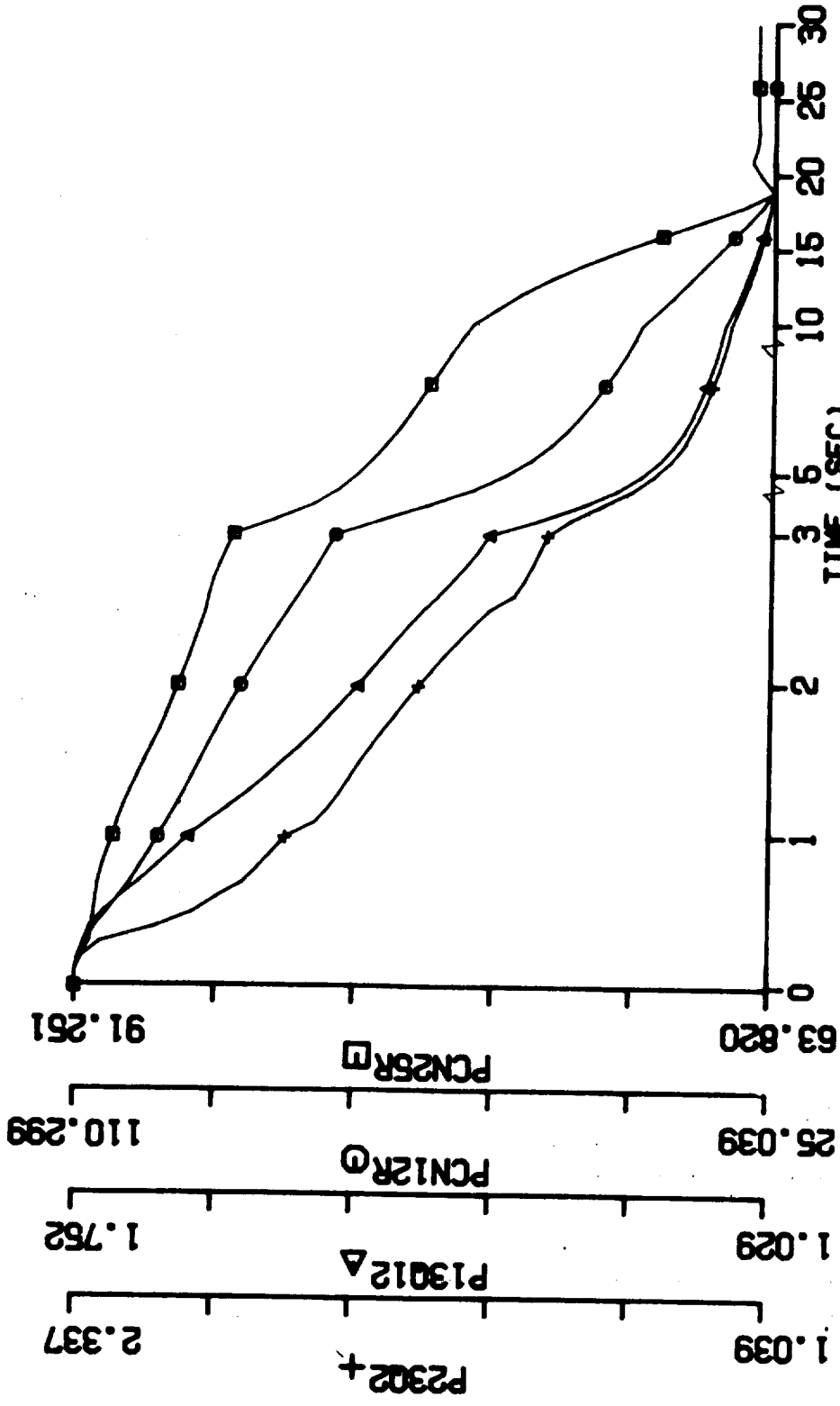

Figure 19.1 Transient Engine Performance: PLA changes from Ground Idle Setting, dry air operation, standard temperature (PCN25R, PCN12R, P13Q12, P23Q2 vs. time)

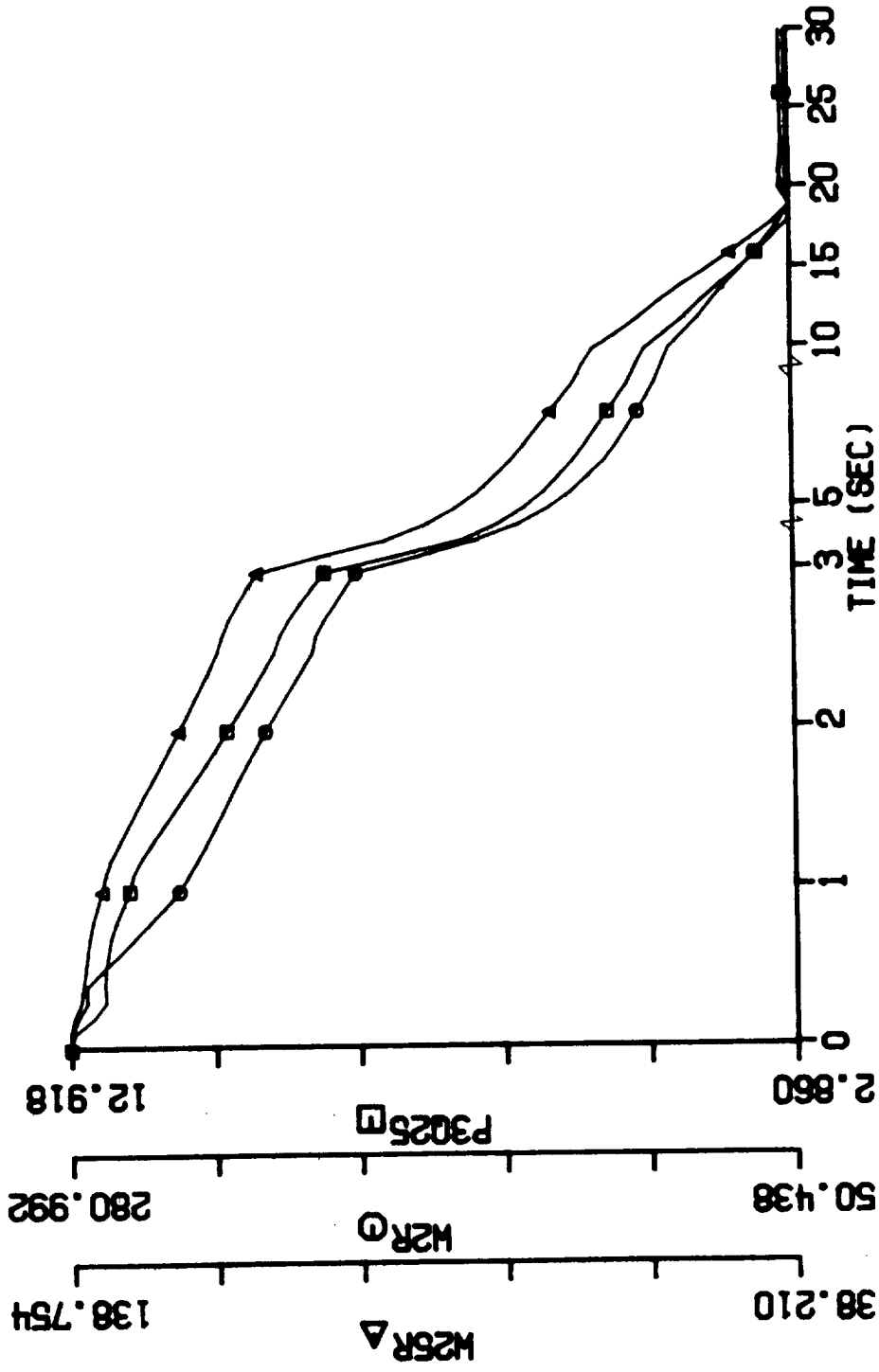

Figure 19.2 Transient Engine Performance: PLA changes from Ground Idle Setting, dry air operation, standard temperature (P3Q25, W2R, W25R vs. time)

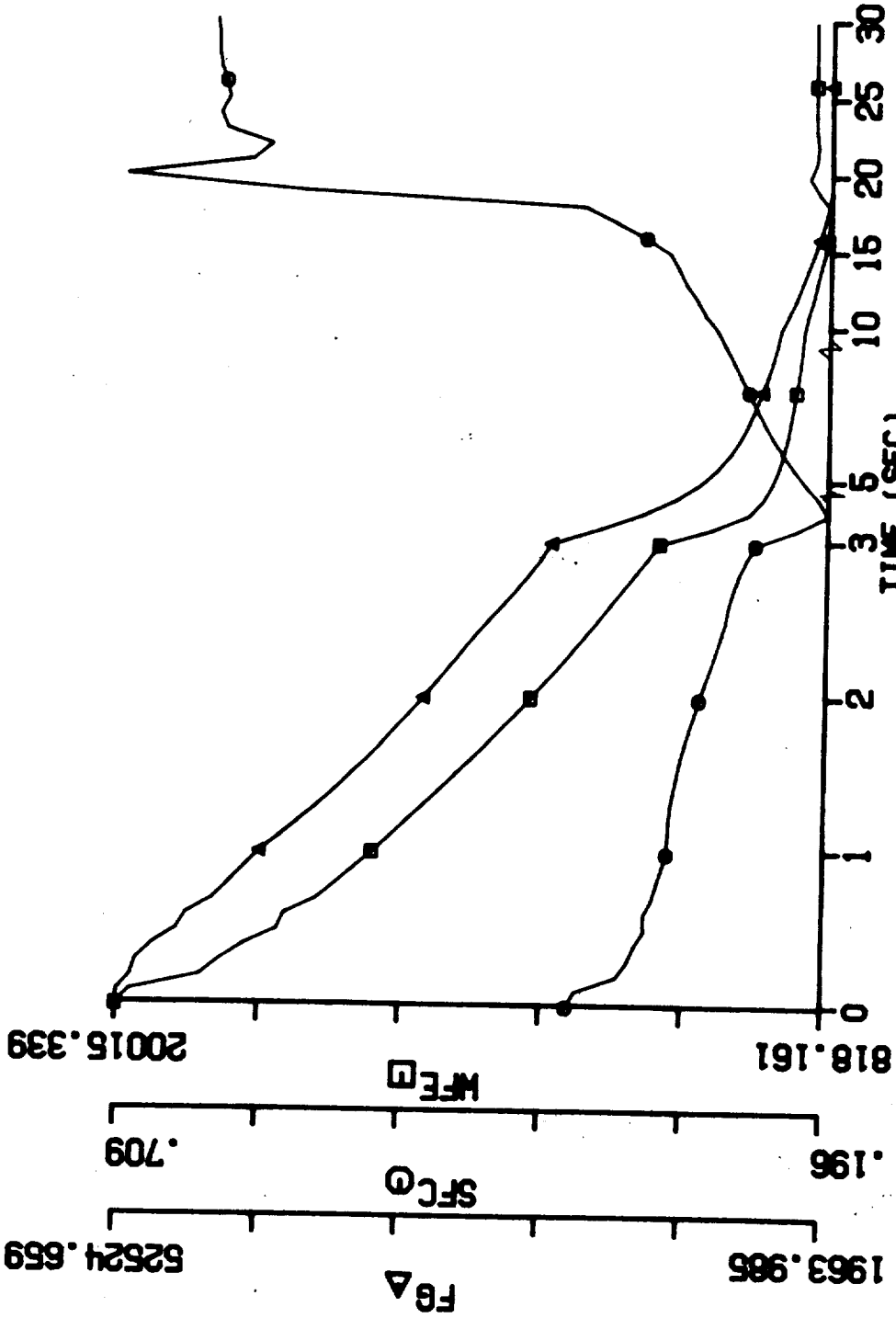

Figure 19.3 Transient Engine Performance: PLA changes from Ground Idle Setting, dry air operation, standard temperature (WFE, SFC, FG vs. time)

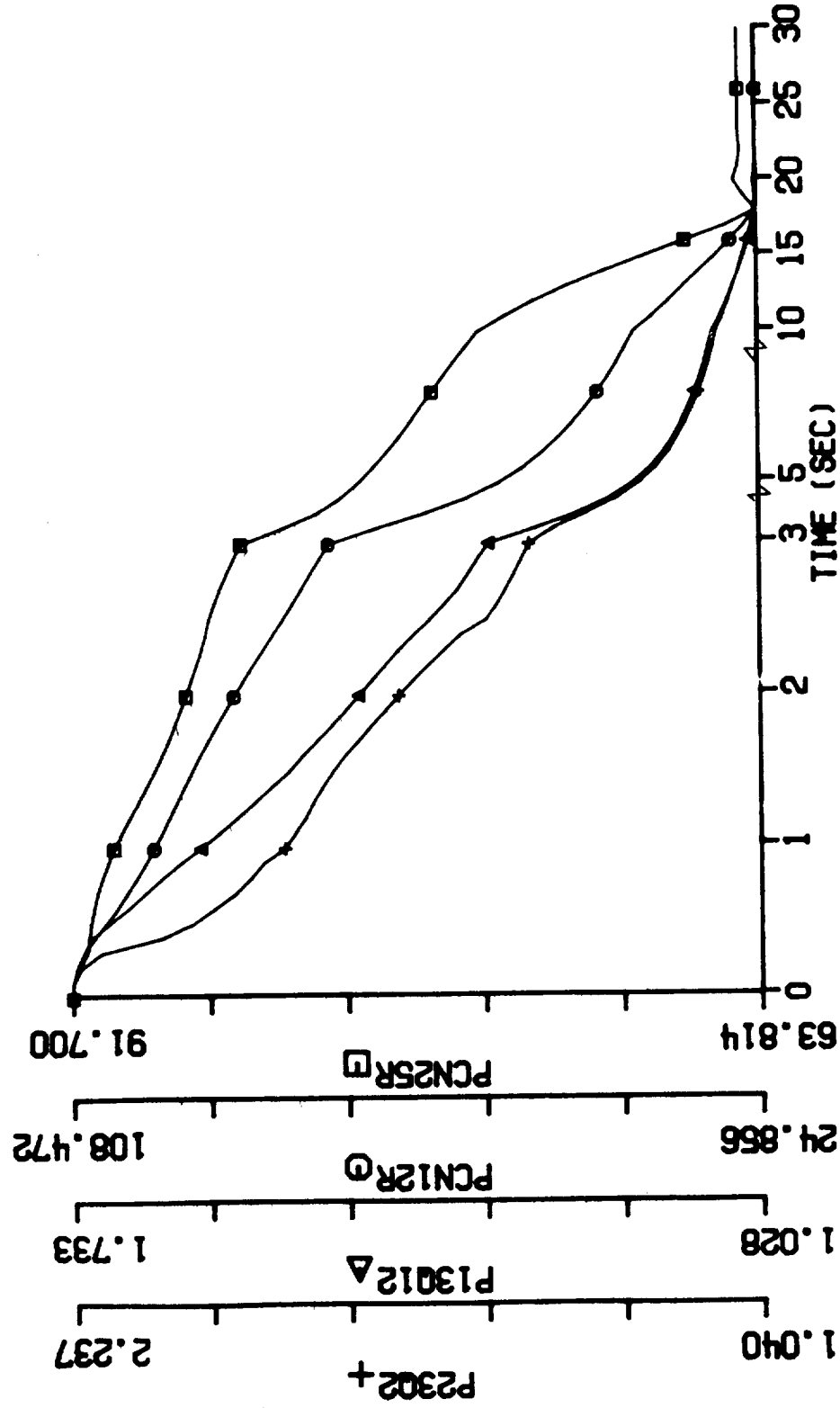

Figure 20.1 Transient Engine Performance: PLA changes from Max Power Setting to Ground Idle Setting, 1% water ingestion with all liquid drained, standard temperature (PCN25R, PCN12R, P13Q12, P23Q2, vs. time)

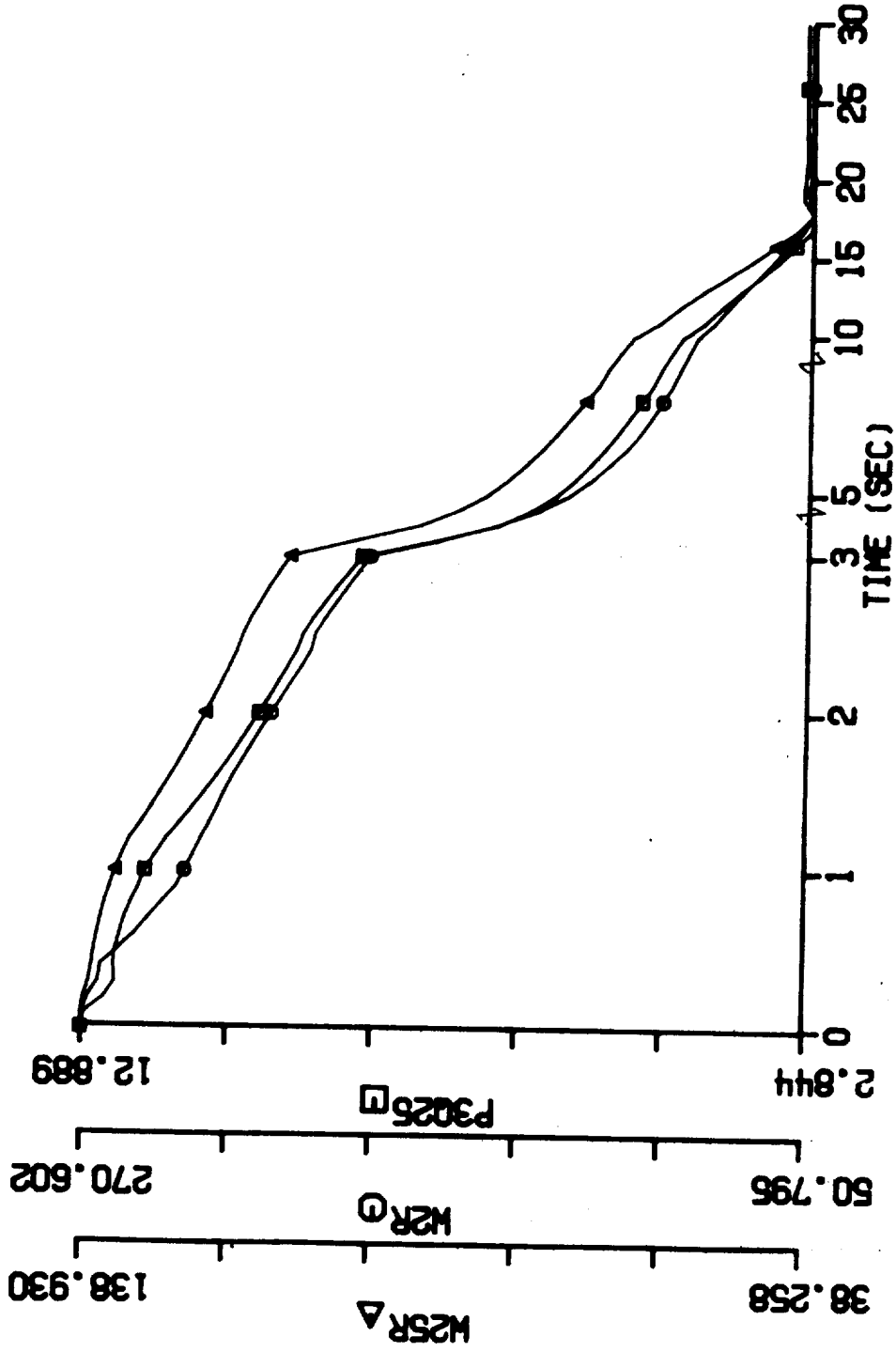

Figure 20.2 Transient Engine Performance: PLA changes from Max Power Setting to Ground Idle Setting, 1% water ingestion with all liquid drained, standard temperature (P3Q25, W2R, W25R vs. time)

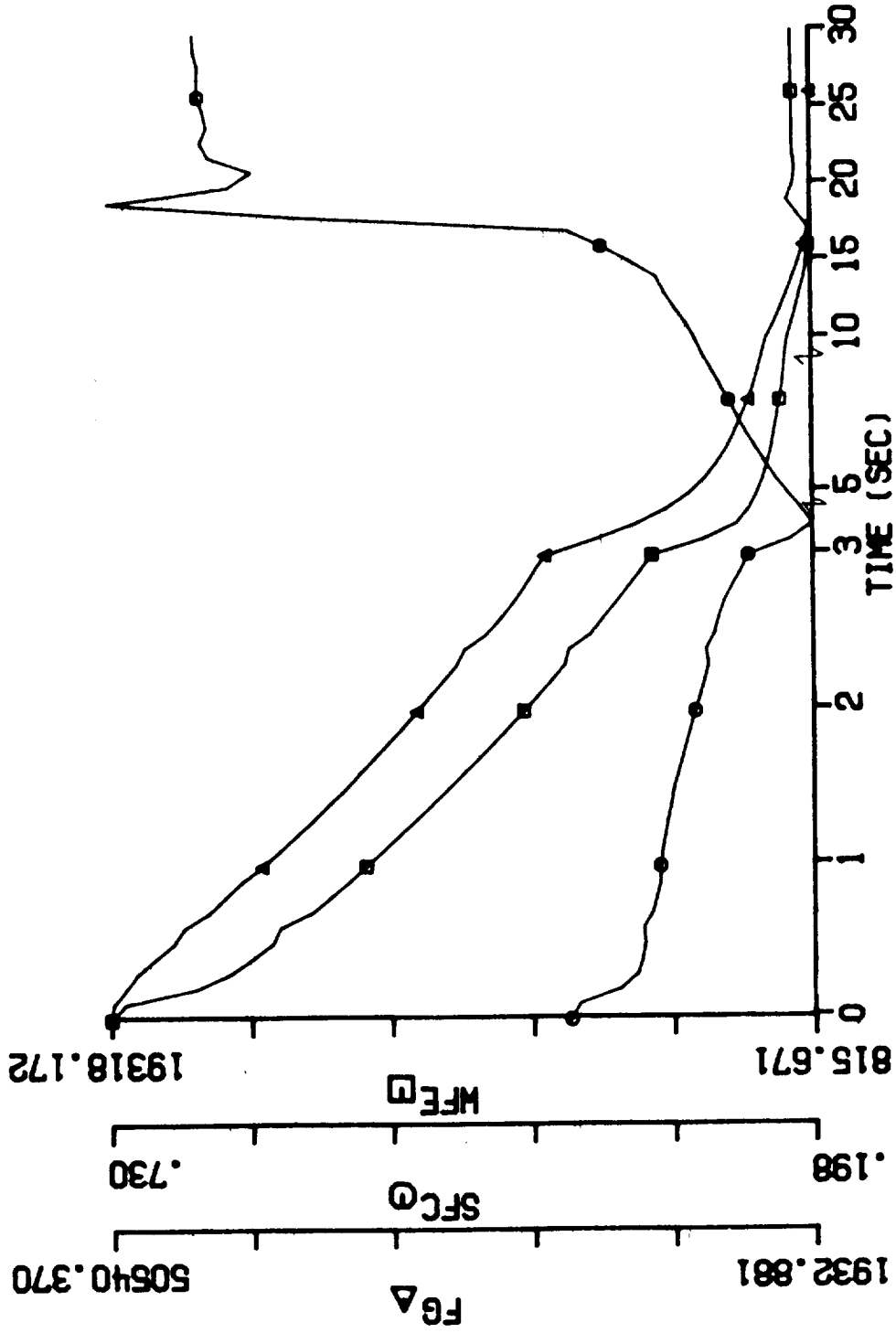

Figure 20.3 Transient Engine Performance: PLA changes from Max Power Setting to Ground Idle Setting, 1% water ingestion with all liquid drained, standard temperature (WFE, SFC, FG vs. time)

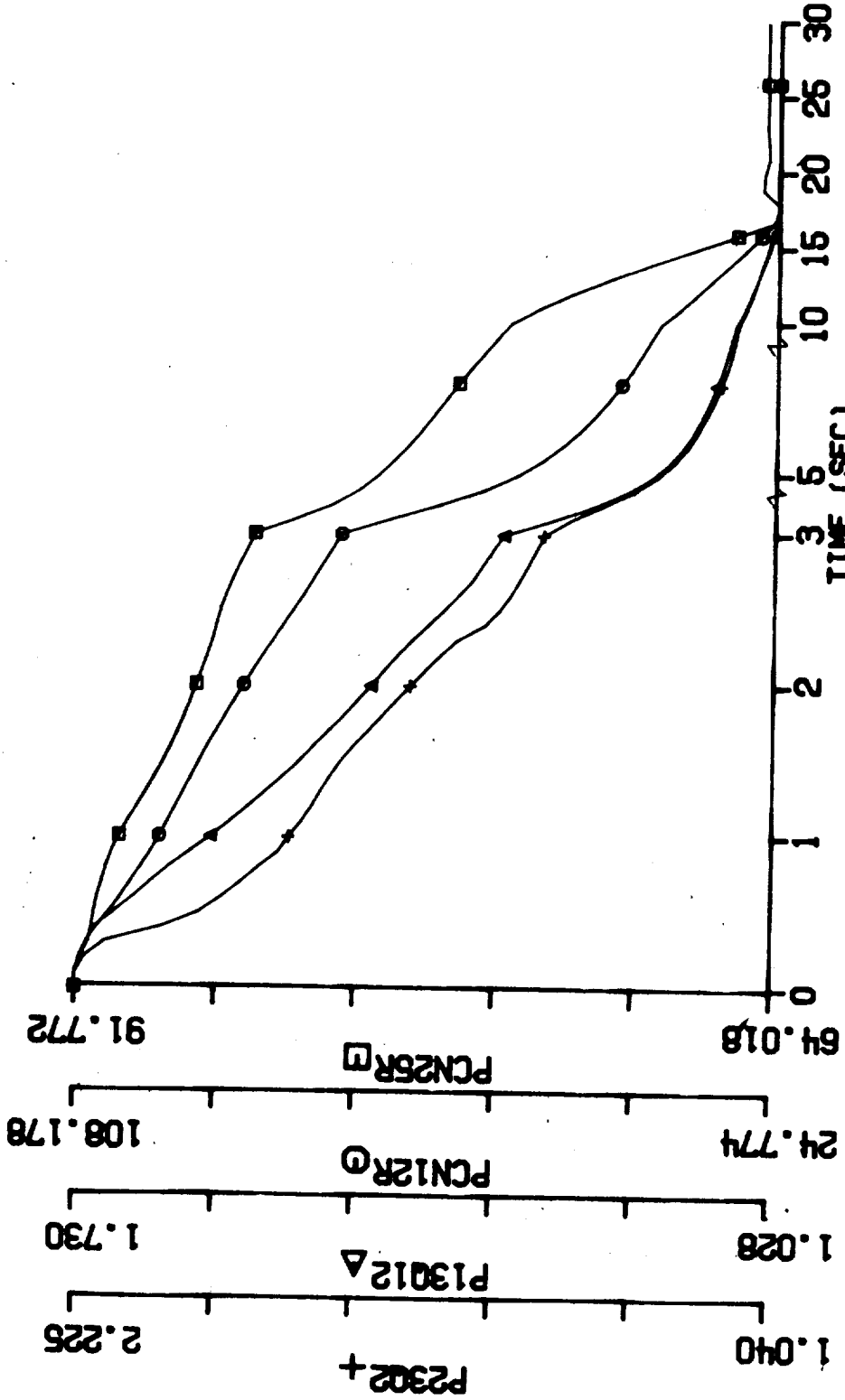

Figure 21.1 Transient Engine Performance: PLA changes from Max Power Setting to Ground Idle Setting, 2% water ingestion with all liquid drained, standard temperature (PCN25R, PCN12R, P13Q12, P23Q2 vs. time)

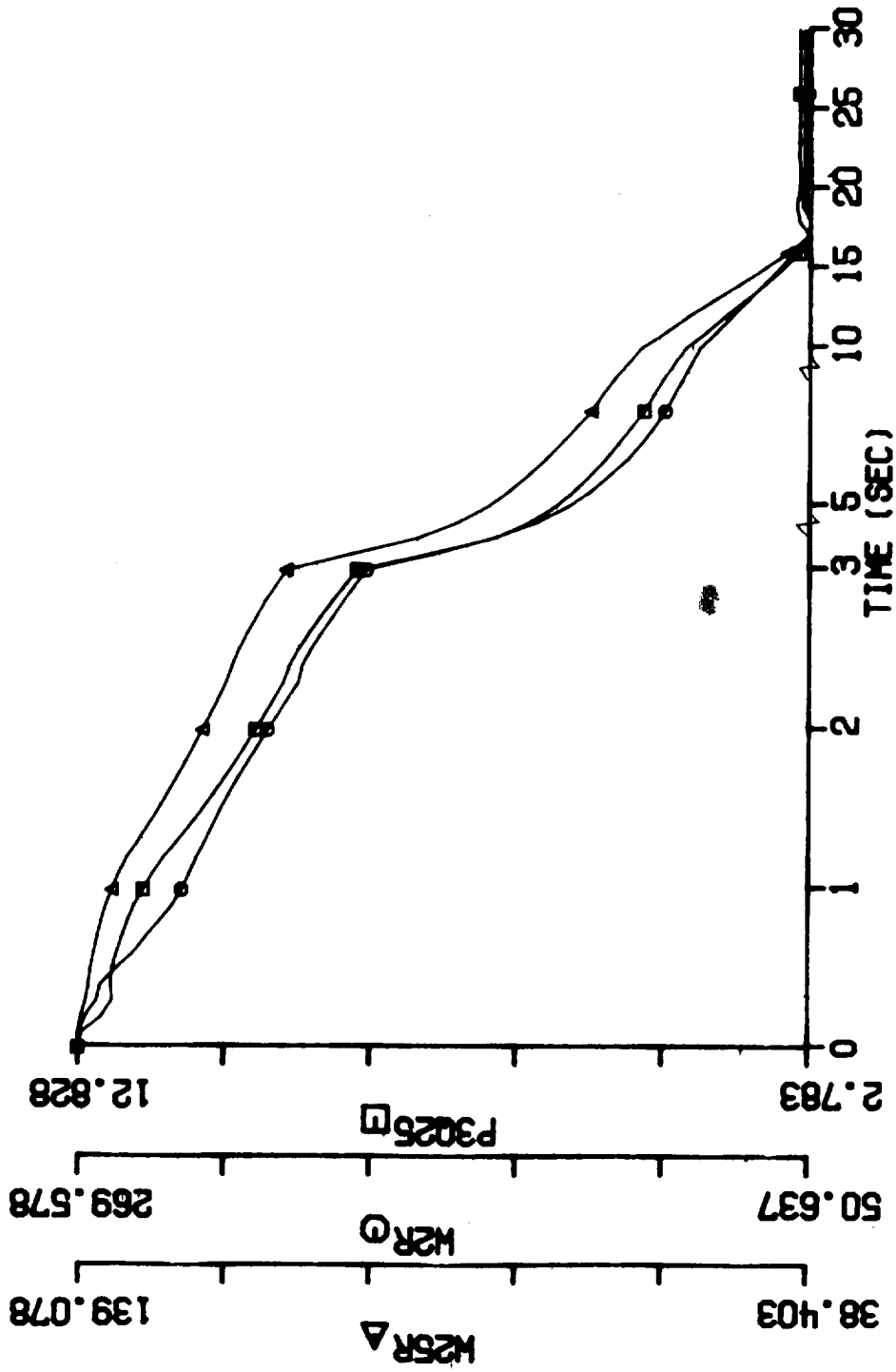

Figure 21.2 Transient Engine Performance: PLA changes from Max Power Setting to Ground Idle Setting, 2% water ingestion with all liquid drained, standard temperature (P3Q25, W2R, W25R vs. time)

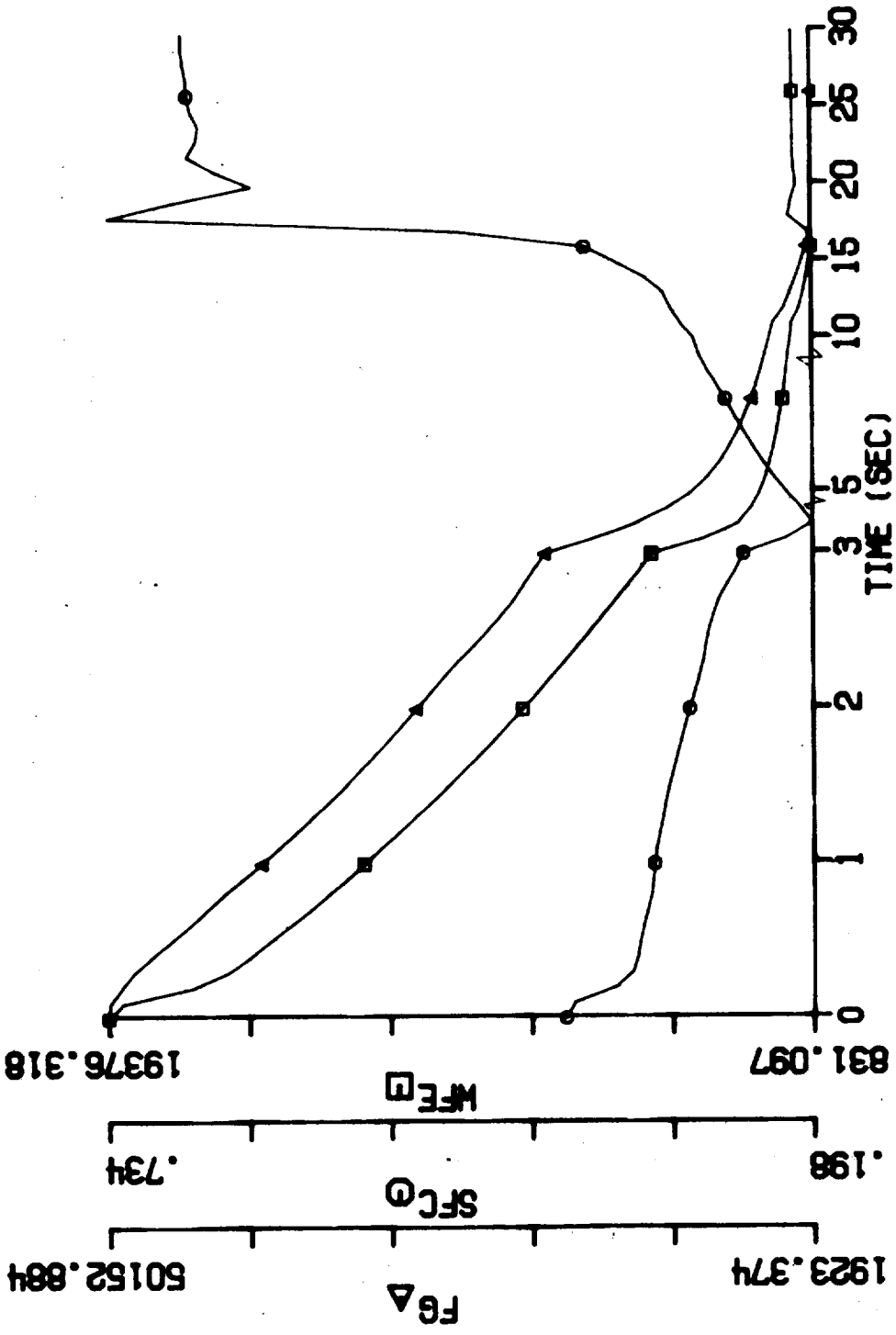

Figure 21.3 Transient Engine Performance: PLA changes from Max Power Setting to Ground Idle Setting, 2% water ingestion with all liquid drained, standard temperature (WFE, SFC, FG vs. time)

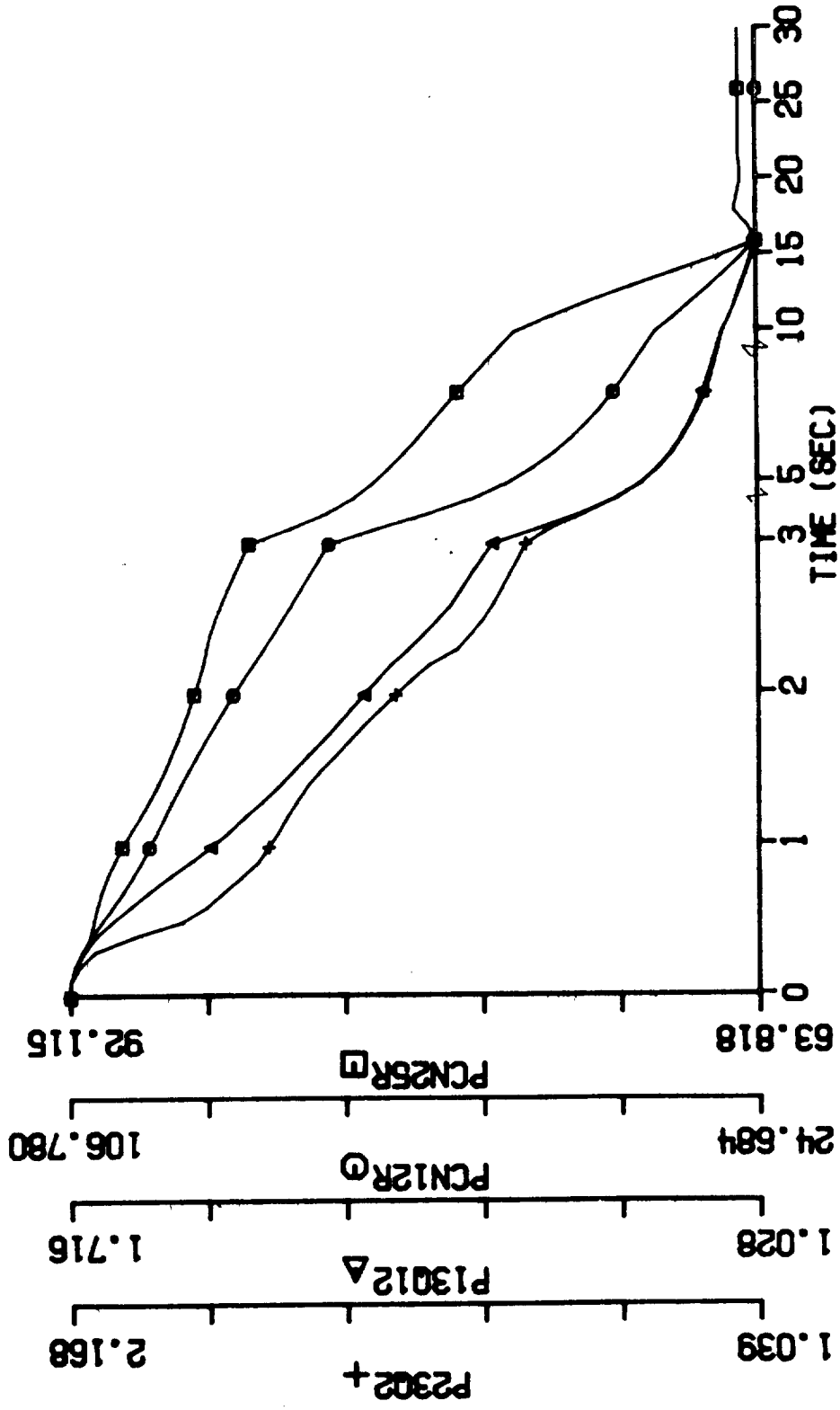

Figure 22.1 Transient Engine Performance: PLA changes from Max Power Setting to Ground Idle Setting, 4% water ingestion with all liquid drained, standard temperature (PCN25R, PCN12R, P13Q12, P23Q2 vs. time)

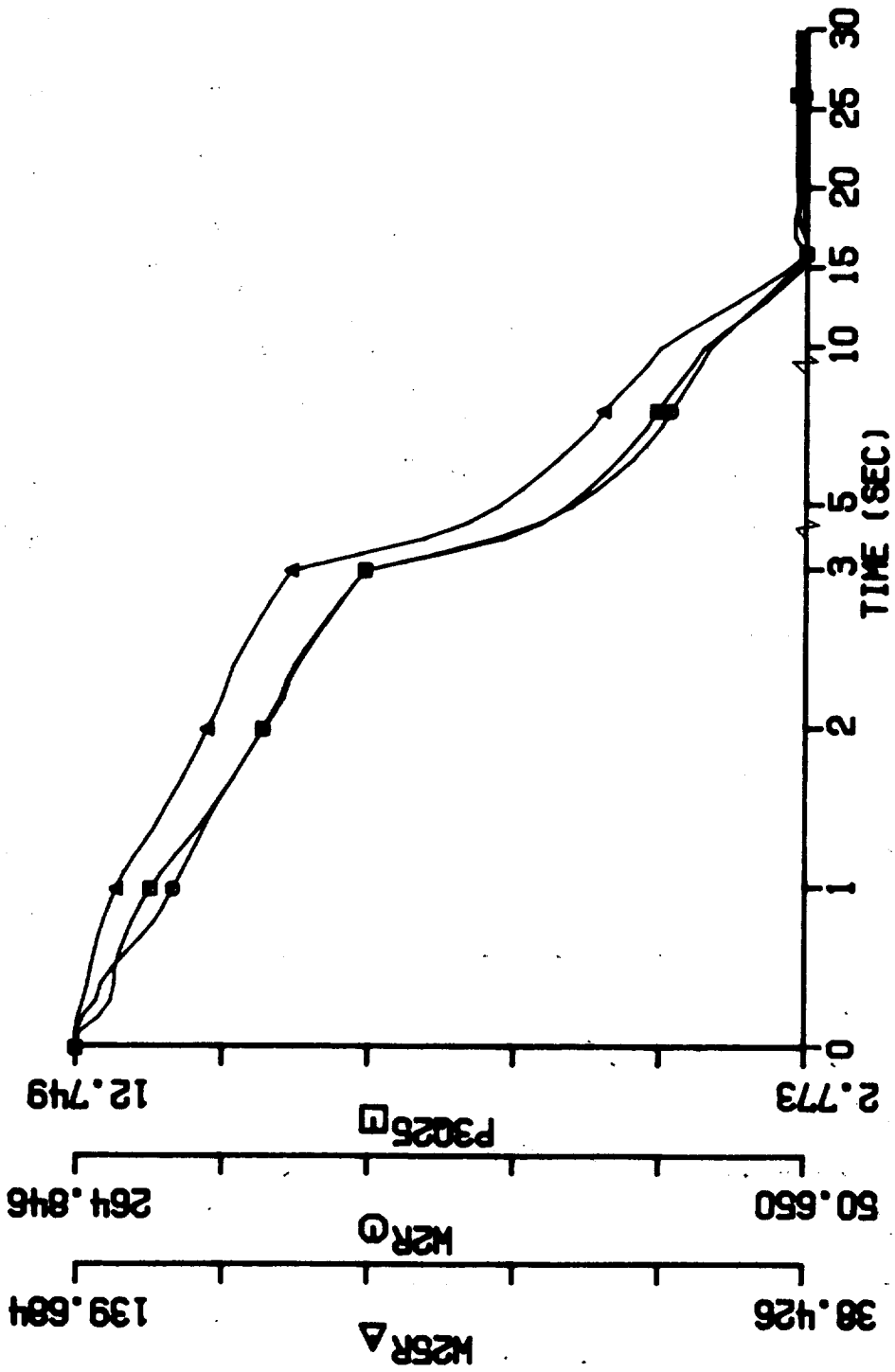

Figure 22.2 Transient Engine Performance: PLA changes from Max Power Setting to Ground Idle Setting, 4% water ingestion with all liquid drained, standard temperature (P3Q25, W2R, W25R vs. time)

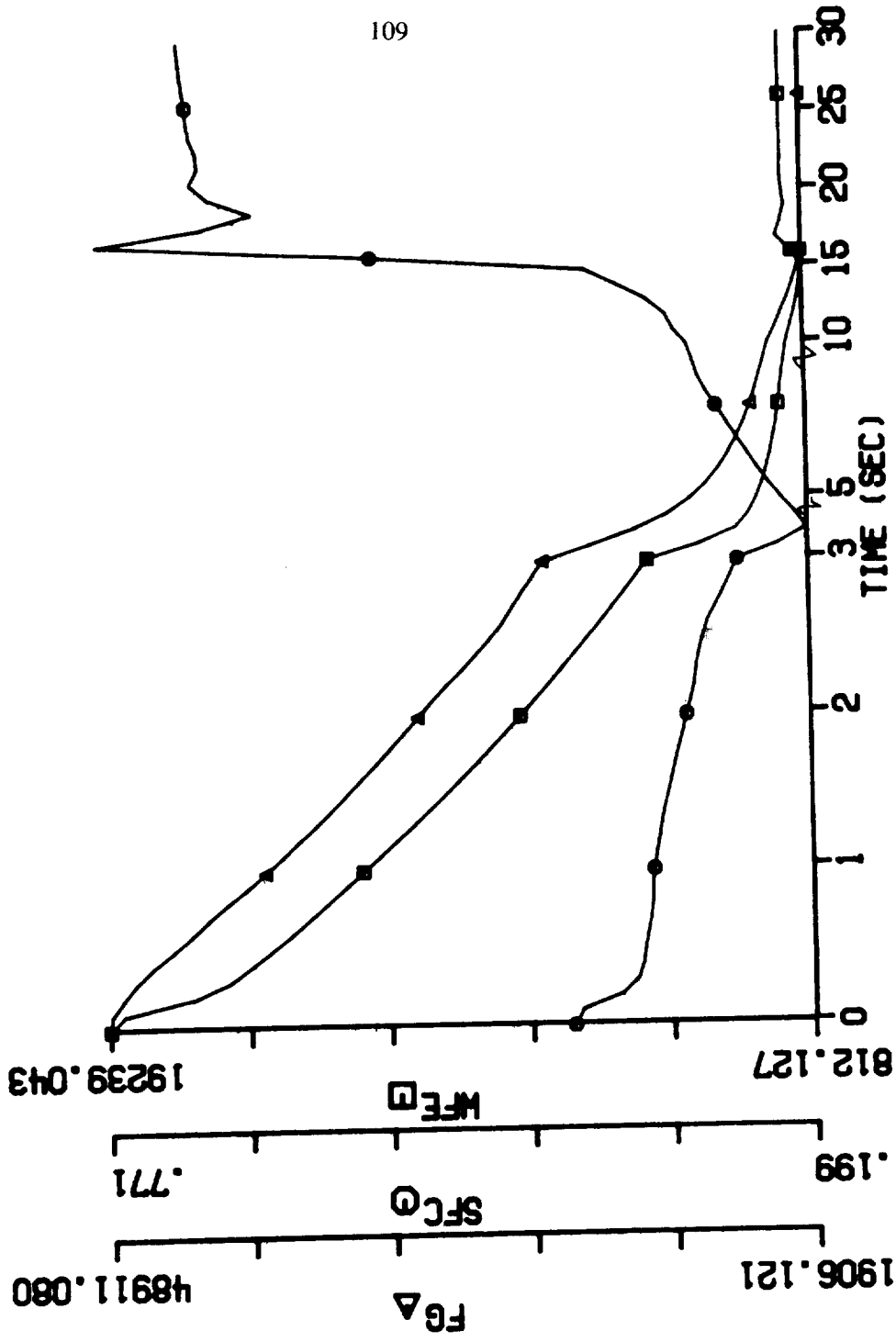

Figure 22.3 Transient Engine Performance: PLA changes from Max Power Setting to Ground Idle Setting, 4% water ingestion with all liquid drained, standard temperature (WFE, SFC, FG vs. time)

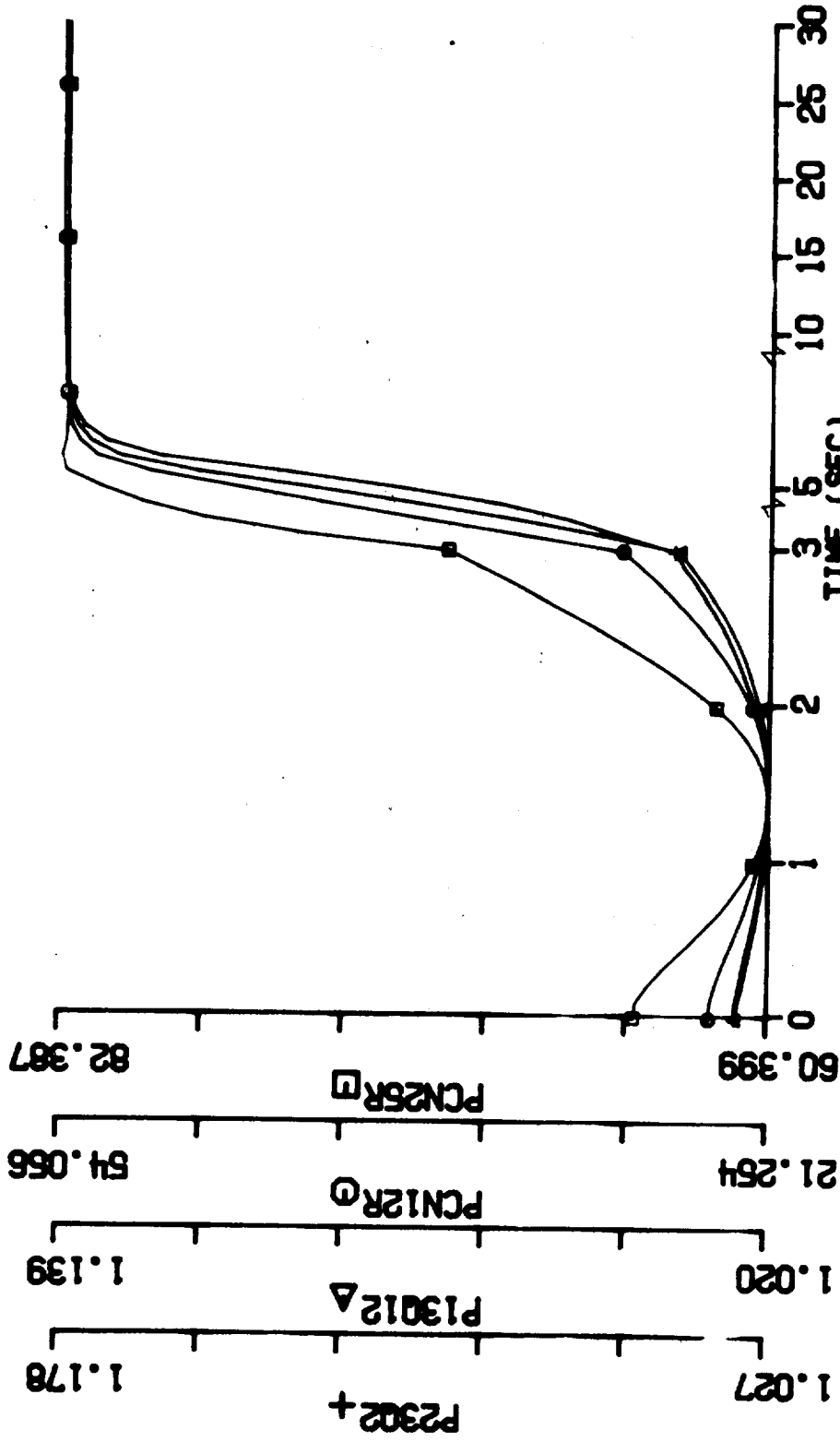

Figure 23.1 Transient Engine Performance: PLA changes from Ground Idle Setting to Max Power Setting, 2% water ingestion with 1% liquid evaporated at burner entry, standard temperature (PCN25R, PCN12R, P13Q12, P23Q2 vs. time)

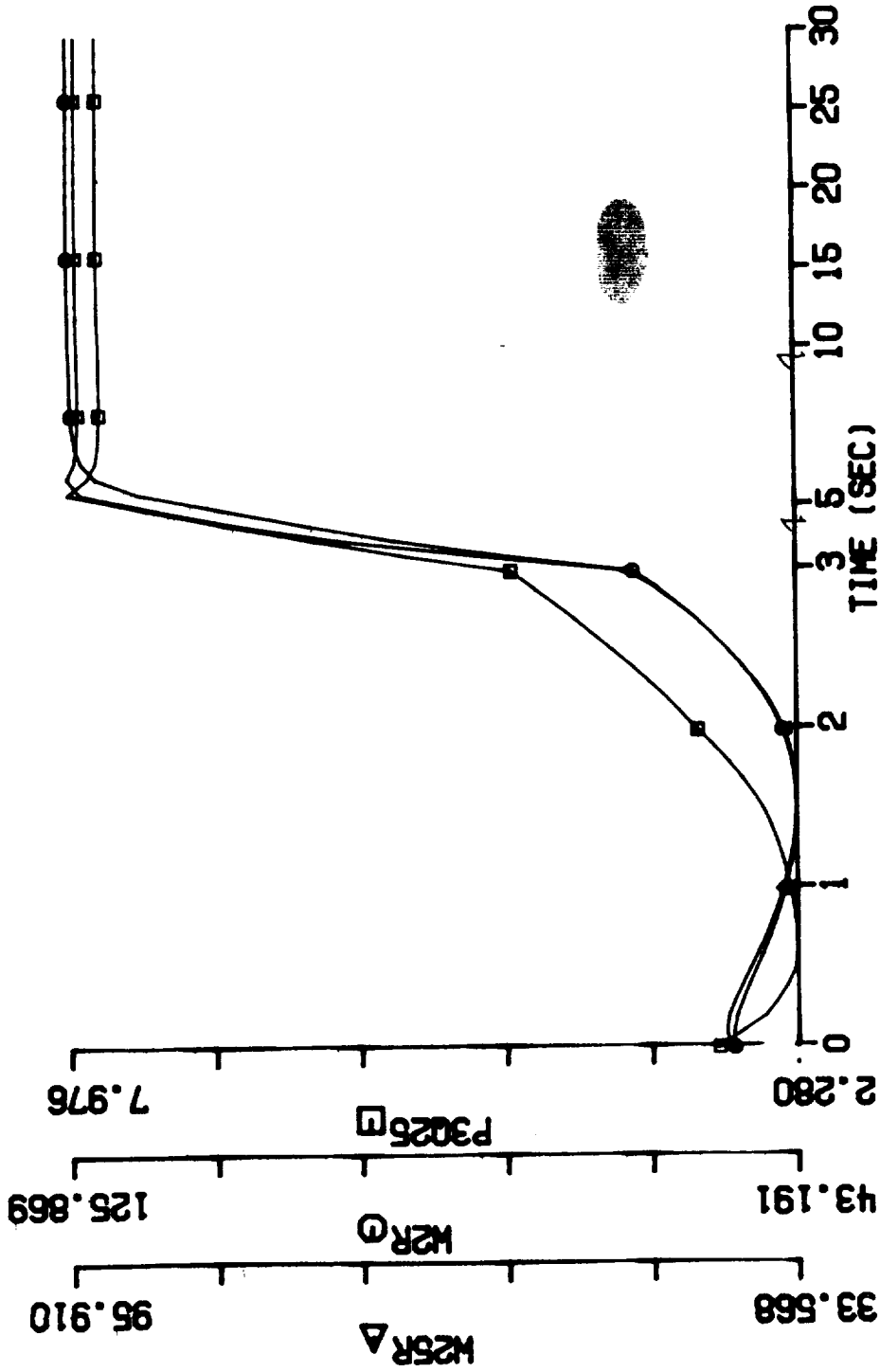

Figure 23.2 Transient Engine Performance: PLA changes from Ground Idle Setting to Max Power Setting, 2% water ingestion with 1% liquid evaporated at burner entry, standard temperature (P3Q25, W2R, W25R vs. time)

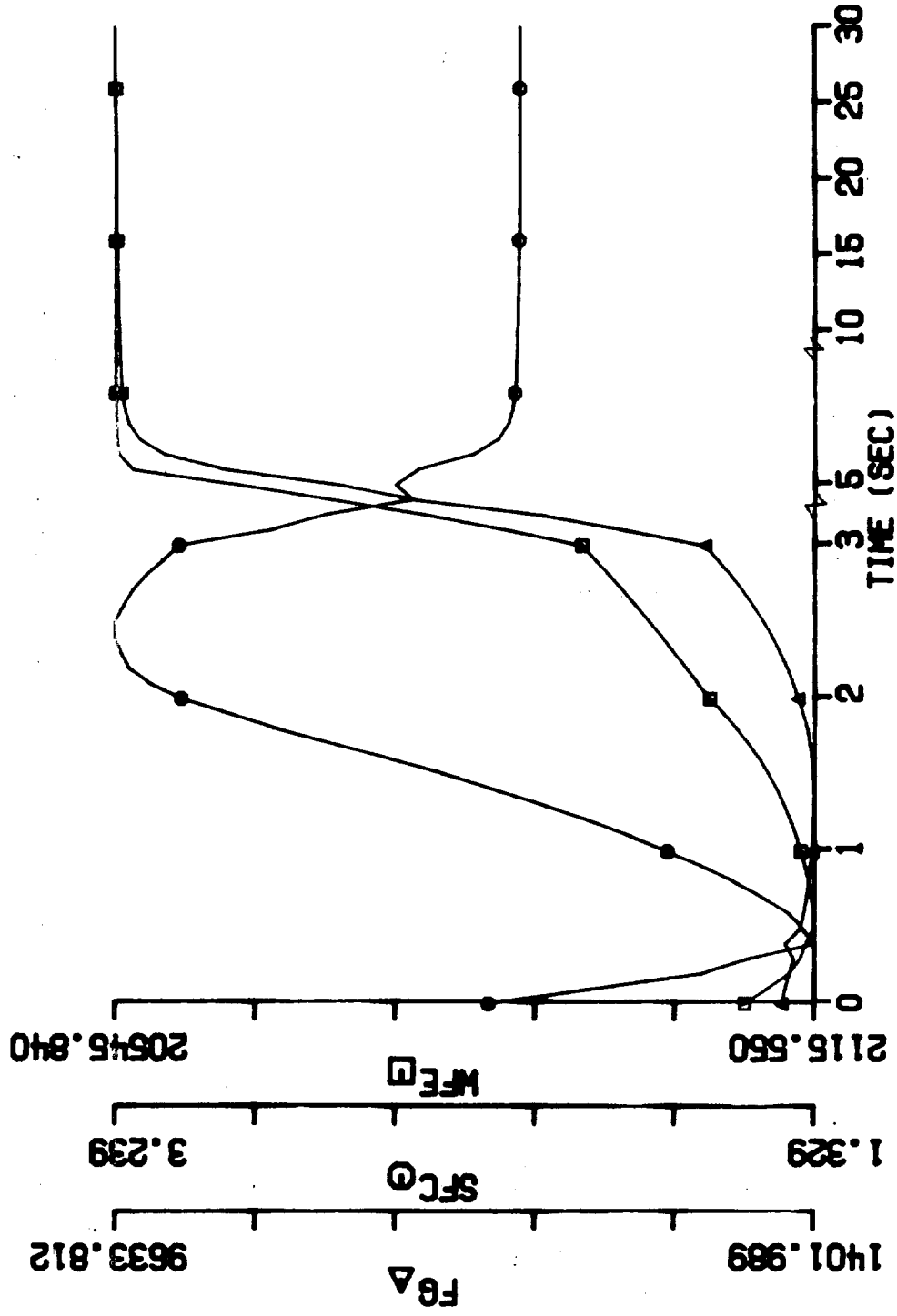

Figure 23.3 Transient Engine Performance: PLA changes from Ground Idle Setting to Max Power Setting, 2% water ingestion with 1% liquid evaporated at burner entry, standard temperature (WFE, SFC, FG vs. time)

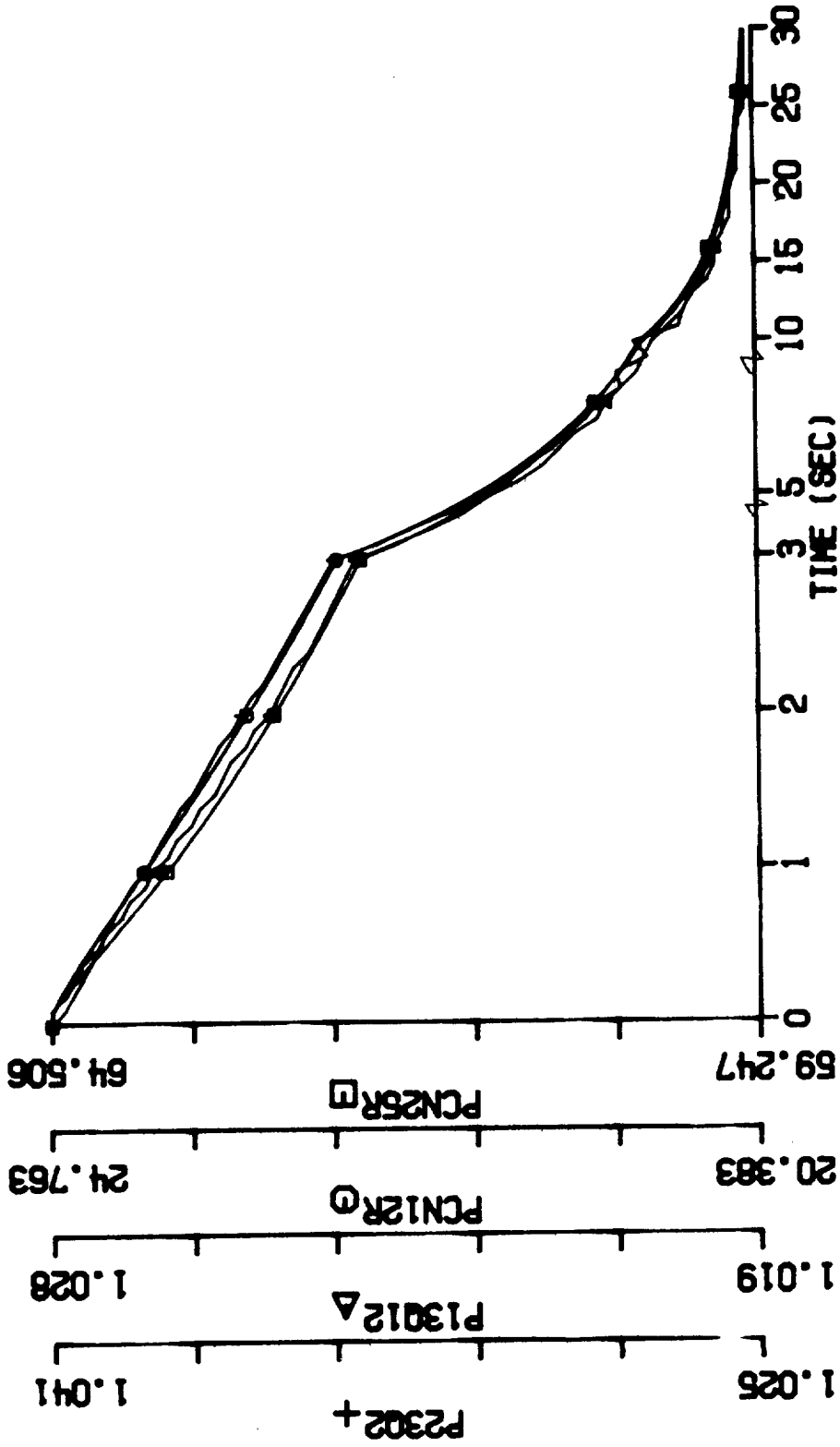

Figure 24.1 Transient Engine Performance: PLA changes from Ground Idle Setting to Max Power Setting, 2% water ingestion with 0.5% liquid evaporated at burner entry, standard temperature (PCN25R, PCN12R, P13Q12, P23Q2 vs. time)

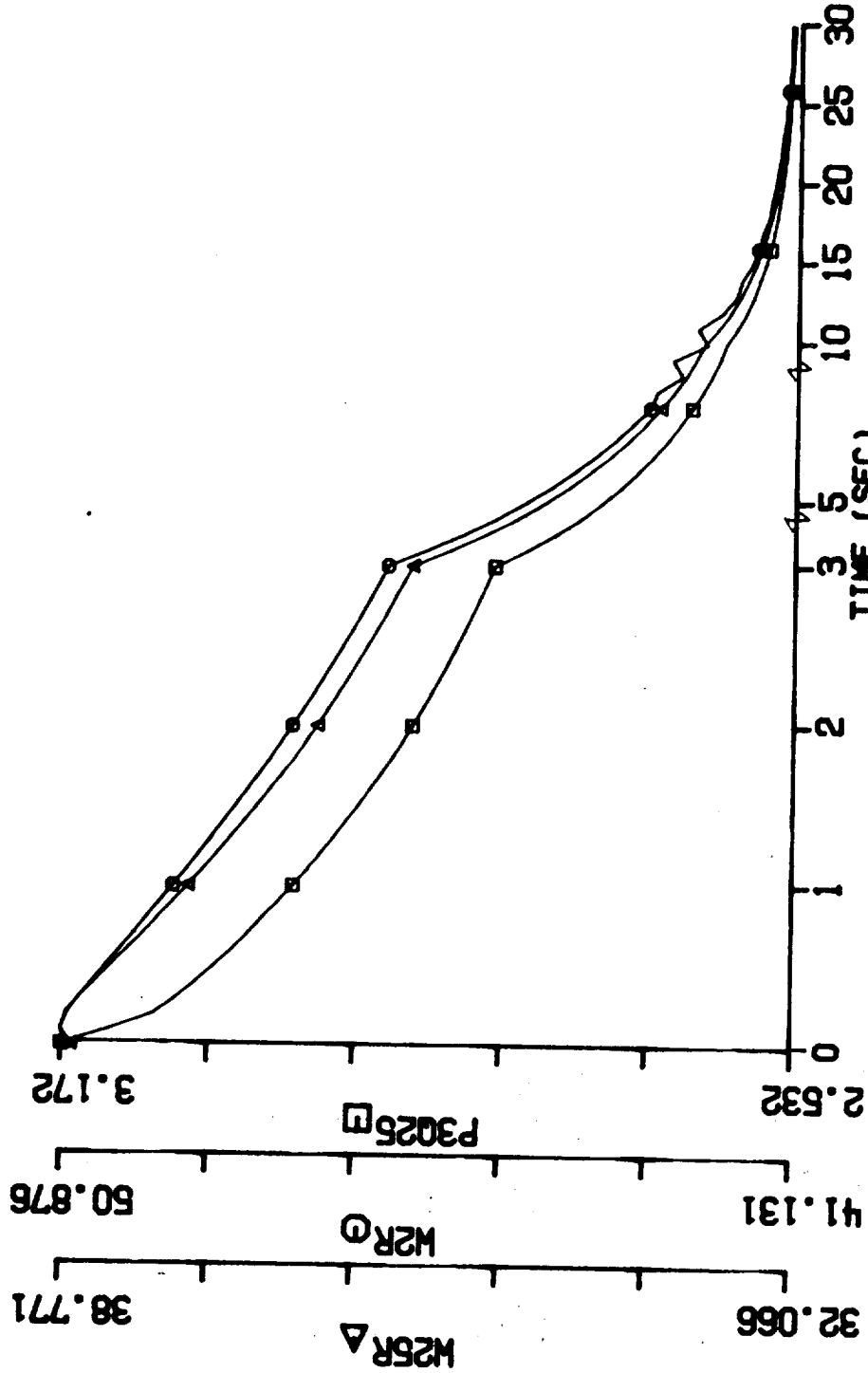

Figure 24.2 Transient Engine Performance: PLA changes from Ground Idle Setting to Max Power Setting, 2% water ingestion with 0.5% liquid evaporated at burner entry, standard temperature (P3Q25, W2R, W25R vs. time)

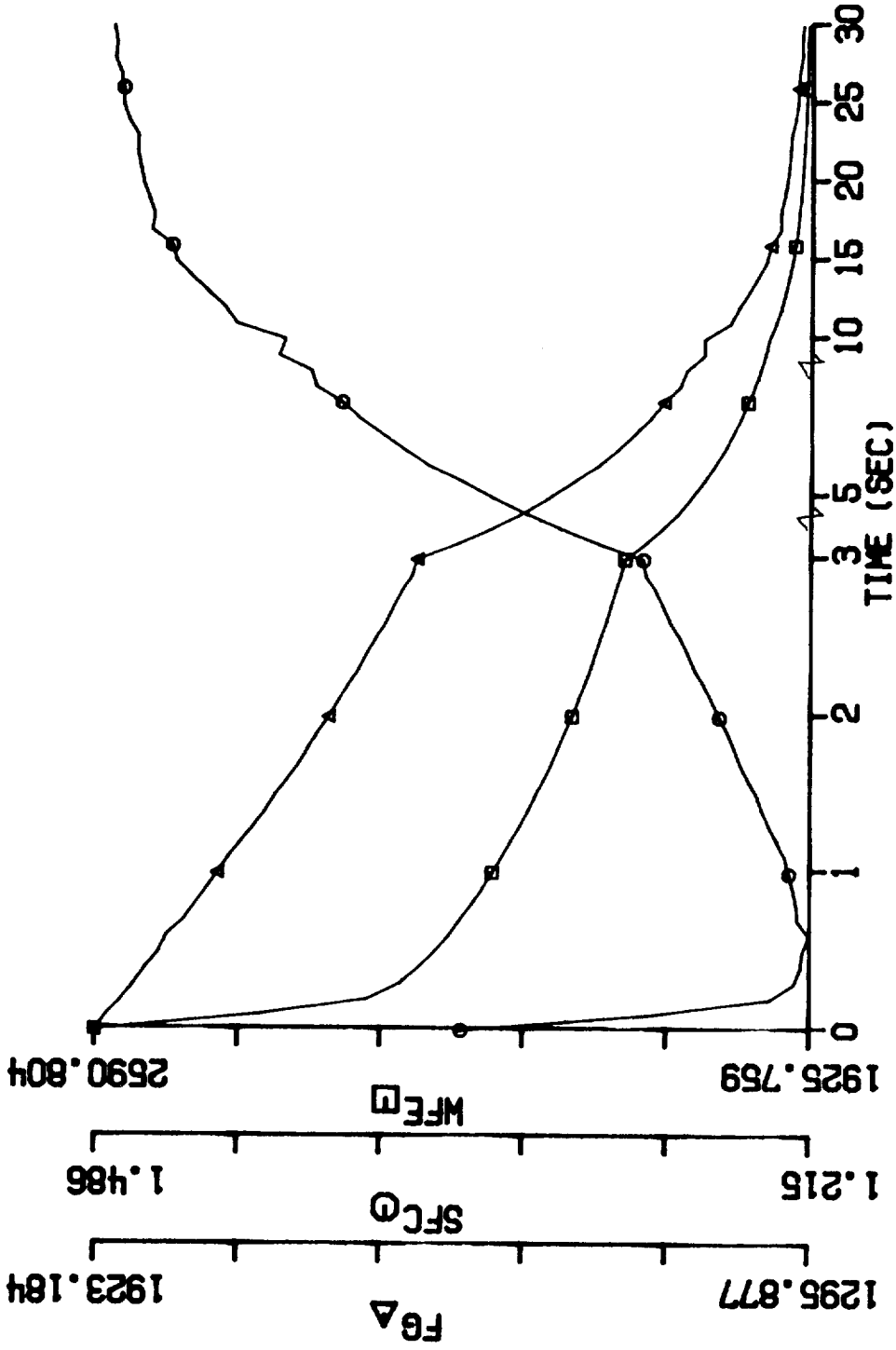

Figure 24.3 Transient Engine Performance: PLA changes from Ground Idle Setting to Max Power Setting, 2% water ingestion with 0.5% liquid evaporated at burner entry, standard temperature (WFE, SFC, FG vs. time)

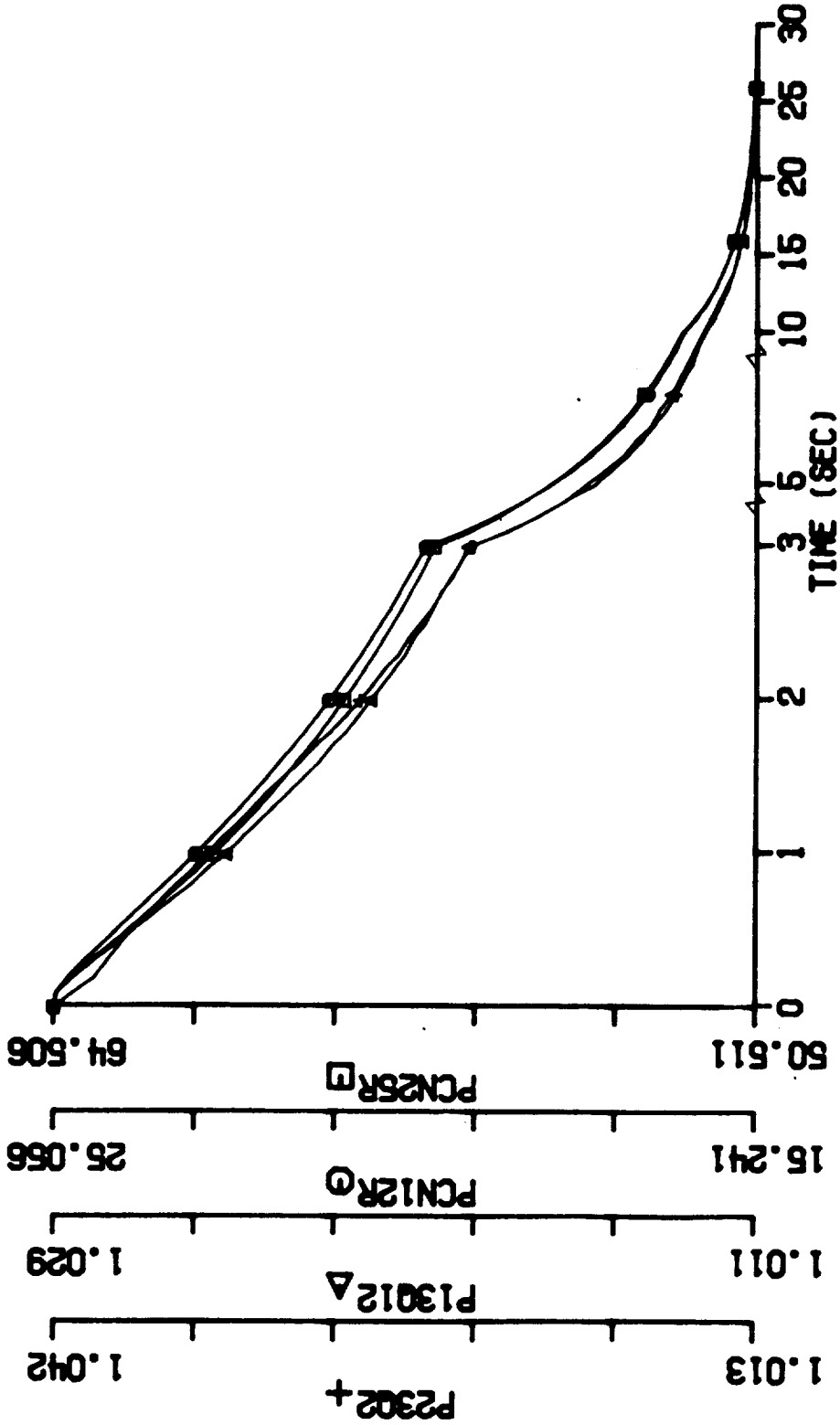

Figure 25.1 Transient Engine Performance: PLA changes from Ground Idle Setting to Max Power Setting, 2% water ingestion with 1% liquid evaporated at burner exit, standard temperature (PCN25R, PCN12R, P13Q12, P23Q2 vs. time)

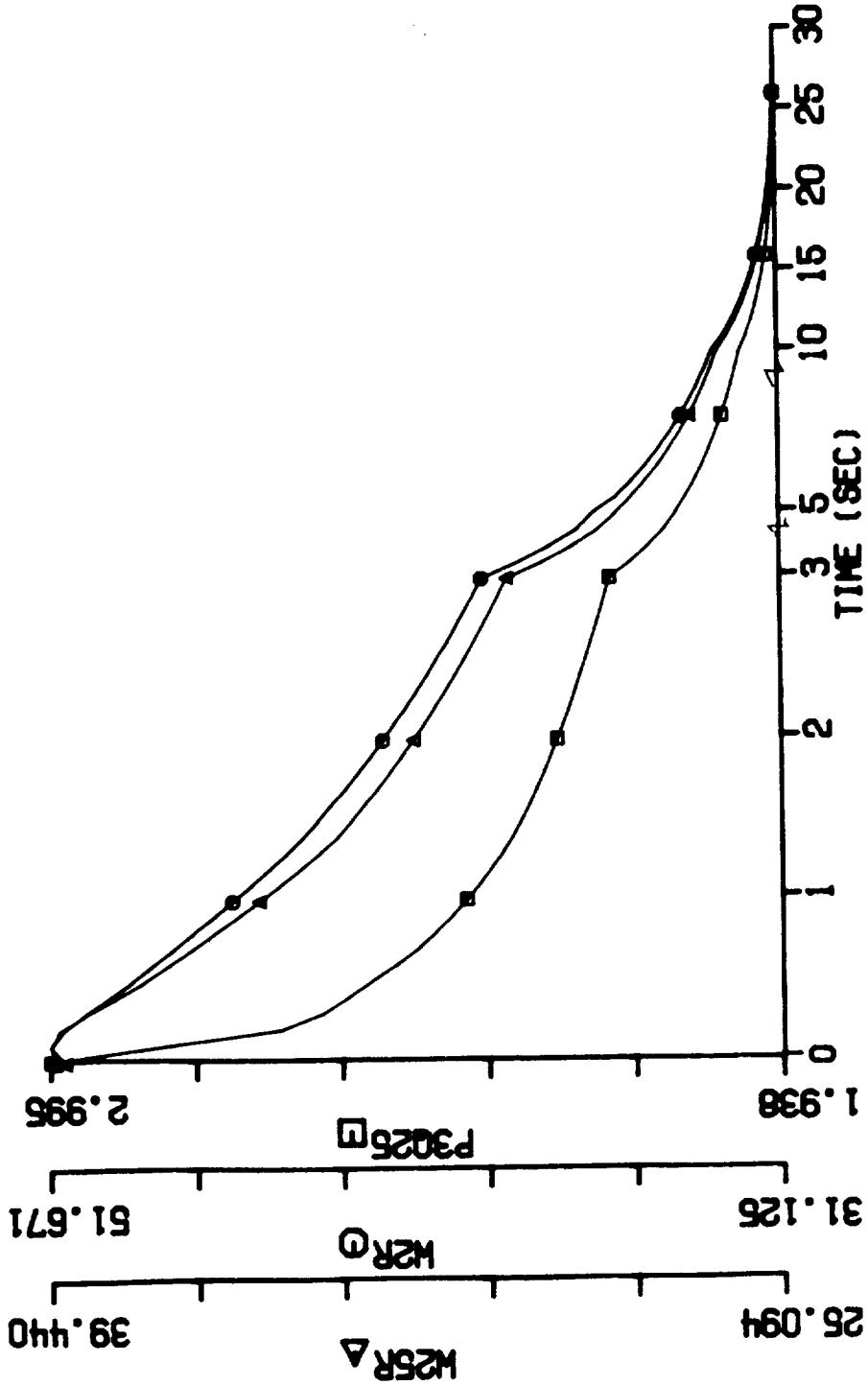

Figure 25.2 Transient Engine Performance: PLA changes from Ground Idle Setting to Max Power Setting, 2% water ingestion with 1% liquid evaporated at burner exit, standard temperature (P3Q25, W2R, W25R vs. time)

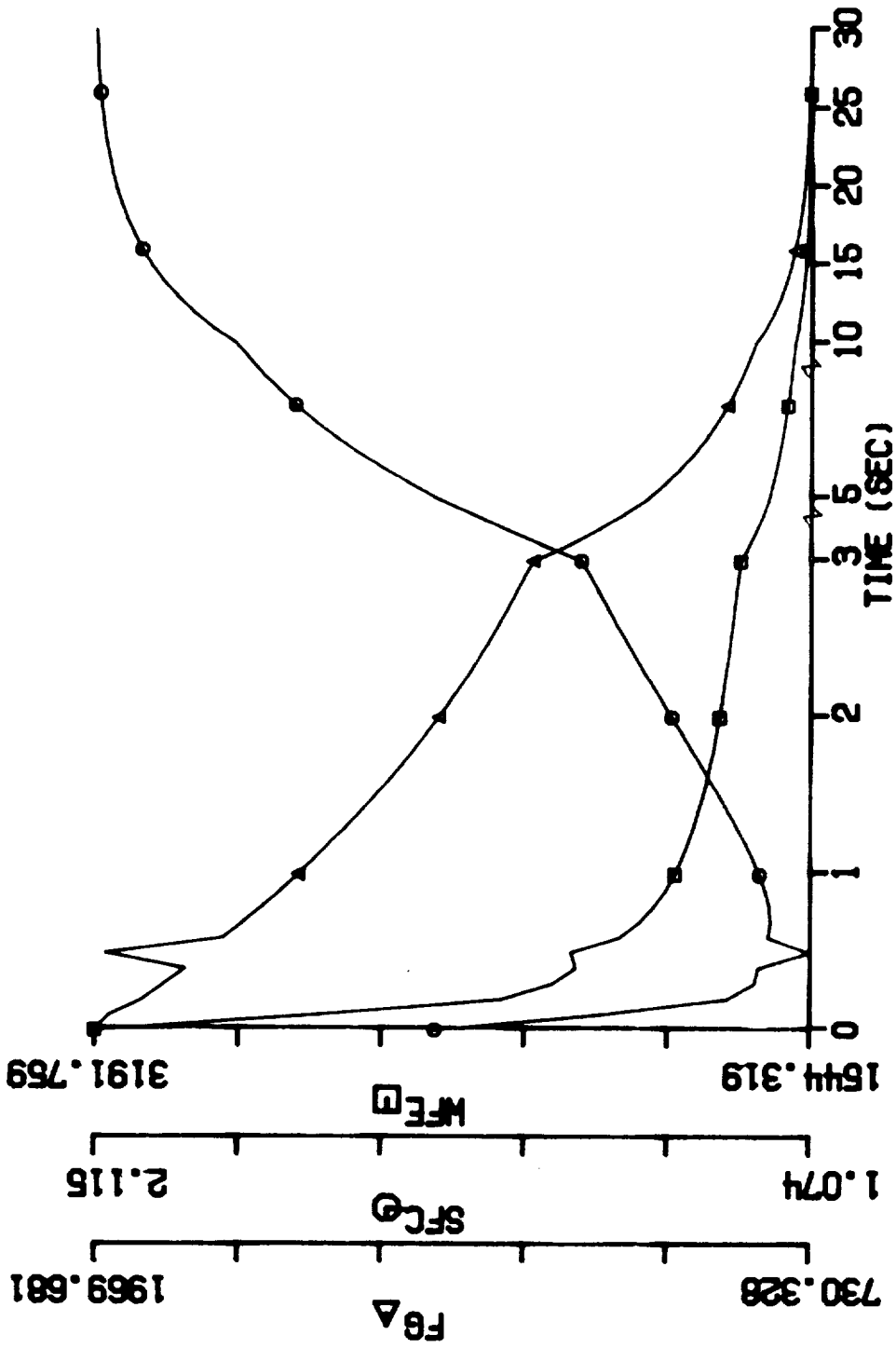

Figure 25.3 Transient Engine Performance: PLA changes from Ground Idle Setting to Max Power Setting, 2% water ingestion with 1% liquid evaporated at burner exit, standard temperature (WFE, SFC, FG vs. time)

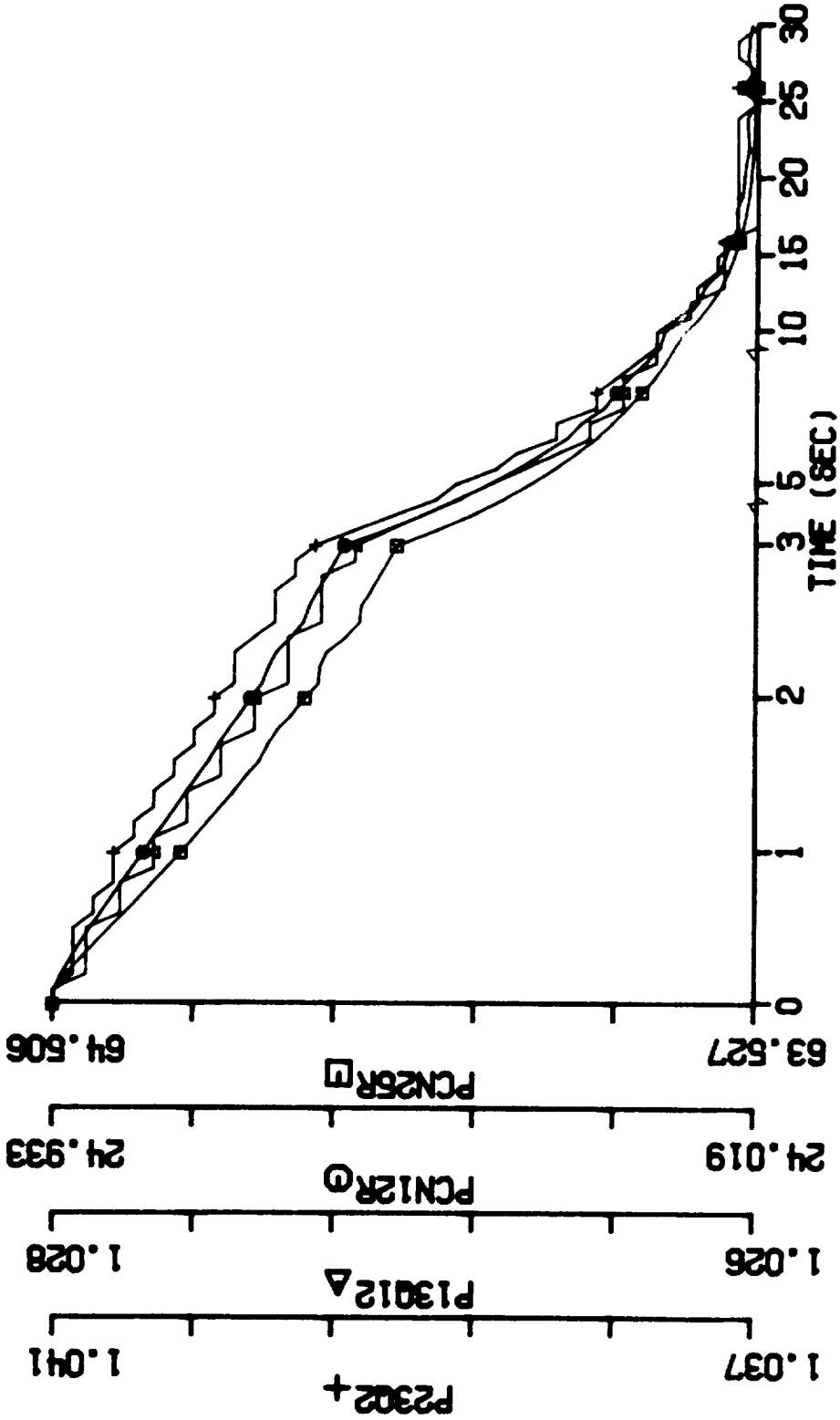

Figure 26.1 Transient Engine Performance: PLA changes from Ground Idle Setting to Max Power Setting, 2% water ingestion with 05% liquid evaporated at burner exit, standard temperature (PCN25R, PCN12R, P13Q12, P23Q2 vs. time)

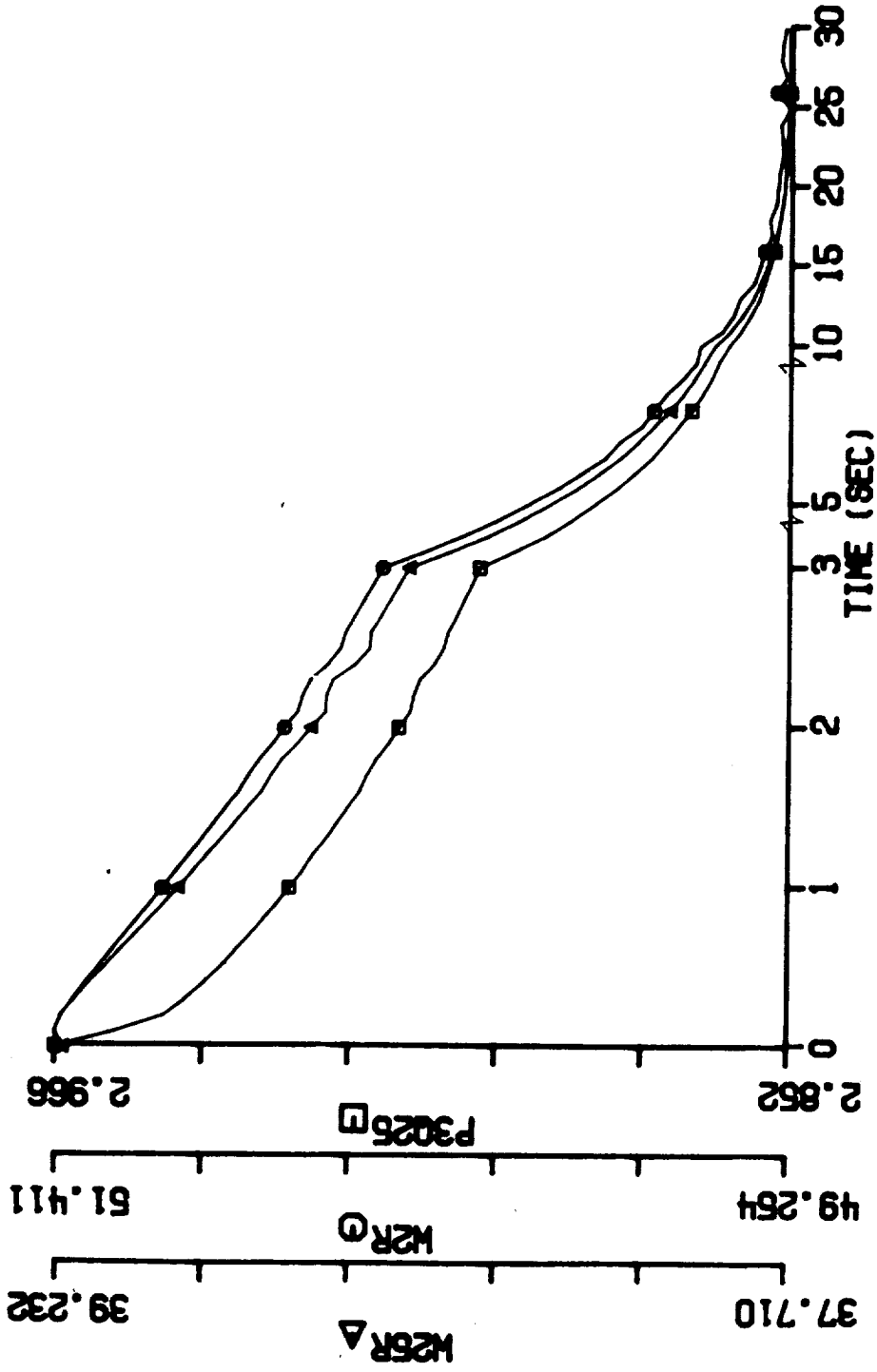

Figure 26.2 Transient Engine Performance: PLA changes from Ground Idle Setting to Max Power Setting, 2% water ingestion with 0.5% liquid evaporated at burner exit, standard temperature (P3Q25, W2R, W25R vs. time)

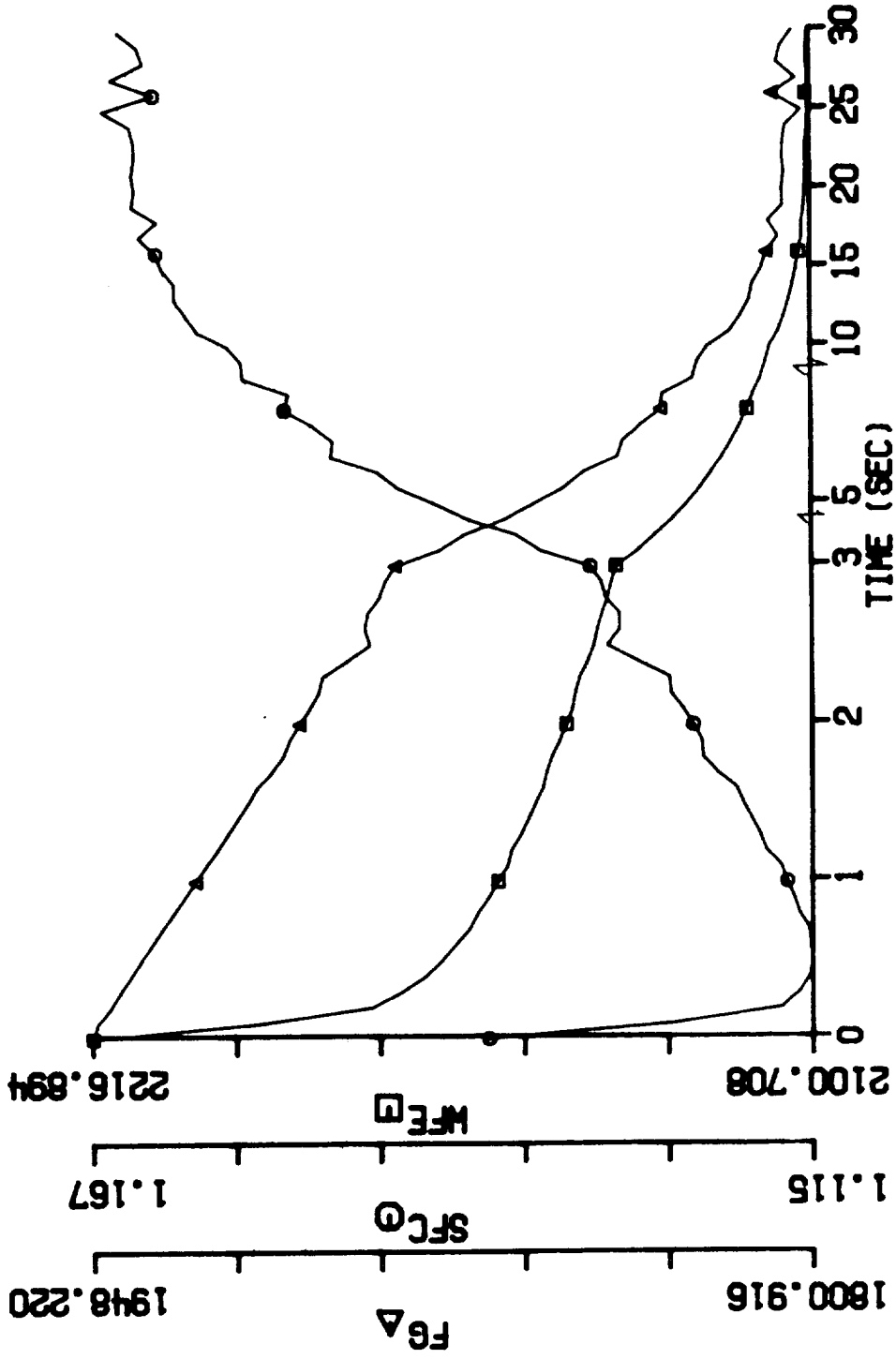

Figure 26.3 Transient Engine Performance: PLA changes from Ground Idle Setting to Max Power Setting, 2% water ingestion with 0.5% liquid evaporated at burner exit, standard temperature (WFE, SFC, FG vs. time)

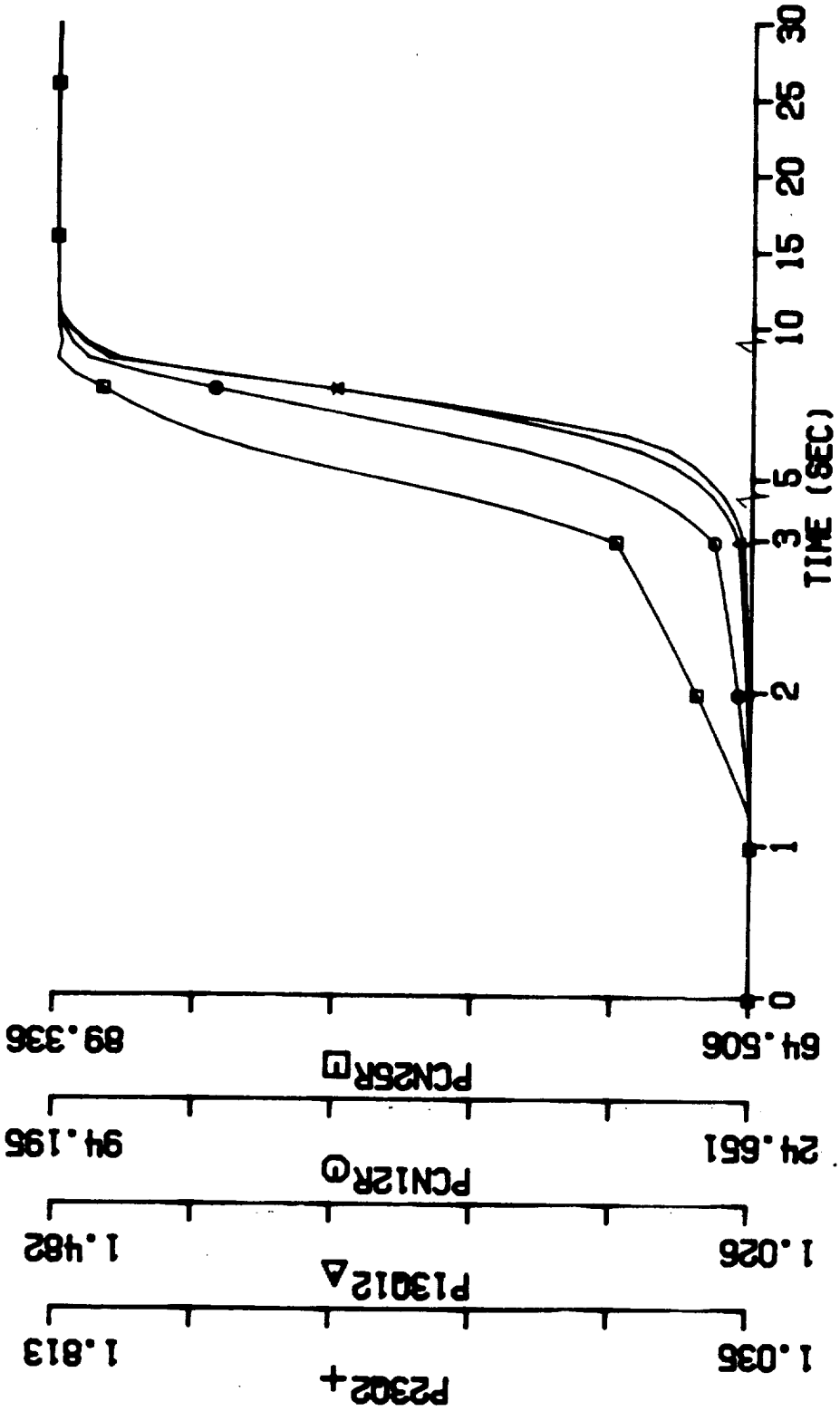

Figure 27.1 Transient Engine Performance: PLA changes from Ground Idle Setting to Max Power Setting, dry air operation, "Hot Day" temperature
(PCN25R, PCN12R, P13Q12, P23Q2 vs. time)

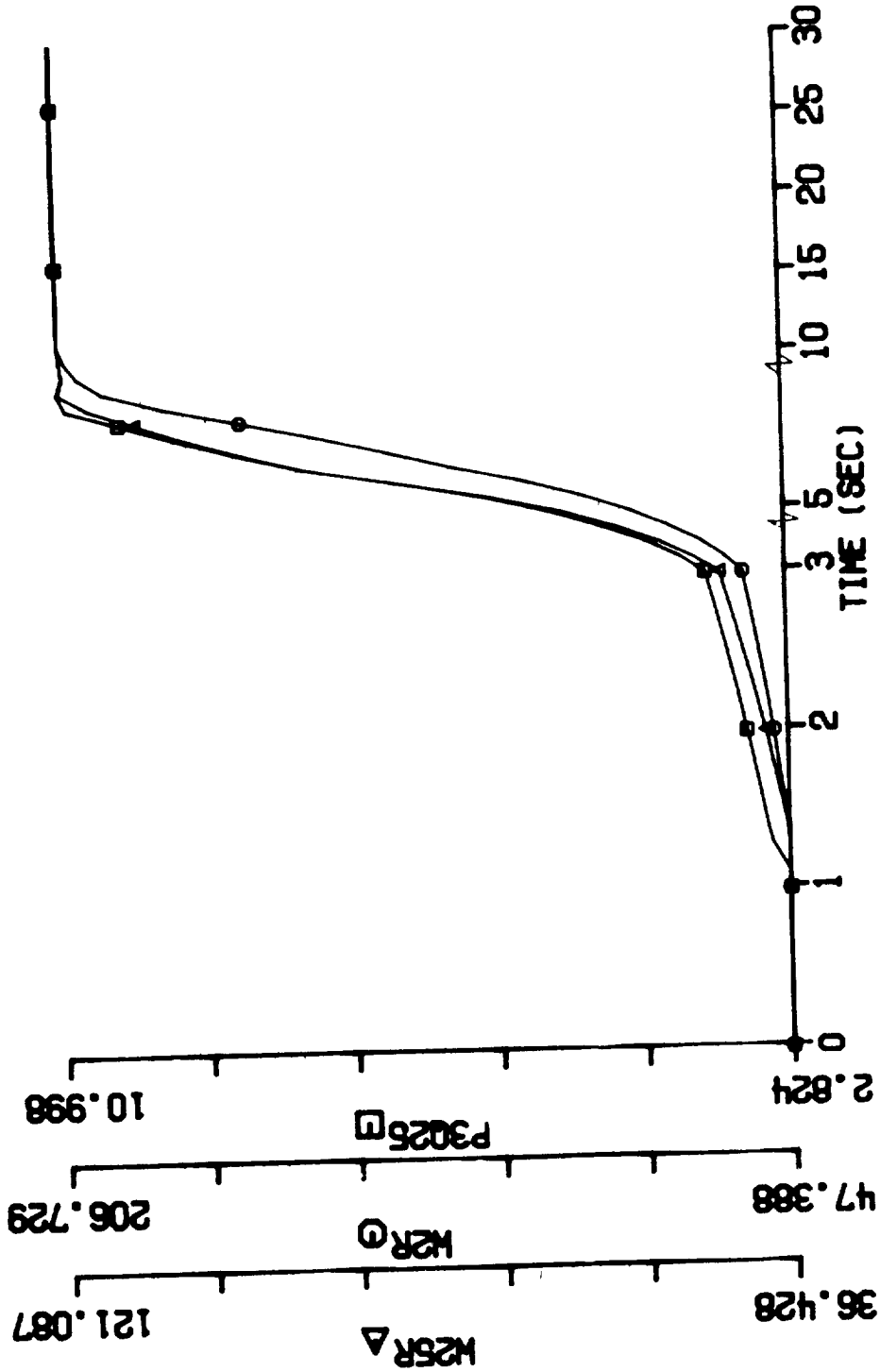

Figure 27.2 Transient Engine Performance: PLA changes from Ground Idle Setting to Max Power Setting, dry air operation, "Hot Day" temperature
(P3Q25, W2R, W25R vs. time)

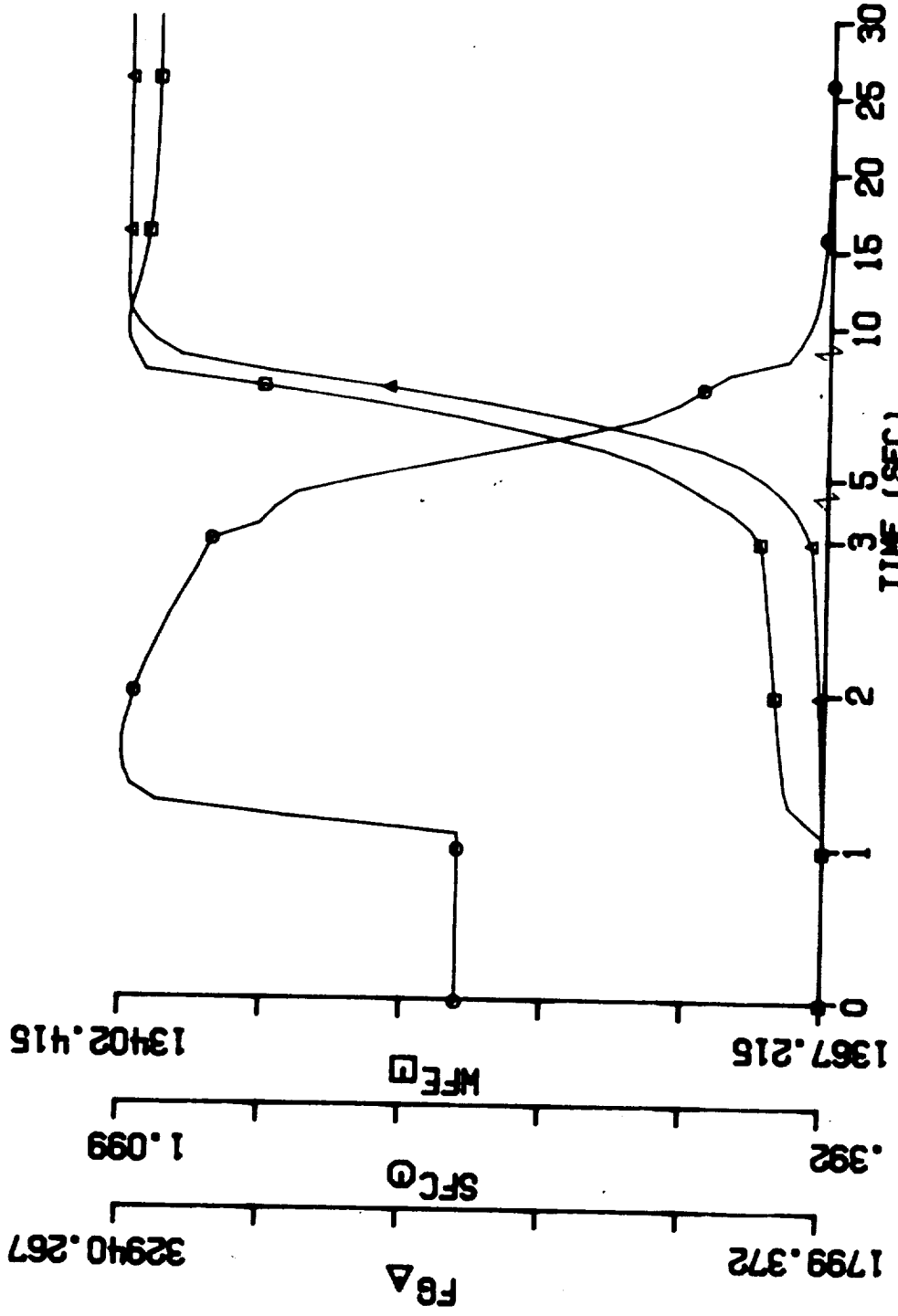

Figure 27.3 Transient Engine Performance: PLA changes from Ground Idle Setting to Max Power Setting, dry air operation, "Hot Day" temperature
(WFE, SFC, FG vs. time)

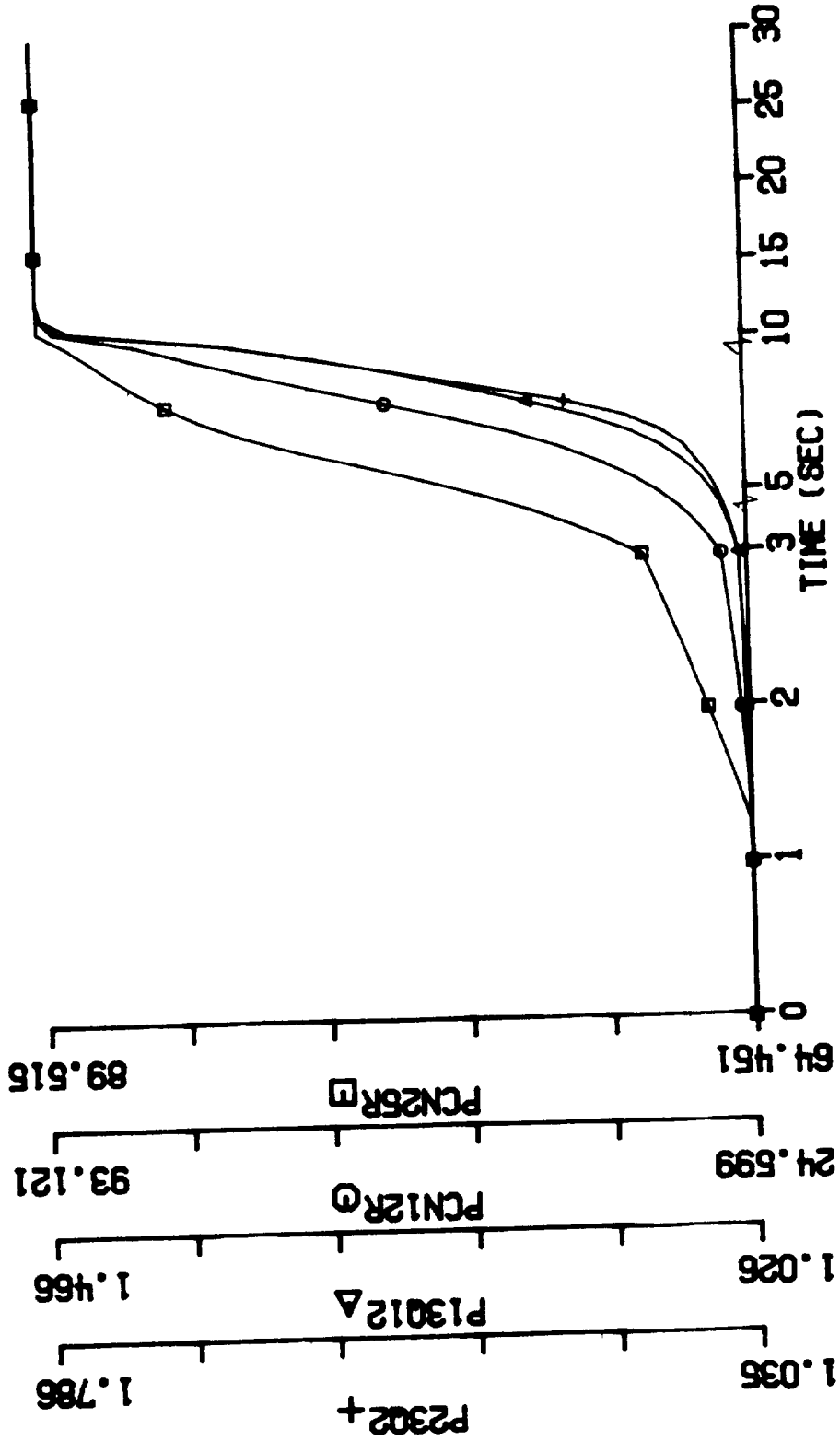

Figure 28.1 Transient Engine Performance: PLA changes from Ground Idle Setting to Max Power Setting, 4% water ingestion with all liquid drained, "Hot Day" temperature (PCN25R, PCN12R, P13Q12, P23Q2 vs. time)

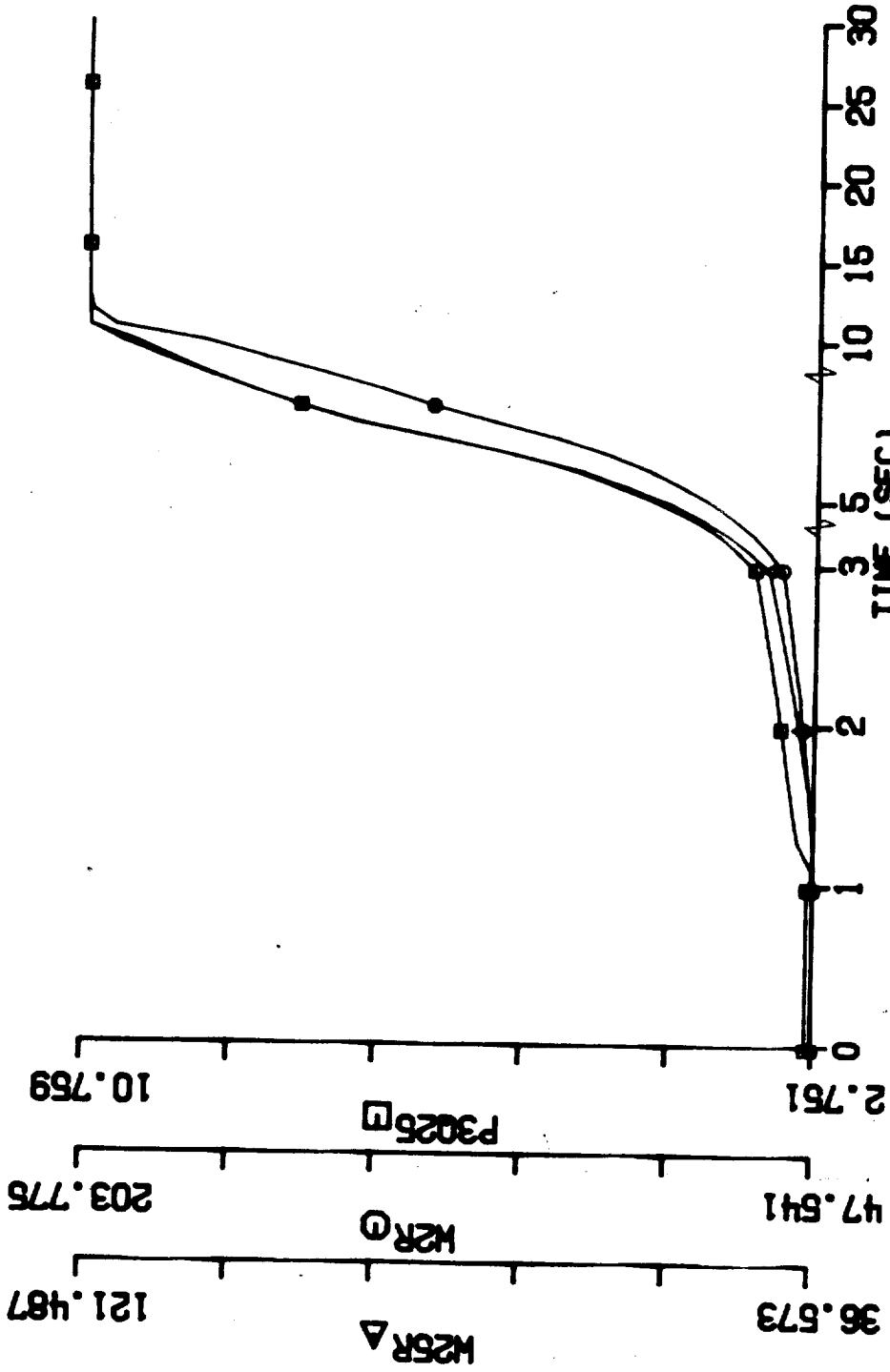

Figure 28.2 Transient Engine Performance: PLA changes from Ground Idle Setting to Max Power Setting, 4% water ingestion with all liquid drained, "Hot Day" temperature (P3Q25, W2R, W25R vs. time)

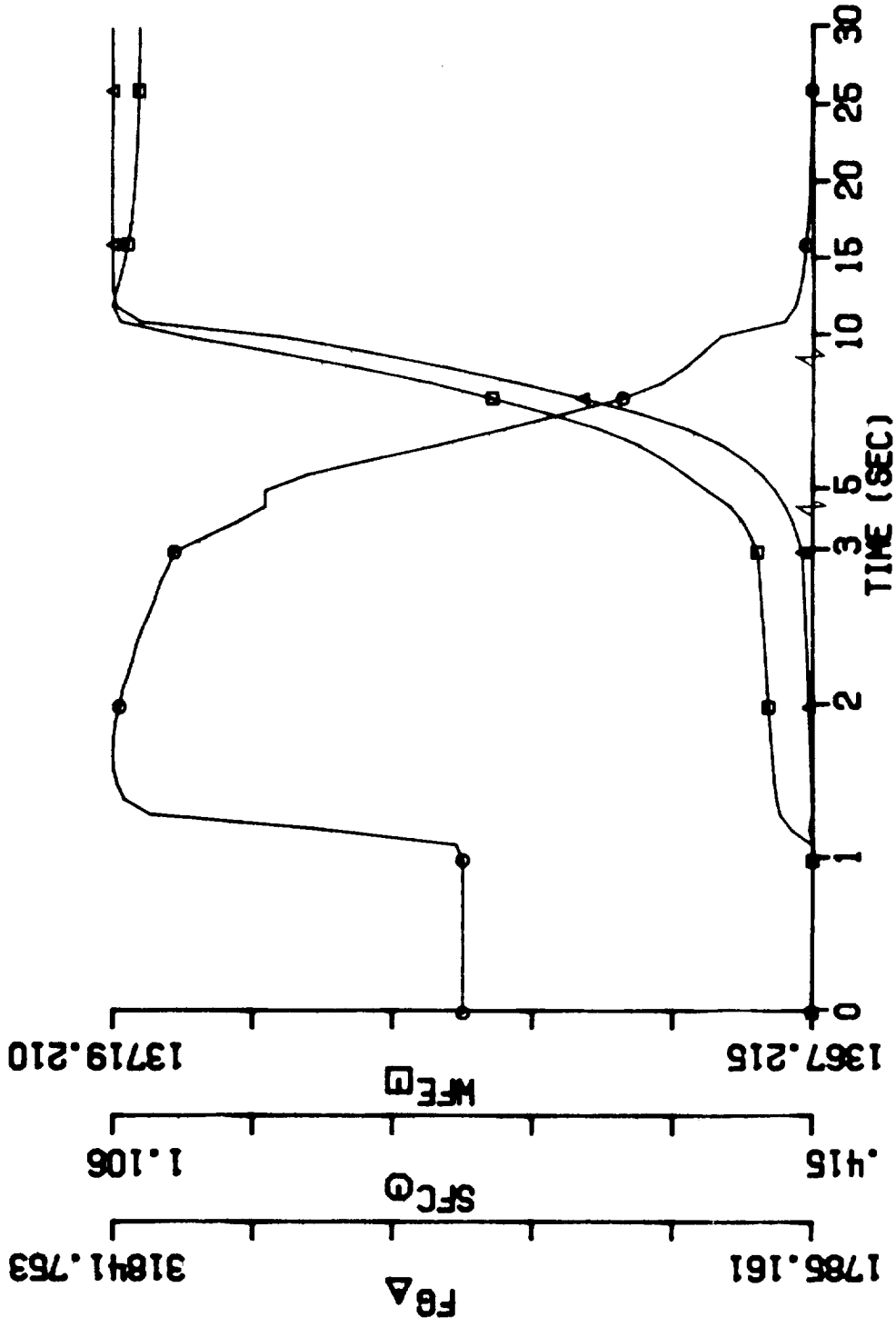

Figure 28.3 Transient Engine Performance: PLA changes from Ground Idle Setting to Max Power Setting, 4% water ingestion with all liquid drained, "Hot Day" temperature (WFE, SFC, FG vs. time)

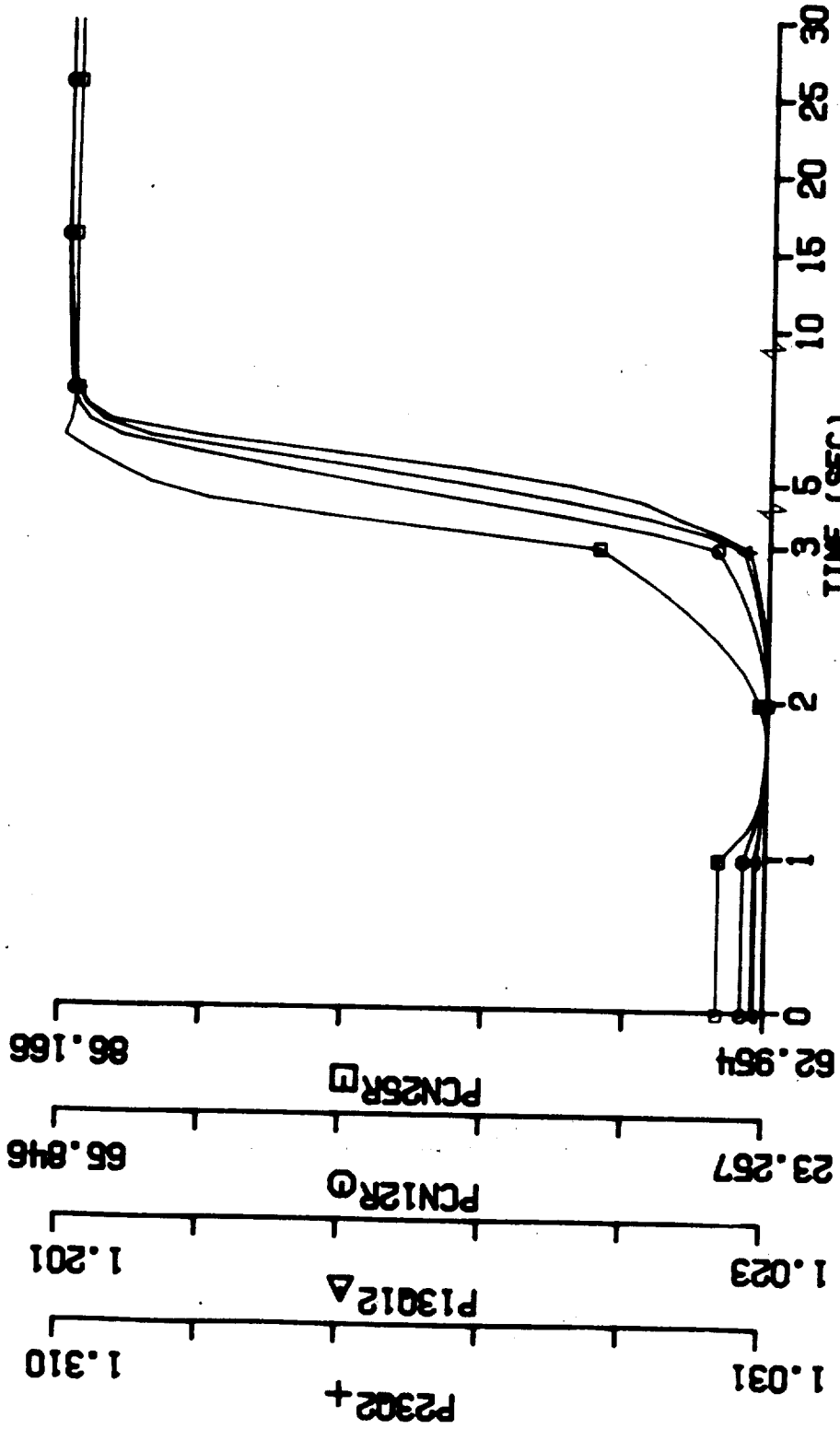

Figure 29.1 Transient Engine Performance: PLA changes from Ground Idle Setting to Max Power Setting, 4% water ingestion with 1% liquid evaporated at burner entry, "Hot Day" temperature (PCN25R, PCN12R, P13Q12, P23Q2 vs. time)

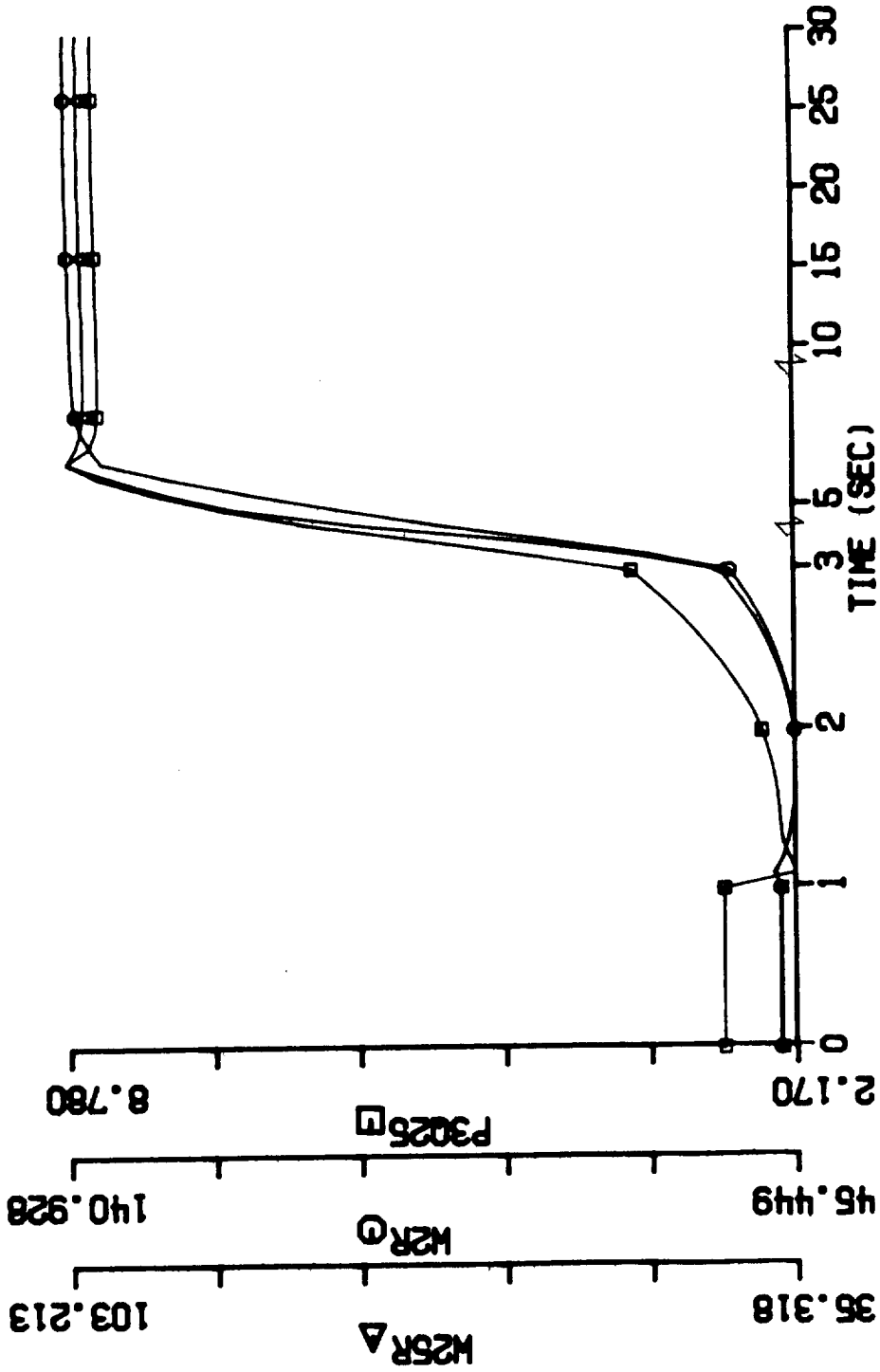

Figure 29.2 Transient Engine Performance: PLA changes from Ground Idle Setting to Max Power Setting, 4% water ingestion with 1% liquid evaporated at burner entry, "Hot Day" temperature (P3Q25, W2R, W25R vs. time)

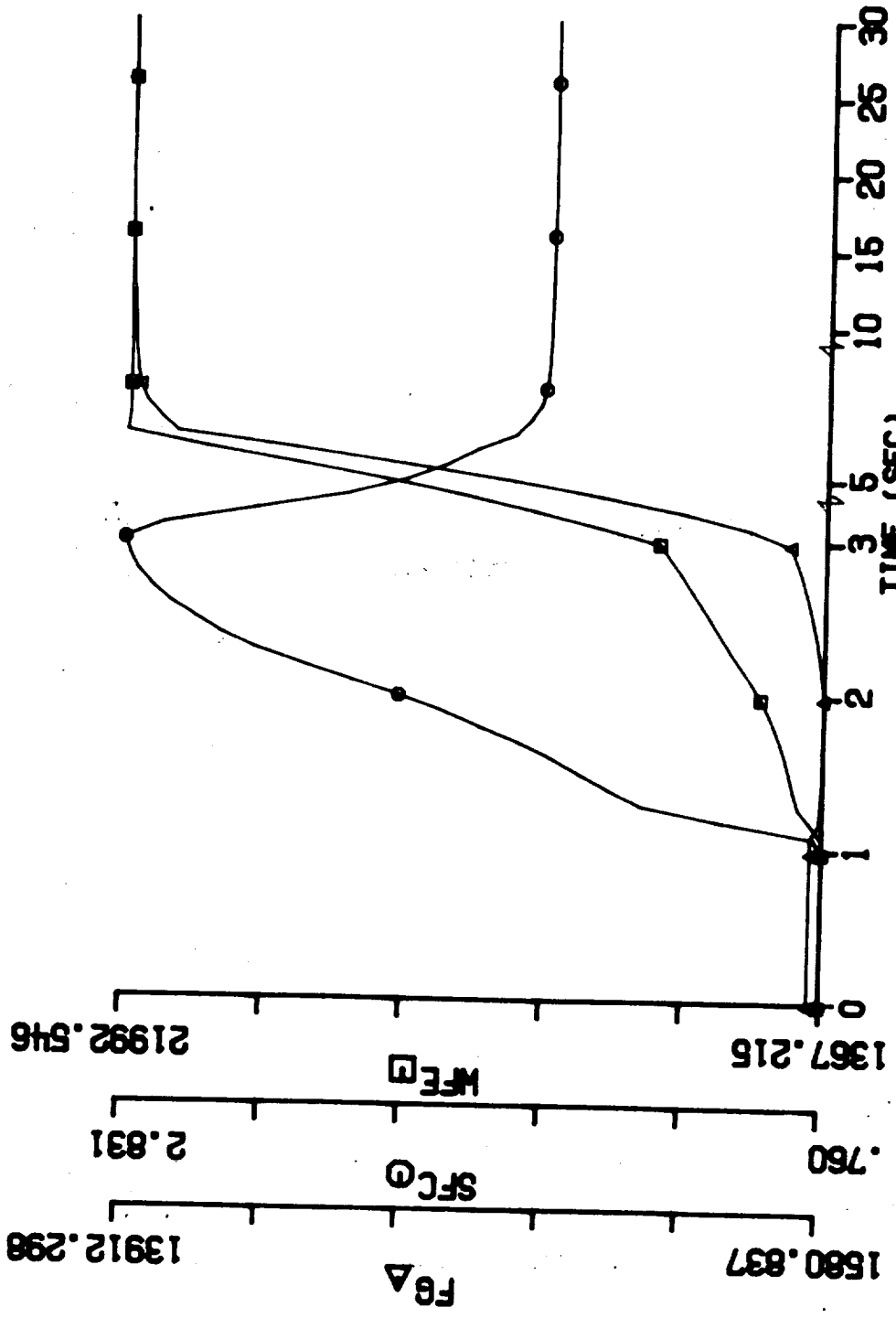

Figure 29.3 Transient Engine Performance: PLA changes from Ground Idle Setting to Max Power Setting, 4% water ingestion with 1% liquid evaporated at burner entry, "Hot Day" temperature (WFE, SFC, FG vs. time)

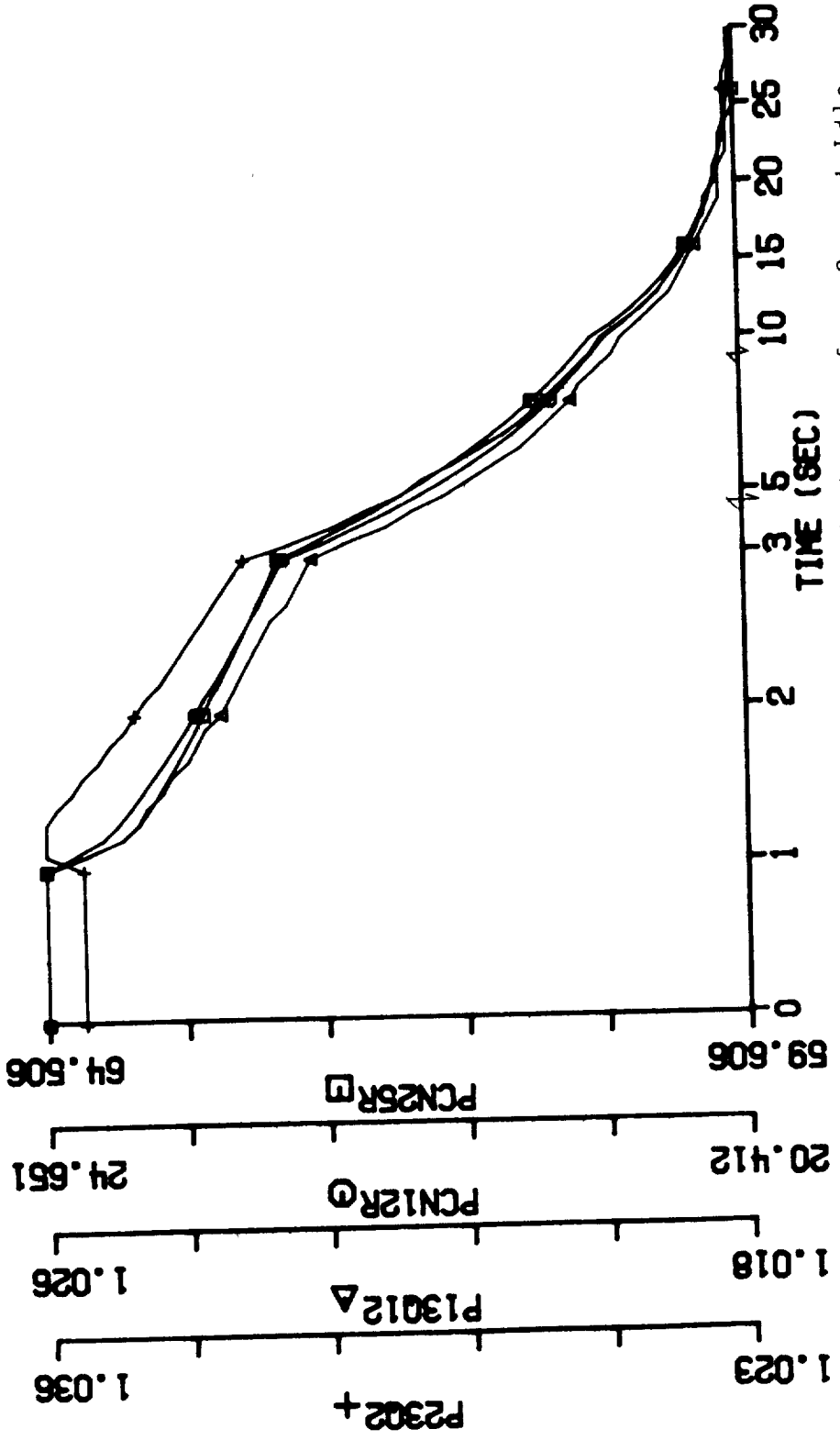

Figure 30.1 Transient Engine Performance: PLA changes from Ground Idle Setting to Max Power Setting, 4% water ingestion with 0.5% liquid evaporated at burner entry, "Hot Day" temperature (PCN25R, PCN12R, P13Q12, P23Q2 vs. time)

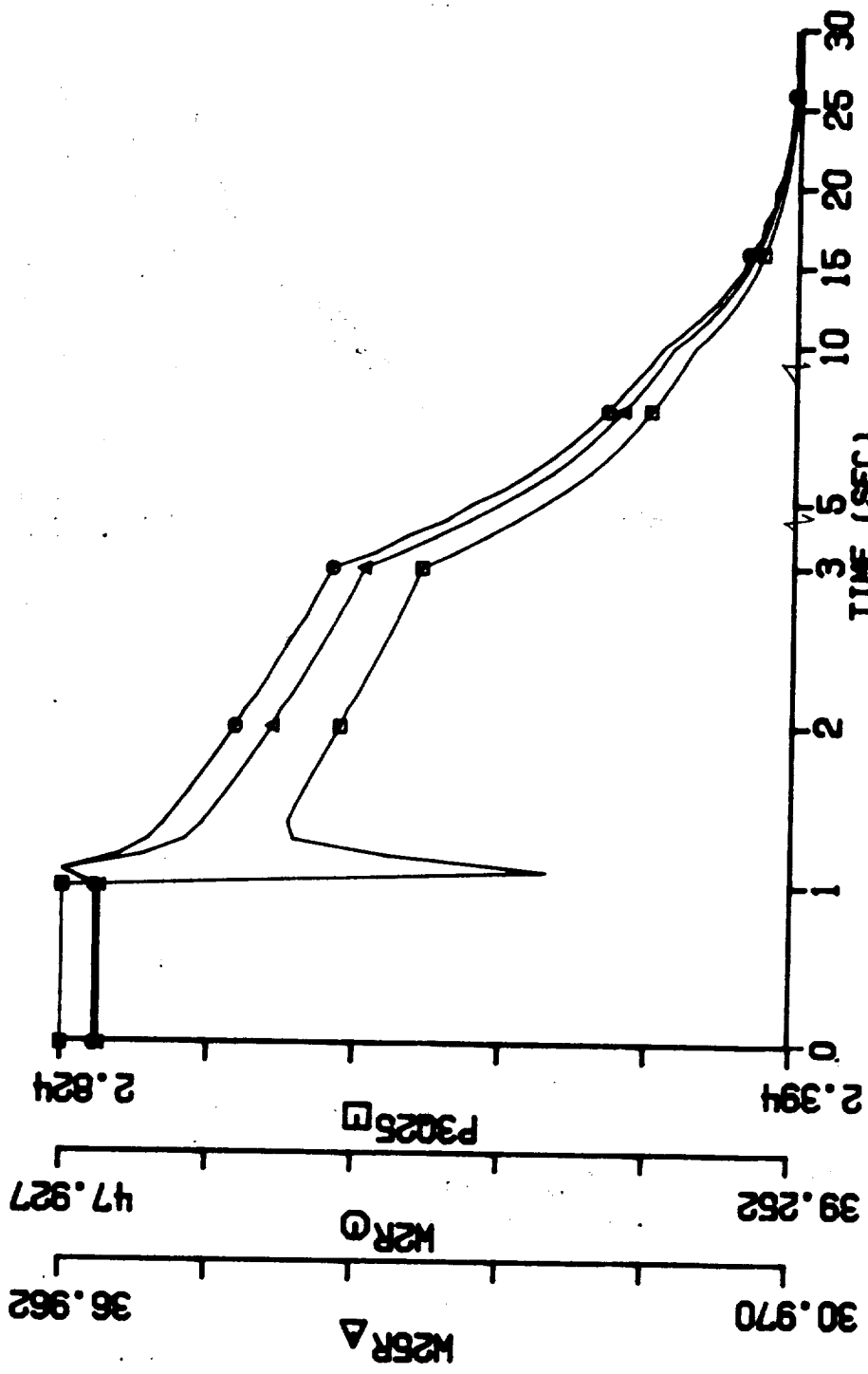

Figure 30.2 Transient Engine Performance: PLA changes from Ground Idle Setting to Max Power Setting, 4% water ingestion with 0.5% liquid evaporated at burner entry, "Hot Day" temperature (P3Q25, W2R, W25R vs. time)

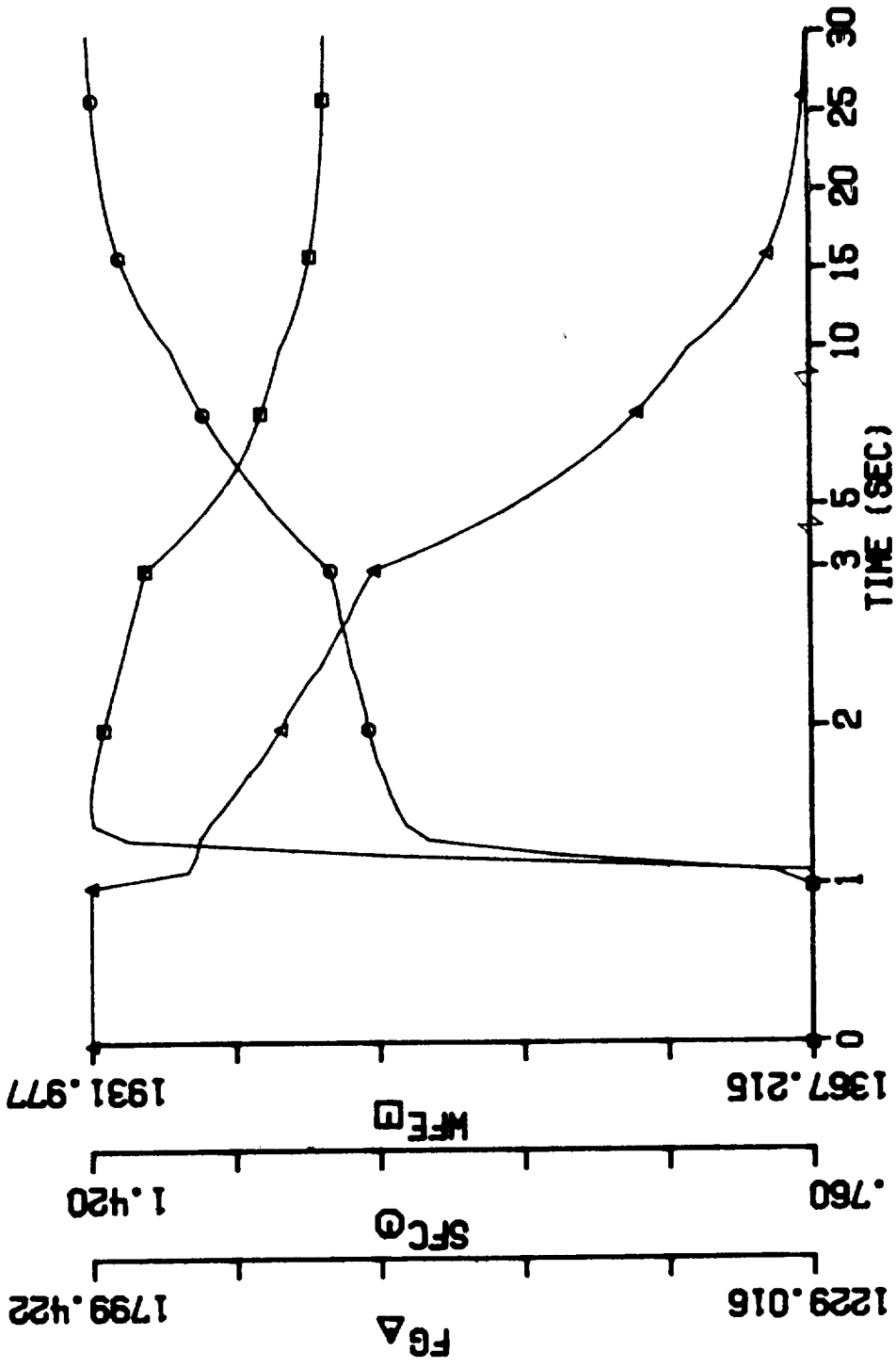

Figure 30.3 Transient Engine Performance: PLA changes from Ground Idle Setting to Max Power Setting, 4% water ingestion with 0.5% liquid evaporated at burner entry, "Hot Day" temperature (WFE, SFC, FG vs. time)

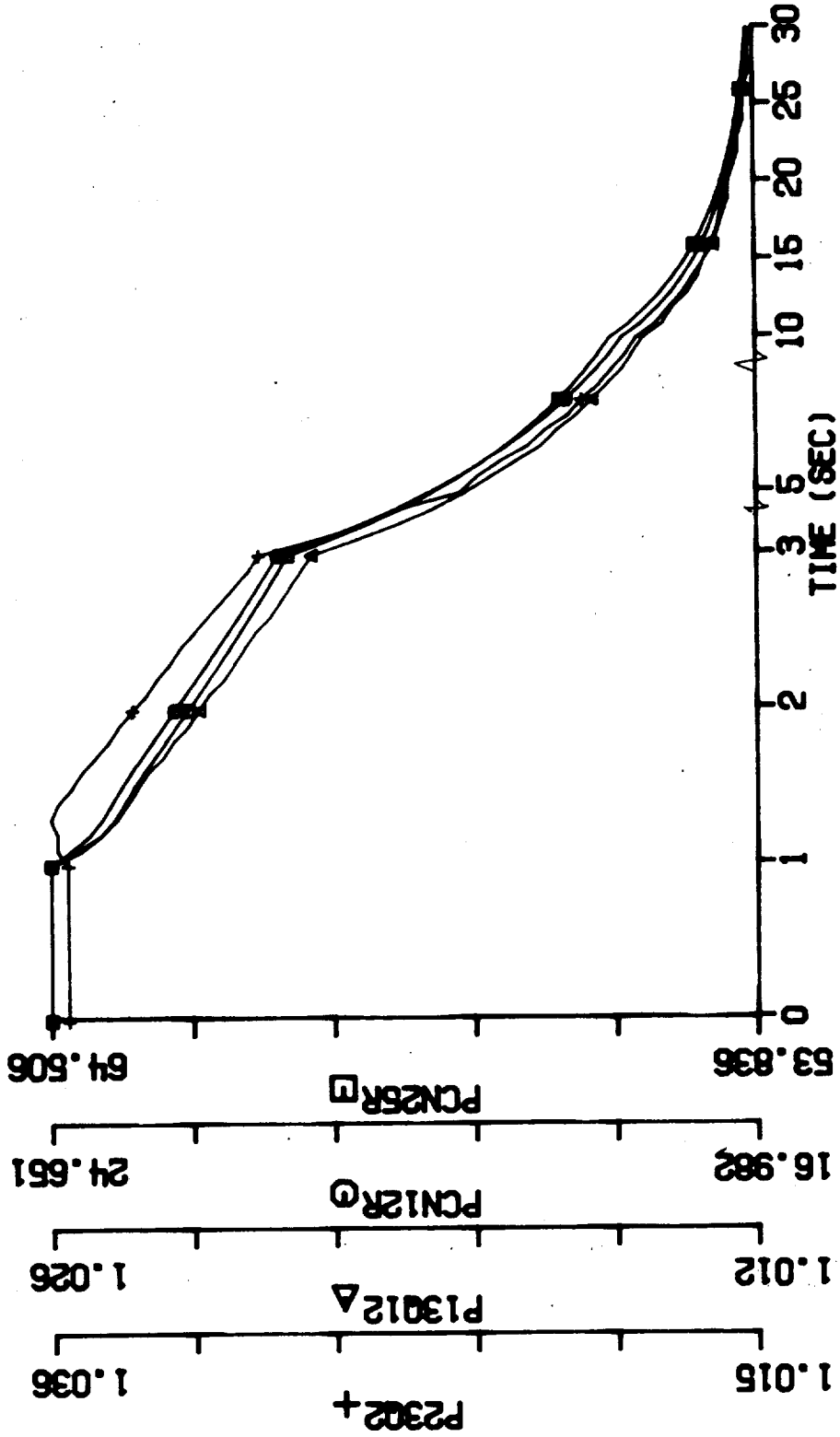

Figure 31.1 Transient Engine Performance: PLA changes from Ground Idle Setting to Max Power Setting, 4% water ingestion with 1% liquid evaporated at burner exit, "Hot Day" temperature (PCN25R, PCN12R, P13Q12, P23Q2 vs. time)

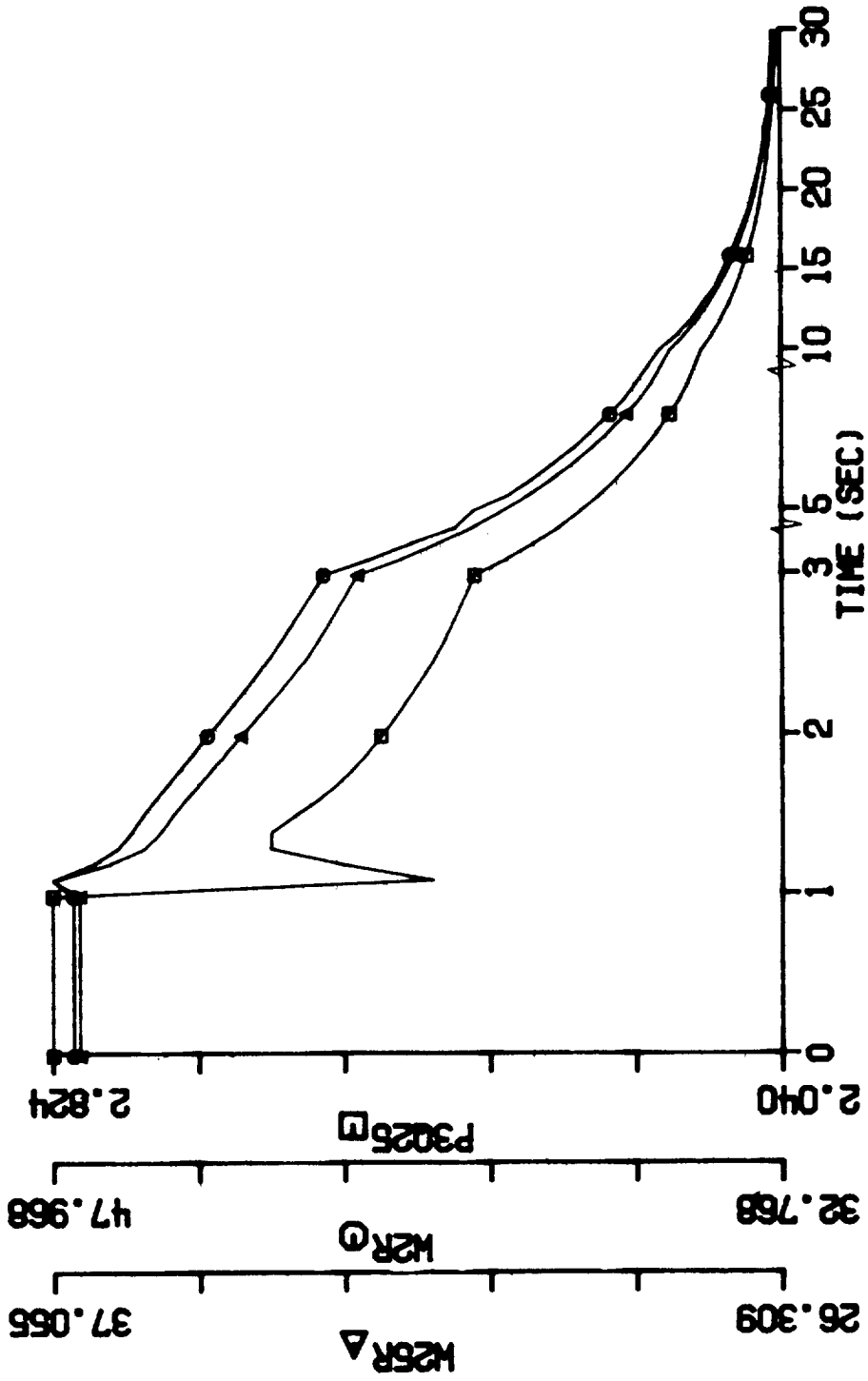

Figure 31.2 Transient Engine Performance: PLA changes from Ground Idle Setting to Max Power Setting, 4% water ingestion with 1% liquid evaporated at burner exit, "Hot Day" temperature (P3Q25, W2R, W25R vs. time)

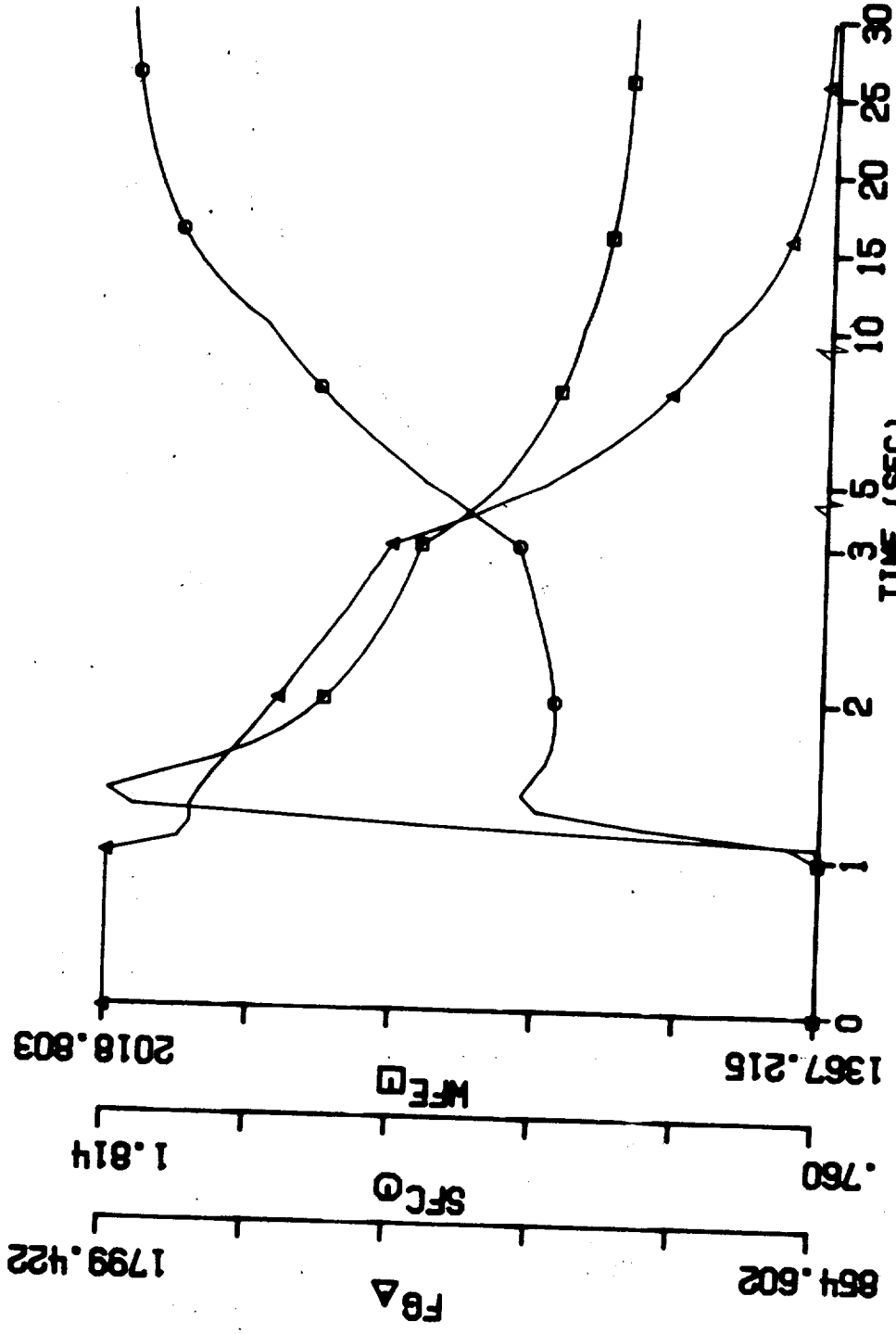

Figure 31.3 Transient Engine Performance: PLA changes from Ground Idle Setting to Max Power Setting, 4% water ingestion with 1% liquid evaporated at burner exit, "Hot Day" temperature (WFE, SFC, FG vs. time)

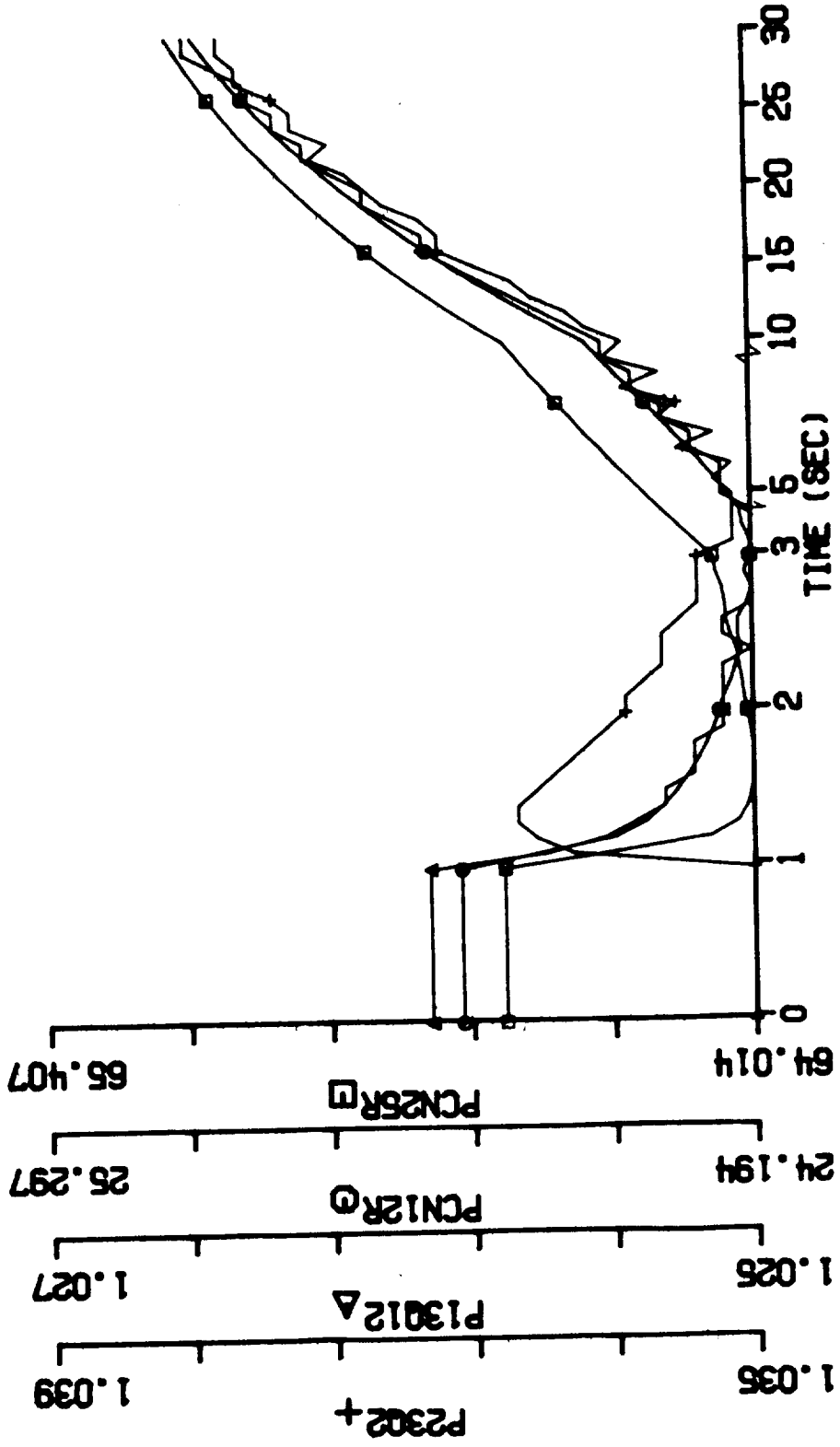

Figure 32.1 Transient Engine Performance: PLA changes from Ground Idle Setting to Max Power Setting, 4% water ingestion with 0.5% liquid evaporated at burner exit, "Hot Day" temperature (PCN25R, PCN12R, P13Q12, P23Q2 vs. time)

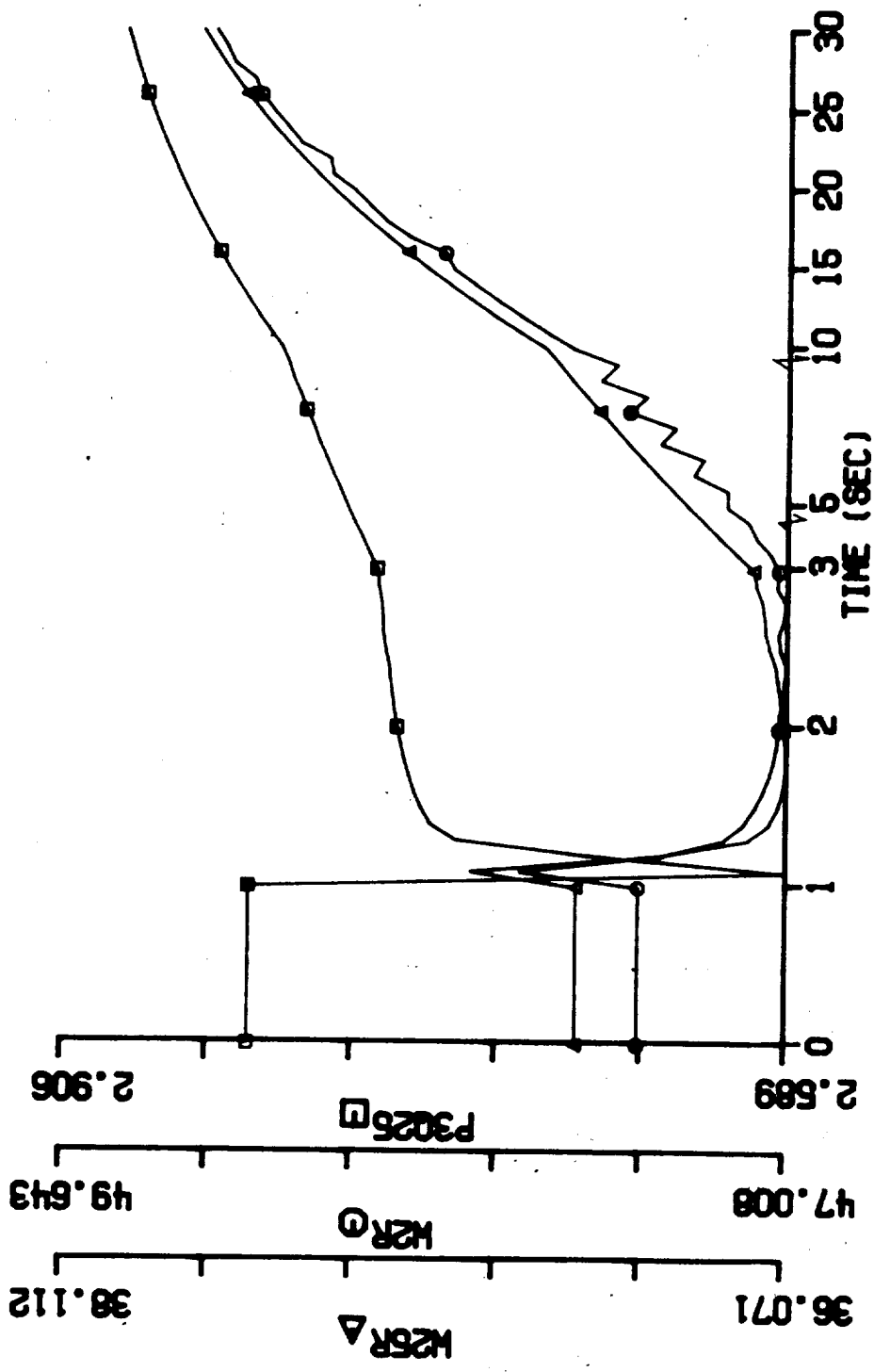

Figure 32.2 Transient Engine Performance: PLA changes from Ground Idle Setting to Max Power Setting, 4% water ingestion with 0.5% liquid evaporated at burner exit, "Hot Day" temperature (P3Q25, W2R, W25R vs. time)

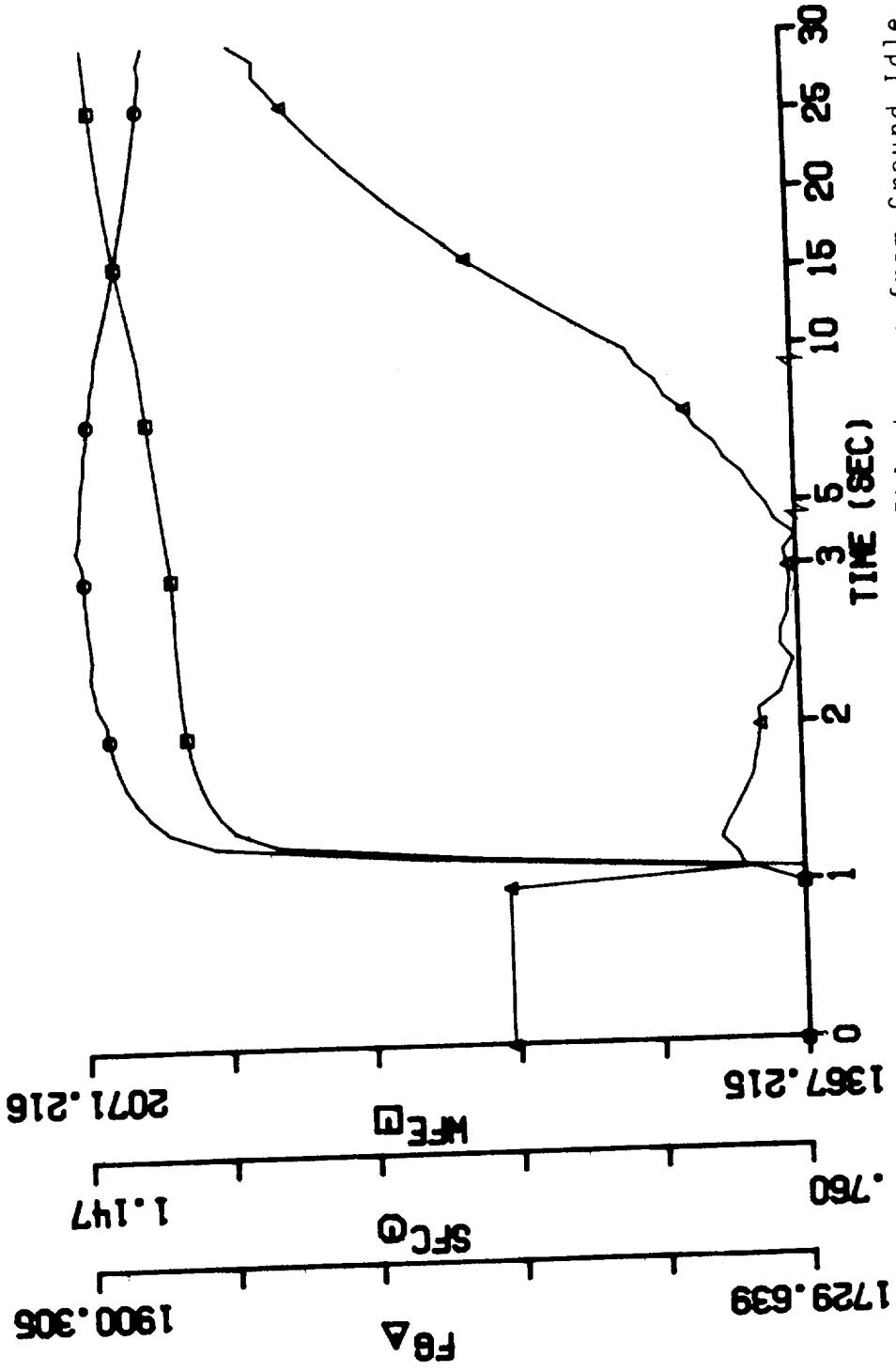

Figure 32.3 Transient Engine Performance: PLA changes from Ground Idle Setting to Max Power Setting, 4% water ingestion with 0.5% liquid evaporated at burner exit, "Hot Day" temperature (WFE, SFC, FG vs. time)

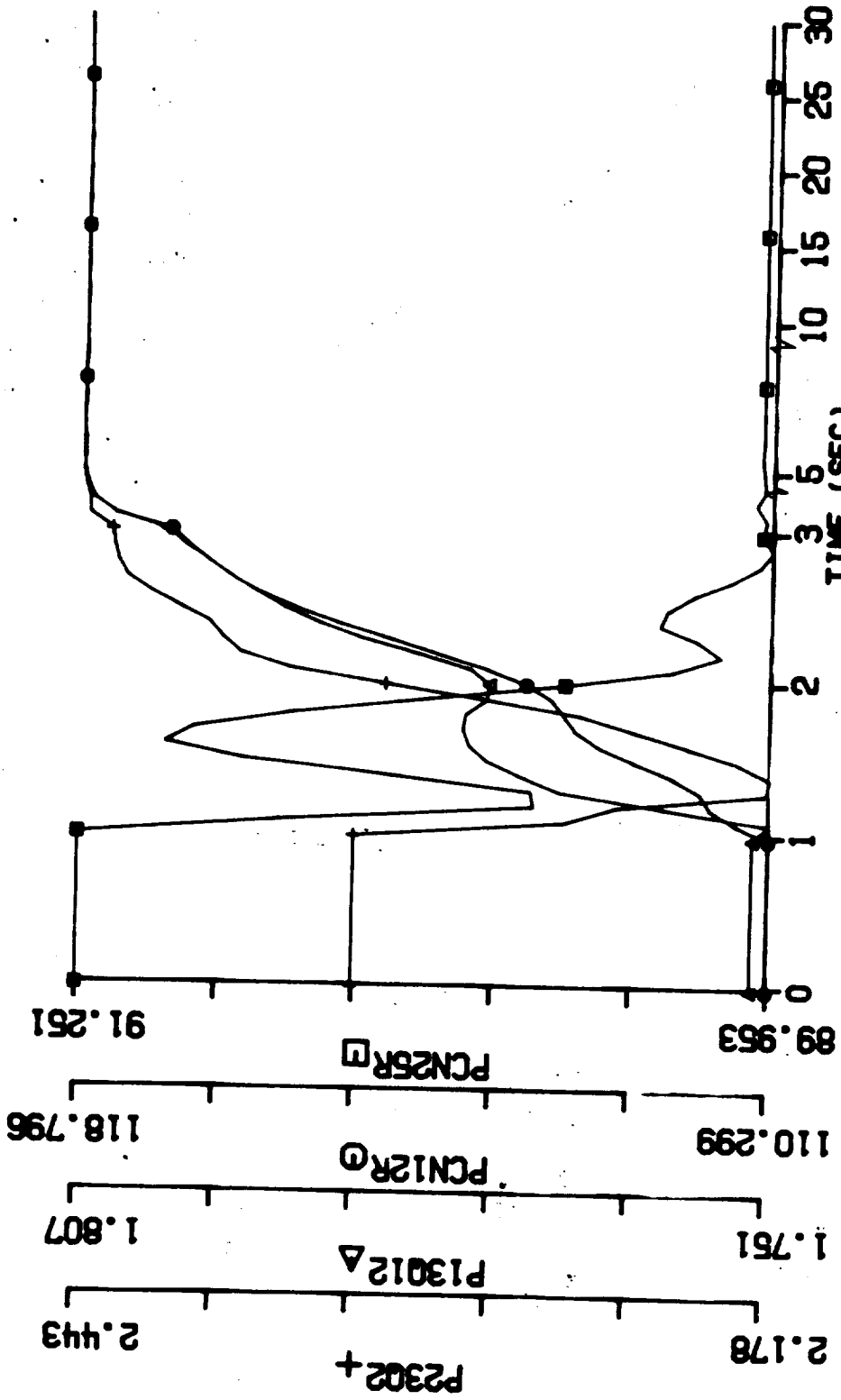

FigOre 33.1 Transient Engine Performance: Max Power Setting, 10 F temperature error, dry air operation (PCN25R, PCN12R, P13Q12, P23Q2 vs. time)

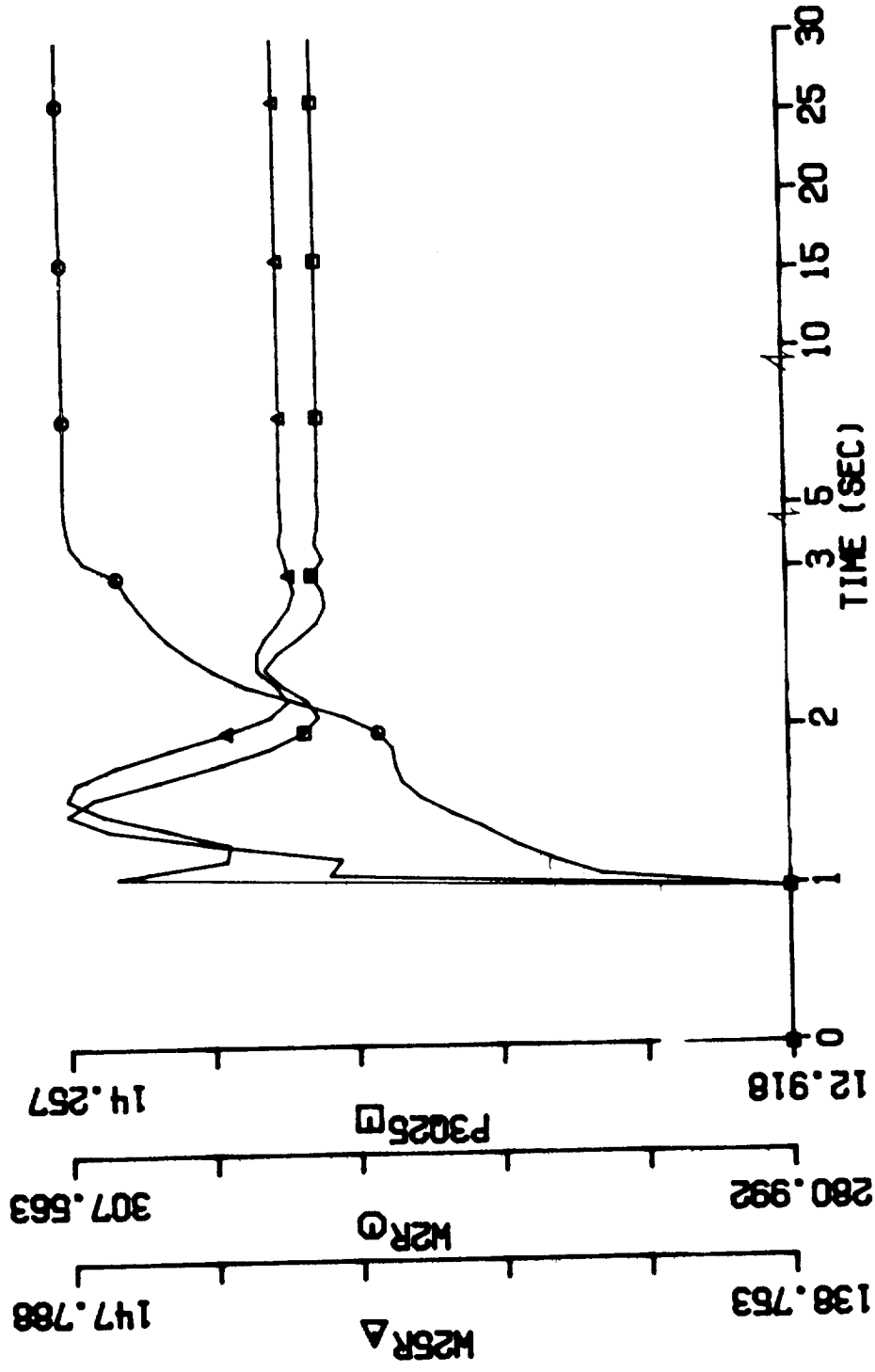

Figure 33.2 Transient Engine Performance: Max Power Setting, 10 F temperature error, dry air operation (P3Q25, W2R, W25R vs. time)

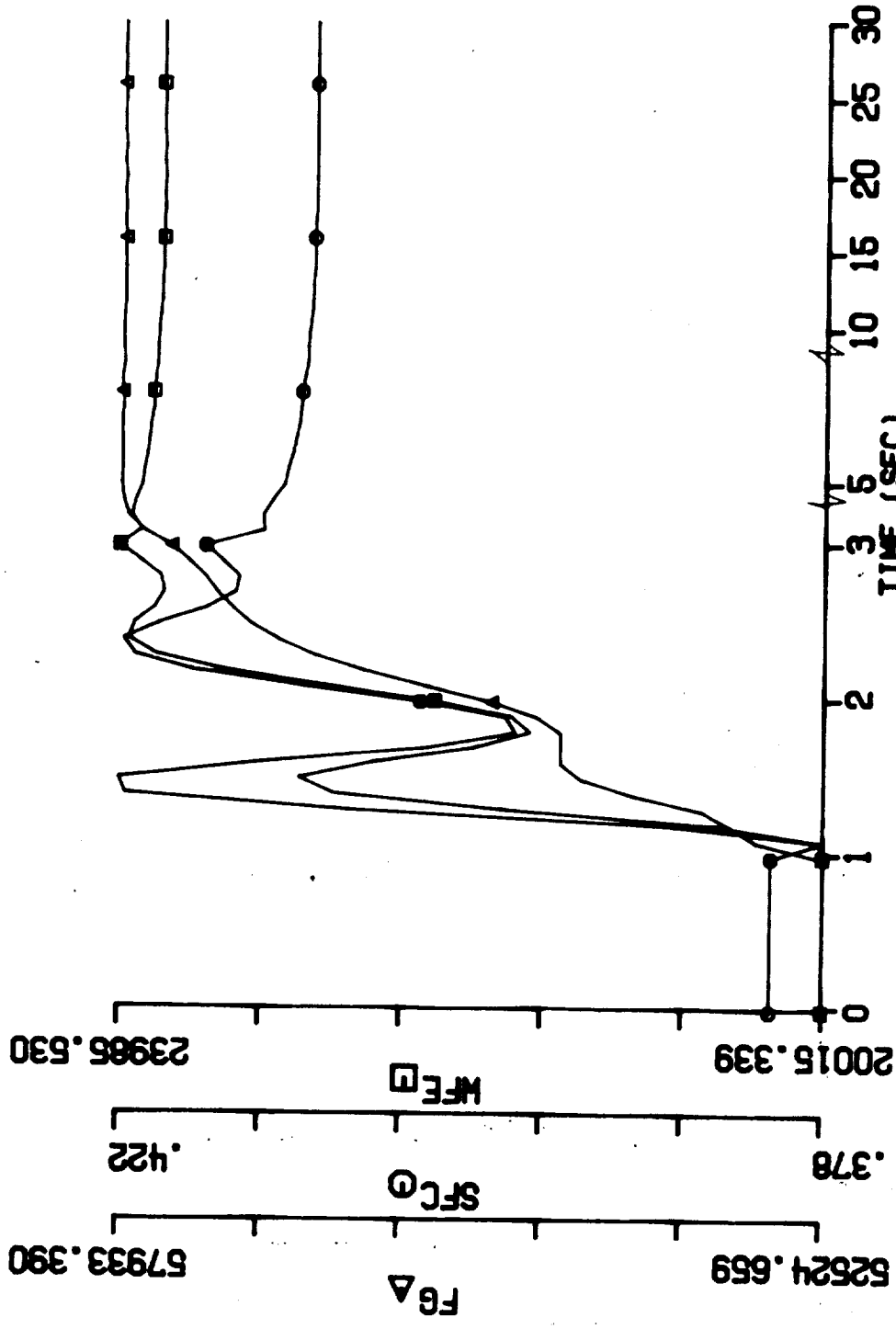

Figure 33.3 Transient Engine Performance: Max Power Setting, 10 F temperature error, dry air operation (WFE, SFC, FG vs. time)

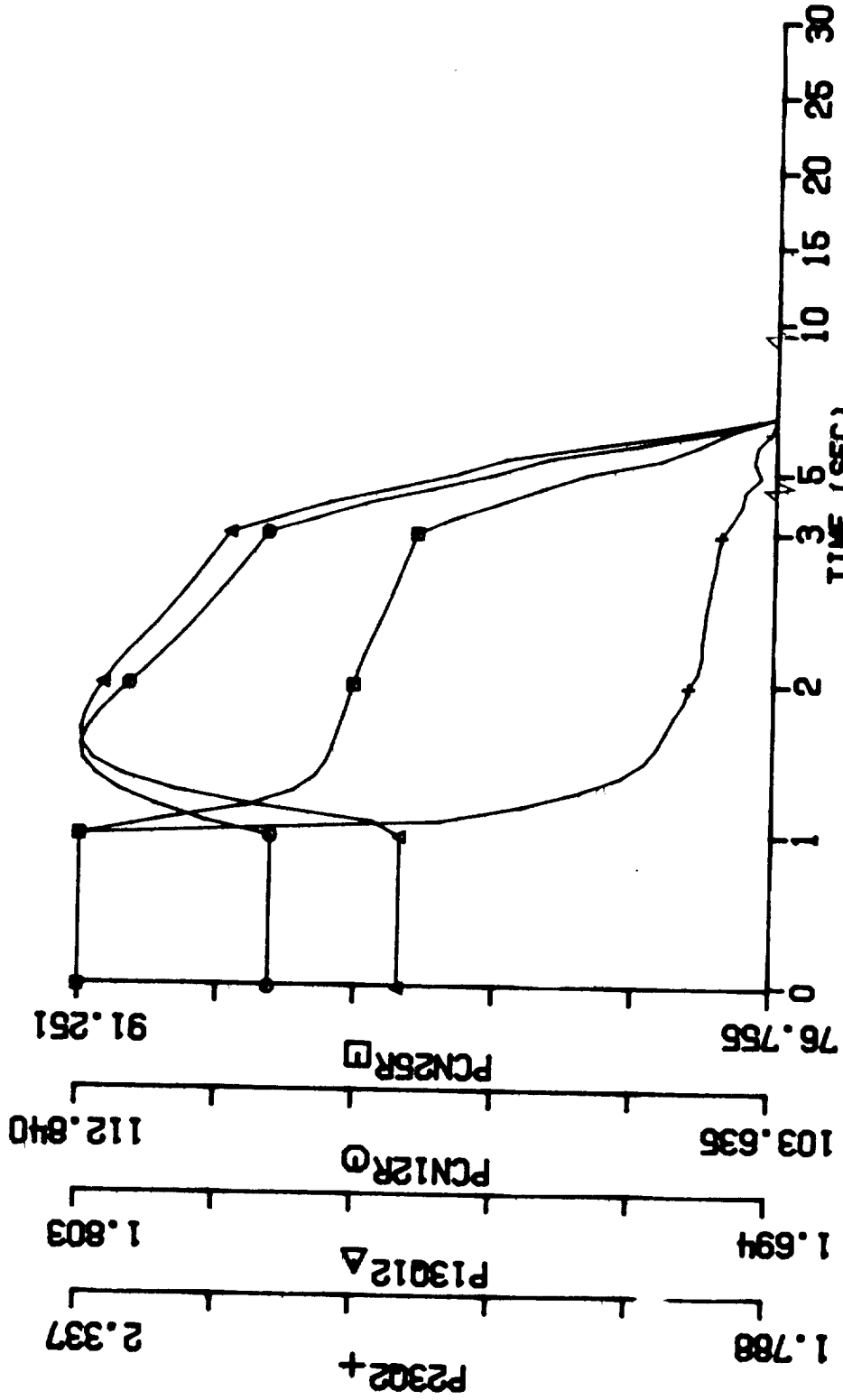

Figure 34.1 Transient Engine Performance: Max Power Setting, 40 F temperature error, dry air operation (PCN25R, PCN12R, P13Q12, P23Q2 vs. time)

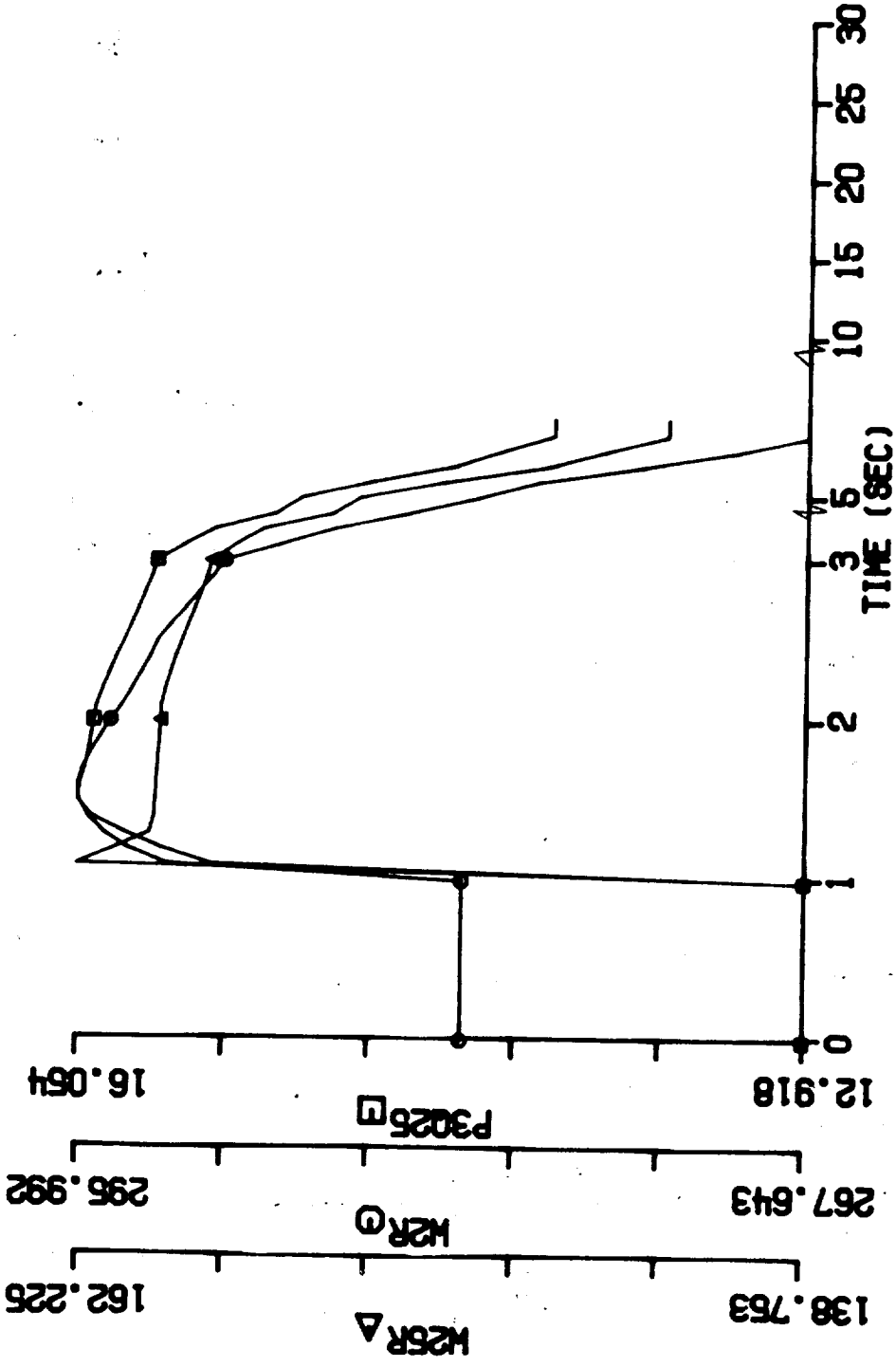

Figure 34.2 Transient Engine Performance: Max Power Setting, 40 F temperature error, dry air operation (P3Q25, W2R, W25R vs. time)

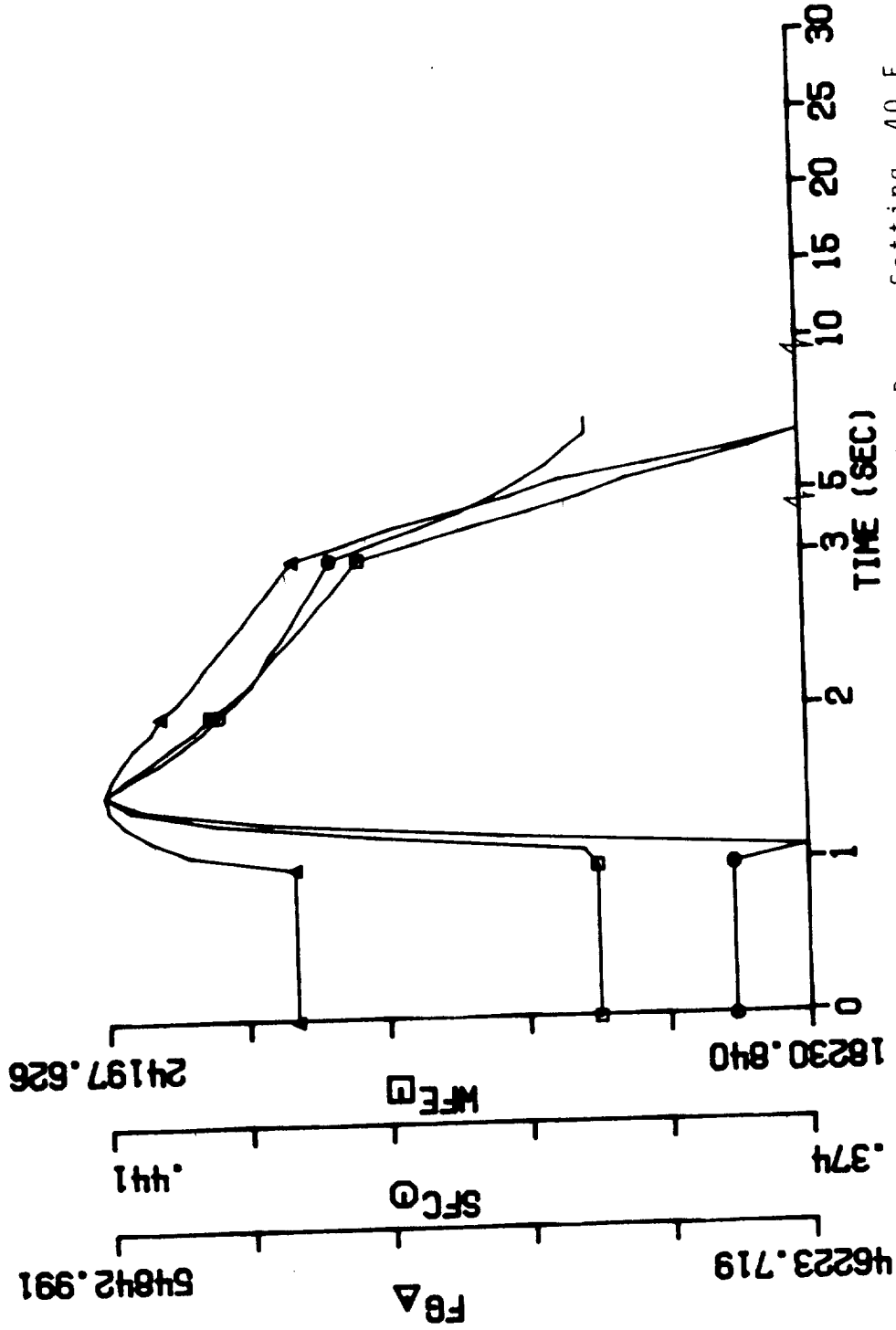

Figure 34.3 Transient Engine Performance: Max Power Setting, 40 F temperature error, dry air operation (WFE, SFC, FG vs. time)

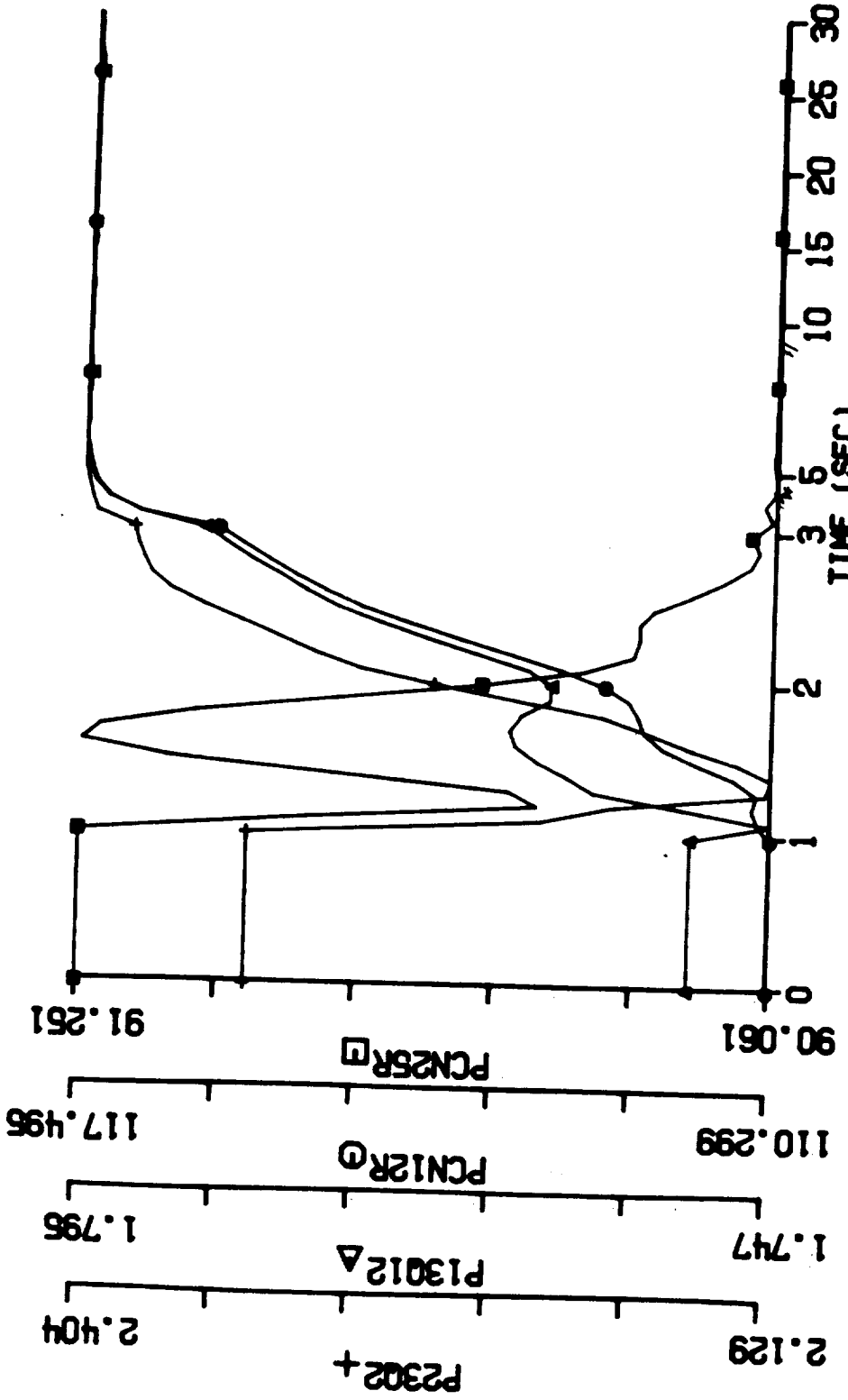

Figure 35.1 Transient Engine Performance: Max Power Setting, 10 F temperature error, 2% ingestion, all liquid drained (PCN25R, PCN12R, P13Q12, P23Q2 vs. time)

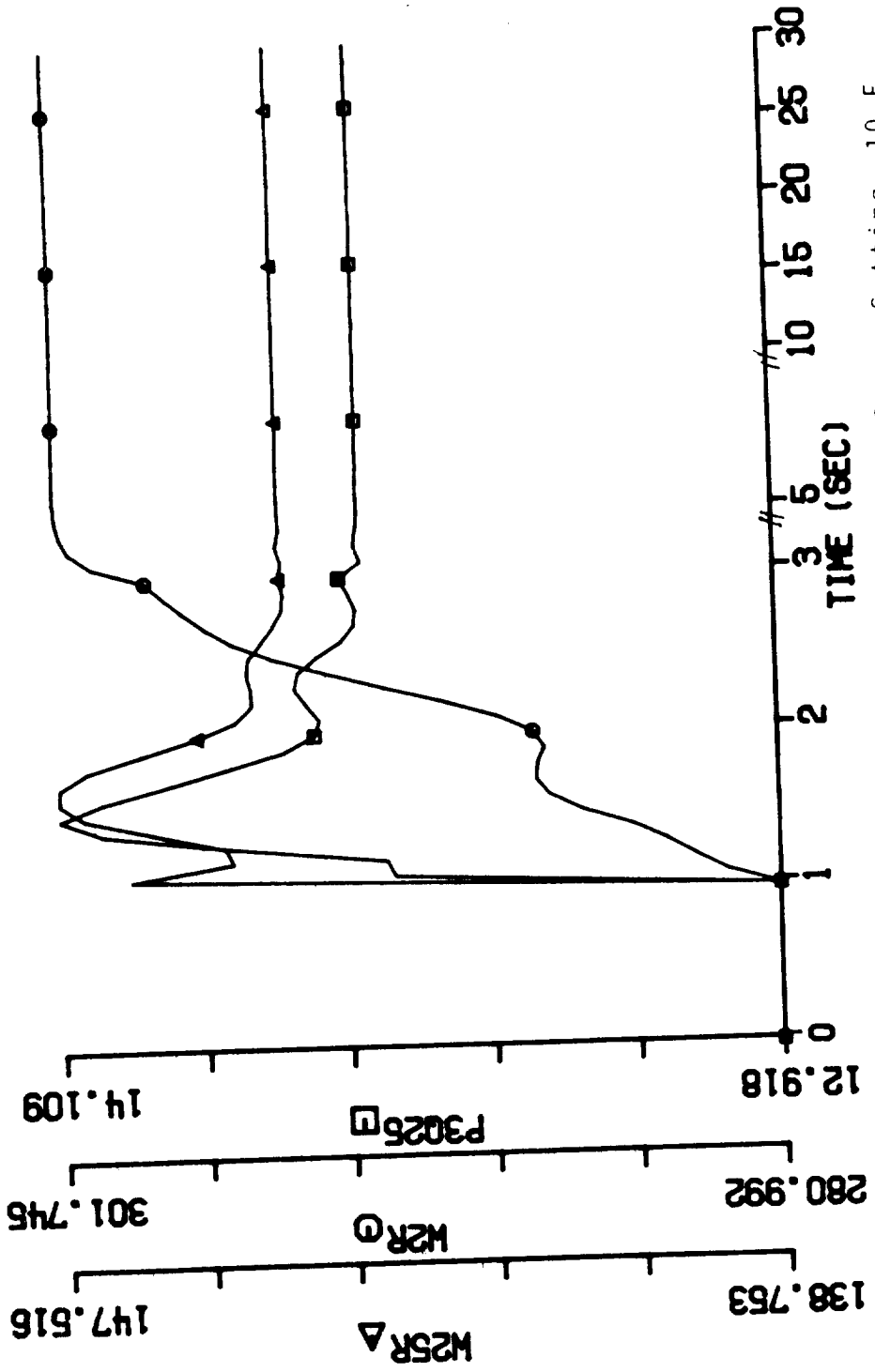

Figure 35.2 Transient Engine Performance: Max Power Setting, 10 F temperature error, 2% ingestion, all liquid drained (P3Q25, W2R, W25R vs. time)

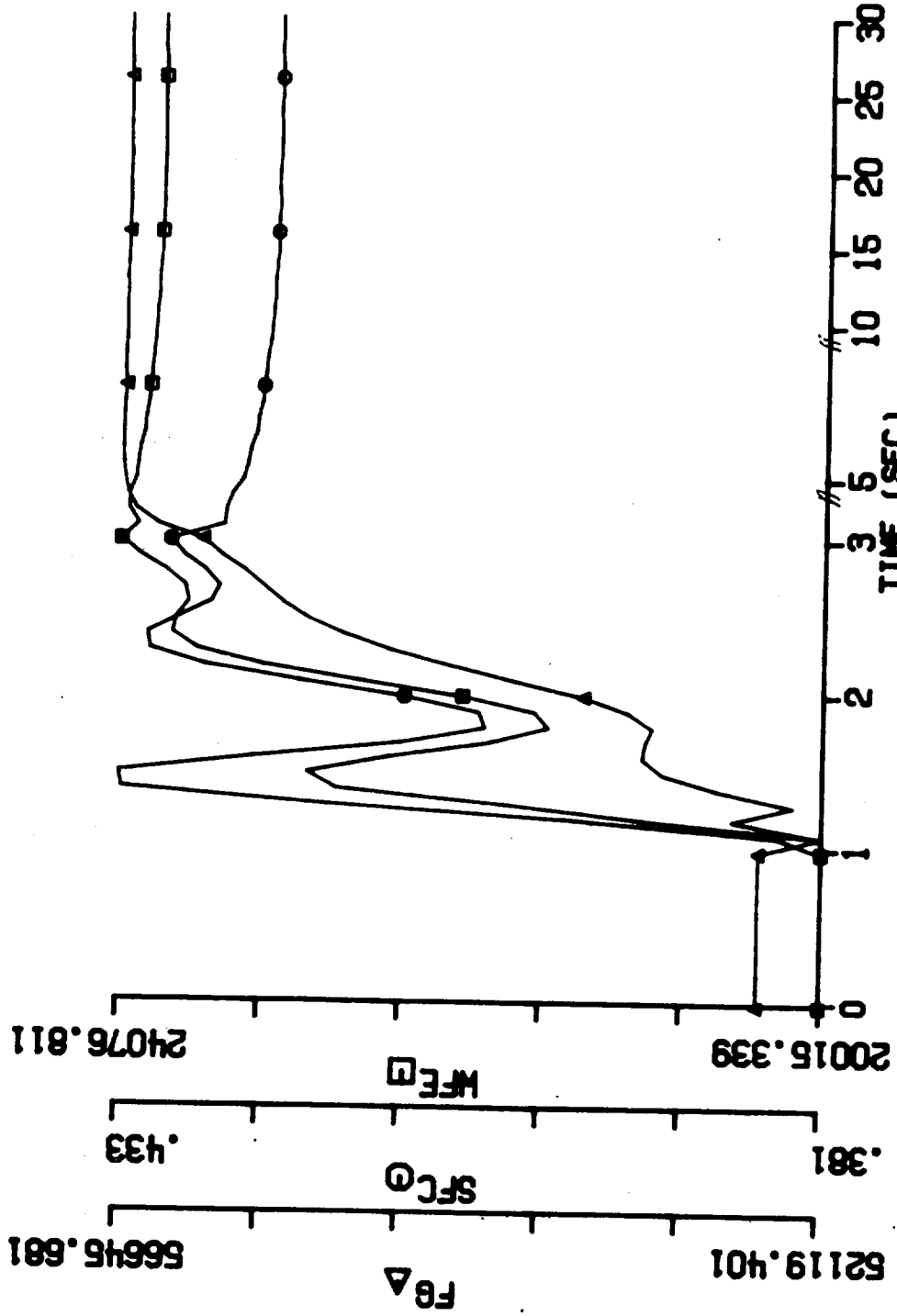

Figure 35.3 Transient Engine Performance: Max Power Setting, 10 F temperature error, 2% ingestion, all liquid drained (WFE, SFC, FG vs. time)

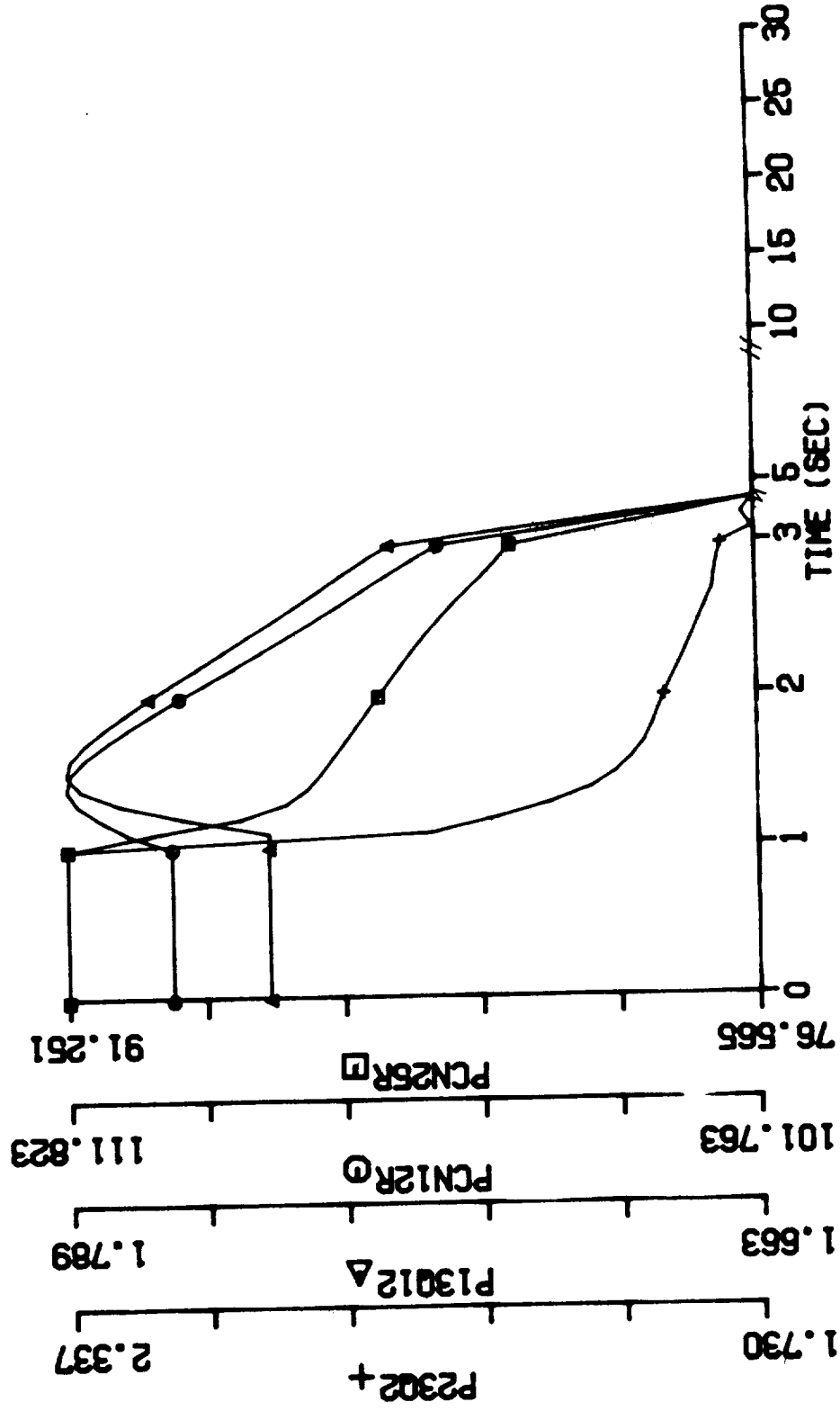

Figure 36.1 Transient Engine Performance: Max Power Setting, 40 F temperature error, 2% ingestion, all liquid drained (PCN25R, PCN12R, P13Q12, P23Q2 vs. time)

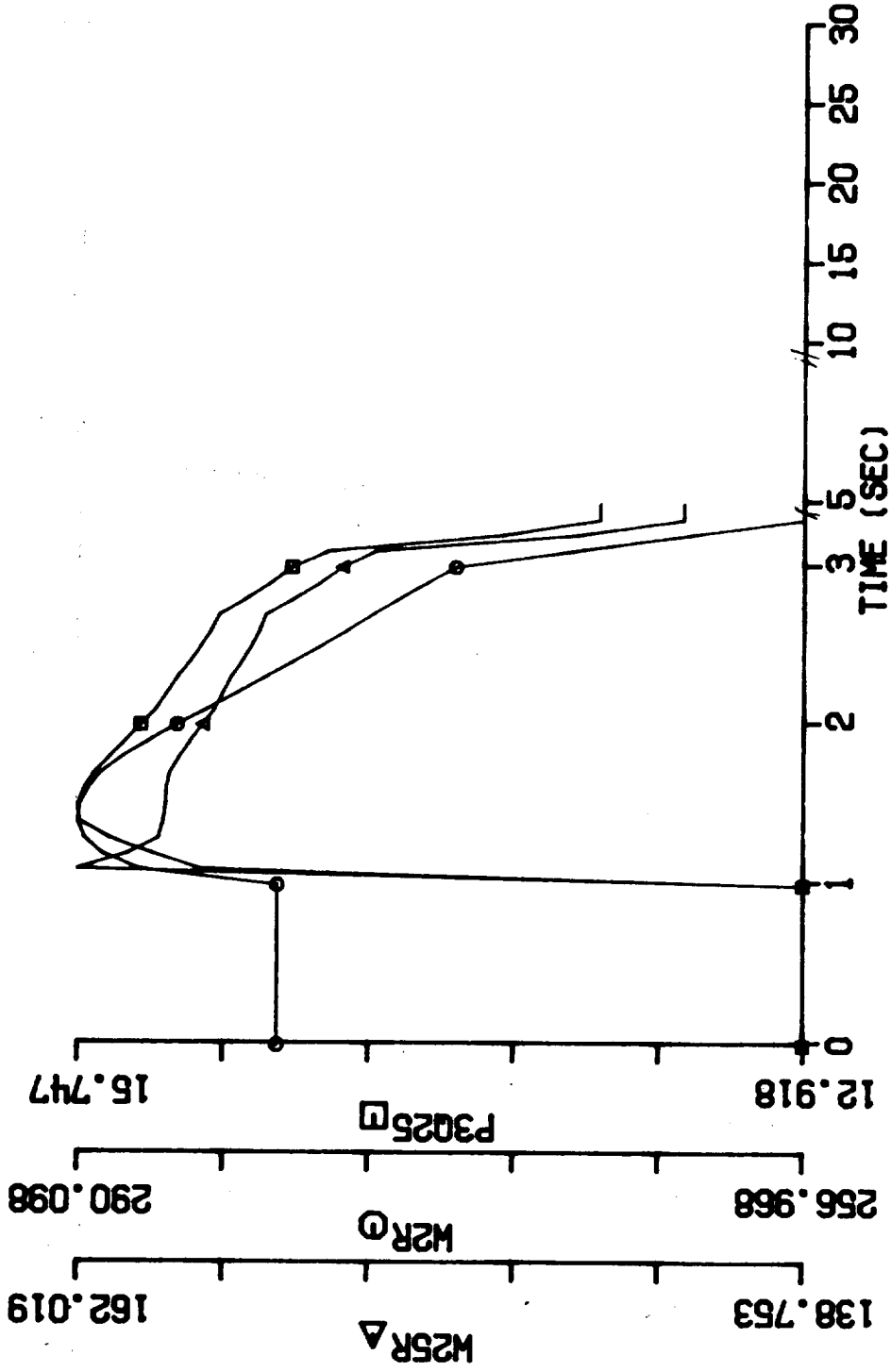

Figure 36.2 Transient Engine Performance: Max Power Setting, 40 F temperature error, 2% ingestion, all liquid drained (P3Q25, W2R, W25R vs. time)

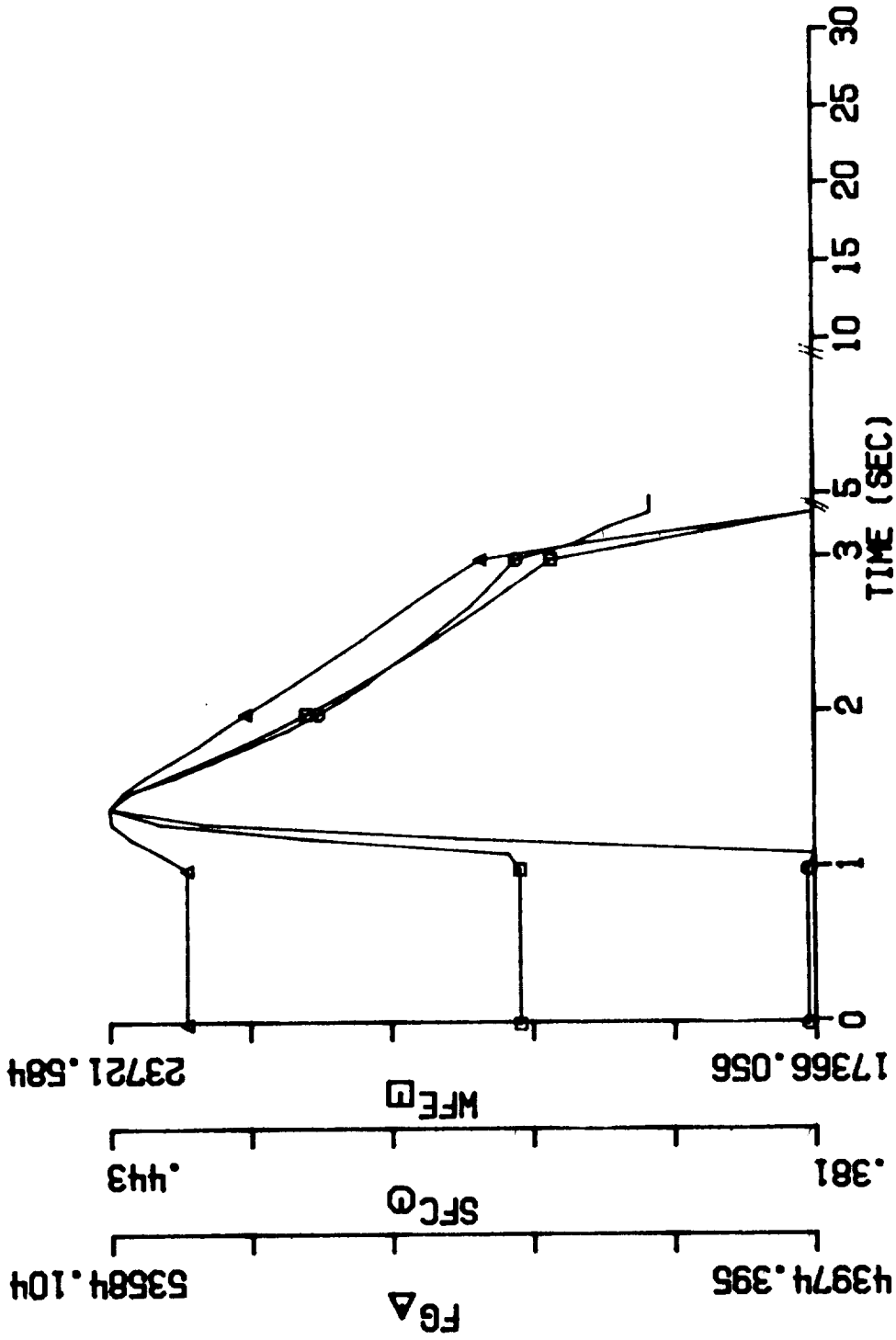

Figure 36.3 Transient Engine Performance: Max Power Setting, 40 F temperature error, 2% ingestion, all liquid drained (WFE, SFC, FG vs. time)

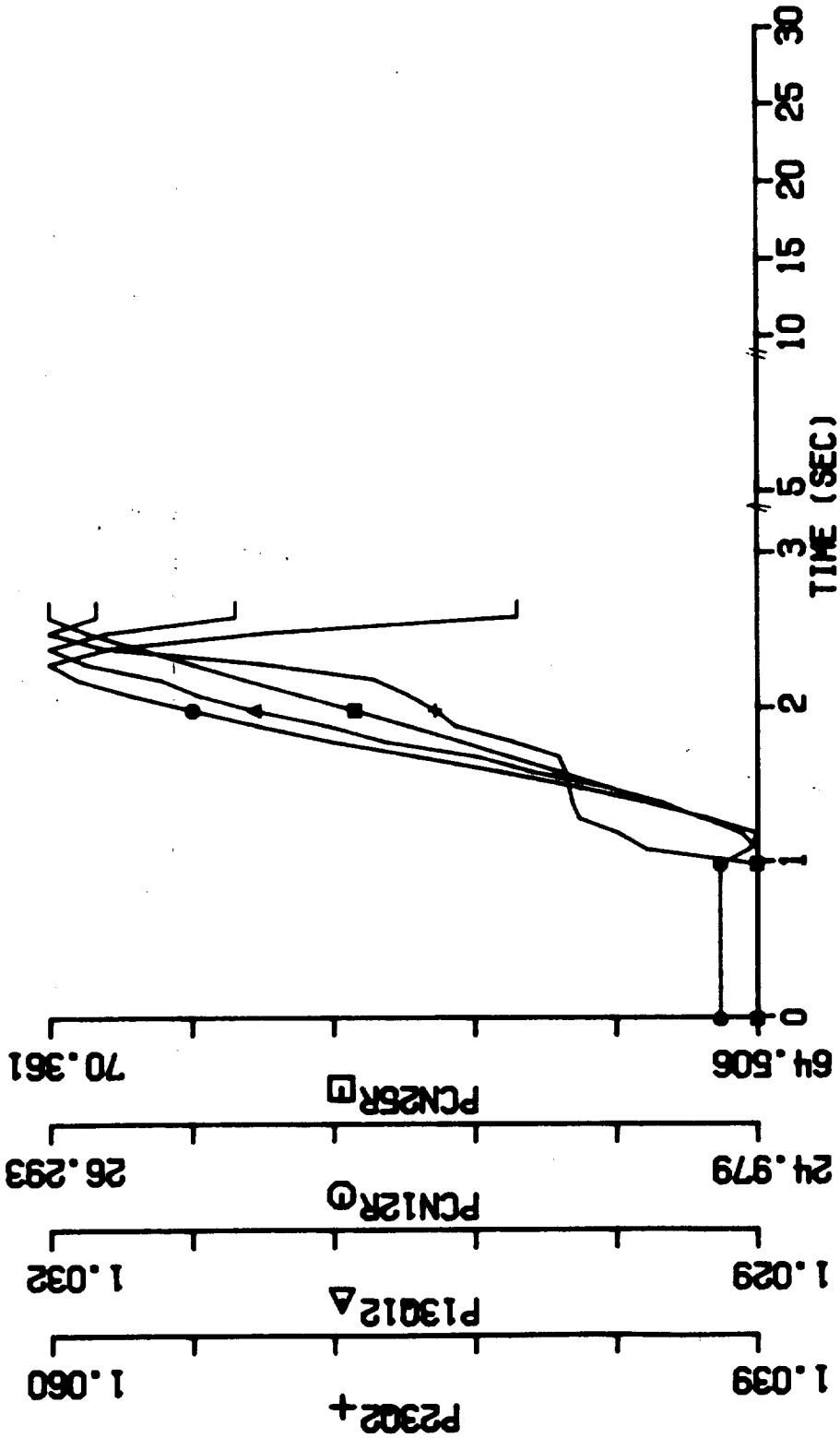

Figure 37.1 Transient Engine Performance: PLA changes from Ground Idle Setting to Max Power Setting, dry air operation, standard temperature,10 F temperature error (PCN25R, PCN12R, P13Q12, P23Q2 vs. time)

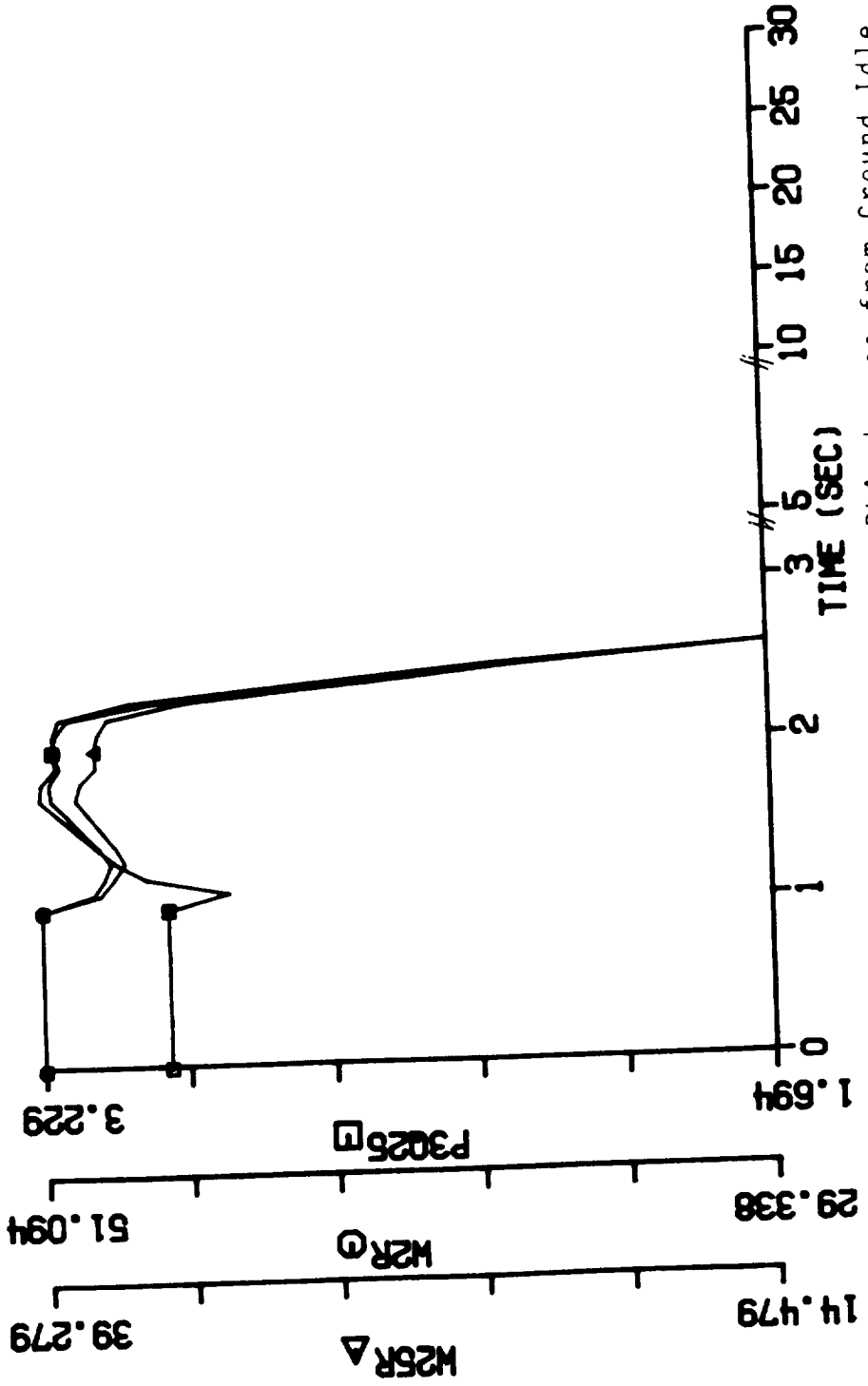

Figure 37.2 Transient Engine Performance: PLA changes from Ground Idle Setting to Max Power Setting, dry air operation, standard temperature,10 F temperature error (P3Q25, W2R, W25R vs. time)

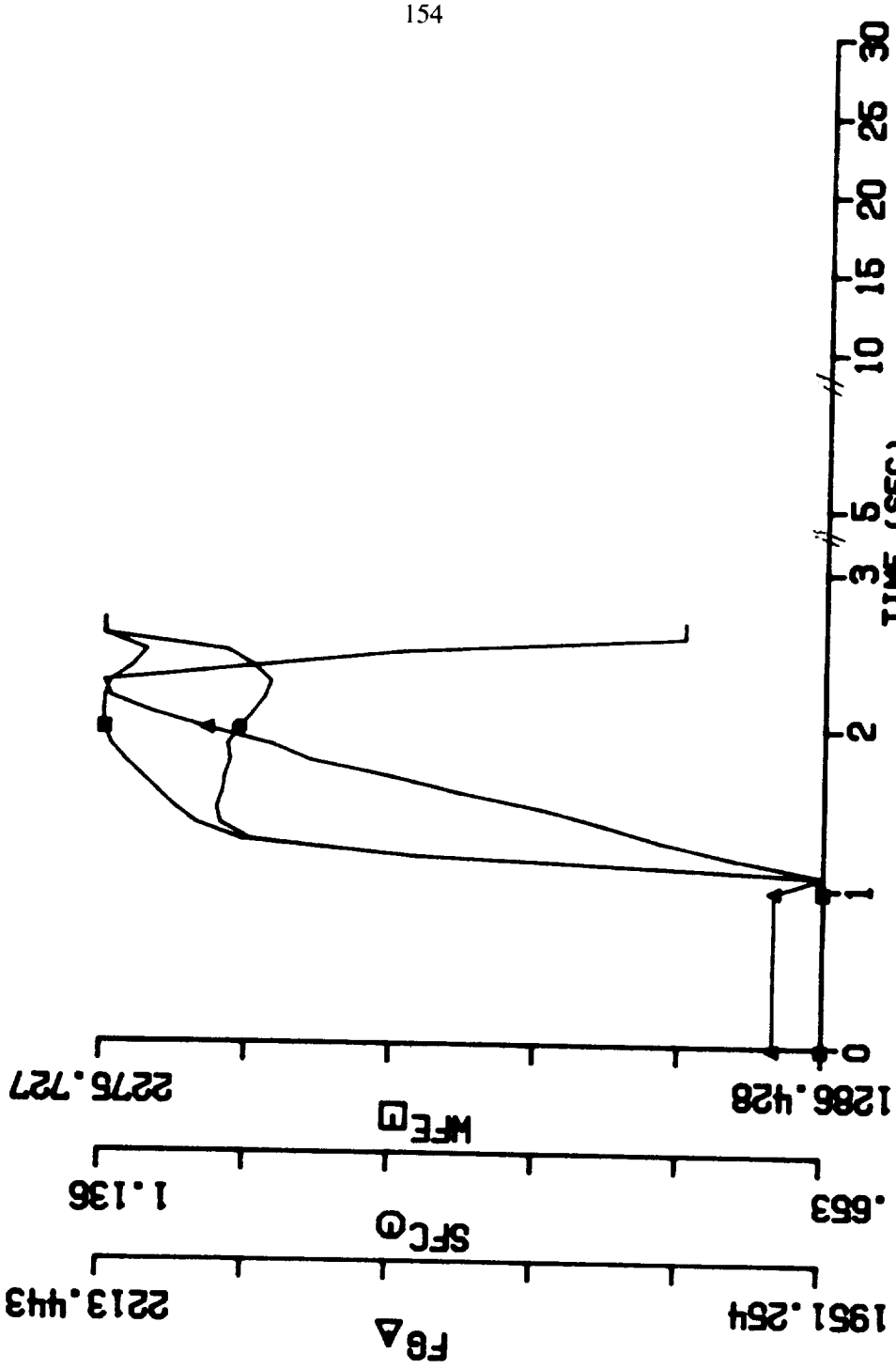

Figure 37.3 Transient Engine Performance: PLA changes from Ground Idle Setting to Max Power Setting, dry air operation, standard temperature,10 F temperature error (WFE, SFC, FG vs. time)

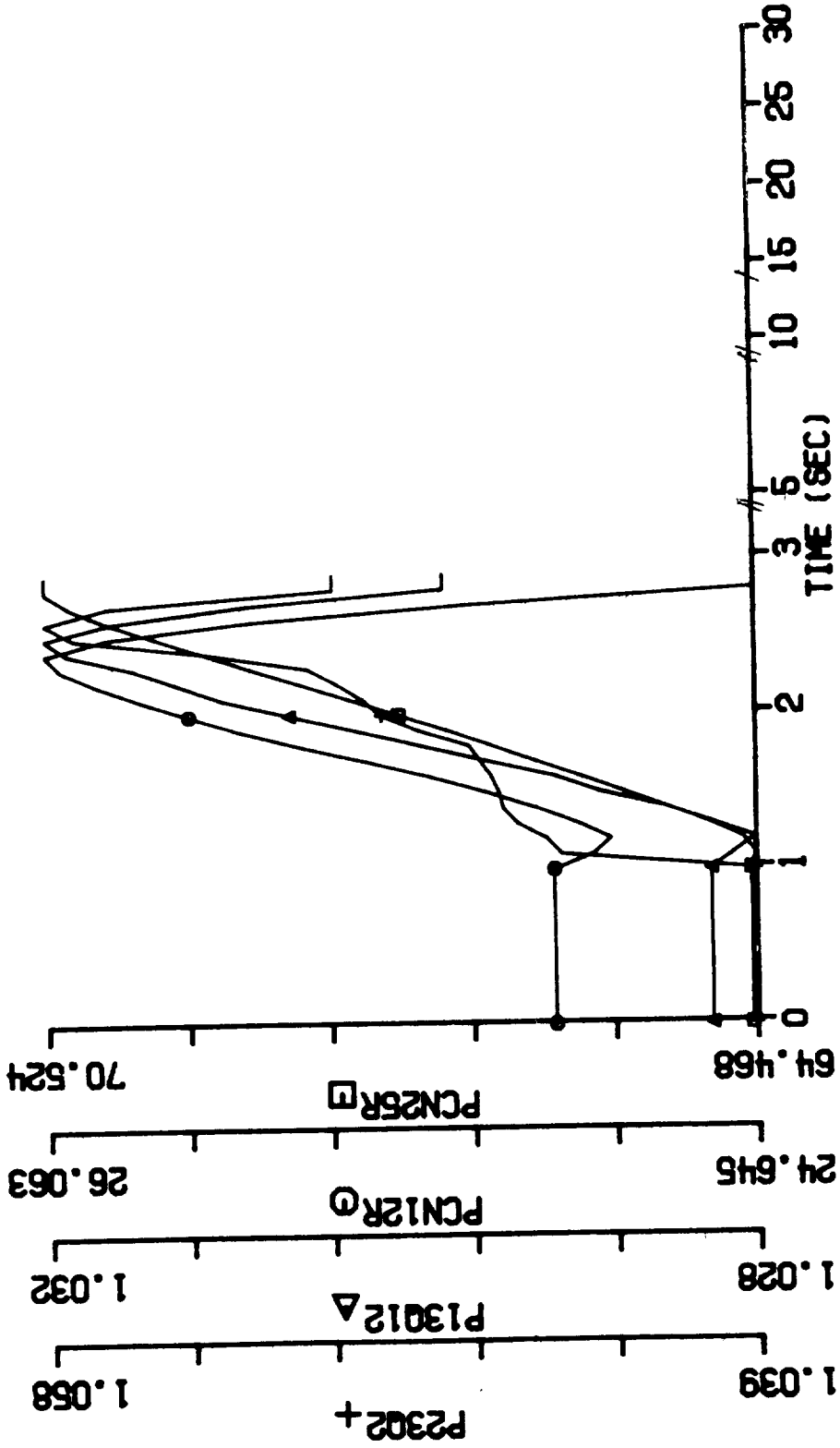

Figure 38.1 Transient Engine Performance: PLA changes from Ground Idle Setting to Max Power Setting, 2% water ingestion with all liquid drained, standard temperature, 10 F temperature error (PCN25R, PCN12R, P13Q12, P23Q2 vs. time)

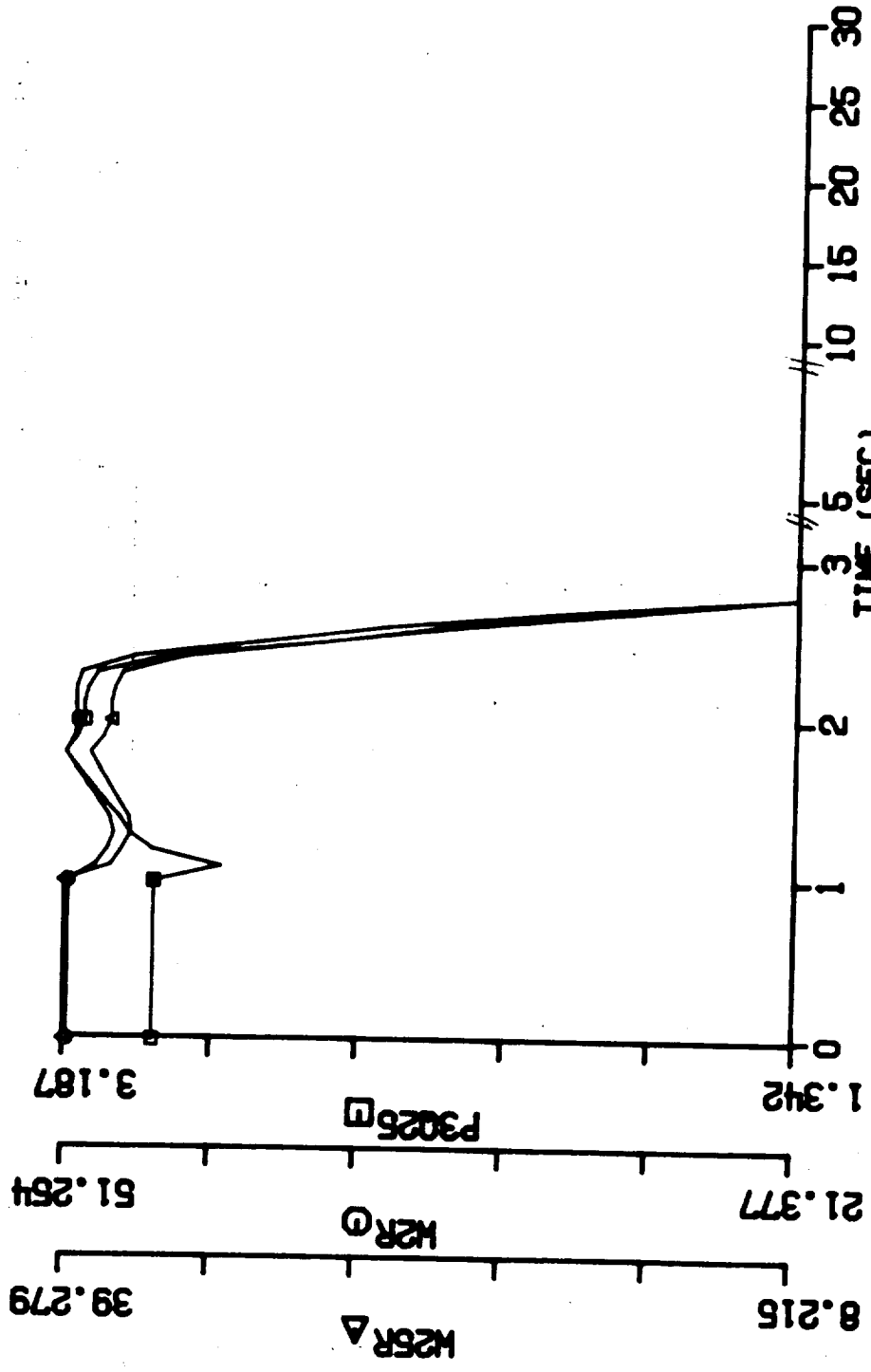

Figure 38.2 Transient Engine Performance: PLA changes from Ground Idle Setting to Max Power Setting, 2% water ingestion with all liquid drained, standard temperature, 10 F temperature error (P3Q25, W2R, W25R vs. time)

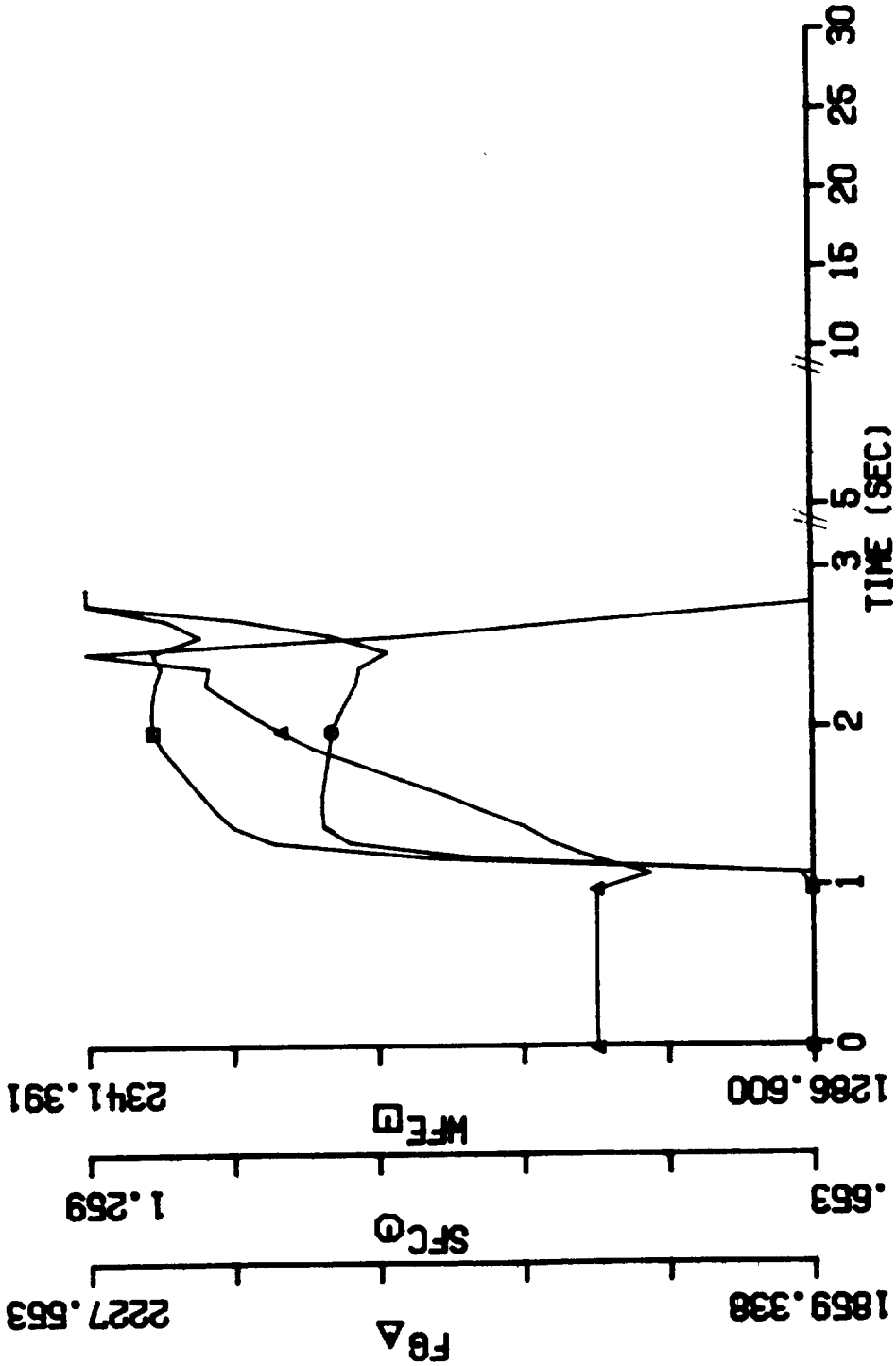

Figure 38.3 Transient Engine Performance: PLA changes from Ground Idle Setting to Max Power Setting, 2% water ingestion with all liquid drained, standard temperature, 10 F temperature error (WFE, SFC, FG vs. time)

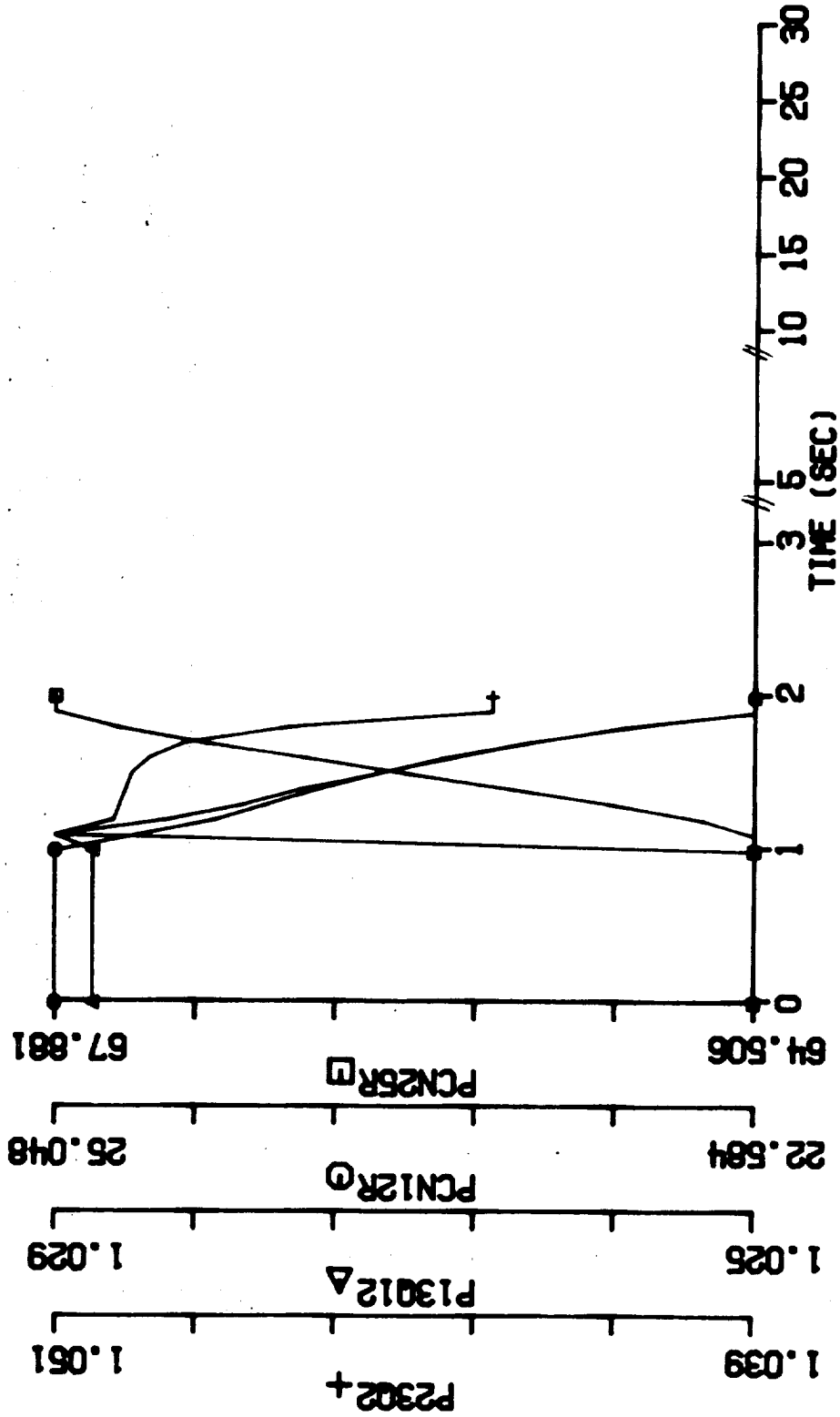

Figure 39.1 Transient Engine Performance: PLA changes from Ground Idle Setting to Max Power Setting, dry air operation standard temperature, 40 F temperature error (PCN25R, PCN12R, P13Q12, P23Q2 vs. time)

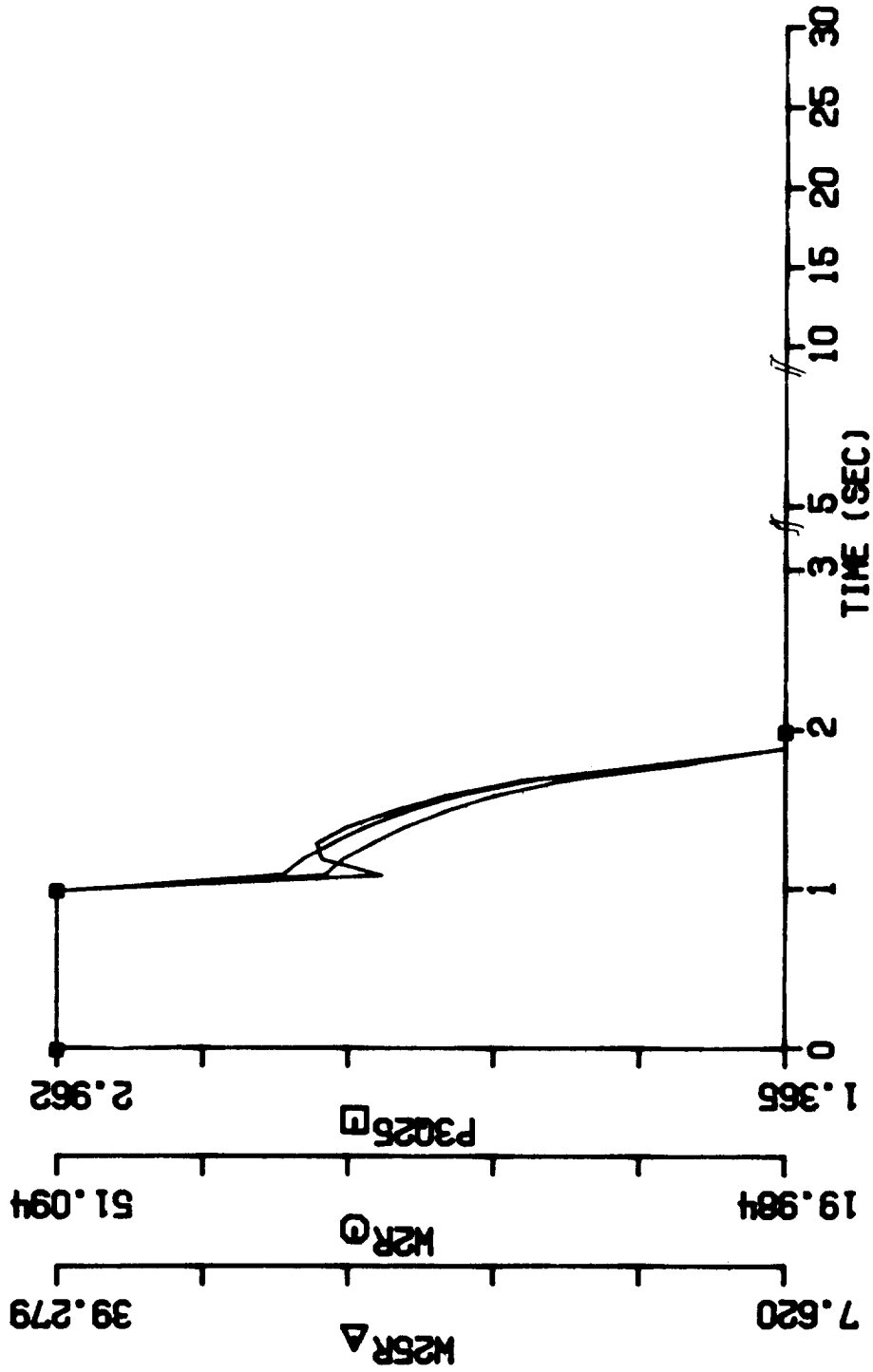

Figure 39.2 Transient Engine Performance: PLA changes from Ground Idle Setting to Max Power Setting, dry air operation standard temperature, 40 F temperature error (P3Q25, W2R, W25R vs. time)

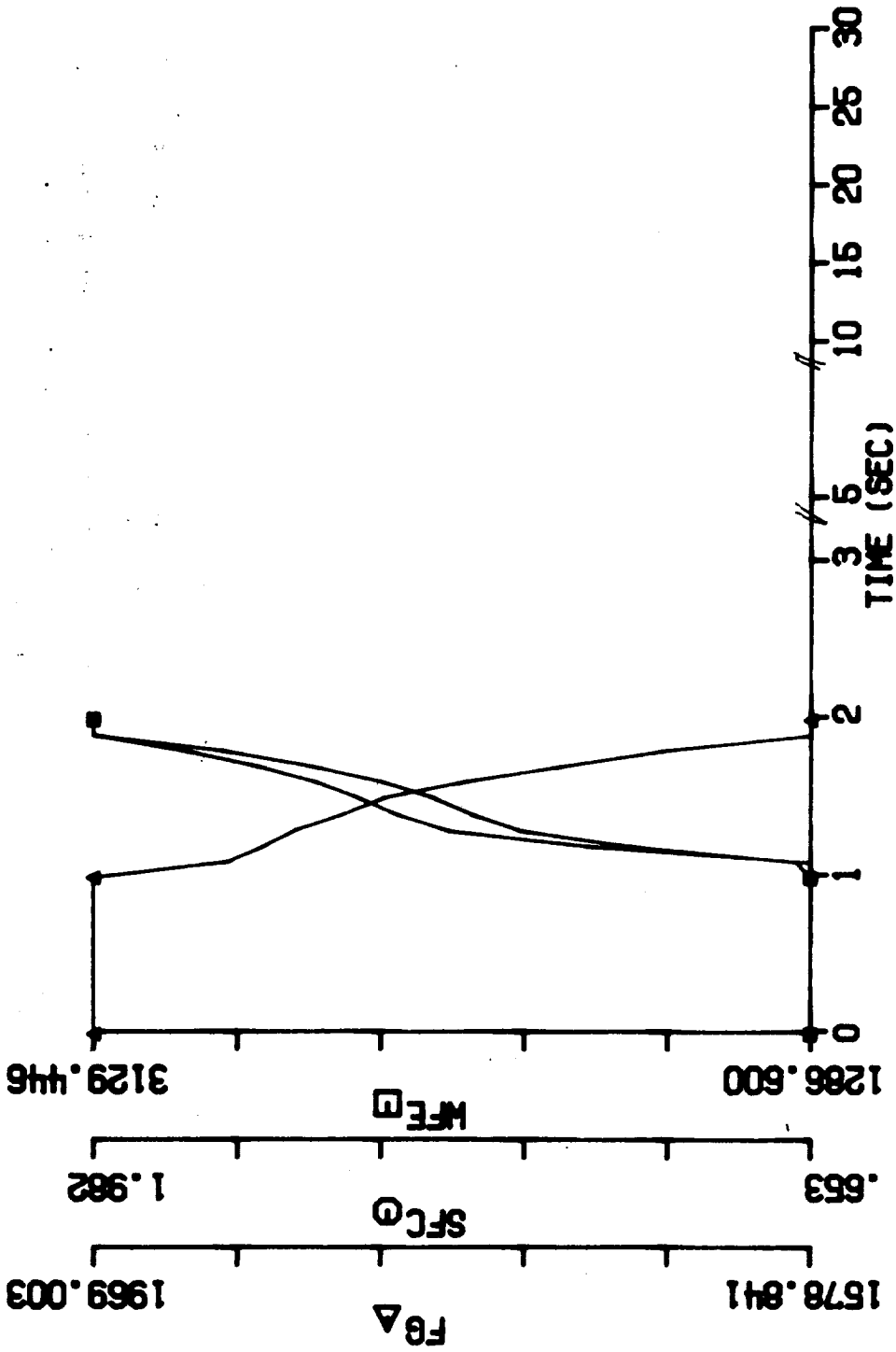

Figure 39.3 Transient Engine Performance: PLA changes from Ground Idle Setting to Max Power Setting, dry air operation standard temperature, 40 F temperature error (WFE, SFC, FG vs. time)

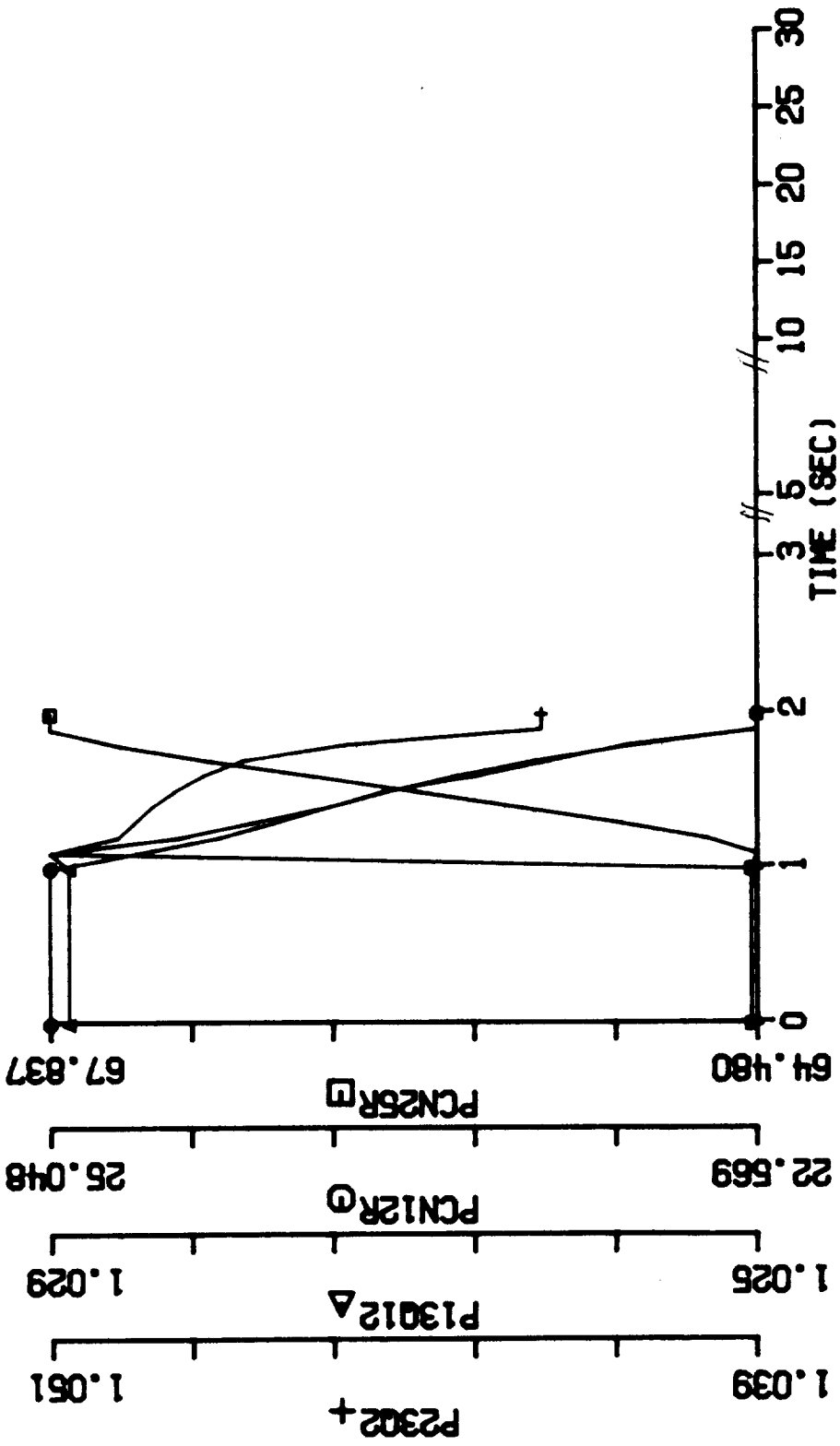

Figure 40.1 Transient Engine Performance: PLA changes from Ground Idle Setting to Max Power Setting, 2% water ingestion with all liquid drained, standard temperature, 40 F temperature error (PCN25R, PCN12R, P13Q12, P23Q2 vs. time)

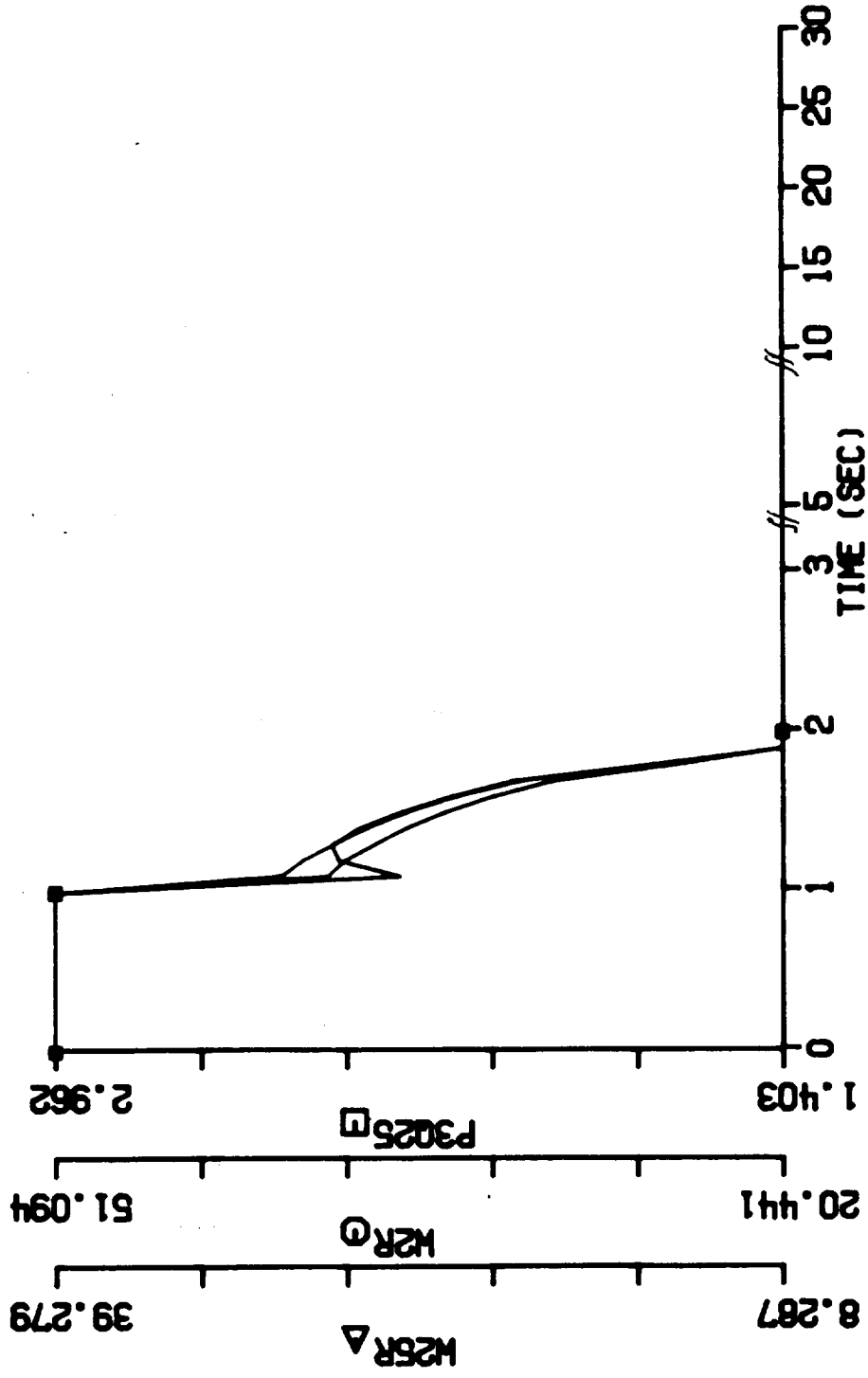

Figure 40.2 Transient Engine Performance: PLA changes from Ground Idle Setting to Max Power Setting, 2% water ingestion with all liquid drained, standard temperature, 40 F temperature error (P3Q25, W2R, W25R vs. time)

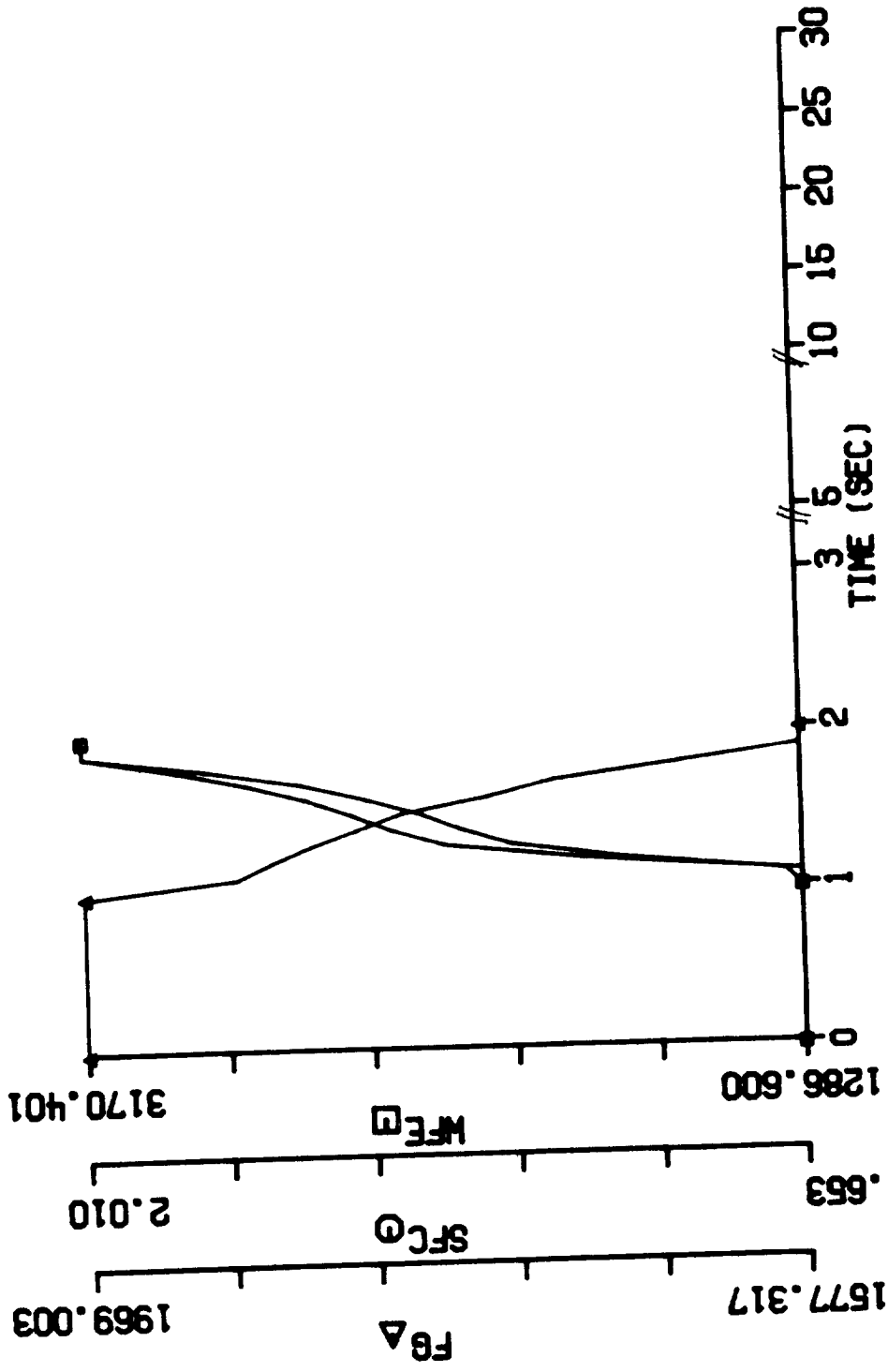

Figure 40.3 Transient Engine Performance: PLA changes from Ground Idle Setting to Max Power Setting, 2% water ingestion with all liquid drained, standard temperature, 40 F temperature error (WFE, SFC, FG vs. time)

1. Report No.	2. Government Accession No.	3. Recipient's Catalog No.
NASA CR-179549 DOT/FAA/CT-TN87/1		

4. Title and Subtitle	5. Report Date
Jet Engine Simulation With Water Ingestion Through Compressor	January 1987
	6. Performing Organization Code
7. Author(s)	8. Performing Organization Report No.
T. Haykin and S.N.B. Murthy	M/NAFA/TR-1
	10. Work Unit No.
	506-62-21
9. Performing Organization Name and Address	11. Contract or Grant No.
Purdue University School of Mechanical Engineering West Lafayette, Indiana 47907	NAG3-481
	13. Type of Report and Period Covered
12. Sponsoring Agency Name and Address	Contractor Report Final
National Aeronautics and Space Administration Lewis Research Center Cleveland, Ohio 44135	14. Sponsoring Agency Code

15. Supplementary Notes

Project Manager, Ronald J. Steinke, Internal Fluid Mechanics Division, NASA Lewis Research Center. Work partially funded by the Department of Transportation, Federal Aviation Administration, Technical Center, Atlantic City, New Jersey 08405 under NASA-FAA Agreement DTFA03-83-A00328.

16. Abstract

Water ingestion into a jet engine affects most directly the performance of the air compression subsystem of the engine, and also the sensors located in that subsystem that provide input to the control system of the engine. Such performance changes can then affect the overall performance of the engine. Considering a generic, high bypass ratio, two-spool gas turbine operating on a stationary test stand with fixed inlet and thrustor nozzle, an attempt has been made to establish the transient performance of the engine under a variety of water ingestion and power setting conditions and also when a temperature sensor providing input to the engine control records a lower temperature than the local gas phase temperature. The principal tools utilized in the investigation have been the so called PURDUE-WINCOF code and an engine simulation code. Performance calculations in each selected case have been made under two limiting sets of conditions: (i) total drainage of water and (ii) partial evaporation of water at the entry or exit of the burner with remaining water drained. Although the results are specialized to the generic engine and its control, it is shown in general that (a) engine performance is degraded during operation with water ingestion and the amount of degradation is a nonlinear function of inlet water mass fraction; (b) controllability of the engine with respect to operator-initiated power setting changes is affected by water ingestion; (c) errors in a temperature sensor providing an input to engine control lead to instability in engine operation, eventually causing a limiting condition or parameter to be exceeded.

17. Key Words (Suggested by Author(s))	18. Distribution Statement
Water ingestion; Rain effects; Compressor performance; Dynamic performance; Engine performance	Unclassified - unlimited STAR Category 01

19. Security Classif. (of this report)	20. Security Classif. (of this page)	21. No. of pages	22. Price*
Unclassified	Unclassified	171	A08

*For sale by the National Technical Information Service, Springfield, Virginia 22161